UNIVERSITY OF SOUTHAMPTON

FACULTY OF ENGINEERING, SCIENCE AND MATHEMATICS

SCHOOL OF CHEMISTRY

AN INVESTIGATION INTO THE MOLECULAR RECOGNITION AND SENSING OF ANIONS, ESPECIALLY OF ALKYLCARBAMATES AND RELATED SPECIES.

By

Peter Richard Edwards

Thesis for the degree of Doctor of Philosophy

March 2010

UNIVERSITY OF SOUTHAMPTON

ABSTRACT

FACULTY OF ENGINEERING, SCIENCE AND MATHEMATICS
SCHOOL OF CHEMISTRY

Doctor of Philosophy

AN INVESTIGATION INTO THE MOLECULAR RECOGNITION AND SENSING OF ANIONS, ESPECIALLY OF ALKYLCARBAMATES AND RELATED SPECIES.

By Peter Richard Edwards

This thesis reports the synthesis and study of the anion recognition properties of a variety of synthetic organic and inorganic receptors. A series of known anion receptors containing a common urea and varying alkyl and aryl substituents have been investigated for their ability to bind the alkylcarbamate portion of two alkylammonium-alkylcarbamate salts and the CO_2 adduct of a cyclic amidine, in an investigation into novel CO_2 fixation strategies. Chemical shift changes were used to observe relative binding strengths for interactions between the alkylcarbamate and the receptors in DMSO-d_6. The results show that it is possible to bind the alkylcarbamate anion in the presence of the primary alkylammonium cation, when a receptor of sufficient strength is employed. The strength of this interaction was increased when 18-crown-6 was added, which acts as a receptor for the alkylammonium cation. The CO_2 adduct of the cyclic amidine, (1,4,5,6,-tetrahydropyrimidine) was shown to have the strongest interactions with the receptor series.

Several Schiff-base and urea containing receptors have been synthesised and assessed for anion complexation properties in solution using ^{1}H NMR in DMSO-d_6 : water mixtures. These are selective for acetate, benzoate and dihydrogen phosphate over chloride and hydrogen sulfate, and exhibit a mixture of 1:1 and 2:1, (guest:host), binding stoichiometries in several cases. Zinc(II) and cobalt(II) chloride complexes of one of this series were synthesised. The cobalt(II)chloride complex was observed to be a stark colorimetric indicator for chloride and dihydrogen phosphate.

A number of isophthalamide derivatives containing activated NH and / or CH protons have been synthesised and assessed for anion complexation solution using ^{1}H NMR in DMSO-d_6. Their interactions with fluoride, chloride and bromide were investigated, which demonstrate a significant contribution from the activated CH protons.

DECLARATION OF AUTHORSHIP

I, Peter Richard Edwards declare that the thesis entitled

An investigation into the molecular recognition and sensing of anions, especially of alkylcarbamates and related species.

and the work presented in the thesis are both my own; and have been generated by me as a result of my own original research. I confirm that:

- this work was done wholly or mainly while in candidature for a research degree at this University;
- where any part of this thesis has previously been submitted for any degree or other qualification at this University or other institution, this has been clearly stated;
- where I have consulted the published work of others, this is always clearly attributed;
- where I have quoted the work of others, the source is always given. With the exception of such quotations, this thesis is entirely my own work;
- I have acknowledged all main sources of help;
- where the thesis is based on work done by myelf jointly with others, I have made clear exactly what was done by others and what I have contributed myself;
- parts of this work have been published as:

Stabilisation of alkylcarbamate anions using neutral hydrogen bond donors. Edwards, P. R; Hiscock, J. R; Gale, P.A. *Tetrahedron. Lett.* **2009**, *50*, 4922.

Carbamate complexation by urea-based receptors: studies in solution and the solid state. Edwards, P. R; Hiscock, J. R; Gale, P. A; Light, M. E. *Org. Biomol. Chem.*, **2010**, *8*, 100.

Signed:……

Date:……

ABBREVIATIONS

A^-	Anion
AAAC	Alkylammonium-alkylcarbamate
ADP	Adenosine diphosphate
AMP	Adenosine monophosphate
ATP	Adenosine triphosphate
ATR	Attenuated Total Reflection
C	Degrees Celcius
CA	Carbonic Anhydrase
Calc.	Calculated
d	Doublet (NMR)
d	Deuterated (NMR)
DAP	1,3-diaminopropane
DBU	1,8-diazabicyclo[5.4.0]undec-7-ene
DCM	Dichloromethane
DMAP	4-Dimethylaminopyridine
DMF	Dimethylformamide
DMSO	Dimethylsulfoxide
DNA	Deoxyribonucleic acid
DPU	Diphenylurea
Eq.	(Molar) Equivalents (of Substance)
ES-	Electrospray Negative (Mass Spectrometry)
ES+	Electrospray Positive (Mass Spectrometry)
FT-ICR-MS	Fourier Transform Ion Cyclotron Resonance Mass Spectrometer
FTIR	Fourier Transform Infra Red (Spectroscopy)
G	Guest
H	Proton (NMR)
H	Host
h	Hours
HRMS	High Resolution Mass Spectrometry
Hz	Hertz
IR	Infra-Red (Spectroscopy)
K	Kelvin
K_a	Association Constant (Binding Constant)
LRMS	Low Resolution Mass Spectrometry
M	Molarity
M	Monoisotopic Mass (Mass Spectrometry)
m	Multiplet (NMR)
m/z	Mass to Charge ratio (Mass spectrometry)

MHz	Mega Hertz
MOF	Metal-Organic Framework
MPt	Melting Point
M-THP	N-methyl-1,4,5,6-tetrahydropyrimidine
NMR	Nuclear magnetic resonance
pKa	Acid dissociation constant
ppm	Parts per million
ppmv	Parts per million (by volume)
RNA	Ribonucleic acid
RT	Room temperature
s	Singlet (NMR)
t	Triplet (NMR)
T	Tesla (Mass Spectrometry)
TBA	Tetrabutlyammonium
TEA	Tetraethylammonium
TFA	Trifluoroacetic acid
THF	Tetrahydrofuran
THP	1,4,5,6-tetrahydopyrimidine
TMA	Tetramethylammonium
TMG	Tetramethylguanidine
tren	Tris-(2-aminoethyl)amine
UV-vis	Ultra-violet / visible (Spectroscopy)
ZIF	Zeolitic Imidazole Framework
Δδ	Chemical shift change
λ	Wavelength (nm) (UV-Visible Spectroscopy)
ν	Wavenumber (cm^{-1}) (Infra Red Spectroscopy)

CONTENTS

ACKNOWLEDGEMENTS

I would like to thank my supervisor Professor Philip A. Gale for his support, guidance and encouragement during the past three years in the lab. I would also like to thank all of the members of the Gale group past; Gareth, Jo, Sergio, Claudia, Roberto, Matt; and present; Jenny, Christine, Steve, Sam, Cally, Masafumi, Agnieszka, and Sarah. I would like to thank Dr. Simon Brooks for his supervision during my third year undergraduate project in the same group. His guidance and enthusiasm was a major contributing factor in my decision to take on a PhD.

I would like to thank the University of Southampton and EPSRC for funding and thank the MS and NMR services at Southampton for their assistance throughout. I would like to thank Dr. Mark. E. Light for running and solving X-ray crystal structures presented in this thesis and recent discussions. I would also like to thank Prof. Gill Reid for productive discussions regarding aspects of Chapter 3.

I would especially like to thank my family for their encouragement and support, and Liz for her never-ending support, especially during the write-up.

CHAPTER 1 - INTRODUCTION

1.1 SUPRAMOLECULAR CHEMISTRY

Supramolecular chemistry was famously described by Jean Marie Lehn in 1988 as "chemistry beyond the molecule".[1] It is the chemistry of systems containing two or more separate chemical entities, bound using interactions weaker than covalent bonds. Because the interactions concerned are relatively weak, supramolecular systems are generally dynamic, i.e. are formed reversibly.

Such systems are often comprised of just two components; a host and a guest. The host is designed to interact favourably with a specific guest or class of guests and is generally the larger of the two components. Guests are normally smaller, and can be neutral or ionic. By appropriate design, supramolecular chemists have synthesised many hosts with very high selectivity for specific guests. These can, for example, bind one particular guest from a mixture of guests in solution. A wide range of intermolecular bonds have been employed in the design of host:guest systems and supramolecular systems as a whole. These include:

i) **Electrostatic interactions** - Interactions between opposite charges. These include ion-ion, ion-dipole and dipole-dipole interactions. Bond energies are high; 100 – 350 kJmol^{-1} (ion-ion), 50 – 200 kJmol^{-1} (ion-dipole), 5 – 50 kJmol^{-1} (dipole-dipole).

Ion - Ion Ion - Dipole Dipole - Dipole

ii) **Hydrogen bonding interactions** – Highly directional partially electrostatic interactions between hydrogen bond donors, which bear an electropositive hydrogen atom, and hydrogen bond acceptors, which bear an electronegative atom or anion. Individual bond energies are moderate; 5 – 120 kJmol^{-1}, but collectively can become much stronger.

iii) **π-π stacking interactions** – Interactions between aromatic rings due to interactions of their π-electron clouds. These may be oriented in either face-to-face or edge-to-face geometries. Bond energies are low; < 50 kJmol^{-1}.

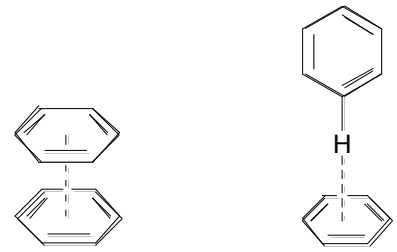

Face-to-face Edge-to-face

iv) **van der Waals interactions** – These are interactions induced between the electron cloud surrounding a nucleus and an adjacent nucleus in another molecule. Bond energies are low; < 5kJmol^{-1}, but collectively may become significantly higher.

v) **Hydrophobic and solvophobic interactions** – Apparent attractive interactions between two or more components of a system, which result from a common hydrophobicity or solvophobicity.

By using combinations of these interactions and correctly positioning them in a host molecule, it is possible make very specific receptors for particular guests. This leads to high selectivity, which should not be confused with a strong interaction.

The strength of a given host:guest interaction is measured by the binding affinity of a system. The binding constant, K_a, for a 1:1 (host:guest) system is defined[2] as:

$$K_a = [HG] / [H][G]$$

where [G] is the concentration of guest (M), [H] is the concentration of host, (M), and [HG] is the concentration of the host:guest complex, (M). Binding constants therefore have units of inverse molar, (M^{-1}). The absolute value depends not only on the strength of host:guest interaction, but also upon on the solvent in which the interaction is studied. Co-ordinating solvents have strong interactions with the host and guest, whereas weakly coordinating solvents do not. Therefore, the same combination of host and guest will produce a larger [HG] in a weakly coordinating solvent than in a highly coordinating solvent. Binding constants will therefore be lower in highly coordinating solvents than weakly coordinating ones. Because of this, it is only possible to directly compare binding constants measured under *identical* conditions. Occasionally binding constants are given as log K_a values, which are proportional to ΔG.

1. 2 ANION RECEPTORS

Many host:guest systems feature anionic guests. This is not only because anions are more easily bound than neutral species due to their charge, but also because they feature in a large number of natural processes and man-made systems, making many of them desirable targets. For example, impermeability of cell membranes to chloride causes the debilitating condition cystic fibrosis.[3] Any non-toxic, artificial receptor capable of binding chloride might find use in new techniques for treating this condition. DNA and RNA are polyanionic structures,[4] and can now be targeted as such by gene therapy. In the environment, eutrophication of waterways is caused by excess nitrate and phosphate from fertilisers. Aside from the ecological damage brought about by algal blooms, this is also reported to be detrimental to human health.[5] Any receptor, therefore, capable of selectively removing nitrate and / or phosphates from the waterway may be of benefit in both regards. Away from the natural world, the nerve gas Sarin, famously used in a terrorist attack in Tokyo,[6] decomposes to give fluoride as a by-product, amongst others, giving reason to design fluoride sensors.

Anions are different sizes and have a large number of different geometries:

i) **Spherical** (eg: halides);

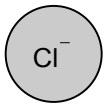

ii) **Linear**, (eg: azide, cyanide);

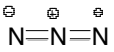

iii) **Y–shape**, (eg: carboxylate);

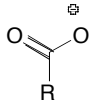

iv) **Trigonal**, (eg: nitrate, carbonate);

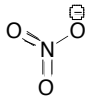

iv) **Tetrahedral**, (eg: phosphates, sulphates);

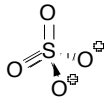

v) **Square planar**, (eg: squarate dianion).

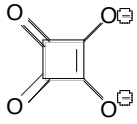

It can be seen that shape is a major discriminating factor between different anions. Therefore, supramolecular chemists usually consider this first when designing receptors, often using hydrogen bonds as the primary method of interaction. Hydrogen bonds are capable of forming highly directional intramolecular bonds, and are therefore excellent for inclusion in shape selective hosts. In addition, multiple hydrogen bonds are very strong. This combination of high directionality and high collective bond strength makes them very powerful anion complexation tools, with other intermolecular interactions often playing only secondary roles.

1.3 CHARGED ANION RECEPTORS

The first synthetic anion receptors were presented by Simmons and Park in 1968 in a series of papers researching the structural equilibria of a series of protonated diazabicycloalkanes, **1** – **4**.[7] In the last of these, they reported an "unprecedented kind of ion-pairing", in which halide ions were observed to enter the internal cavity of the macrocycles, (Figure 1.1). In acidic aqueous media, the opposing terminal tertiary amine groups are protonated, and can form hydrogen bonds to anionic guests within the binding cavity. Receptors **1** and **2**, do not bind chloride, bromide or iodide in 50% TFA:D_2O, (by analysis of the chemical shift changes in the ^1H NMR spectra). In the same solvent system, the binding cavity of **3** is large enough to accommodate chloride ($K_a = 4M^{-1}$), but not bromide ($K_a = 1M^{-1}$), or iodide, ($K_a = 0M^{-1}$). This receptor therefore prefers smaller anions. Receptor **4** binds all halides equally ($K_a > 10M^{-1}$), within the limits of the experiment, because of its large internal cavity. It can be seen that different sized cages favour different sized halides to different extents, demonstrating the important principle of size complementarity in this field. The authors highlight that many of the structures involve two hydrogen bonds, which shows the power of using multiple hydrogen bonds. They also note that external binding is observed, in which only one hydrogen bond is formed between the halide and the protonated amine. It should also be noted that these receptors and many of those that follow are pH dependant, in that they may only be employed where the pH range enables protonation of the host, whilst keeping the guest deprotonated.

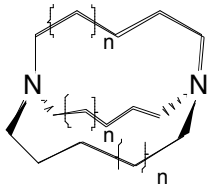

1 n = 3
2 n = 4
3 n = 5
4 n = 6

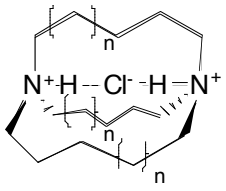

Fig 1.1 Chloride complex of **3**

Lehn and co-workers subsequently synthesised similar receptors, such as **5** with longer side chains and additional amines. This more elongated type of structure was developed to accommodate azide,[8] a linear anion with formal negative charges at its termini. In acidic aqueous conditions, the six secondary amines are protonated. Upon the addition of azide, (as its sodium salt), a 1:1 complex is formed with a total of six charged hydrogen bonds between the protonated amine groups and the termini of azide, (Figure 1.2). Azide is bound far more strongly by receptor **5** than chloride or bromide, (log K_a (N_3^-) = 4.6, log K_a (Cl^-) < 1.0, log K_a (Br^-) = 2.0), by ^{13}C NMR titration in aqueous perchloric acid. Acetate (log $K_a \approx 2.0$), nitrate and nitrite (log $K_a \approx 3.0$), and iodide (log $K_a < 1.0$), were also studied. The authors remark that the binding trend observed is not due to the relative hydration energies of the anions studied and therefore **5** is a bona-fide azide selective receptor, based on shape complementarity.

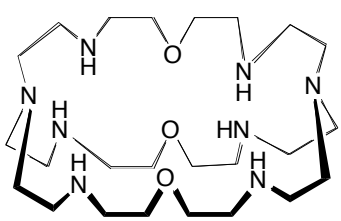

5

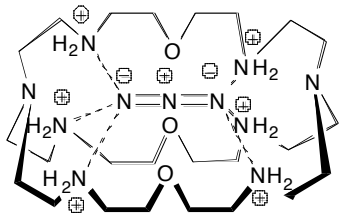

Fig 1.2 Azide complex of **5**

Many similar examples of anion complexation by cationic species have subsequently been published. Kimura and co-workers, for example, reported that simple polyamines such as receptor **6** can act as receptors for triscarboxylate citrate (K_a = 1,000M^{-1}), in preference over biscarboxylates such as succinate (K_a < 10M^{-1}), malonate (K_a < 10M^{-1}), and malalate (K_a < 10M^{-1}).[9]

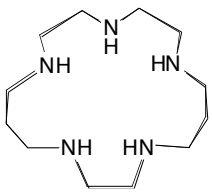

6

These results were obtained by electrochemical means in dimethoxyethane, and were confirmed by observing the changes in elution times of the receptors in electrophoresis experiments with and without carboxylates. The longer the elution time, the stronger the complex. Similar receptors in the series showed that the biscarboxylates; fumarate, tartrate and maleate, were unbound. This is because citrate has a triple negative charge, whereas the biscarboxylates have only a double negative charge. Therefore, receptor **6** is primarily an electrostatic receptor, which is not greatly affected by the geometry of the anion. Due to the biological relevance of triscarboxylates, the authors remark that systems similar to **6** may lead to synthetic transporters for anions, such as those that have more recently been developed.[10]

Also with reference to the potential for biological applications, Martell and co-workers studied the behaviour of a similar macrocycle **7** with various phosphate species.[11] The hexa-protonated form of **7** showed significant preference for triphosphate (log K_a = 13.05) over monophosphate (log K_a = 3.51). The stark difference in binding is again due to a largely electrostatic effect. Lehn and co-workers have shown that receptors such as these can be used as catalysts in the hydrolysis of adenosine triphosphate,[12] a key biological process which is an important step in cell energy usage.[13]

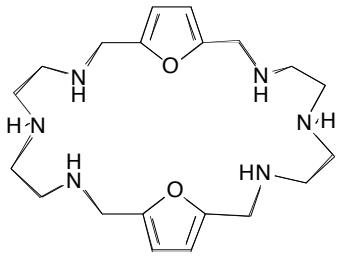

7

Examples of purely electrostatic receptors by Schmidtchen and co-workers were also presented around this time. In this series, alkyl cages were synthesised which contained quarternary amines at the four corners of the tetrahedron.[14] The receptors were designed to bind anions within their central cavities, held entirely by electrostatic interactions. Different sized cages were shown to have different binding affinities for anions. Because they are methylated rather than protonated, they are pH-independent receptors.

Receptor **8** has an internal cavity 4.6Å in diameter and the most strongly bound anion in H_2O is bromide (log K_a = 3.7) over iodide (log K_a = 2.2) and chloride, (log K_a = 1.3). Receptor **9** binds the halides in this order with a marginally increased preference for bromide, (log K_a = 3.9), over iodide (log K_a = 2.4), and chloride (log K_a = 0.5).

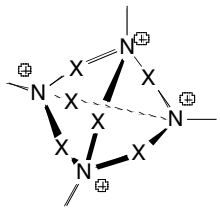

8 X = -((CH)$_2$-)$_6$ -
9 X = -((CH)$_2$-)$_8$ -

Because these receptors have 4+ charge, they are associated with counter-anions. It is therefore conceivable that the counter anions used may have competed with the anion for the receptor, giving a distorted picture of the anion complexation properties of the series. Thus, a second generation was synthesised, in which the counter-anions were covalently attached to the quaternary ammonium cage.[15] This series is typified by receptor **10**.

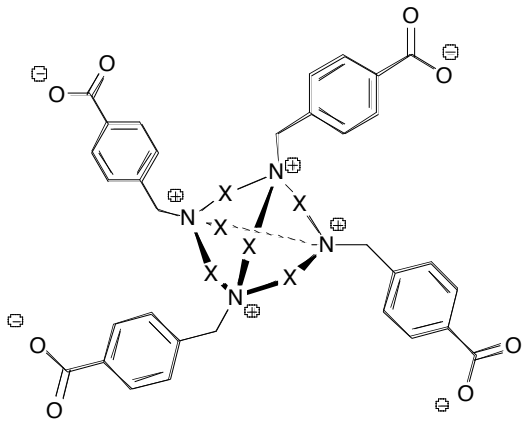

10 X = - ((CH)$_2$-)$_6$ -

In dilute solutions, such as the solution in the titration experiments, it is assumed that opposite charges from two different molecules of **10** cannot come into close contact. In addition, it is not possible for the counter-anions to rotate into the binding cleft of receptor it is attached to. The cage can therefore freely accept analyte anions. Receptor **10** is selective for iodide (K_a = 6,480M^{-1}), over bromide (K_a = 2,150M^{-1}) and chloride (K_a = 270M^{-1}), by NMR titration in D_2O. This is a different selectivity from the previous receptor of the same size, **8**. As the only difference is the presence of the covalently attached counter-anions, one could surmise that in the case of **8** iodide is prevented from entering the binding cavity, due to the presence of bound counter-anions, leading to a low binding affinity for this large anion.

There have also been many examples of receptors for anions based on guanidinium salts. First described as anion receptors by Lehn and co-workers in 1978,[16] these employ both electrostatic and hydrogen bonding interactions to bind anions. Typical of these types of receptors are those such as **11** by Lehn and co-workers, which contain a central guanidinium salt and bulky substituents.[17]

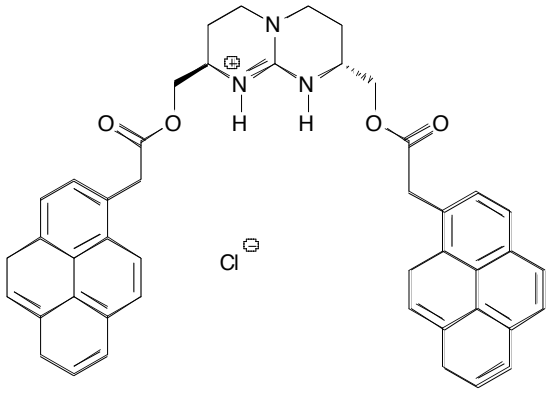

11

Receptor **11** was found to be a good oxo-anion receptor, due to the near-perfect match between the geometries of the guanidinium hydrogen bond donors and the oxygen atoms of the anions. It was found to bind *p*-nitrobenzoate with K_a = 1,609M^{-1} by ^{1}H NMR titration in $CDCl_3$ when the anion was added as its TEA salt. Because **11** is chiral, it is also capable of differentiating between L- and D-enantiomers of amino acids. SS-**11** was shown to bind L-tryptophan with K_a = 1,051M^{-1} and D-tryptophan with K_a = 534M^{-1}. This difference is caused by the steric repulsion between the bulky side groups of **11** and the indole ring of the tryptophan.

1.4 NEUTRAL ANION RECEPTORS

It was observed in the 1990's, that receptors did not have to be cationic to bind anions strongly. Neutral systems were developed which operated in organic media. Many neutral receptors were much more synthetically accessible than charged receptors. Another significant advantage of these was that they were open to almost limitless adaptation and tuning, as proven by the explosion of interest in anion recognition since the late 1990s.[18] For these reasons, neutral hydrogen-bonding motifs now form the majority of new synthetic anion receptors.

1.4.1 Amide-based Anion Receptors

The first example of a neutral anion receptor, **12** was presented by Pascal and co-workers in 1986.[19]

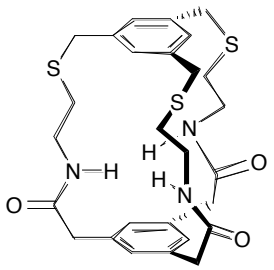

12

It has several characteristics of the electrostatic receptors, as it is a macrocyclic, cage-type molecule, with three amides in alkyl chains, connected at both ends by different 1,3,5-trisubstituted benzene rings. The receptor has C_{3v} symmetry, with the amides positioned into the cavity.

X-ray crystallography shows that this arrangement is not maintained in the solid state, (Figure 1.3). Instead, two of the amide protons are convergent, with the third not oriented in the same direction.

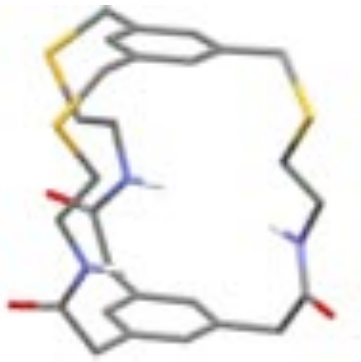

Fig 1.3 Crystal structure of **12**.
(Solvent molecules and non-acidic protons omitted for clarity).

Receptor **12** was shown to respond to the addition of fluoride when this was added as its TBA salt to a DMSO-d_6 solution of **12** by study of the chemical shift changes in the ^{1}H and ^{19}F NMR spectra. This work showed that when several neutral hydrogen bonds are arranged to work cooperatively, they can act as effective anion receptors.

Several years later, Reinhoudt and co-workers, appended the tris amine, tris-(2-aminoethyl)amine, (tren), with amides, producing systems similar to acyclic versions of **12**.[20] Opening up the macrocycles to provide anion binding clefts such as those seen in **13** – **18**, provided much larger cavities for binding anions.

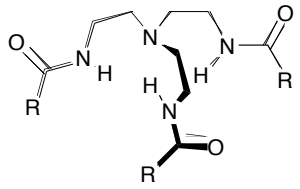

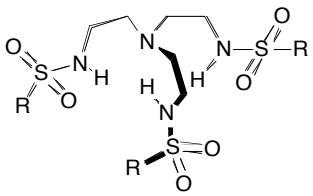

13 (R = CH_2Cl)
14 (R = $(CH_2)_4CH_3$)
15 (R = Ph)
16 (R = 4-$MeOC_6H_4$)

17 (R = 4-MeC_6H_5)
18 (R = 2-naphthyl)

This series of receptors was selective for dihydrogen phosphate when studied by UV-vis titration techniques in acetonitrile, because this anion is fairly basic and matches the C_3 symmetry of the series of receptors. It does not bind hydrogen sulfate as strongly because hydrogen sulfate is far less basic than dihydrogen phosphate. Receptor **18** is the strongest receptor of the series, binding dihydrogen phosphate, (K_a = 14,200M^{-1}), over chloride, (K_a = 1,600M^{-1}), and hydrogen sulfate (K_a = 38M^{-1}), when studied by conductimetry techniques in acetonitrile. (Anions added as their TBA salts). It is the strongest in the series because it has sulfonamides instead of amides, which are more acidic than amides. This is because the nitrogen lone-pair of electrons is delocalised into two S=O bonds instead of a single C=O bond. In addition to this advantage, **18** also has naphthalene substituents, which participate in secondary π-π stacking interactions with each other. This keeps the three strands of **18** together, and pre-organises them into a cleft.

This work shows the simplicity with which a series of anion receptors can be synthesised and demonstrates that the rapid optimisation of a given receptor series was an achievable goal. Once trends in a given series are established, it is then possible to optimise selectivity or to increase binding affinity for particular anions rationally.

It was not until 1997, however, that the full potential of amide-based receptors was demonstrated by Crabtree and co-workers.[21] They showed that very small bis-amide based receptors such as **19** – **23**, could bind anions such as the halides using just one binding cleft, (Figure 1.4). The series of receptors was synthesised such that the two NH bonds converge at a point. This happens when the molecule adopts a convergent, *syn-syn* conformation. The strongest receptor of the group is **19,** selective for chloride (K_a = 61,000M^{-1}), over fluoride (K_a = 30,000M^{-1}), and acetate, (K_a = 17,000M^{-1}) when studied by ^{1}H NMR titration techniques in CD_2Cl_2. (Anions added as their PPh_4 salts). The most selective receptor however, **23**, is selective for fluoride (K_a = 24,000M^{-1}), over chloride (K_a = 1,500M^{-1}), and acetate (K_a = 525M^{-1}) in the same solvent system. In the case of **23** there are intra-molecular hydrogen bonds between the NH and the nitrogen of the central pyridine ring, which pre-organises the molecule into a *syn-syn* conformation, ideal for a binding cleft for small anions. It is also possible that in the *anti-anti* and *syn-anti* conformations, the (sulf)amide proton(s) clash with the protons on the central ring, further disfavouring these conformations.

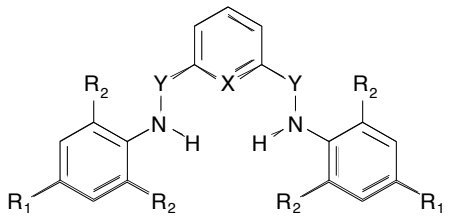

19 X = CH, Y = CO, $R_1 = R_2 = H$
20 X = CH, Y = CO, $R_1 = {}^nBu$, $R_2 = H$
21 X = CH, Y = CO, $R_1 = R_2 = CH_3$
22 X = CH, Y = SO_2, $R_1 = R_2 = H$
23 X = N, Y = CO, $R_1 = R_2 = H$

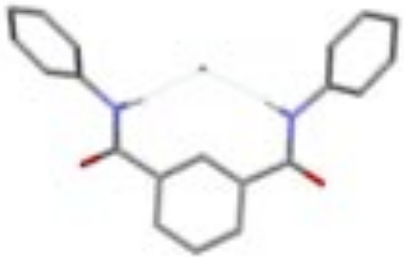

Fig 1.4 Crystal structure of bromide complex of **19**.
(Solvent molecules, PPh_4 cations, and non-acidic protons omitted for clarity.)

Contemporaneously, B. D. Smith and co-workers produced similar amide-based receptors, such as **24,** which are activated by the presence of bound boranate groups.[22] The boronate groups are positioned such that they can accept electrons from the carbonyl oxygen upon complexation of anions. This transfers a formal negative charge to the boron atom, which allows the nitrogen lone pair to form a full N=C bond. A full positive charge is therefore formed on the amide nitrogen, (Figure 1.5), which greatly enhances the anion binding abilities compared to receptors without boronates, due to the electrostatic interactions. Compound **24** binds acetate around 20 times more strongly than the best Crabtree receptor, **23**, because of this interaction, when added as its TBA salt and studied by ^{1}H NMR techniques in DMSO-d_6, (K_a (**24**) = 2,100M^{-1}, K_a (**23**) = 110M^{-1}). It should be noted that **24** does not have a central pyridine ring. A receptor incorporating boronates and the pre-organisation afforded by the presence of pyridine would be likely to have even stronger anion binding properties.

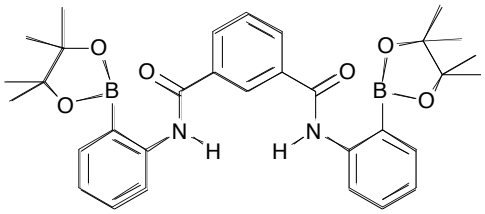

24

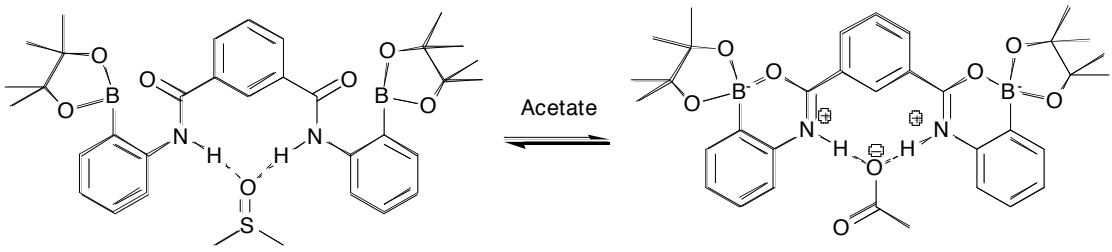

Fig 1.5 Internal electron transfer brought about in **24** upon the addition of acetate in DSMO

The combined works of Crabtree and Smith led to amides becoming a popular choice for the synthesis of neutral anion receptors. Gale and co-workers, for example produced receptor **25,** which was shown to be selective for dihydrogen phosphate (K_a = 149M^{-1}), over acetate (K_a = 98M^{-1}), benzoate (K_a = 43M^{-1}) and chloride (K_a = 13M^{-1}) in 0.5% H_2O:DMSO-d_6 by ^{1}H NMR titration techniques, (anions added as their TBA salts).[23] This is not a particularly successful receptor, but shows that even simple electron rich amides can bind anions with a degree of selectivity in competitive solvents.

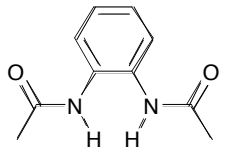

25

Kondo and co-workers have extended Crabtree motifs to include further amides, and pyridine sustituents, which can act as hydrogen bond acceptors. This combination of acceptors and donors makes these receptors very selective for dihydrogen phosphate,[24] an anion which contains both hydrogen bond donors as well as acceptors. To achieve a favourable interaction with dihydrogen phosphate, the receptor twists, (Figure 1.6). Dihydrogen phosphate was shown to bind around 60 times more strongly than acetate with receptor **26**, (K_a ($H_2PO_4^-$) > 1,000,000 M^{-1}, K_a ($CH_3CO_2^-$) = 17,000M^{-1}) by UV spectroscopy in 0.5% DMSO:CH_3CN, (when the anions were added as their TBA salts), due to a combination of shape and charge complementarity.

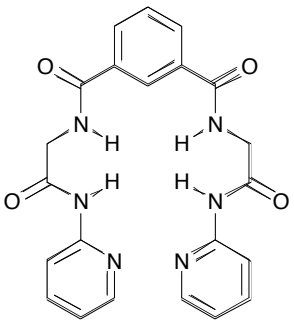

26

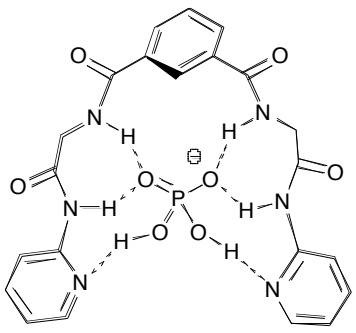

Fig 1.6 Dihydrogen phosphate complex of **26**

Recent work by Rybak-Akimova and co-workers has yielded double-ended amide macrocycles such as **27**, which have opposing 2,6-bisamino pyridine units, linked by polyamines.[25] Having two anion binding clefts enables the binding of dianinonic species, such as biscarboxylates. The group studied several biscarboxylates, with different length carbon chains. Macrocycle **27** is selective for TBA succinate (K_a = 30,000M^{-1}) and other biscarboxylates such as oxalate (K_a = 1,300M^{-1}), malonate (K_a = 6,000M^{-1}), glutarate (K_a = 1,200M^{-1}) and fumarate (K_a = 5,700M^{-1}) by ^{1}H NMR techniques in DMSO-d_6 over monocarboxylates, such as acetate (K_a = 88M^{-1}), and benzoate (K_a = 35M^{-1}), (anions added as their TEA salts.) The proposed succinate complex is shown, (Figure 1.7). Receptor **27** still has the same bis-amide motif as the work of Crabtree twelve years previously and this continues to be an important motif in anion recognition.

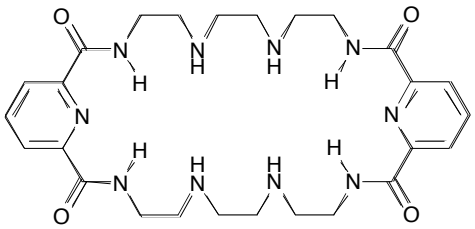

27

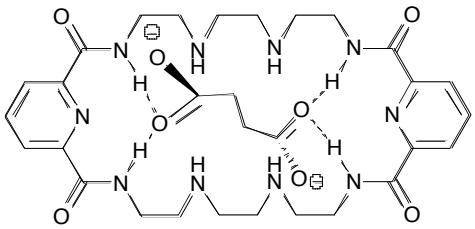

Fig 1.7 Succinate complex of **27**

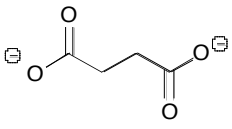

Succinate

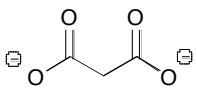

Malonate

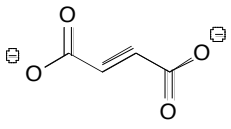

Fumarate

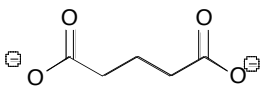

Glutarate

Bowman-James and co-workers have produced similar macrocycles, **28 – 31** and macro-bicycles, **32** and **33**.[26] Despite having more hydrogen bond donors, the bicyclic systems actually show poorer binding with the majority of anions than the corresponding macrocycles, by ^{1}H NMR titration in DMSO-d_6. Receptor **31** binds dihydrogen phosphate, (log K_a = 4.05), over chloride, fluoride, bromide (log $K_a \approx$ 2.60-2.70), and hydrogen sulfate (log K_a = 2.03) when studied by ^{1}H NMR titration techniques in DMSO-d_6, (anions added as their TBA salts). Receptor **33**, however, binds fluoride most strongly, (log K_a = 5.90), over chloride (log K_a = 3.48), dihydrogen phosphate (log K_a = 3.31) hydrogen sulfate (log K_a = 1.83), and bromide (log K_a = 1.60), under the same conditions.

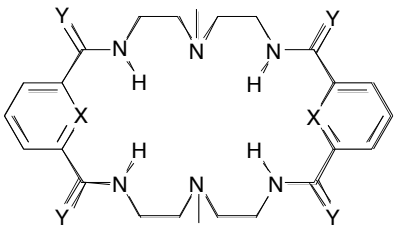

28 (Y=S, X=CH)
29 (Y=S, X=N)
30 (Y=O, X=CH)
31 (Y=O, X=N)

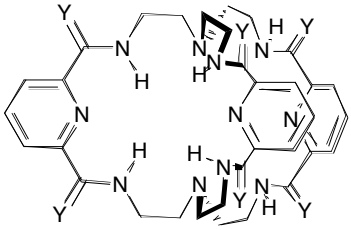

32 (Y=S)
33 (Y=O)

The group has obtained a crystal structure for the complex of **33** and fluoride, which shows C_3 symmetry, with the fluoride held by three pairs of hydrogen bonds, (Figure 1.8).

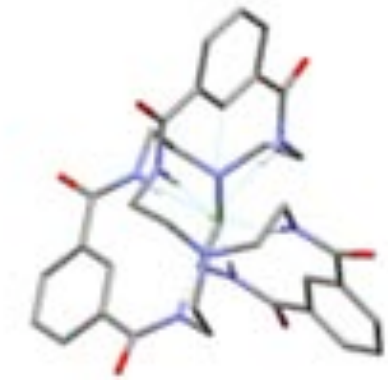

Fig 1.8 View of the crystal structure of fluoride complex of **33**

In general, the macro-bicyclic systems are poor anion receptors compared to the macrocycles. The decreased affinity for anions shows that steric congestion can be a major obstacle regarding the diffusion of anions to a binding site. Large structures such as these can also have extensive intra-molecular hydrogen bonding networks, which may incur significant energy penalties upon anion complexation, and in extreme cases, can give rise to very unpredictable binding characteristics. Böhmer and co-workers, for example, have synthesised many tri-, tetra-, and hexa-urea macrocycles, which whilst rationally designed for various anions, have a large number of intramolecular hydrogen bonding equilibria, which confuses the binding patterns and makes further rational design very difficult.[27]

Other groups have had greater success with macro-tricyclic systems. In 1997, Anslyn and co-workers produced receptor **34**.[28] It is similar to Pascal's fluoride receptor, with hydrogen bond donors held between a 1,3,5-trisubstituted benzene ring, but with a far larger binding cavity, (73.8Å). It comprises of six amides converging in a central cleft, and was designed to be selective for the trigonal anion nitrate, with each pair of amides positioned to converge on one nitrate oxygen atom, (Figure 1.9).

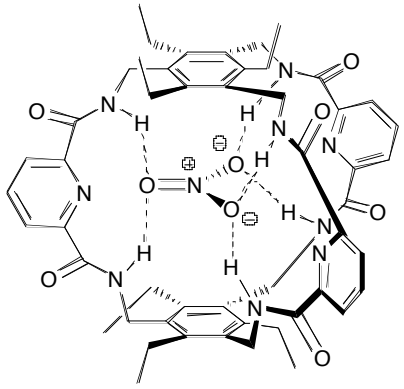

Fig 1.9 Proposed solution complex of **34** with nitrate.

Receptor **34** is selective for acetate ($K_a = 770M^{-1}$), over nitrate ($K_a = 300M^{-1}$), and other anions, (added as their TBA salts), by ^1H NMR titration in $CDCl_3$ / CD_3CN, (1:3 v/v). Despite the apparent failure to produce a nitrate selective system, it must be recognised that selectivity for acetate over nitrate is normally much greater, due to the fact that it is 10^6 times more basic than nitrate. That the two binding constants are in the same order of magnitude is remarkable, and proves that **34** is a successful shape selective receptor for nitrate.

Amides are not limited to use in small receptors. For example, cyclic- and poly-peptides have been used to bind larger anions, such as phosphate, sulfate and iodide. Kubik and co-workers, for example, have produced, (among other systems), receptor **35**, which is a bis-hexapeptide containing alternating L-proline and 6-aminopicolinic acid subunits.[29] This structure shows a preference for large anions such as sulfate (K_a = 350,000M^{-1}) and iodide, ($K_a \approx$ 10,000M^{-1}), over smaller ones such as bromide (K_a = 5,300M^{-1}), chloride, (K_a = 710M^{-1}) and nitrate, (K_a = 130M^{-1}) in 50% D_2O:CD_3CN, (anions were added as their Na or K salts). The preference for large anions is in line with the large cavity formed upon anion complexation, described by the authors as a "molecular oyster", (Figure 1.10). The reason that anions can be bound in such competitive solvents is that they can become completely surrounded by the two halves of the receptor, enabling them to be completely shielded from the solvent. In addition, the lipophilic regions of the **35** are oriented away from the anion and toward the organic solvent upon complexation. Sulfate is bound most strongly because it is doubly negative, which adds a significant electrostatic contribution to the overall binding strength.

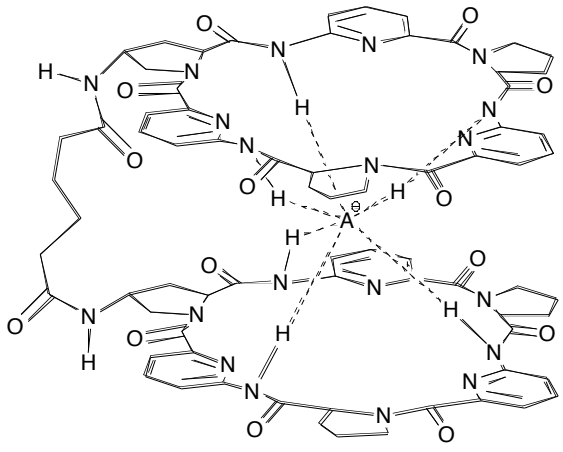

Fig 1.10 "Molecular oyster" anion complex of **35**

1.4.2 Urea-based Anion Receptors

Despite first being shown to bind anions in 1992, the use of (thio)-ureas took longer to become widespread than that of amides. They are stronger than single amides because they can form multiple hydrogen bonds to the same anion, but they are not convergent. Wilcox and co-workers, showed that the geometry of ureas is perfectly matched to bind oxo-anions and carboxylate anions in particular,[30] (Figure 1.11).

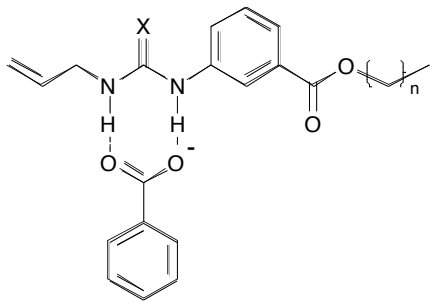

Fig 1.11 Benzoate complex of **36** (X = O, n = 7); **37** (X = S, n = 7).

Compound **36**, for example was shown to bind benzoate (K_a = 27,000M^{-1}) more strongly than diphenylphosphate, (K_a = 9,000M^{-1}), tosylate (K_a = 6,100M^{-1}), and adamantyl-sulphonate, (K_a = 6,900M^{-1}) as determined by UV-visible spectroscopy in chloroform. (Anions added as their TBA salts).

As with the early amide receptors, B. D. Smith and co-workers demonstrated that the anion binding characteristics of this motif could be greatly enhanced by appending boron-containing groups in appropriate positions to make the NH of the urea more acidic.[22] As before, the boron atom can take a full negative charge, leaving a full positive charge delocalised between the two urea nitrogen atoms. This effects causes the binding constant of **39** with acetate to be 200 times that of **38** in DMSO-d_6, (K_a (**38**) $\approx 300M^{-1}$; (**39**) $\approx 60{,}000M^{-1}$) when studied by ^1H NMR techniques, (anions added as their TBA salts).

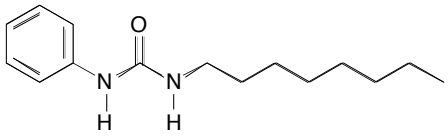

38

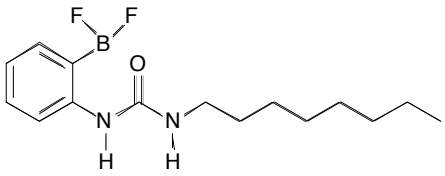

39

In 1993, Rebek and co-workers added a second urea to the Wilcox type of receptor, synthesising receptors such as **40** [31] in which the two ureas are appended to a xanthene scaffold. This type of structure enables the strength of ureas to be used in convergent hydrogen bond clefts. The group observed significantly larger carboxylate binding constants with **40**, compared to **41**, the analogous mono-urea.

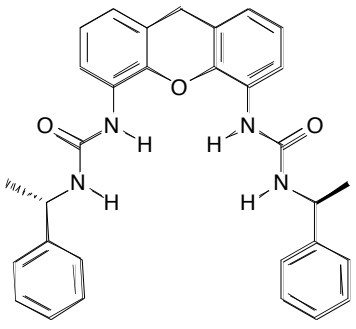

40

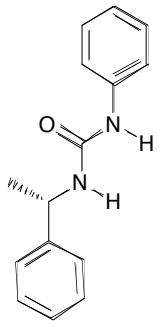

41

Receptor **40** binds benzoate (K_a = 200,000M^{-1}), over 500 times more strongly than **41** (K_a = 400M^{-1}), in $CDCl_3$ by ^{1}H NMR titration, (anions added as their TMA salts). Each urea forms two hydrogen bonds to each of the benzoate oxygen atoms, and shows the collective strength of ureas when arranged into clefts.

The convergent bis-urea motif has also been employed by Gale and co-workers, who have replaced amides with ureas in some of their receptors. This has led to significant improvements in anion binding constants.[23] For example, **42**, a urea-based analogue of *o*-phenylenediamine derived receptor **25**, binds carboxylates far more strongly than **25**. In 0.5% H_2O:DMSO-d_6, it was observed to bind acetate (K_a = 3,210M^{-1}), over benzoate (K_a = 1,330M^{-1}), and dihydrogen phosphate, (K_a = 732M^{-1}), by ^{1}H NMR titration. (Anions added as their TBA salts).

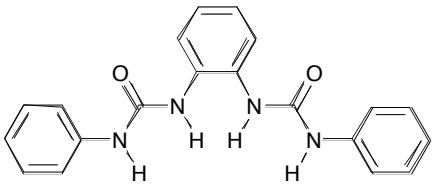

42

The group have obtained crystals of **42** complexed to benzoate by slow evaporation from acetonitrile, (Figure 1.12). The structure shows a total of four hydrogen bonds between the receptor and anion, with each carboxylate oxygen atom bound by the two NH protons of one urea moiety. This is similar to the binding mode proposed by Rebek and co-workers with reference to their work.[31]

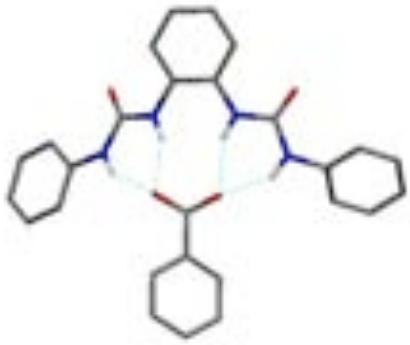

Fig 1.12 Crystal structure of benzoate complex of **42**.
(TBA groups and non-acidic protons omitted for clarity).

From the same paper, the group has also produced other versions of **42**, such as **43** and **44**, which incorporate electron withdrawing substituents.

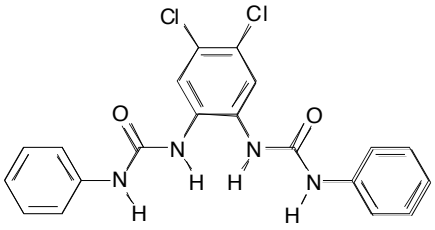

43

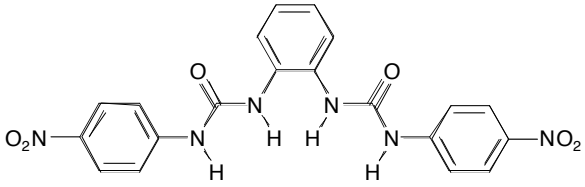

44

Both have higher oxo-anion binding affinities than **42** because of their electron withdrawing groups, which cause the urea NH protons to become more acidic. Receptor **43** binds acetate (K_a = 8,079M^{-1}), in preference over dihydrogen phosphate (K_a = 4,724M^{-1}), and benzoate, (K_a = 2,248M^{-1}). Receptor **44** binds acetate (K_a = 4,018M^{-1}), in preference over benzoate (K_a = 1,399M^{-1}), and dihydrogen phosphate, (K_a = 666M^{-1}) under the same titration conditions as used for **42**. One might expect **44** to be the better anion receptor, because nitro groups have a mesomeric effect whereas chlorides are only inductive, but the opposite is clearly true.

The authors believe that this is because **44** can freely rotate at the central benzene ring. This means that a significant proportion of **44** is not in the optimum *syn-syn* conformation in solution, and the receptor must rotate prior to binding. In receptor **43** however, the chloride groups activate the adjacent protons, causing intramolecular hydrogen bonds to form between these and the carbonyl oxygen atoms, (Figure 1.13). This causes a larger proportion of the receptor to adopt a syn-syn conformation, which enhances the binding strength of **43**, compared to both **44** and **42**.

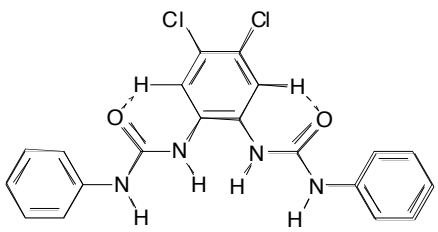

Fig 1.13 The *syn-syn* conformation of **43** is stabilised by enhanced intramolecular hydrogen bonding between the protons adjacent to the chloride substituents

As in the development of amide-based receptors, many bis-, tris- and tetra-ureas have been synthesised by appending urea groups to a wide range of organic scaffolds. Werner and Schneider have produced tris-ureas appended to tren, similar to the amides made by Reinhoudt and co-workers. A series of receptors, which incorporated **45**, was shown to be chloride selective in DMSO-d_6 (K_a = 1,979M^{-1}) relative to the larger halides. (Anions added as their TBA salts).[32] An energy minimised computer model of a similar receptor **46** complexed to chloride shows that the anion is bound using contributions from all six hydrogen bond donors, as intended.

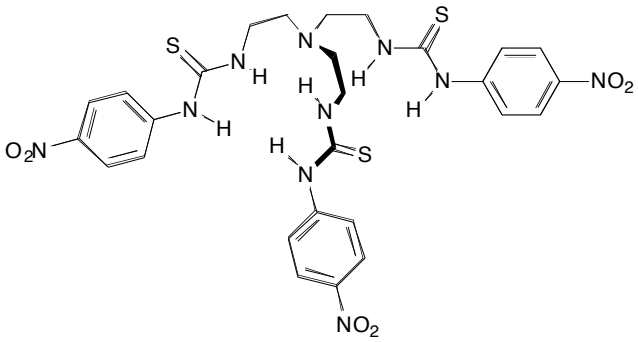

45

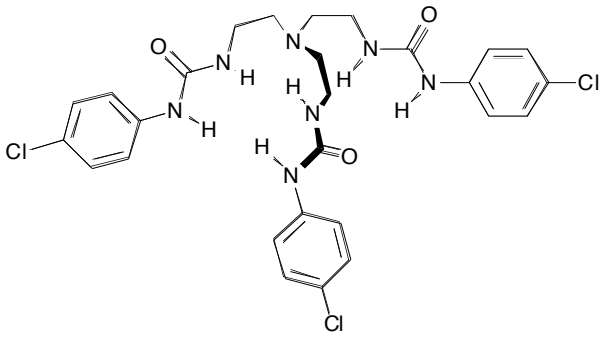

46

Tren based urea receptors such as these, have yielded some exceptional single crystal X-ray structures. In 2007, Ghosh and co-workers published a structure of a similar receptor, **47** bound to hydrogen-phosphate,[33] (Figure 1.14). It shows two dihydrogen phosphate anions bound in a phosphate dimer, with all eight oxygen atoms hydrogen bonded to the urea NH protons of two receptor molecules. The crystal structure also shows π-π stacking interactions between the two receptors, which aids the formation of this dimeric structure.

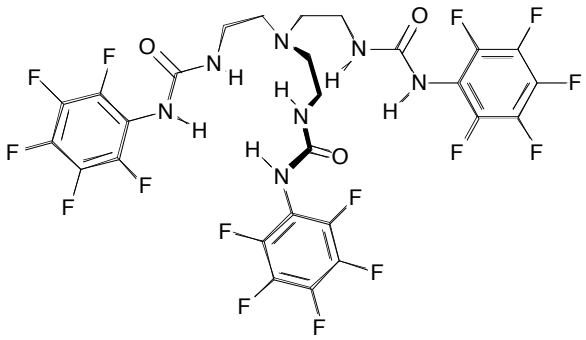

47

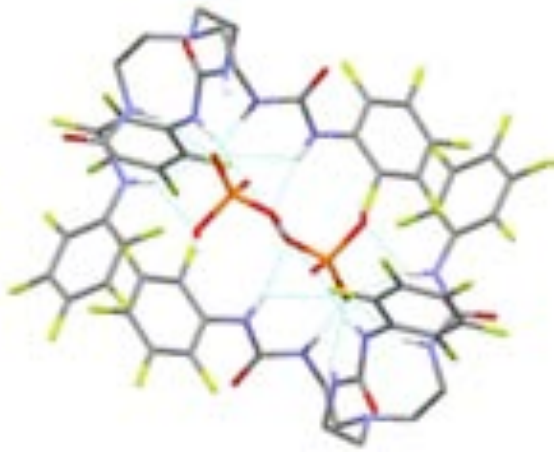

Fig 1.14 Hydrogen phosphate dimer complex of **47**
(Counter-cations and non-acidic protons omitted for clarity).

Similarly, Custelcean and co-workers have recently appended tren with pyridyl-urea groups to produce the sufate-selective receptor **48**.[34] In the solid state, a single sulfate anion is bound by twelve hydrogen bonds, from two receptor molecules, such that it is completely encapsulated, (Figure 1.15). Only a 1:1 interaction was evident in solution, a similar to the findings of Ghosh. These crystals were obtained from a solution containing other anions such as selenate in addition to sulfate. This work demonstrates that selective crystallisation can be a powerful tool for anion separation in situations where different anions are competing for a binding site.

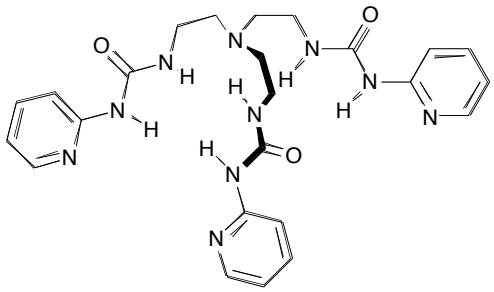

48

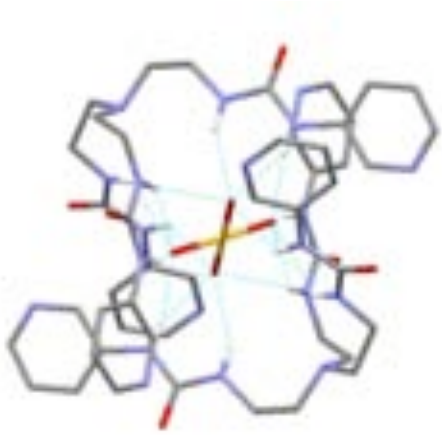

Fig 1.15 Crystal structure of sulfate complex of **48**
(Counter-cations and non-acidic protons omitted for clarity).

Tris-(thio)ureas have also been incorporated into macrocycles. Inspired by the work of Pascal, Anslyn and others, Tobe and co-workers developed the thiourea containing macro-tricycle, **49** which is similar to those of Pascal and Anslyn.

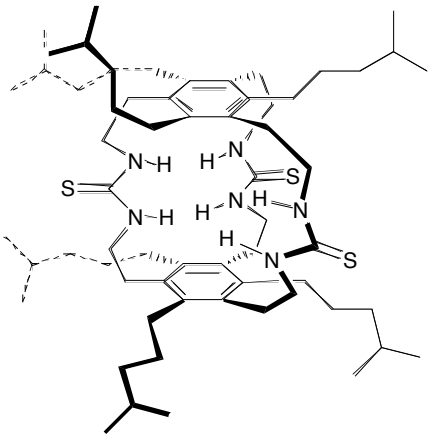

49

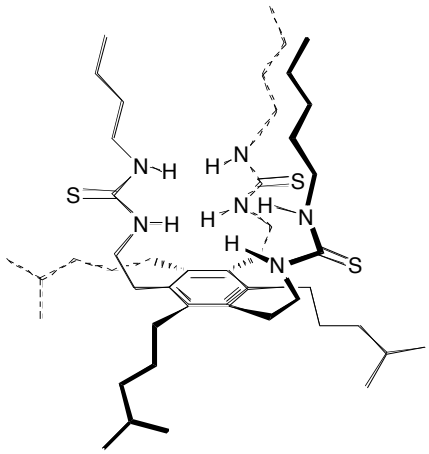

50

Receptor **49** has three urea hydrogen bond donor clefts attached at 1,3,5-trisubstituted benzene rings.[35] It was anticipated that this would bind anions more strongly than an acyclic analogue, **50** because of pre-organisation. Proton NMR titration experiments were conducted in $CDCl_2CDCl_2$ at 373K for both receptors with the TBA salts of acetate, chloride and fluoride, (Table 1.1).

	K_a **(49) / M^{-1}**	K_a **(50) / M^{-1}**
Acetate	116 (8)	3030 (11)
Chloride	112 (3)	3700 (12)
Fluoride	93 (11)	1770 (5)

Table 1.1 Binding constants (with associated % errors) for receptors **49** and **50** with various anions in $CDCl_2CDCl_2$ at 373K

The results show that the macrocycle, **49** is not as strong a receptor as its acyclic counter-part, **50**. This is because the three ureas are well positioned to form intramolecular hydrogen bonds to each other, around the outside of the receptor, which need to be broken in the event of anion complexation. This has a detrimental enthalpic effect and was described above with reference to the work of Bowman-James.

1.4.3 Amido-urea based anion receptors

Ureas are particularly potent anion receptors when appended with additional functional groups. Often, the additional groups used are amides because these are good hydrogen bond donors, which are synthetically accessible and relatively straightforward to derivitise.

Gale and co-workers have developed an array of carboxylate binding receptors by appending bis-phenyl urea with amides.[36] Receptors such as **52** (K_a (AcO^-) = 2,470M^{-1}), were shown to be far better carboxylate receptors than bis-phenyl urea itself **51**, (K_a = 1,260M^{-1}) in 0.5% H_2O:DMSO-d_6, (anions added as their TBA salts).[36b] The addition of the two amides to bisphenylurea has therefore increased the acetate binding constant by a factor of two, again demonstrating the cumulative strength of multiple hydrogen bonds.

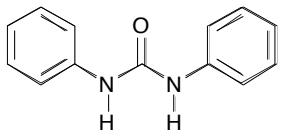

51

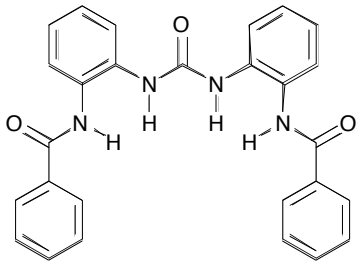

52

This work culminated in the synthesis of a macrocyclic amido-urea, **53**, which comprises the structure of **52**, macrocyclised by incorporation of a Crabtree-type 2,6-amido-substituted pyridine.[36c] Designed as a carboxylate receptor, it binds acetate strongly, (K_a =16,500M^{-1}), in 0.5% H_2O:DMSO-d_6, and was also shown to be selective for acetate in 5% H_2O:DMSO-d_6, (K_a = 5,170M^{-1}) over benzoate (K_a = 1,260M^{-1}) and dihydrogen phosphate, (K_a = 1,452M^{-1}).

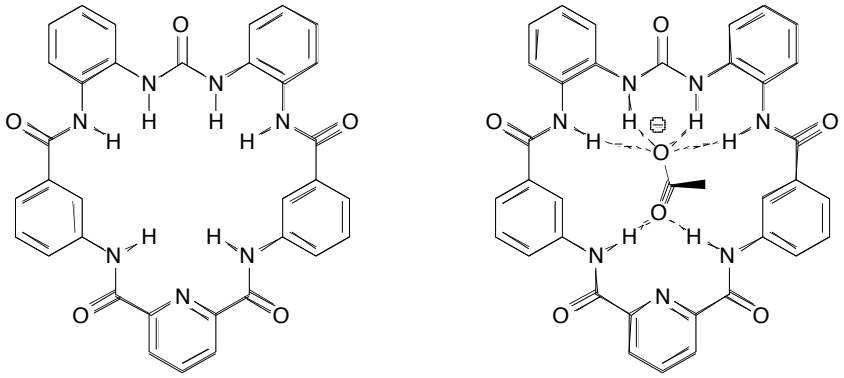

53 **Fig 1.16** Acetate complex of **53** - Solution

During the NMR titrations, the urea NH protons and lower amide protons were observed to undergo the largest chemical shift changes with carboxylates, indicating that these protons contribute the most to binding. The amides adjacent to the urea are not greatly involved in binding these anions in solution, leading the authors to conclude that a symmetrical complex is formed in solution, relative to the NMR timescale (Figure 1.16). In the solid state, this average structure is not seen. A crystal suitable for X-ray crystallography was obtained from slow evaporation of a DMSO solution of **53** and TBA acetate, which instead shows acetate bound asymmetrically by three amides, (Figure 1.17). The ureas are bound to a water molecule, from the wet DMSO. This highlights that differences in binding modes may be observed between the solution state and the solid state.

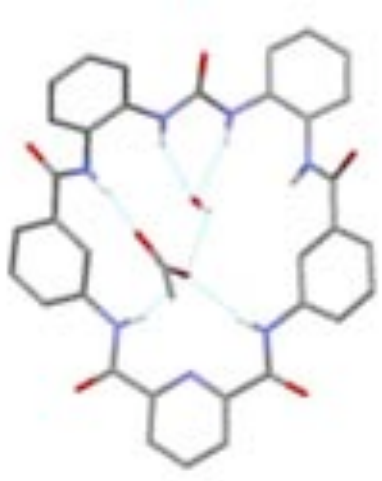

Fig 1.17 Crystal structure of acetate complex of **53**.
(TBA groups and non-acidic protons omitted for clarity).

The same authors have also presented work in which the 1,2 phenylenediamine derived bis-urea, **42**, has been appended by amides, producing receptors such as **54** and **55.**[37] It was anticipated that adding further hydrogen bond donors to this successful carboxylate receptor would produce even higher binding constants. Receptor **54** was studied for anion complexation using ^{1}H NMR titration techniques in 0.5%H_2O:DMSO-d_6. It bound acetate most strongly (K_a = 3,200M^{-1}), in preference over dihydrogen phosphate (K_a = 2,290M^{-1}), and benzoate, (K_a = 974M^{-1}). All anions were bound by this receptor in a 1:1 stoichiometry. Receptor **55**, a structural isomer of **54**, was observed to bind only chloride in a 1:1 stochiometry under the same conditions, (K_a = 17M^{-1}). The oxo-anions were bound in a 2:1 (guest:host) stoichiometry. In this case, benzoate (K_1 = 10,110M^{-1}, K_2 < 10M^{-1}), was bound preferentially over dihydrogen phosphate (K_1 = 7,780M^{-1}, K_2 = 24M^{-1}) and acetate, (K_1 = 6,100M^{-1}, K_2 < 10M^{-1}), (anions added as their TBA salts). The formation of 2:1 (guest:host) complexes is a result of a twist in the conformation of **55** at the central phenyl ring such that the two halves of the cleft diverge, providing two sites for anions.

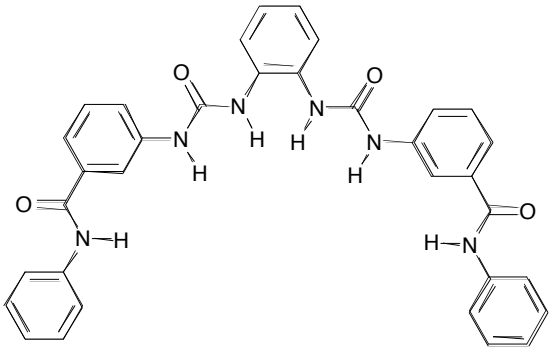

54

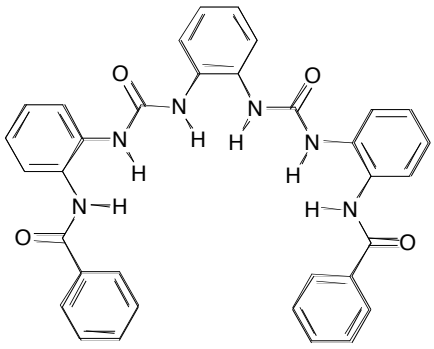

55

1.4.4 Anion receptors with heterocyclic hydrogen bonds

Whilst having the capability to form very strong hydrogen bond donors to anions, amides and ureas can also act as hydrogen bond acceptors with other receptor molecules through their carbonyl oxygen atoms. This means that in order to complex anions, they must often break bonds to the other receptors. This can represent a significant energy barrier, and so it is desirable to synthesise receptors, less able to act as hydrogen bond acceptors. To this end researchers have used various heterocyclic hydrogen bond donors, in increasingly sophisticated systems.

Pyrroles

Calixpyrrole, **56** has been known as a receptor since 1996,[38] despite itself dating back to 1886.[39] In seminal work carried out by Sessler and co-workers, the cleft of calixpyrrole was seen to orientate into a cone conformation upon the addition of chloride or fluoride in the solid state, (Figure 1.18). Using ^{1}H NMR titration techniques (CD_2Cl_2), it was shown that fluoride is bound more strongly than chloride, (K_a (F^-) = 17,000M^{-1}, K_a (Cl^-) = 350M^{-1}). (Anions added as their TBA salts).

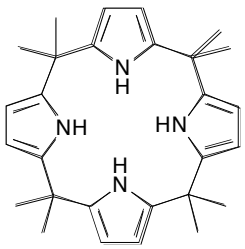

56

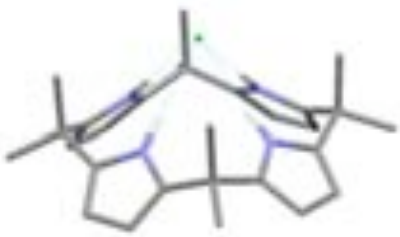

Fig 1.18 Crystal structure of chloride complex of **56**.
(Counter-cations and non-acidic protons omitted for clarity).

Pyrrole itself is a popular neutral hydrogen bond donor for anion complexation, and has been incorporated into acyclic anion receptors by Gale and co-workers.[23] Receptor **57** was shown to bind dihydrogen phosphate (K_a = 295M^{-1}) over acetate, (K_a = 251M^{-1}) and benzoate (K_a = 113M^{-1}), by ^{1}H NMR in 0.5%H_2O:DMSO-d_6, (anions added as their TBA salts).

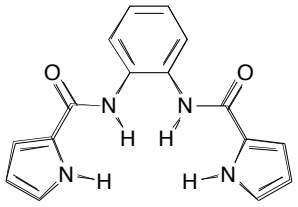

57

Sessler and co-workers have made many acyclic and macrocyclic receptors incorporating multiple pyrroles as well as amides. One particular example, **58** was seen to be highly selective for tetrahedral anions, with dihydrogen phosphate, (K_1 = 34,000M^{-1}, β_2 = 2,600M^{-1}) binding 2:1 (guest:host) and hydrogen sulfate (K_a = 64,000M^{-1}) by UV titration in acetonitrile.[40] (Anions added as their TBA salts).

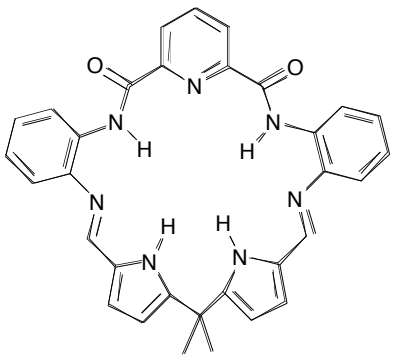

58

Subsequent computer modelling of **58** identified **59** as a receptor, which would not undergo 2:1 (guest:host) binding with dihydrogen phosphate. This receptor was duly synthesised and was found to be selective for hydrogen sulfate (K_a = 108,000M^{-1}), over dihydrogen phosphate (K_a = 29,000M^{-1}), and acetate (K_a = 12,600M^{-1}), by the same titration technique. This receptor was not able to twist into unfavourable conformations due to being sterically restricted by the bulky toluene group appended to the bispyrrolomethane.

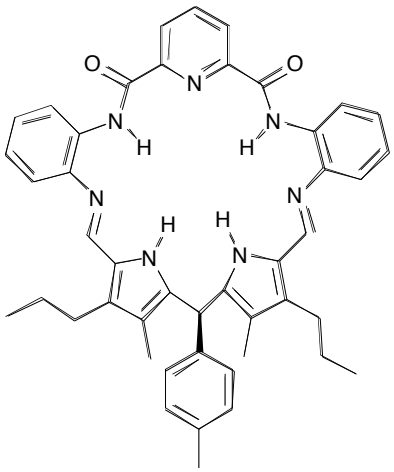

59

Katayev and co-workers have shown the anion binding properties of other pyrrole containing macrocycles, **60** and **61**, which also incorporate Crabtree-type bis-amide units and further secondary amides.[41]

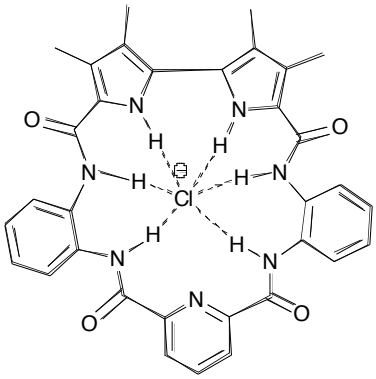

60 (bound to chloride)

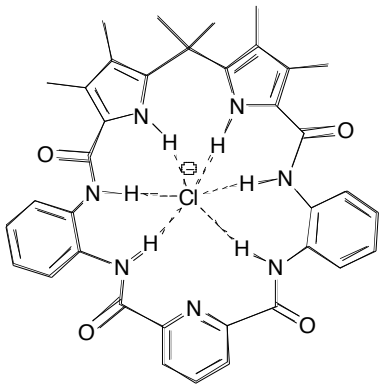

61 (bound to chloride)

Receptor **59** is selective for hydrogen sulfate (log K_a = 5.26), over benzoate (log K_a = 4.36), fluoride (log K_a = 4.63), chloride (log K_a = 4.37), and dihydrogen phosphate, (log K_a = 3.83). Receptor **60** is selective for benzoate (log K_a = 6.00), and dihydrogen phosphate, which is bound 2:1 (guest:host), (logK_1 = 5.24), (logβ_2 = 8.29).

Indoles, carbazoles and indolocarbazoles

Despite the widespread use of pyrrole, the use of these more acidic pyrrole analogues, such as those below, was not explored substantially until 2005.

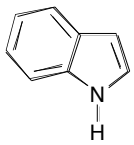

Indole

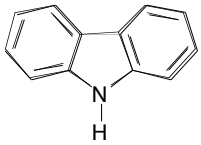

Carbazole

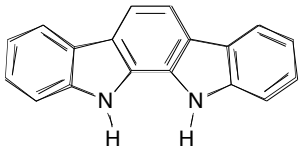

Indolocarbazole

Jeong and co-workers were the first to investigate these types of anion receptors, with macrocyclic structures such as **62**,[42] which contain two 1,10-disubstituted indolocarbazole groups linked by alkynes. This provides a small rigid binding cleft comprising four indolocarbazole NH protons. It was studied for anion complexation properties with various TBA salts by UV-vis titration in MeCN. Receptor **62** binds fluoride (K_a = 200,000,000M^{-1}), over acetate (K_a = 5,900,000M^{-1}), dihydrogen phosphate, (K_a = 2,100,000M^{-1}), chloride (K_a = 1,500,000M^{-1}), azide (K_a = 88,000M^{-1}), hydrogen sulfate (K_a = 65,000M^{-1}), and cyanide (K_a = 65,000M^{-1}), when these are added as their TBA salts. The value for fluoride was obtained using competition assays with chloride in MeCN.

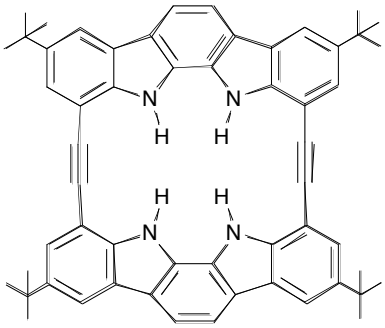

62

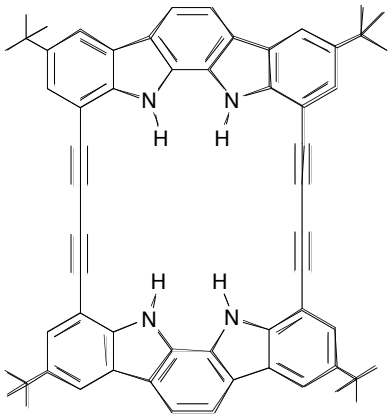

63

Receptor **62** has subsequently been extended producing **63**, which is of an optimum geometry to accommodate azide.[43] Receptor **63** is not selective for azide (it binds benzoate (K_a = 170,000M^{-1}) and dihydrogen phosphate (K_a = 220,000M^{-1}), but it was shown to bind azide in 10% MeOH:Acetone (K_a = 81,000M^{-1}), by UV-visible spectroscopy. This is roughly 35 times stronger than it is bound by **62** under identical conditions, (K_a = 2,300M^{-1}), (added as its TBA salt). Crystal structures of receptors **62** and **63** bound to azide were obtained, (Figure 1.19), which show different binding modes. Receptor **62** binds to azide only at one end, because it cannot be accommodated length-ways by the receptor. With receptor **63**, azide is bound between the two ends in the plane of the receptor.

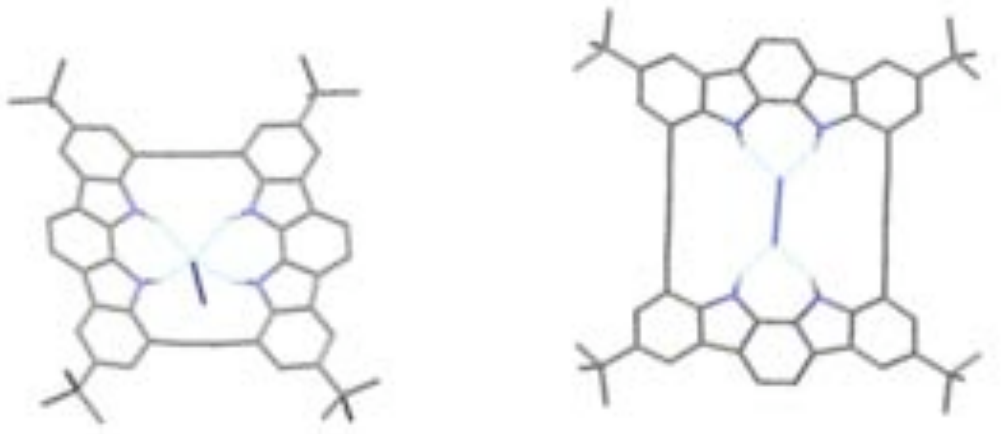

Fig 1.19 Crystal structures of azide complexes of **62** and **63**
(Counter-cations and non-acidic protons omitted for clarity).

The group has since appended this type of structure with amides and urea to give structures such as **64** and **65,**[44] which has given indole-containing receptors with clefts similar to the bis-ureas of Rebek.

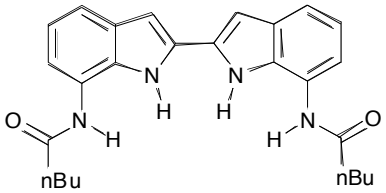

64

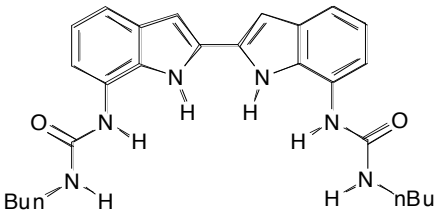

65

They found good selectivity for oxo-anions, specifically pyrophosphate, ($P_2O_7^{2-}$), which was bound by **65** (K_a > 5,000,000M^{-1}) as determined by UV titration in DMSO:0.1-0.2% H_2O, (anion added as its TBA salt). A proposed solution-state complex is presented, (Figure 1.20). The exceptionally high binding strength was attributed to the high number of strong hydrogen bond donors in receptor **65** and good shape complimentary with pyrophosphate. In contrast, receptor **64** bound this anion less strongly by a factor of ten.

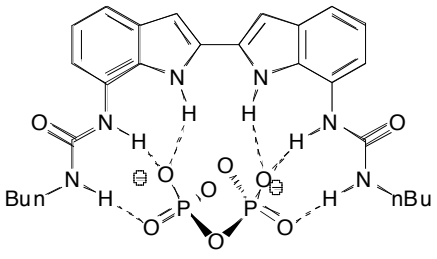

Fig 1.20 Pyrophosphate complex of **65**

The same group has also appended indolocarbazole with hydroxyl groups to produce receptor **66**.[45] This was found to be exceptionally selective for acetate (K_a = 1,100,000M^{-1}) over dihydrogen phosphate, (K_a = 29,000M^{-1}) as determined by ^1H NMR titration techniques in 1%H_2O:CD_3CN, (anions added as their TBA salts). This is presumably due to steric restrictions due to the bulky groups at the other end of the alkynes, which restrict the binding of the larger dihydrogen phosphate anion.

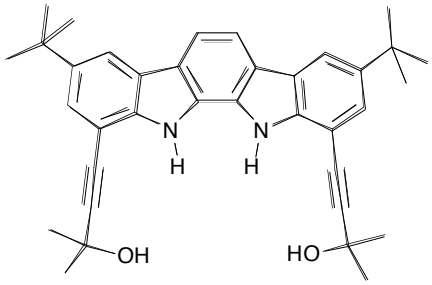

66

Beer and co-workers have demonstrated the effects of appending electron withdrawing groups and electron donating groups to the indolocarbazole scaffold. The group studied receptors **67** and **68**, observing the strongest binding with **68**, presumably due to the electron withdrawing effect of the bromide substituents.[46] Receptor **68** was shown to bind benzoate most strongly (log K_a = 5.90), over fluoride (log K_a = 5.00), and chloride (log K_a = 4.90) by UV titration in acetone, (anions added as their TBA salts). This trend was also observed for **67**, (log K_a ($C_6H_6CO_2^-$) = 5.90), (log K_a (F^-) = 4.70), (log K_a (Cl^-) = 4.10), and indolocarbazole, (log K_a ($C_6H_6CO_2^-$) = 5.30), (log K_a (F^-) = 4.70), (log K_a (Cl^-) = 4.50).

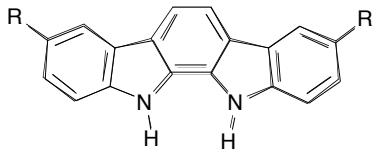

67 (R = Me) **68** (R = Br)

At the same time as Jeongs initial work on indolocarbazoles, Jurczak and co-workers first used carbazole as a scaffold for anion receptors.[47] They described 1,8-diamino-3,6-dichlorocarbazole derived receptors **69** and **70**. Somewhat surprisingly, receptor **70** is selective for benzoate, (K_a = 8,340M^{-1}) over other anions, as determined by ^{1}H NMR titration in 0.5%H_2O:DMSO-d_6, (anions added as their TBA salts.) One may have expected this tightly convergent receptor to be selective for halides. The authors conclude that the high binding constants observed across the series of anions are due to increased rigidity from the carbazole scaffold, which assists in pre-organisation, and from having the strongly acidic carbazole NH hydrogen bond, which is activated by the electron withdrawing chloride substituents.

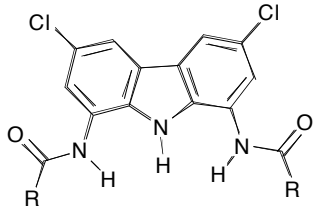

69 (R = Ph) **70** (R = Pr)

The group obtained crystals of the chloride complex of **69** by diffusion of Et_2O into a DCM solution of **69** and TBA chloride, (Figure 1.21). The structure obtained shows four hydrogen bonds between chloride and the receptor, from the three NH hydrogen bond donors and one CH hydrogen bond donor on one of the phenyl substituents. The shortest hydrogen bond is that between the chloride and the carbazole, showing that this bond is the most significant hydrogen bond in the interaction with chloride, and presumably with other anions. It may be that benzoate is able to bind to two CH protons from both of the appended phenyl rings, which gives rise to its surprisingly high binding affinity for this receptor.

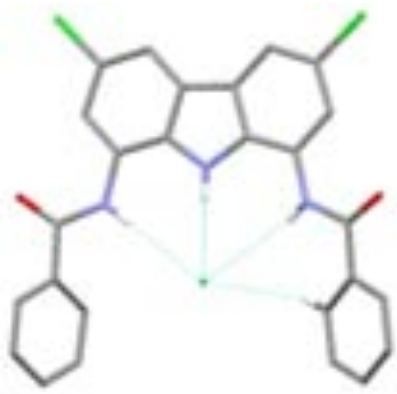

Fig 1.21 Chloride complex of **69**. (Counter-cations and non-acidic protons omitted for clarity).

The first use of indoles in anion recognition, can be attributed to Pfeffer and co-workers in 2007.[48] They connected an indole (appended at the 7 position), to amide and urea groups with different length alkyl chains, producing a series of receptors **71** - **73**.

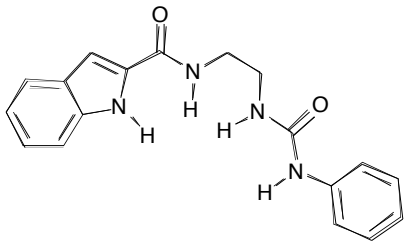

71

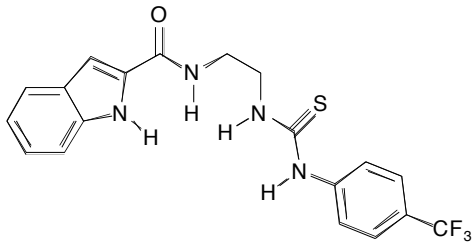

72

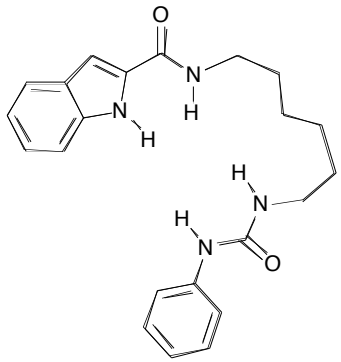

73

These bound dihydrogen phosphate acetate and chloride in a 1:1 stoichiometry with hydrogen bonding contributions from all of the hydrogen bond donors. Generally the three receptors exhibit similar strength binding to acetate (log ß (**71**) = 3.1, log ß (**72**) = 2.8, log ß (**73** = 3.9) and dihydrogen phosphate (log ß (**73**) = 3.5, log ß (**72**) = 3.5, log ß (**71**) = 3.4), which are bound significantly more strongly than chloride (log ß (**72**) = 2.1, log ß (**73**) = 2.2.), as determined by ^{1}H NMR titration in DMSO-d_6. (Anions added as their TBA salts). Oxo-anions are bound most strongly. Dihydrogen phosphate is bound slightly more strongly than acetate overall. It is thought that the short alkyl linkers in receptors **71** and **72** restrict binding to acetate because they cannot form convergent clefts. Where the alkyl linker is significantly extended, **73**, there is increased freedom to produce an optimal binding site.

More recently, Gale and co-workers have produced receptors in which 2-amido-indole is appended to established anion receptor cores.[49] They showed that replacing the phenyl group of Crabtree receptor **19** with an indole to give **74**, increases the affinity for some anions by up to a factor of ten in 0.5% H_2O:DMSO-d_6. Under these conditions, receptor **74** binds to dihydrogen phosphate with K_a ($H_2PO_4^{2-}$) = 1,250M^{-1}, (compared to K_a = 10 M^{-1} for receptor **19**).[49] The increase in binding affinity is due to the two additional hydrogen bond donors. Compound **74** is selective for dihydrogen phosphate over acetate (K_a = 880M^{-1}), benzoate (K_a = 120M^{-1}) and chloride (K_a = 17M^{-1}). (Anions added as their TBA salts).

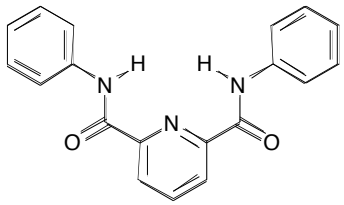

19

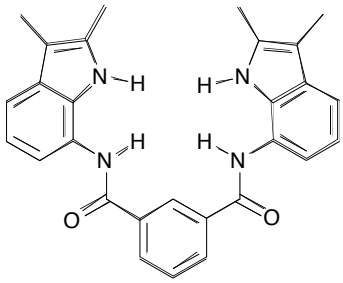

74

The group obtained crystals suitable for single crystal X-ray diffraction of **74** bound to chloride and **74** bound to fluoride. With chloride, the receptor was bound in a 1:1 stoichiometry, with the anion sitting above the plane of the receptor, (Figure 1.22).

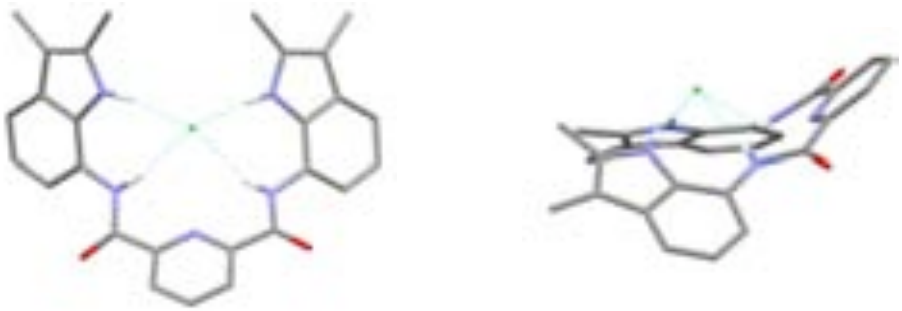

Fig 1.22 Views of the crystal structure of the chloride complex of **74**

With fluoride, the receptor was bound also bound in a 1:1 stoichiometry, but the receptor was twisted around the anion in a helix, (Figure 1.23). It is clearly the different sizes of the two anions, which causes this striking difference. Fluoride is a small anion, and as such can be wrapped up inside the receptor, whereas chloride is too large for this binding mode, and instead is bound on one side of the receptor, which bends towards the anion.

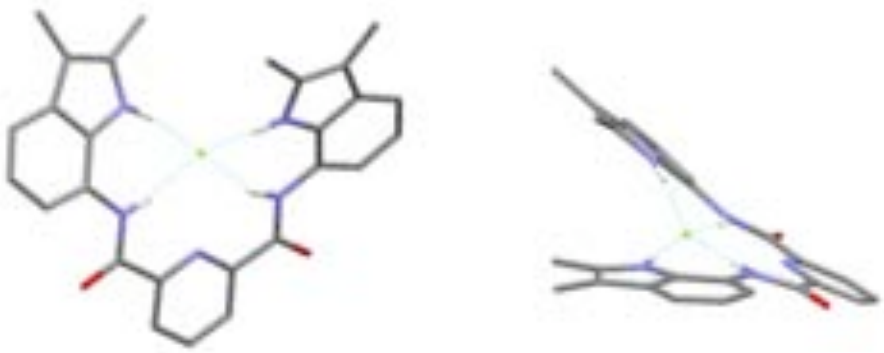

Fig 1.23 Views of the crystal structure of the fluoride complex of **74**

Both crystal structures show that receptor **74** is capable of significant twisting. The combination of this twisting ability and opposing hydrogen bond donors may explain why it is selective for dihydrogen phosphate.

Under identical NMR titration conditions to those used by Gale and co-workers, Jurczak and co-workers found the same anion preferences with a similar receptor, **75**. It incorporates two indole groups appended with amides to a 1,3-disubstituted azulene scaffold, (K_a ($H_2PO_4^-$) = 2,300M^{-1}, K_a ($C_6H_5CO_2^-$) = 544M^{-1}, K_a (Cl^-) = 50M^{-1}).[50] This showed marginally better anion binding than the receptors of Gale and co-workers, which is likely to be due, not to the change in the central scaffold, but to the removal of the methyl groups from the two indoles moieties . The anion binding properties of receptors with non-substituted indoles like these have subsequently been shown to be slightly superior to methylated ones.[50] This effect is presumably due to the electron donating effect of the methyl substituents

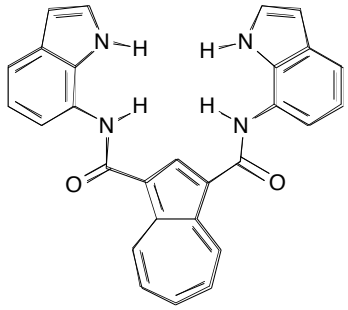

75

Recently, Caltagirone and co-workers have produced receptors in which indoles are appended to bipyridine.[51] Receptor **76** and **77**, (a platinum complex of **76)**, were shown to bind dihydrogen phosphate (K_a (**76**) = 90M^{-1}, K_a (**77**) = 3,644M^{-1}), more strongly than benzoate (K_a (**76**) = 35M^{-1}, K_a (**77**) = 280M^{-1}), and acetate (K_a (**76**) = 58M^{-1}, K_a (**77**) = 189M^{-1}), using ^{1}H NMR titration techniques in 0.5% H_2O: DMSO-d_6, (anions added as their TBA salts.) Receptor **77** is a vastly superior receptor in the case of each anion, especially with dihydrogen phosphate, which is bound over 40 times more strongly than by **76**. The stark differences between the two receptors are due to the conformational restriction of the binding cleft in **77** due to the metal centre. Receptor **77** has a fixed conformation, **76** does not.

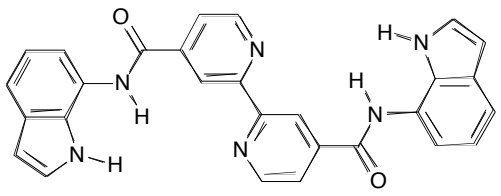

76

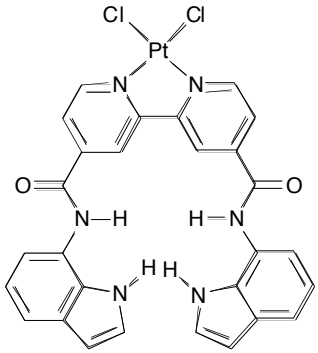

77

The group has obtained crystal structures of **76** bound to acetate in a 2:1 (guest:host) stoichiometry. The structure shows the receptor twisted about the central pyridine-pyridine bond, such that it forms a divergent conformation. This shows that the receptor is flexible in the solution state. Indeed, when fitting the titration data, the authors found that neither a 1:1 or 1:2 binding model provided a proper fit for the interaction between **76** and acetate, and concluded that in this case, a mixture of binding conformations had been observed.

In 2008, Gale and co-workers published work on diindolylurea receptors, such as **78**, in which two methyl-appended indoles were linked at the 7-position by a urea.[52] It was found to be an exceptionally strong receptor for dihydrogen phosphate in 0.5% H_2O:DMSO-d_6, (K_a > 10,000M^{-1}) and was also observed to bind this anion well in 10% H_2O:DMSO-d_6 (K_a = 4,790M^{-1}). Also strongly bound in 0.5% H_2O:DMSO-d_6 were acetate (K_a > 10,000M^{-1}), and benzoate (K_a > 10,000M^{-1}). In 10% H_2O : DMSO-d_6, (K_a ($CH_3CO_2^-$) = 736M^{-1}, K_a ($C_6H_5CO_2^-$) = 567M^{-1}, they were bound to a lesser extent than dihydrogen phosphate, (anions added as their TBA salts). This combination of extremely selective and strong anion binding is a remarkable result. (Anions added as their TBA salts).

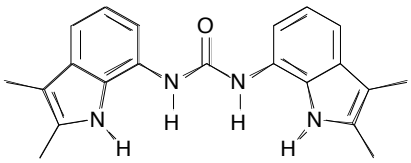

78

The group have obtained a single crystal structure of **78**, bound to phosphate, which is formed by a double deprotonation of dihydrogen phosphate, during crystallisation from a solution of **78** and TBA dihydrogen phosphate in DMSO, (Figure 1.24). The crystal shows three molecules of **78** bound around one phosphate anion, held by a total of six hydrogen bonds.

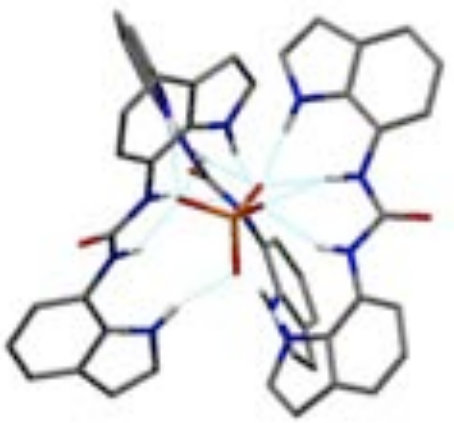

Fig 1.24 Crystal structure of the 3:1, (host:phosphate), complex of **78**.
(TBA groups and non-acidic protons omitted for clarity).

Single crystals were also obtained from a mixture of **78** and TEA hydrogen carbonate, also by evaporation from DMSO-d_6, (Figure 1.25). When resolved, these showed two receptor molecules bound to a central carbonate anion, it too having been deprotonated in solution.

Fig 1.25 Crystal structure of the 3:1, (host:phosphate), complex of **78**.
(TBA groups and non-acidic protons omitted for clarity).

The group have also produced similar biscarbazole and mixed indole-carbazole systems based on **78**,[53] and have appended amides to produce receptors **79 - 82.**[54]

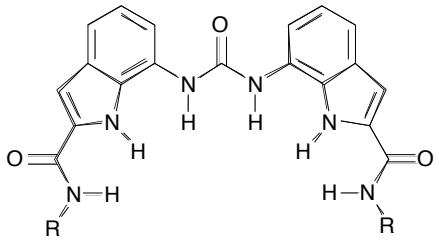

79 (R = Ph)
80 (R = ^{n}Bu)
81 (R = 2-pyridyl)
82 (R = CH_2-C_6H_5)

Receptors **79** –**82** are selective for oxo-anions in 10% H_2O:DMSO-d_6 by ^1H NMR titration. Of these, **80** is the most selective. It binds acetate (K_a = 1,422M^{-1}), over benzoate (K_a = 481M^{-1}). (Anions added as their TBA salts.) Despite it being clear from chemical shift changes that dihydrogen phosphate was also strongly bound by **80**, it was not possible to fit the titration data for this anion to either a 1:1 or 2:1 binding model. The origin of this behaviour was found to be due to anion-to-anion proton transfer between bound and unbound dihydrogen phosphate. When further dihydrogen phosphate was added to a 1:1 mixture of **80** and dihydrogen phosphate, the bound dihydrogen phosphate was deprotonated by the additional dihydrogen phosphate to leave phosphoric acid in solution, and hydrogen phosphate bound to **80**. The authors assert that this type of process may happen with other neutral oxo-anion receptors, and that this may be hard to detect by normal NMR titration. This type of process, for example, may explain the formation of the crystal structures seen with **78**, (Figure 1.24 and Figure 1.25).

1.5 AIMS OF THIS THESIS

The examples discussed in the introductory chapter are provided to give an overview of the area of anion complexation, highlighting recent advances in the binding of common anionic species in the solution and solid state. As this area of chemistry develops it is becoming ever broader, targeting new and existing guests with increasingly sophisticated and complex systems.

This thesis discusses the synthesis, characterisation and anion recognition properties of simple acyclic hydrogen bond receptors for anions and has been divided into three sections.

- Investigations into novel methods of carbon dioxide fixation using combinations of covalent and hydrogen bond formation. These include using existing monotopic receptors and a novel ditopic receptor.
- The synthesis, characterisation and anion binding studies, of a series of simple bis-ureas with central Schiff-base moieties. The synthesis, characterisation and studies of colorimetric response to anions, of metal complexes derived from one of the aforementioned receptors.
- The synthesis, characterisation and anion binding studies, of a series of isophthalamide derivatives featuring activated CH protons, emphasising the role of the activated CH protons.

CHAPTER 2 - CARBON DIOXIDE FIXATION USING COVALENT AND HYDROGEN BOND FORMATION

2.1 INTRODUCTION

2.1.1 Carbon dioxide in the atmosphere

The emission of carbon dioxide, (CO_2), a greenhouse gas, has increased substantially in the recent past due to increased fossil fuel consumption.[55] This has caused concentrations of CO_2 to rise from 315ppmv to 385ppmv since reliable measurements began at Mauna Loa in Hawaii in 1958.[56] During the same period, the average global temperature has increased by around 0.50ºC.[57] The rate of warming is predicted to accelerate in the future, and is anticipated to cause widespread detrimental effects to the climate.[57]

The perceived threats of climate change have prompted research in several areas. Firstly, alternative energy sources, such as hydroelectric, solar, wind, nuclear, wave and tidal are now firmly established. These sources accounted for around 24% of

global electricity generation in 2008.[58] Carbon sequestration and capture is also currently in extensive development. This involves permanent storage of CO_2 underground after it is produced, such that it cannot get into the atmosphere. It is estimated to have the potential to drastically reduce CO_2 emissions from conventional power stations.[59] A third area of significant interest is the chemical fixation of CO_2. Work has been conducted in this area with a view to storage and transportation of CO_2 and the incorporation of waste CO_2 into other processes, such as the synthesis of bulk and fine chemicals, as described below.

2.1.2 Carbon dioxide fixation by covalent bond formation

There are many facile, covalent bond forming reactions between CO_2 and small molecules, which are rapid, reversible and quantitative.

Primary Amines

When primary amines are exposed to CO_2, for example, they convert rapidly to alkylammonium-alkylcarbamate, (AAAC) salts.[60] Weiss and co-workers have shown using proton NMR that the two species are indistinguishable on the NMR timescale.[61] This is because the two components of the salt exchange a proton and CO_2 rapidly. The two components of the salt are therefore in close association, due to electrostatic interactions. The process may be reversed by moderate temperature elevation. Industrial processes commonly use alkanolamines such as monoethanolamine, diethanolamine, diisopropanolamine, 2-amino-2-methyl-1-propanol because these are easily processed in an industrial applications,[62] but the reaction proceeds with any primary or secondary alkylamine, (Figure 2.1).

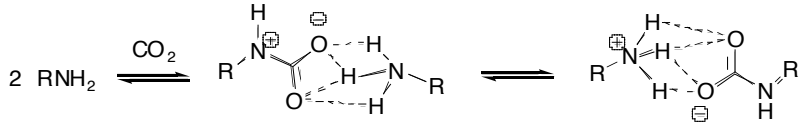

Fig 2.1 Reaction between amine and CO_2

This interaction has subsequently been used in a variety of supramolecular systems by Rudkevich and co-workers. In 2002, they proposed a fluorescent carbon dioxide detection system using the fluorescent amine, 1-methylaminopyrene, **83**.[63]

83

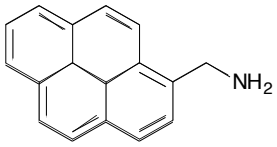

In the absence of carbon dioxide, the pyrene groups do not fluoresce because the intramolecular nitrogen lone-pairs quench the photo-induced electron transfer fluorescence emission of the pyrenes.[64] After bubbling CO_2 through the DMSO solution, AAAC salts are formed, (Figure 2.2). The formation of the AAAC salt is accompanied by increased fluorescence, because the nitrogen lone pairs are involved in covalent interactions with either the CO_2 or the proton, and can no longer quench this emission.

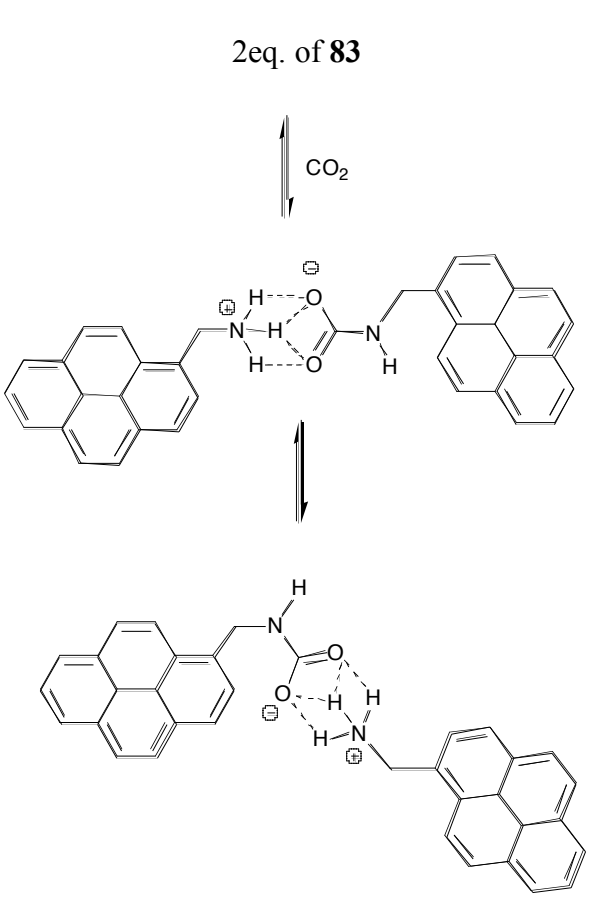

Fig 2.2 Two equivalents of **83** form an AAAC salt upon reaction with CO_2

In 2004, the same group published details of amine and urea-appended calixarenes, such as **84**.[65] When dissolved in organic solvents, the ureas hydrogen-bond to those in adjacent molecules, forming dimers. Upon addition of carbon dioxide, the dimers aggregate due to AAAC salt interactions, forming supramolecular polymers.

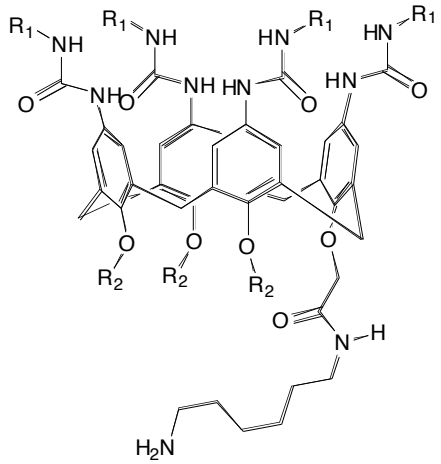

84

This work has since been extended into a novel separation technique. Compound **85** can bind sodium inside a modified calixarene cavity by electrostatic interactions from its eight oxygen atoms.[66] Upon addition of carbon dioxide to form a polymer, AAAC salt bridges are again formed, with the sodium incorporated into the polymer matrix as it precipitates. This enables sodium to be separated from solution and other cations in the bulk, (Figure 2.3).

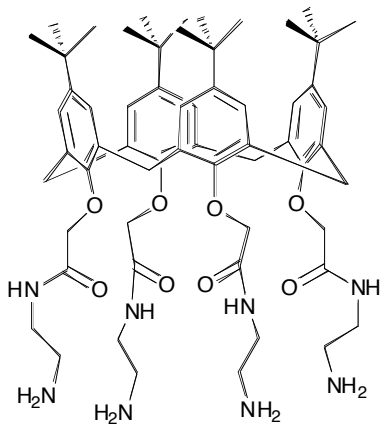

85

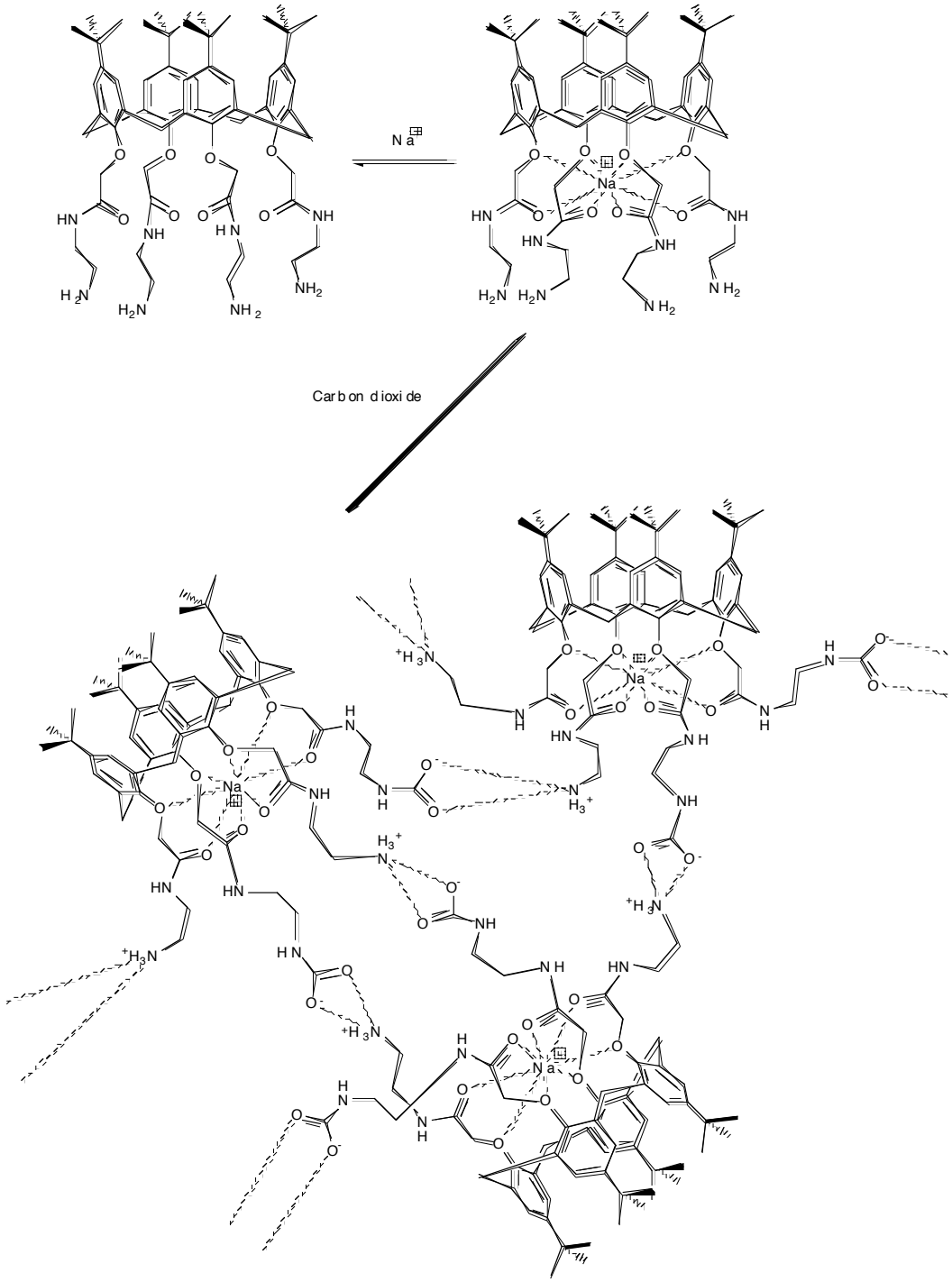

Fig 2.3 Receptor **85** removes sodium from solution using AAAC salt formation

Further separation systems have been developed[67] and the group has produced work, in which lysine groups are made into AAAC salts, giving novel supramolecular materials.[68]

Amidines

When amidines are exposed to CO_2 they form adducts. As in the reaction with amines, moderate temperature elevation reverses the process. Amidines are generally less reactive with carbon dioxide than amines, but some cyclic amidines, such as 1,8-diazabicyclo[5.4.0]undec-7-ene (DBU), and N-methyl-1,4,5,6-tetrahydropyrimidine (M-THP), are as rapid,[69-70] (Figure 2.4). M-THP converts to 100% adduct after 1h under an atmosphere of CO_2. Bubbling CO_2 through a solution of either amidine causes this conversion to be almost instantaneous.

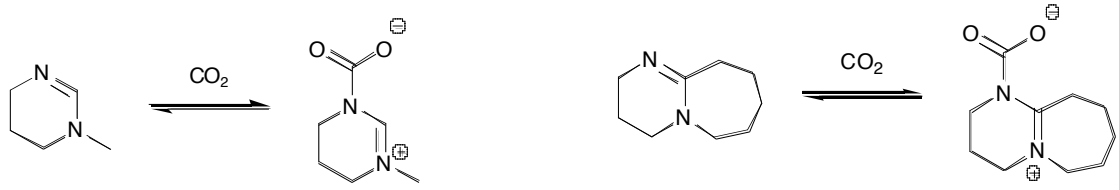

M-THP **M-THP-CO_2** **DBU** **DBU-CO_2**

Fig 2.4 Example reactions between cyclic amidines and carbon dioxide

In order to improve the handling of M-THP, Endo and co-workers attached it to a polystyrene backbone, which was made into a thin film.[71] Under a flow of carbon dioxide the film was observed to be around 25% efficient compared to M-THP, presumably due to the difficulty of diffusing carbon dioxide through the film. The process maintained its reproducibility however, with no significant degradation of the system.

The carbon dioxide chemistry of amidines is not limited to forming simple adducts. Jessop and co-workers combined 1eq. DBU with 1eq. alcohol,[72] a mixture which upon exposure to carbon dioxide, produces the corresponding carbonate and $DBUH^+$, (Figure 2.5). With an appropriate choice of alcohol, the mixture can be transformed from a liquid as non-polar as chloroform to one as polar as DMF. The authors postulate that solvent systems in which the polarity can be readily changed just by the addition of a gas, may find use in novel separation or precipitation techniques.

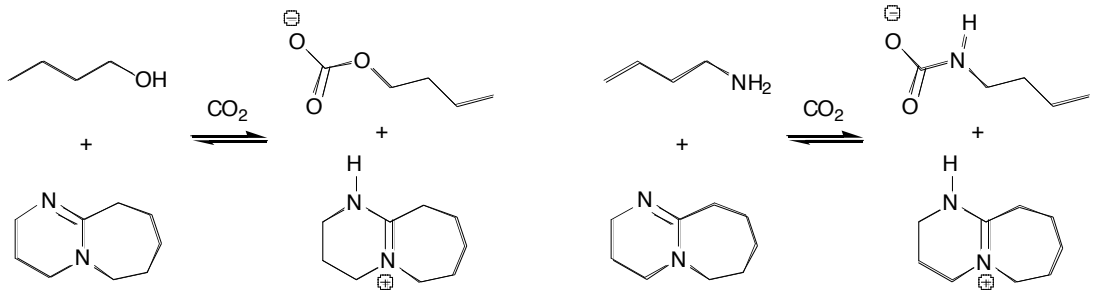

Fig 2.5 Example reactions of DBU and alcohol / amine and CO_2

In a similar reaction, DBU has been combined in a 1:1 mixture with amines. After exposure to CO_2 the resultant mixture consists of $DBUH^+$ and the corresponding carbamate,[73] (Figure 2.5). It has also been shown that under an atmosphere of carbon dioxide, DBU can catalyse the reaction of CO_2 with simple alkynes to produce pharmaceutically relevant intermediates,[74] highlighting the uses of CO_2 fixation agents in fine chemical synthesis.

Carbenes

Heterocyclic carbenes, such as that contained in compound **86** are also able to reversibly bind and release CO_2 by a covalent reaction,[75] (Figure 2.6). The product of this reaction is similar to THP-CO_2 or M-THP-CO_2 in that it is a neutral adduct. FTIR shows that compound **86** is quantitatively converted to its adduct after 10 minutes exposure to CO_2 at 20ºC. The process can be reversed by heating at 100ºC in the absence of CO_2 for 30 minutes.

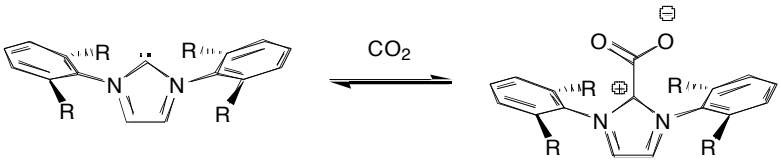

86

Fig 2.6 Compound **86** and its reaction with CO_2.

In 2009, Rosi and co-workers showed that this effect was also possible within an expanded structure, a zinc-adeninate.[76] The structure is held together with hydrogen bonds, with two of the nitrogen atoms of an adenine bound to a zinc centre, (Figure 2.7). This enables activation of the carbon between these two atoms and enables binding of carbon dioxide.

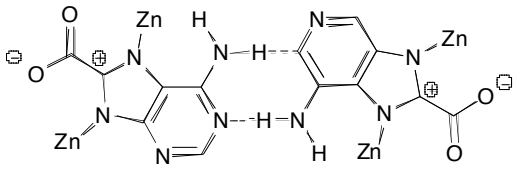

Fig 2.7 Sub-unit of a zinc-adeninate complex after reaction with CO_2.

2.1.3 Carbon dioxide fixation by hydrogen bond formation

Carbon dioxide

Hydrogen bonds were first used as a method of carbon dioxide fixation by Leigh and co-workers in 1996.[77] They adapted a benzoquinone macrocycle, previously prepared by Hunter,[78] in an attempt to form macrocycle **87**. Initially, this synthesis produced [2]-catenane **88** in high yield via a self-templation mechanism,[79] but compound **87** was subsequently synthesised by a different route.[77]

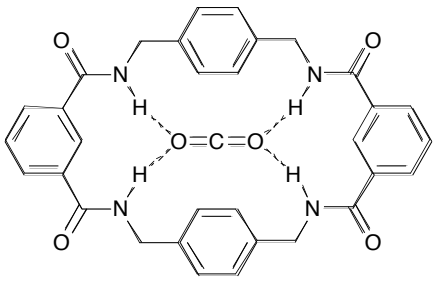

87

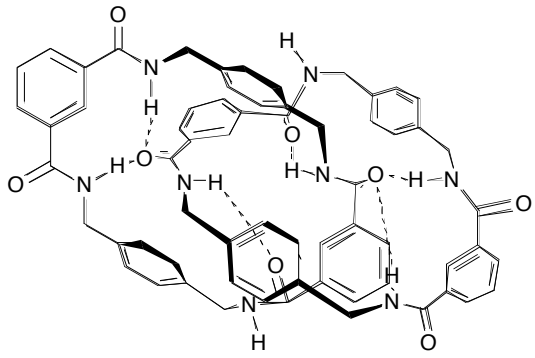

88

When exposed to a CO_2 atmosphere, a crystal coated with a thin layer of macrocycle **87** was observed to oscillate at a lower frequency, an effect indicative of mass gain. This result is not observed with other gases and remains the only example of hydrogen bonding between a synthetic receptor and non-activated CO_2.

Activated carbon dioxide

Generally, the hydrogen bonding of activated CO_2, as carbonate or hydrogen carbonate, is more easily attained than the fixation of un-activated carbon dioxide. This is because activated CO_2 species are anionic, making them far more likely to form favourable hydrogen bonding interactions with hydrogen bond donors than neutral CO_2. One method to convert CO_2 into carbonate is the use of salt hydrates. This process involves partially hydrated basic salts such as TBA fluoride. The pK_a of the water molecules in the salt hydrate, is lowered by the close proximity of fluoride, enabling it to act as a nucleophile towards CO_2, forming hydrogen carbonate. Further deprotonation by a second fluoride may then occur to provide carbonate and HF_2^-.[80]

It has been shown by Gale and co-workers that it is possible to hydrogen bond the carbonate anion formed by this process. In 2006 they reported a macrocyclic amido-urea, **53**, discussed earlier with relevance to carboxylate complexation, (Chapter 1.4.3).[81]

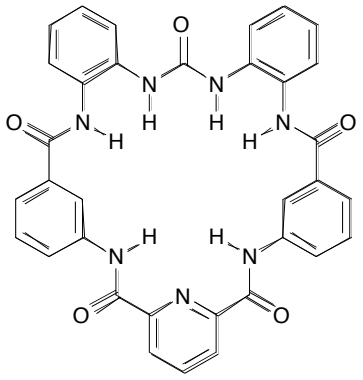

53

During an attempted crystallisation of the TBA fluoride complex of **53**, crystals were obtained suitable for X-ray crystallography. Upon resolution of the structure, it was observed that instead of being bound to fluoride, **53** was bound to carbonate which

had been fixed from CO_2 by the salt hydrate mechanism. In the solid-state structure of the mixed carbonate / fluoride salt, the carbonate is accommodated by six hydrogen bond donors, which provide an almost perfect geometric match, (Figure 2.8). The fluoride anions are exterior to **53**.

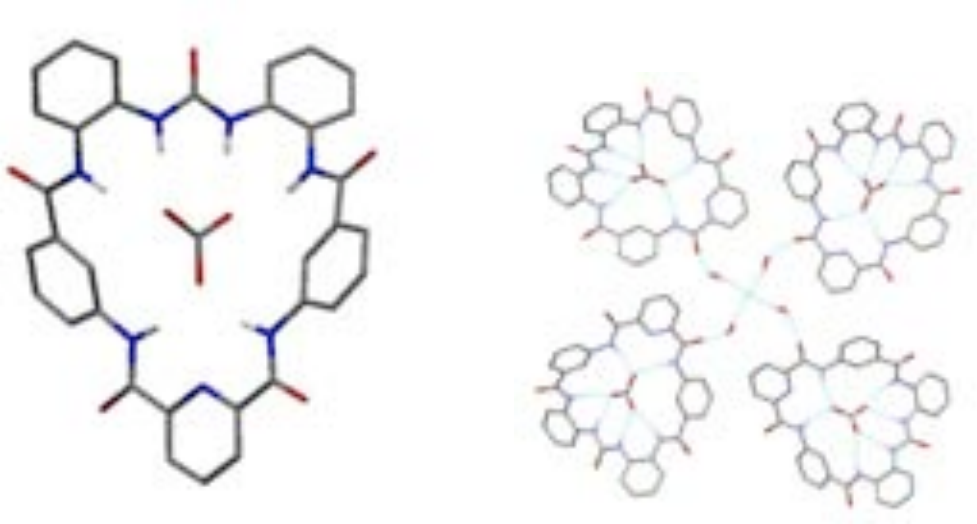

Fig 2.8 Views of crystal structure of mixed carbonate / fluoride complex of **53**. (Non-acidic protons and TBA groups omitted for clarity).

This system has since been modelled by Tossell, who calculated the binding constant between the macrocycle and carbonate to be several orders of magnitude greater than the binding constant between the macrocycle and chloride.[82]

Gunnlaugsson and co-workers have described a salt-hydrate type system in which a different result is observed. The amido-naphthalimide, **89**, deprotonates upon addition of TBA fluoride in DMSO solution, undergoing a stark colour change from green to red.[83] Over time exposed to air, the colour of the solution reverts to green, suggesting that the receptor is protonated once again.

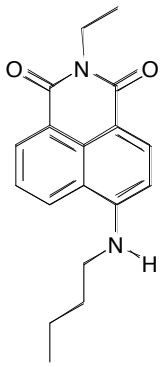

89

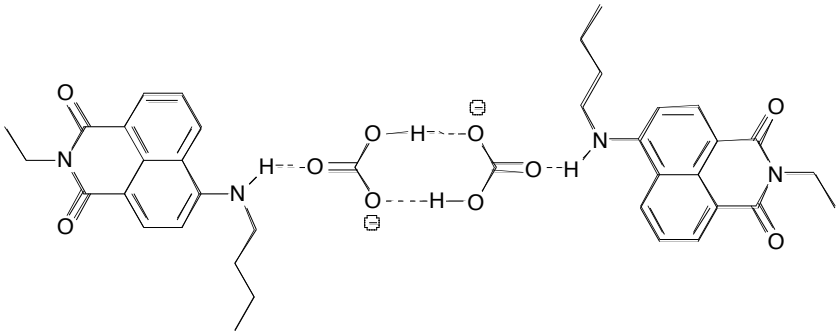

Fig 2.9 Schematic representation of the crystal structure of **89** with hydrogen-carbonate fixed from ambient carbon dioxide.

Crystals obtained after exposure to air, show two hydrogencarbonate anions associated in a carboxylate dimer structure, which had been fixed from ambient CO_2 in the atmosphere, (Figure 2.9). The hydrogen carbonate oxygen atoms not involved in forming the dimer are bound to the amines in the two receptors. In the solid state, the receptor is neutral, which leads the authors conclude that the base responsible for forming the hydrogen carbonate species is not fluoride, but infact deprotonated **89**.

2.1.4 Carbon dioxide fixation at metal centres

There are many examples in the literature of CO_2 fixation at metal centres. Transition metals are featured in many of these because of their multiple stable oxidation states, which enable the facile addition of extra ligands. In 1991, Calderazzo and co-workers reported simple hafnium, zirconium and titanium carbamato complexes formed from the reaction between simple metal halides, an amine and CO_2.[84] The resultant structures have one or two metal centres, co-ordinated to four *N*,*N*`-carbamato ligands, formed by the reaction between the amine and CO_2, (Figure 2.10). Others have shown the identical behaviour of chromium and molybdenum,[85] lithium[86] and several lanthanides,[87] (Figure 2.10). Oxalate formation and binding is also observed,[88] (Figure 2.10).

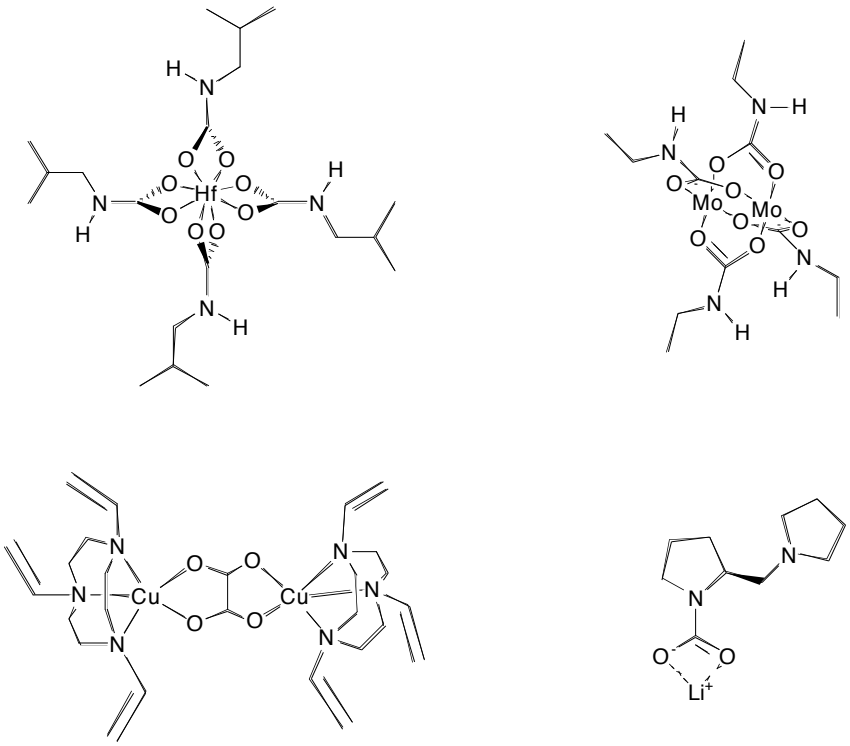

Fig 2.10 Example structures of metal-carbamato complexes.

More complex systems have also been developed. Copper and zinc, for example, have been utilised in systems mimicking enzyme activity. Both metal centres bind CO_2 in enzymes such as carbonic anhydrase (CA), which converts water and CO_2 to carbonic acid for transport in the blood.[89] In 1996, Bazzicalupi et al. showed that hydrated copper and zinc complexes of [15]aneN_3O_2, **90**, could fix ambient CO_2 in aqueous solution to form carbonate.[90] In the solid state, carbonate is bound between three metal centres, (Figure 2.11). The metal centres are held by three nitrogen atoms from the ligand, similar to the active site in CA.

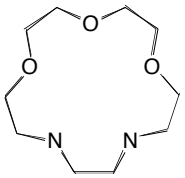

90

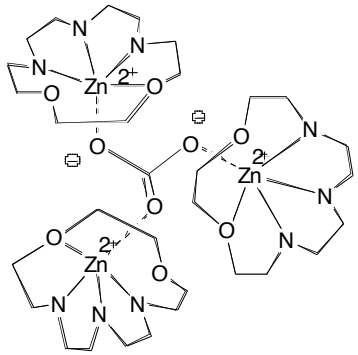

Fig 2.11 Carbonate co-ordinated to three metal centres.

Garcia-España and co-workers have produced macrocycle **91**, which features a terpyridine unit and a polyamine chain.[91] When **91** reacts with 1 eq. of copper, a complex is formed in which the copper is bound at the terpyridine site. Upon exposure to CO_2, one of the amines reacts to form a carbamate, which is then stabilised by the copper centre, (Figure 2.12).

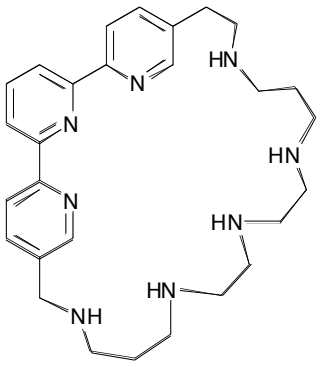

91

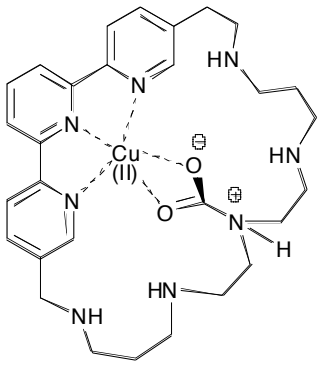

Fig 2.12 Mono-copper / CO_2 complex of **91**.

This is similar to the behaviour of the enzyme rubisco, which is involved in the first steps of photosynthesis.[92] In rubsico, a nitrogen containing lysine residue is used to form a carbamate with CO_2. The carbamate is then stabilised by a magnesium or manganese centre in its active site, before subsequent reactions to make glycerate-3-phosphate, the building block of glucose and more complex carbohydrates.

Nickel has been shown to behave similarly, in that it can stabilise carbamates formed by the reaction of CO_2 with nitrogen containing compounds. Walther et al. have produced a complex 24-member metallocycle **92**, which is held together by six nickel centres bound to neighbouring carbamate ligands,[93] (Figure 2.13). Each nickel centre in **92** is coordinated to its original ligand, the carbon from the Schiff base and two oxygen atoms of different carbamate moieties.

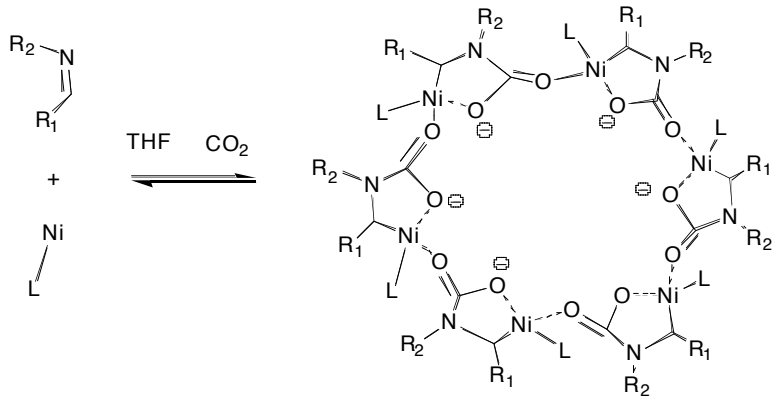

92

Fig 2.13 Nickel metallocycle, **92**, synthesised in THF using CO_2.

2.1.5 Reactions of carbon dioxide at metal centres

Metals are efficient catalysts due to their ability to adopt multiple stable oxidation states. They have found use in CO_2 chemistry in the synthesis of:

i) cyclic- and poly-carbonates from epoxides[94]
ii) ureas from amines[95]
iii) carbonates / carbamates from alcohols / amines and alkyl halides[96]
iv) specific chemical intermediates for further synthetic procedures[97]
v) fuels, such as syn-gas[98]
vi) carbon monoxide[99]

Because this chapter concerns only the fixation of CO_2, these transformations are included for perspective only, and this list is by no means exhaustive.

2.1.6 Carbon dioxide absorption within porous structures

Novel methods of storing CO_2 have recently emerged, many from gas separation studies using various porous substances. Porous structures capable of significant CO_2 sorbtion include:

i) zeolites
ii) aluminophosphates
iii) metal organic frameworks, (MOFs)
iv) metal based sorbants
v) partially porous organic crystals

Zeolites, such as zeolite 13X, have been known to fix CO_2 selectively for several years.[100] Recently, this behaviour was probed in aluminophosphates,[101] which whilst structurally similar, are not generally as efficient at CO_2 fixation as zeolites. MOFs have shown the best capacities so far, partly due to their massive internal surface areas.[102] Yaghi and co-workers, for example have developed excellent carbon dioxide

selective MOFs, some of which can achieve loadings of up to ~83L gaseous CO_2 for every 1L of MOF.[102e]

Other groups have combined the use of AAAC salt-based systems with solid supports, so that AAAC salts can be formed in the solid state. The CO_2 absorption properties of silica,[103] zeolites,[104] and some MOFs,[105] can be improved by appending amines. For example, Rayalu and co-workers have shown that the absorption properties of zeolite 13X can be improved by a factor of up to 3.5 by incorporating monoethanolamine into the synthesis.[104] Couck et al. have shown the excellent CO_2 selectivity of the MOF, "MIL-53(Al)", when 2-aminoterephthalic acid was incorporated as the linker.[105] This substance shows an almost infinite selectivity for CO_2 over methane at 1 bar, compared to a ratio of 7:1 (CO_2:CH_4) for unappended MIL-53(Al). Also, Atwood and co-workers have shown absorption behaviour in dimerised calixarene crystals, such as those of *p-tert*-butylcalix-[4]-arene.[106] Recently, they have shown that crystals of calix-[5]-arene are also capable of similar behaviour, showing selectivity for CO_2 over hydrogen.[107]

2.1.7 Summary

Many methods of CO_2 fixation are seen in the literature. Several examples employ more than one of these at a time, such as; covalent interactions and metal centres; hydrogen bonding and activation by salt-hydrates, and covalent interactions within porous structures. The work that follows also uses two methods of CO_2 fixation, namely covalent fixation by amine or amidine, followed by stabilisation of the resultant anion by hydrogen bonding. This represents a novel approach.

2.2 STABILISATION OF ALKYLAMMONIUM-ALKYLCARBAMATE SALTS USING HYDROGEN BOND DONORS – INITIAL STUDIES

2.2.1 Introduction

As shown in the first chapter, there are many examples of receptors, in which neutral hydrogen bond donors are arranged into convergent clefts in order to efficiently bind anions. It was hypothesised that the anionic component of alkylammonium-alkylcarbamate (AAAC) salts could also be bound in the same way; a novel approach to CO_2 stabilisation. The alkylcarbamate anions of AAAC salts closely resemble carboxylates in terms of their size, shape and electronic structure, and as such might be expected to hydrogen bond to ureas in a similar manner.

Whilst such an interaction would be favourable in isolation, the anions and cations of AAAC salts are very closely associated by electrostatic charge pairing because the alkylammonium cations have one or more proton substituents. This makes them less innocent than tetrabutlyamonium salts or other cations used in routine anion complexation studies. The hydrogen bonding interaction between any receptor and the alkylcarbamate anion therefore needs to be strong in order to compete with the electrostatic interaction between the alkylammonium and the alkylcarbamate. Below, a mode of binding is suggested for these interactions, in which the electrostatic charge pairing of the AAAC salt is disrupted by the introduction of the hydrogen bond donor, (Figure 2.14 and Figure 2.15).

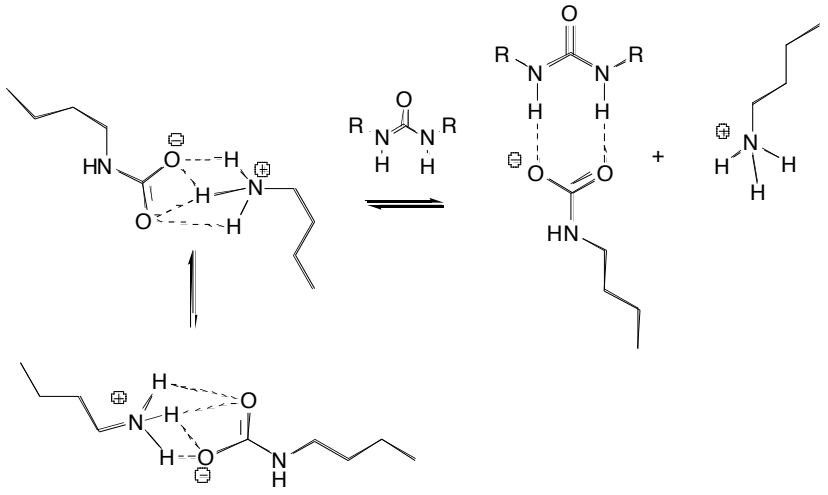

Fig 2.14 Proposed binding equilibria between ureas and AAAC salt formed from n-butylamine and CO_2

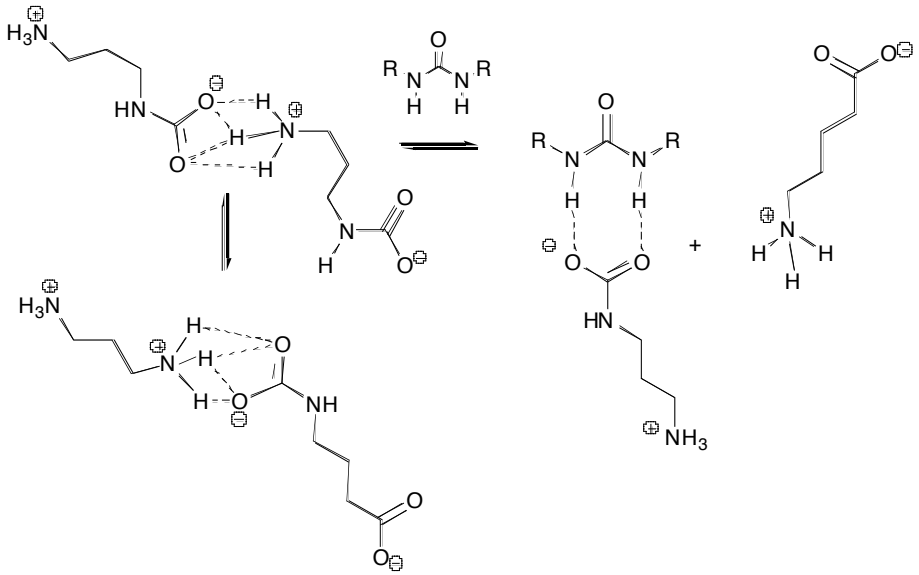

Fig 2.15 Proposed binding equilibria between ureas and DAP-CO_2

Previously, the group has produced oxo-anion receptors **93 – 102**, some of which are very selective for dihydrogen phosphate, even in exceptionally competitive solvents.[51-53] Receptors **93** and **94** were produced during this project, receptor **95** was prepared by Dr. Simon Brooks during his PhD candidature and receptors **96-102** had previously been prepared for publication[52-53] by Dr. Claudia Caltagirone and Jenny Hiscock and have been have been re-synthesised by myself according to their procedure where further material was required.

Receptor **98** is selective for dihydrogen phosphate over acetate in 10% H_2O:DMSO-d_6, (K_a ($H_2PO_4^-$) = 5,170M^{-1}, K_a ($CH_3CO_2^-$) = 774M^{-1}, and in 25% H_2O:DMSO-d_6, (K_a ($H_2PO_4^-$) = 160M^{-1}, K_a ($CH_3CO_2^-$) = 20M^{-1}). Despite being bound more weakly than dihydrogen phosphate, carboxylates are still bound strongly in 0.5% H_2O:DMSO-d_6, K_a (AcO^-) > 10,000M^{-1}, K_a (BzO^-) > 10,000M^{-1}.

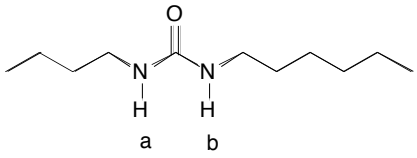

93

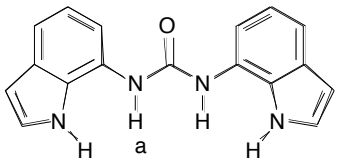

98

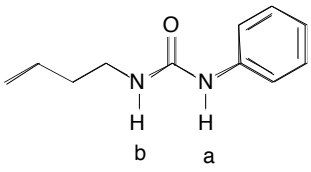

94

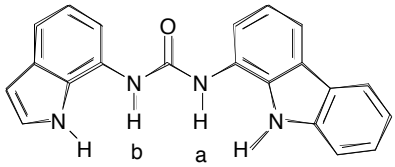

99

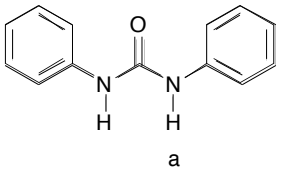

95

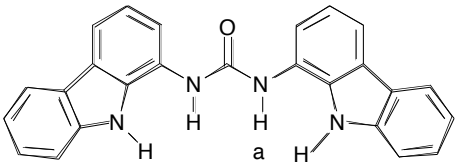

100

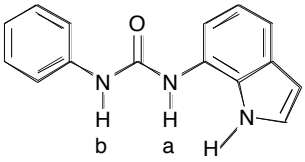

96

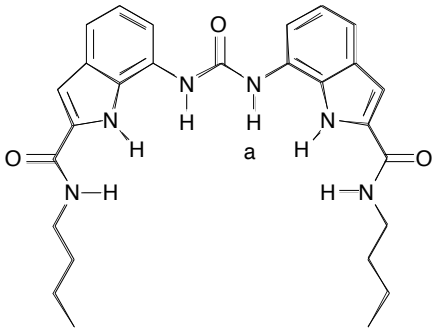

101

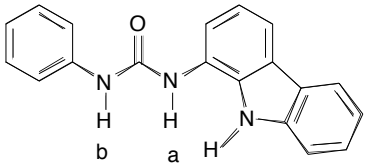

97

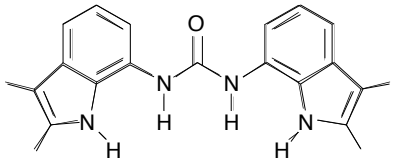

102

It was hypothesised that similarly large binding constants may be obtained for interactions between these receptors and alkylcarbamate alkylcarbamates, by way of ^{1}H NMR titration experiments.

2.2.2 Proton NMR titration with AAAC salts

Initially, proton NMR titrations were conducted in DMSO-d_6 at 298K between receptor **101** and the zwitterionic AAAC salt formed from 1,3-diaminopropane, (DAP-CO_2). Receptor **101** was selected because it is a strong receptor for oxo-anions and thus it was thought that it would provide a good chance of observing strong hydrogen bonding with AAAC salts. (At this point it was unknown whether or not they would hydrogen bond at all). The titration data set was fitted to a 1:1 binding model using WinEqNMR,[108] which gave $K_a = 4{,}300M^{-1}$ (± 16%), (Appendix 3). This value is of a similar order to the binding constants with TBA benzoate, and was an encouraging result. Unfortunately, repeat studies under identical conditions, which gave $K_a = 724M^{-1}$ (± 10%) and $K_a = 1{,}194M^{-1}$(±11%), showed the method to be unreliable, (Figure 2.16), (Appendix 3). Similar titrations were also carried out between **102** and DAP-CO_2, (K_a = $711M^{-1}$(± 11%)), but given the unreliability of the other results, no further titrations were conducted with AAAC salts.

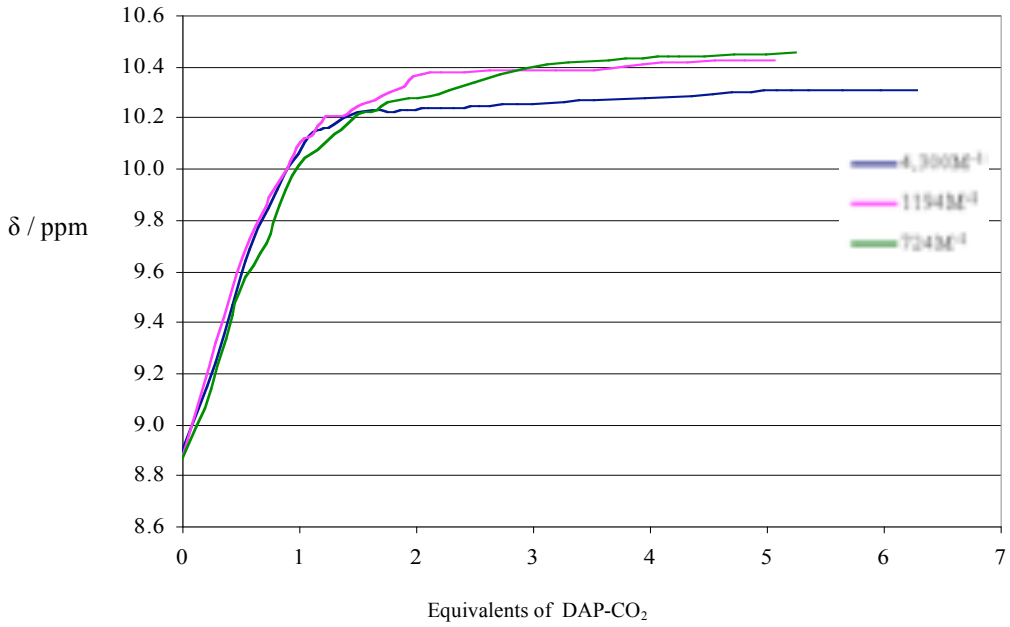

Fig 2.16 Plot of chemical shift (ppm) against equivalents of DAP-CO_2 added to a solution of **101**

It is thought that the differences in the binding constants arise from CO_2 loss from solution during the titration experiment. Loss of CO_2 shifts the equilibrium of the

CO_2 / amine reaction so as to lower the concentration of the AAAC salt in solution. This leads to unknown amounts of AAAC salt in solution, which directly affects the calculated binding constant. The largest differences between the three titrations curves appear later in the titration, lending credence to the notion that the loss of CO_2 from solution becomes more significant with time. The rate of CO_2 loss is likely to be dependant upon ambient temperature, atmospheric pressure, and the extent to which the mixtures are agitated during the titration process. Variations in these parameters appear to make it impossible to perform several titrations under identical conditions.

2.2.3 Relating chemical shift changes to binding constants

Despite the difficulty of obtaining reliable binding constants for the interaction between AAAC salts and the selected anion receptors, it was clear that favourable hydrogen bonding interactions were formed in many cases. These interactions are evidenced by the chemical shift changes (Δδ) of the urea, indole and amide NH protons of the receptors of receptor **101**, upon addition of AAAC salts.

It has previously been observed in other anion complexation studies, that the magnitude of Δδ experienced by a hydrogen bond donor is generally related to the strength of the hydrogen bonding between the receptor and anion, and hence may be related to the binding constant of that particular combination.[7, 36, 42, 109]
An anion which strongly binds to a given receptor, will cause a greater proportion of receptor-anion complex at a given concentration of anion, and hence a greater Δδ than an anion which is poorly bound by the receptor. Indeed, this is the basis on which binding constants are calculated by non-linear binding models.[108]

At this stage, it was necessary to assess the relationship between Δδ values and binding constants observed for a series of structurally related receptors interacting with the same anion. To this end, the binding constants and Δδ values (at 1eq.) for the interactions between receptors **93 – 101** and TBA benzoate were obtained, either from the literature, (**95, 98 – 101**)[52-53] or from performing new titrations, (**93**, **94**, **96**), (Appendix 3). Benzoate was selected because it gave a large range of values in 0.5%H_2O:DMSO-d_6.

Results

Receptors **93**, **94** and **95** have stability constants between $17M^{-1}$ and $674M^{-1}$ with benzoate, and average Δδ values of 1.20ppm, (Table 2.1). Receptors **97**, **99** and **100**, have stability constants between 3,400 M^{-1} and 5,880 M^{-1}, and average Δδ values of 1.75ppm. Receptors **96**, **98** and **101** all have stability constants greater than 10,000 M^{-1} and average Δδ values of 2.40 ppm. Whilst it is possible that these receptors may have different binding modes to benzoate, there is a general correlation between K_a and the chemical shift change for the urea NH protons.

	K_a / M^{-1}	Δδ / ppm
93	17	0.25
94	140	1.20
95	647	2.10
96	>10000	2.25
97	3400	1.85
98	>10000	1.84
99	5880	1.70
100	5670	1.70
101	>10000	2.70

Table 2.1 Binding constants (M^{-1}) and Δδ values for the 1:1 (receptor: benzoate) complexes of **93 - 101**

There are likely to be similar relationships between the Δδ values and K_a values for other anions with this set of receptors, including alkylcarbamate anions in AAAC salts. In this case, where it is not possible to obtain reliable binding constants by titration, it may therefore be possible to observe relative binding affinities of these for AAAC salts by considering Δδ values. It is likely that a degree of correlation between the Δδ value of the urea NH protons in the absence and presence of one equivalent of AAAC salt and the associated stability constant will be evident. Therefore, a binding strength trend can be ascertained from Δδ values of a 1:1 (receptor : alkylcarbamate anion) solution, relative to the chemical shift of the same proton in a solution containing only receptor, despite not knowing the absolute value of the binding constants.[7, 36, 42, 109] It is unlikely that the relative receptor:anion binding strengths will show the same trend as those seen with benzoate, because it is a different anion.

2.3 STABILISATION OF ALKYL AMMONIUM ALKYL CARBAMATE SALTS USING HYDROGEN BOND DONORS – CHEMICAL SHIFT CHANGES

2.3.1 Introduction

Solutions containing a receptor, **93** – **101** (1mM), (Page 72), and either **a)** n-butylamine (2mM) or; **b)** 1,3-diaminopropane (1mM) were made in DMSO-d_6. Each solution was bubbled with CO_2 for three minutes, ensuring saturation of the solution, (Appendix 2C). The chemical shifts of the urea proton(s) were then recorded, and these values were compared to the chemical shift of the urea proton(s) of the appropriate receptor in DMSO-d_6 in the absence of the AAAC salt. This gave a Δδ value for each combination of receptor and AAAC salt. For each combination, a mean was obtained from three identical repeats.

2.3.2 Results and Discussion

Positive Δδ values were observed for the urea NH protons of several of the receptors upon addition of AAAC salts, (Table 2.2), (Appendix 2A). As stated earlier, this observation is consistent with favourable interactions between the AAAC salts and the receptors, and was expected following the initial titration experiments.

i	Δδ NH (a) / ppm	Δδ NH (b) / ppm
93	0	0
94	0	0
95	0.11 (13)	-
96	0.26 (6)	0.28 (6)
97	0.27 (13)	0.30 (15)
98	0.71 (7)	-
99	0.67 (10)	0.68 (12)
100	0.63 (5)	-

ii	Δδ NH(a) / ppm	Δδ NH (b) / ppm
93	0	0
94	0	0
95	0.08 (23)	-
96	0.28 (14)	0.30 (15)
97	0.37 (9)	0.42 (10)
98	0.70 (10)	-
99	0.50 (7)	0.51(6)
100	0.56 (6)	-

Table 2.2 a) Chemical shift changes for urea NH protons (with associated % errors) for receptors **93 - 100** in the presence of **i)** AAAC salt formed by the reaction of 2eq. n-butylamine and CO_2; **ii)** AAAC salt formed by the reaction of 1eq. 1,3-diaminopropane and CO_2. (Solvent = DMSO-d_6).

Smaller Δδ values are observed in cases in which the receptor has a low number of hydrogen bond donors, and larger Δδ values are seen where the receptor has a larger number of hydrogen bond donors. Receptors **93** and **94** have only two hydrogen bond donors and Δδ = 0 in the presence of 1eq. of alkylcarbamate anion in DMSO-d_6. Receptor **95** also has two hydrogen bond donors and has electron withdrawing phenyl groups. Its urea NH protons have only small Δδ values of around 0.1 ppm. Receptors **96** and **97** have three hydrogen bond donors, including an acidic indolyl or carbazoyl moiety. Their urea NH protons have substantially Δδ values, between 0.26 – 0.42 ppm. When a further hydrogen bond donor is added, such as in receptors **98** – **100**, the Δδ values for the urea NH are again larger; 0.50 – 0.71 ppm. Receptor **98** has the highest Δδ values; 0.70 ppm with DAP-CO_2 and 0.71 ppm with the AAAC salt resulting from the reaction of n-butylamine with CO_2. Δδ values for the urea NH protons could not be obtained for the urea NH protons of receptor **101**, (which has six hydrogen bond donors), due to peak broadening.

2.3.3 Conclusion

In line with the argument presented in Chapter 2.2.3, one can conclude that out of this series, the strongest receptor for both of the AAAC salts studied is **98**. The weakest receptors are those with negligible or very small Δδ values, **93** – **95**. The Δδ values for the urea NH protons of the other receptors are between these extremes, and follow a similar, but not identical trend to that seen for the same receptors with benzoate. Considering the strong charge pairing between the alkylammonium and alkylcarbamate components of an AAAC salt, it is remarkable that a degree of stabilisation of the AAAC salts can be achieved by complexation with neutral hydrogen bonding arrays. Although these experiments have been performed in a competitive solvent, which will assist in separating the charges of the AAAC salts, this result is significant, because it demonstrates that collective hydrogen bonding interactions can compete with electrostatic interactions in cases where the counter-cation is strongly ion-paired to the anion.

2.4 STABILISATION OF ALKYLAMMONIUM-ALKYLCARBAMATE SALTS USING HYDROGEN BOND DONORS AND 18-CROWN-6

2.4.1 Introduction

The experiments described previously, (Chapter 2.3), were repeated in the presence of 1eq. 18-crown-6. This crown is of an appropriate size to hydrogen bond to protonated amines and so should also compete with the electrostatic charge pairing of the AAAC salt.

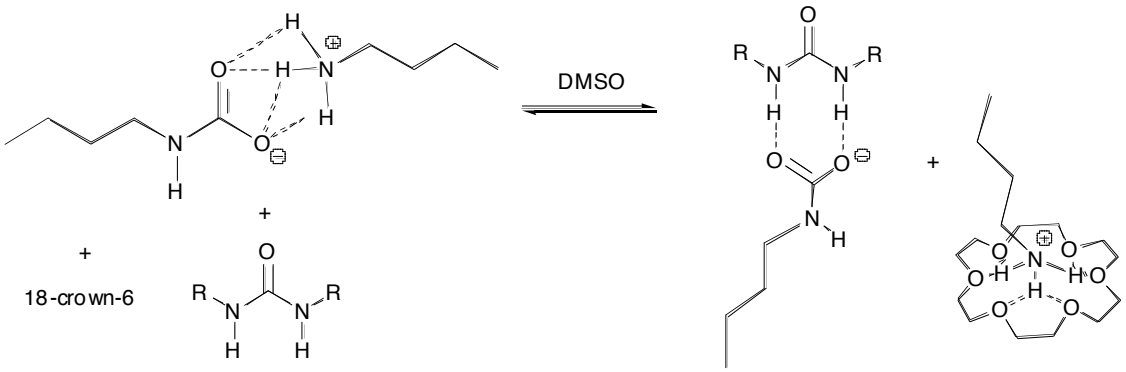

Fig 2.17 Proposed binding mode between AAAC salt and anion receptor in presence of 18-crown-6

It was thought that this would increase the concentration of unbound alkylcarbamate anion. The presence of increased amounts of unbound alkylcarbamate was anticipated to cause larger Δδ values for the urea NH protons of receptors **93-101**, (Page 72), than was observed without 18-crown-6.

2.4.2 Results and Discussion

In the majority of cases, the effect of adding 1eq. of 18-crown-6 is an increase in the Δδ values of the urea NH protons compared to the initial experiment without 18-crown-6, (Table 2.3), (Appendix 2A). As before, receptors **93** and **94** the urea NH protons have Δδ = 0 with both AAAC salts. The urea NH protons of receptor **95** have Δδ values similar to the case without 18-crown-6, of around 0.1 ppm. The Δδ values for

the urea NH protons of receptors **96** and **97** however, are larger, between 0.34 ppm and 0.45 ppm. The Δδ values for **99** and **100** are also generally larger, than the comparable case without 18-crown-6. The exception is the case of receptor **99** and 18-crown-6 / butylamine, which has the same Δδ value as the case without 18-crown-6.

i	Δδ NH (a) / ppm	Δδ NH (b) / ppm
93	0	0
94	0	0
95	0.10 (6)	-
96	0.34 (15)	0.37 (7)
97	0.36 (13)	0.39 (13)
98	0.45 (1)	-
99	0.66 (1)	0.66 (1)
100	1.18 (3)	-

ii	Δδ NH (a) / ppm	Δδ NH (b) / ppm
93	0	0
94	0	0
95	0.15 (6)	-
96	0.43 (4)	0.46 (5)
97	0.40 (2)	0.45 (2)
98	0.59 (6)	-
99	0.78 (5)	0.78 (5)
100	0.77 (10)	-

Table 2.3 a) Chemical shift changes for urea NH protons / ppm (with associated errors / %) for receptors **93 – 100** and 1eq. 18-crown-6 in the presence of, **i)** AAAC salt formed by the reaction of n-butylamine and CO_2; **ii)** AAAC salt formed by the reaction of 1,3-diaminopropane and CO_2. (Solvent = DMSO-d_6)

Another exception to the trend of increased Δδ values is receptor **98**, the urea NH protons of which, have a significantly Δδ with both AAAC salts in the presence of the crown-ether, (0.45ppm and 0.59ppm), than in the absence of crown-ether, (0.70 ppm and 0.71ppm). Why this should be so is not apparent, but it causes the Δδ values to increase with both the number of hydrogen bond donors in the receptor and the acidity of the receptor, (pK_a (indole) = 21.0, pK_a (carbazole) = 19.1).[110]

2.4.3 Conclusion

The addition of 1 eq. of 18-crown-6, has the effect of increasing the Δδ values, relative to the initial experiments, (Chapter 2.3). This observation is attributed to the presence of a higher proportion of "free" alkyl-carbamate anion, which arises from competition with the crown ether for the alkyl-ammonium cation. This will be expanded upon in the conclusion, (Chapter 2.6).

2.5 STABILISATION OF AN AMIDINE-CO_2 ADDUCT USING HYDROGEN BOND DONORS

2.5.1 Introduction

In a further attempt reduce the extent of charge pairing within this system, the response of the urea NH protons of the receptor series were studied upon the addition of the CO_2 adduct of the cyclic amidine, 1,4,5,6-tetrahydropyrimidine (THP). The adduct, THP-CO_2 has little charge pairing in solution compared to the AAAC salts. It was anticipated that this would be reflected in increased Δδ values for the urea NH protons of receptors **93** – **101,** (Page 72), than had been observed for the AAAC salts, even when these are in the presence of 18-crown-6, (Figure 2.18).

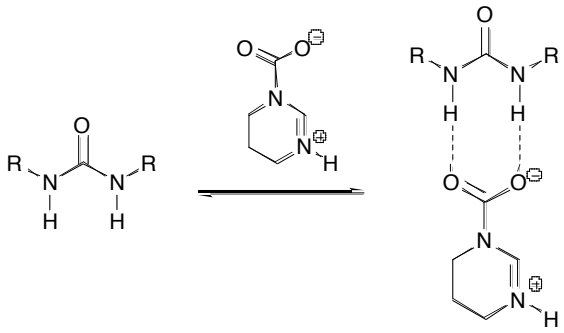

Fig 2.18 Proposed binding mode between THP-CO_2 and generic urea receptor

An identical procedure to that used for the previous studies was used to obtain Δδ values for the urea NH protons of the receptors in the presence of 1eq. THP-CO_2, (Chapter 2.3 / 2.4).

2.5.2 Results

For each receptor, the Δδ values in the resonance(s) of the urea NH proton(s) are significantly higher than the corresponding chemical shift changes with AAAC salts, even in the presence of 18-crown-6, (Table 2.4), (Appendix 2A).

	Δδ NH (a) / ppm	**Δδ NH (b) / ppm**
93	0.03 (37)	0.03 (37)
94	0.22 (13)	0.23 (13)
95	0.75 (4)	-
96	1.09 (12)	1.32 (10)
97	1.06 (4)	1.25 (4)
98	1.17 (5)	-
99	1.31 (4)	1.34 (4)
100	1.42 (3)	-
101	0.87 (6)	-

Table 2.4 Chemical shift changes for urea NH protons / ppm (with associated errors / %) for receptors **93 – 101** and 1eq. THP-CO_2. (Solvent = DMSO-d_6)

The smallest Δδ values were observed for the urea NH protons of receptor **93**. Receptor **94** has significantly enhanced Δδ values of 0.22 ppm and 0.23 ppm for the urea NH protons. The urea NH protons receptor of **95** have Δδ =0.75 ppm, which is significantly greater than the Δδ values seen with AAAC salts. Receptors **96** – **98** all have similar average Δδ values between 1.16 and 1.32 ppm. Receptors **99** and **100** have slightly larger Δδ values; 1.31 – 1.42 ppm. For the first time, the urea NH protons of receptor **101** were not broadened by the addition of anion, and give Δδ = 0.87 ppm. This data is also presented graphically, (Figure 2.19).

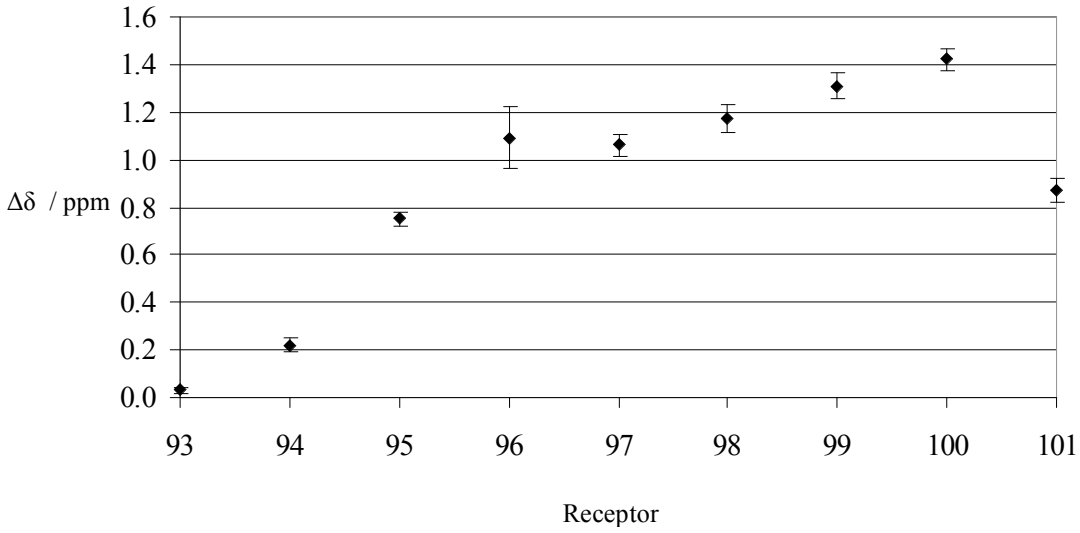

Fig 2.19 Δδ values for downfield urea NH proton for receptors **93 - 101** upon addition of 1eq. THP-CO_2. (Solvent = DMSO-d_6)

2.5.3 Discussion

The Δδ experiments with THP-CO_2 appear to confirm that a guest that does not undergo significant charge pairing in solution provides significantly greater proportions of "free" anion in solution, reflected in higher Δδ values. The greater availability of "free" anion is shown by the fact that the urea NH protons of receptor **94**, (and to a lesser extent **93**), undergo a change with THP-CO_2. This is not the case with the AAAC salts. Again, it is the urea NH protons of the most acidic receptors, which have the largest Δδ values.

This trend is the same as the trend of the receptors with AAAC salts in the presence of 18-crown-6, in that the Δδ values increase with both the number of NH hydrogen bond donors present and the acidity of the receptor. This is unlike the case of AAAC salts in the absence of 18-crown-6, which has a trend based on other factors.

2.6 CONCLUSION

For each of the five sets of experiments described in Chapter 2.3, 2.4 and 2.5, there is clear evidence of favourable hydrogen bonding interactions between the receptors **93 - 101**, (Page 72), and AAAC salts or THP-CO_2 adduct. The receptor(s) which are strongest, (ie: those with the highest $\Delta\delta$ values), are not the same, in each case. This is to be expected, because the five experiments have different effective anions, as expanded upon below.

2.6.1 Chemical shift changes upon addition of THP-CO_2 and AAAC salts - (in the presence of 18-crown-6)

With THP-CO_2 and the AAAC salts in the presence of 18-crown-6, the $\Delta\delta$ values of the urea NH protons increase in a clear trend. They increase in line with the number of hydrogen bond donors present in the receptor and the relative acidity of its substituents, (Figure 2.20 and Figure 2.21). It is thought that this trend is seen because there is a low to negligible amount of AAAC salt charge-pairing in solution, which makes the alkylcarbamate anion relatively basic, and will therefore bind strongly to the more acidic receptors of the series, **99** and **100**. Indeed, this is the trend seen for the basic anion acetate with the same receptors.[52-53]

2.6.2 Chemical shift changes upon addition of AAAC salts - (no 18-crown-6)

In the case of the AAAC salts in the absence of 18-crown-6, it is the urea NH protons of receptor **98**, (the least acidic of the receptors with four NH protons) which has the largest $\Delta\delta$, (Figure 2.20 and Figure 2.21). It is thought that this is because there is a significant degree of AAAC salt charge-pairing in solution, which makes the alkylcarbamate anion less basic than in the cases described above. It has previously been shown that receptor **98** binds dihydrogen phosphate preferentially over (more basic) acetate,[50-51] which shows that whilst strong, **98** is not ideal for binding the most basic anions. Hence, it will bind alkylcarbamate anions most strongly when they are weakly basic, ie: in the absence of 18-crown-6. The more acidic receptors, **99** and **100**

do not bind anions of low basicity as well as those of high basicity and so do not interact strongly with alkylcarbamates in the absence of 18-crown-6.

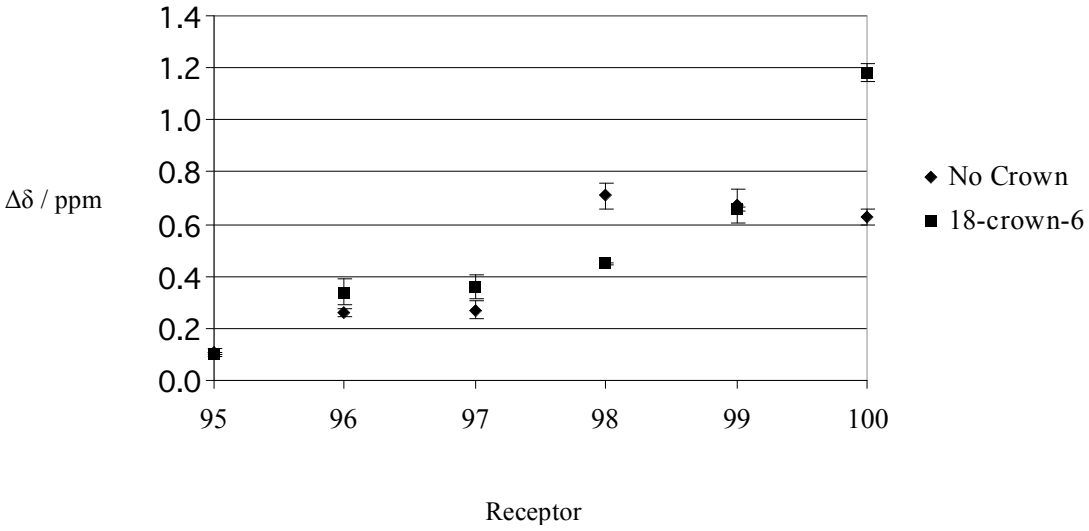

Fig 2.20 Graph of Δδ / ppm for urea NH proton (a) of receptors **95 - 101** upon addition of 2eq. AAAC salt from reaction of n-butylamine and CO_2 in absence and presence of 1eq. of 18-crown-6. (Solvent = DMSO-d_6)

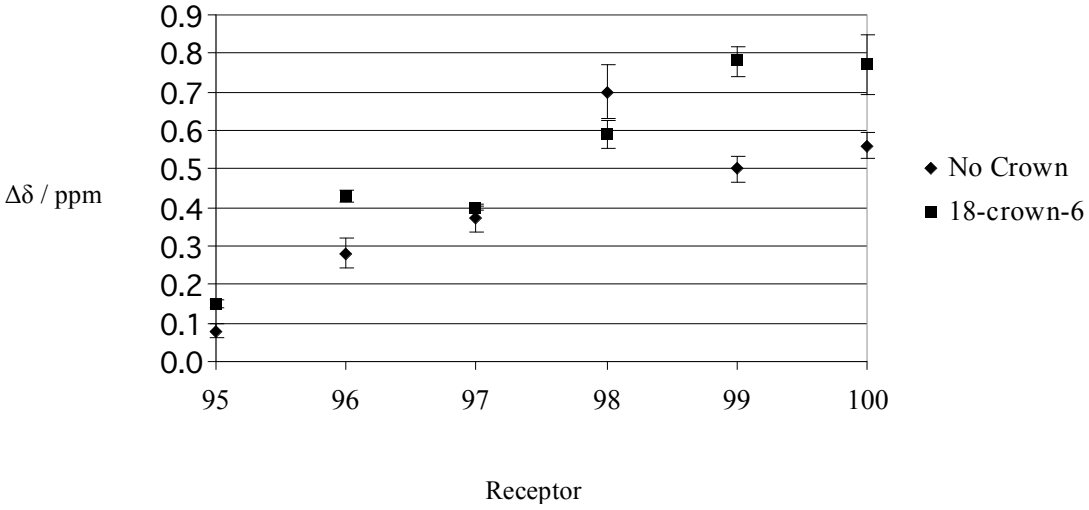

Fig 2.21 Graph of Δδ / ppm for the downfield urea NH proton (a) of receptors **95 - 101** upon addition of 1eq DAP-CO_2 in absence and presence of 1eq. of 18-crown-6. (Solvent = DMSO-d_6)

2.7 SOLID STATE ANALYSIS

Crystals suitable for X-ray diffraction were formed by slow evaporation from a DMSO solution of receptor **101**, (Page 72), 18-crown-6, and DAP-CO_2, (Appendix 1B). The structure was resolved and showed a 1:1:1 ternary crystal structure comprising of the receptor, 18-crown-6, and the zwitterionic species DAP-CO_2 bound to both of these, (Figure 2.22).

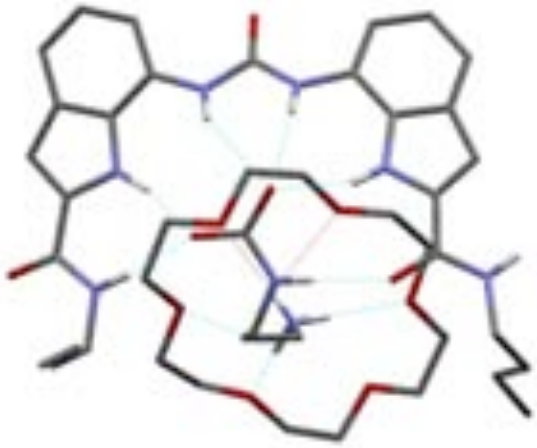

Fig 2.22 A view of one of the two complexes in the asymmetric unit of the ternary complex of the AAAC salt formed by the reaction of 1,3-diaminopropane and CO_2, receptor **101** and 18-crown-6

The alkylammonium group of DAP-CO_2 is hydrogen bonded to18-crown-6, with donor-acceptor bond lengths between 2.74 - 3.07Å. The carbamate moiety of DAP-CO_2 is bound to receptor **101** by six hydrogen bonds, with the two carbamato oxygen atoms receiving a total of five hydrogen bonds from the two urea NH protons (3.29Å, 2.77Å), the two indolyl NH protons (2.69Å, 2.78Å), and one of the amide NH protons, (2.85Å). The carbamato NH proton acts as a hydrogen bond donor to the carbonyl oxygen of the other amide (2.89Å), the NH proton of which is oriented away from the binding site. This amide NH is bound to an adjacent host molecule, binding to the carbonyl oxygen of its amide, (2.89Å). This interaction is repeated along the length

of the crystal giving rise to two in-equivalent receptor molecules in an asymmetric complex, (Figure 2.23 and Figure 2.24).

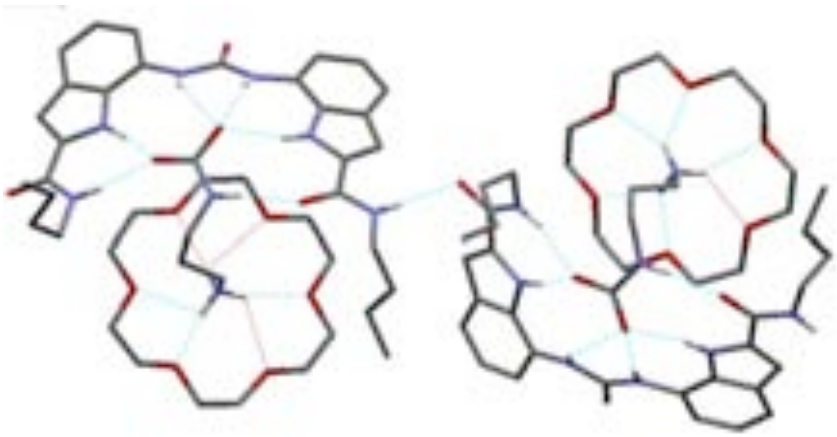

Fig 2.23 Extended structure of ternary crystal structure of **101**, 18-crown-6 and DAP-CO_2

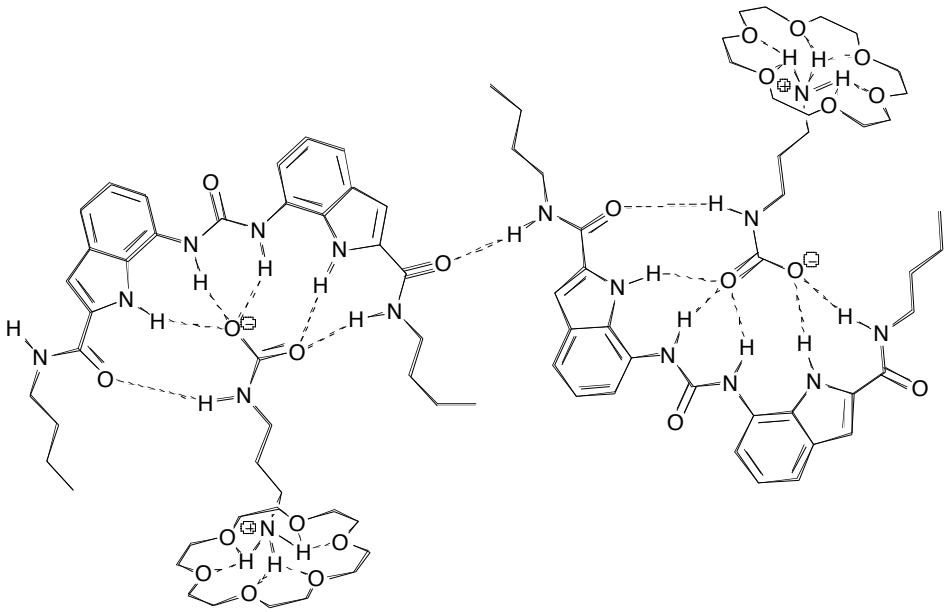

Fig 2.24 Schematic representation of the full solid state structure of the ternary complex of **101**, DAP-CO_2 and 18-crown-6, showing both asymmetric units

This is a novel type of structure, the first to show binding of an alkylammonium-alkylcarbamate zwitterion bound to two neutral hydrogen bonding receptors.

2.8 STABILISATION OF ALKYL-AMMONIUM ALKYL-CARBAMATE SALTS USING A DITOPIC RECEPTOR

2.8.1 Introduction

The presence of 18-crown-6 has been shown to increase the proportion of alkylcarbamate anion bound to a series of receptors, because it increases the Δδ values of the urea NH protons in receptors **93** – **100**, (Page 72), forming what is thought to be a ternary complex in solution. This is certainly the case in the solid state, as demonstrated by the ternary crystal structure of **101**, 18-crown-6 and DAP-CO_2. However, it is likely that in solution the formation of this ternary structure suffers a large entropic penalty compared to the binary receptor:alkylcarbamate complex which forms in the absence of 18-crown-6. It was therefore thought that ditopic receptors would be able to condense two of these three components into one molecule, and hence would be desirable targets for enhanced AAAC salt binding by reducing the entropic penalty.

There are a wealth of ion-pair receptors in the literature, which can be fitted into two main categories; heteroditopic receptors, which have separate anion and cation binding sites; contact-ion pair receptors, in which the ions are bound at a distance closer than the sum of their van-der-Waals radii. Examples of hetero ditopic receptors include amino-acid receptors such as **103** by Späth and König, which contain guanidine and crown-ether moieties.[111] These accept both of the ends of amino acids, (Figure 2.25).

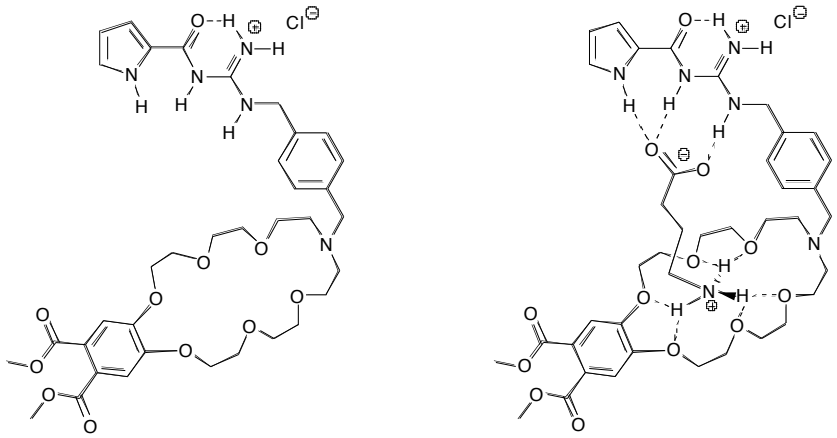

103

Fig 2.25 Receptor **103** bound to an amino acid

The group of de Mendoza has previously used chiral receptors such as **104**, which contain guanidine and a crown-ether in order to differentiate between L and D amino acids,[112] a principle discussed with relation to the work of Lehn and co-workers (Chapter 1.3).[17]

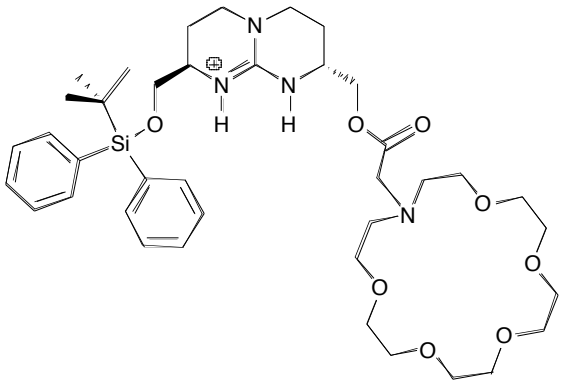

104

Non-contact ion-pair receptors have also been presented by Beer and co-workers, who have developed calixarenes appended with Crabtree-type isophthalamides such as **105** for alkali-metal halides.[113] Kilburn and co-workers have developed similar receptors such as **106**, which have urea that bind oxo-anions in the presence of sodium.[114]

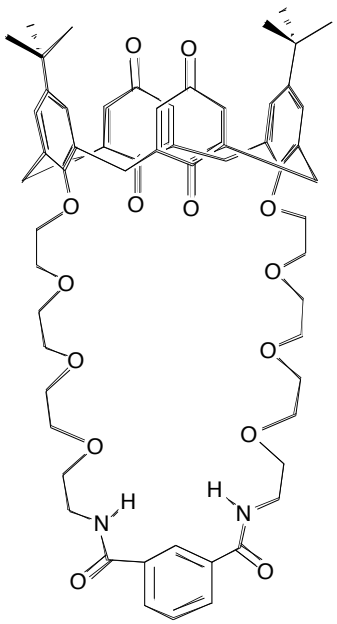

105

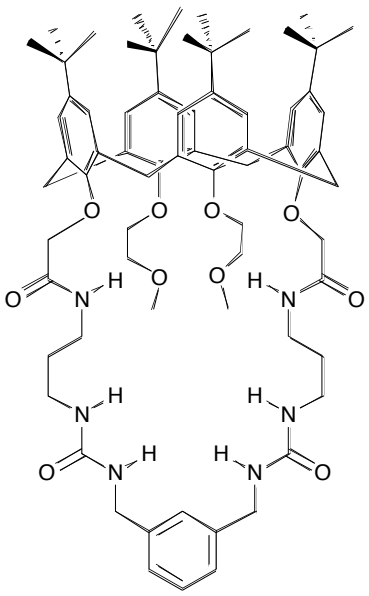

106

Gale, Custelcean and co-workers have probed the ion-pair binding ability of calix-[4]-pyrrole.[115] Steed and co-workers have recently demonstrated simple contact silver salt receptors based on **107**, in which the anion (NO_3^-, $CH_3CO_2^-$ or PF_6^-) are bound by hydrogen bond donors and the metal ion.[116]

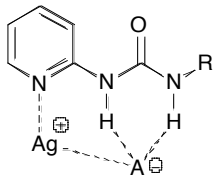

107

Tasker and co-workers have conducted extensive work on metal salt extraction techniques, notably for sulfates, with contact ion-pair receptors such as **108** that undergo internal proton transfer upon complexation of the ion-pair.[117]

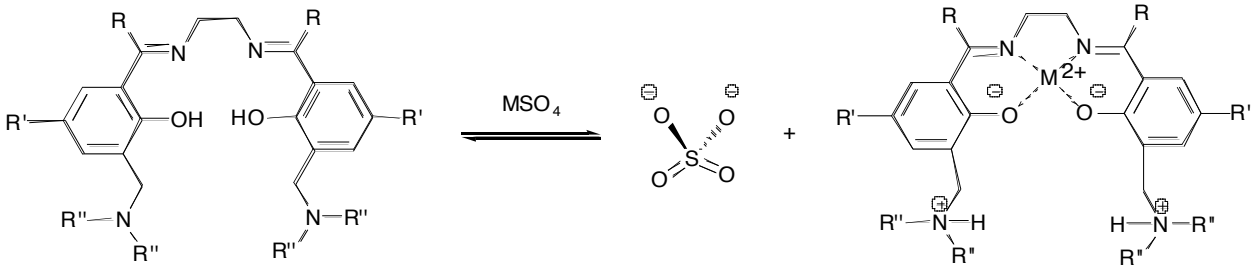

108

Figure 2.26 Receptor **108** undergoes internal proton transfer upon complexation of metal sulfate salt.

2.8.2 Synthesis

The urea NH protons of receptor **95** have the same chemical shift changes with AAAC salts in the presence and absence of 18-crown-6, making this a good receptor on which to test the hypothesis that a ditopic receptor should increase Δδ. Receptor **94** is also relatively simple to derivatise compared to some of the other receptors. Receptor **109**, was synthesised for this purpose from phenylisocyanate and 4,4`- aminobenzo-18-crown-6 in good yield, (Scheme 2.1). It is a bis-phenyl urea, in which one phenyl ring has been replaced with a benzo-18-crown-6 substituent.

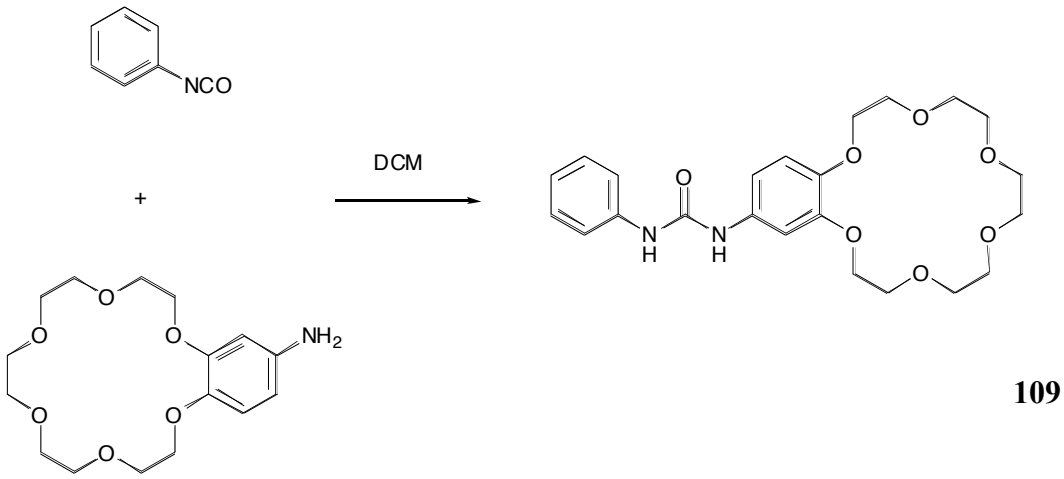

109

Scheme 2.1 *Reagents and Conditions:* DCM, RT, 2h, 81%.

In the solution state, it was anticipated that this receptor would bind to both the alkylcarbamate and alkylammonium moieties of AAAC salts, (Figure 2.27). It was also thought that extended tapes may form in the solid state by incorporation of DAP-CO_2.

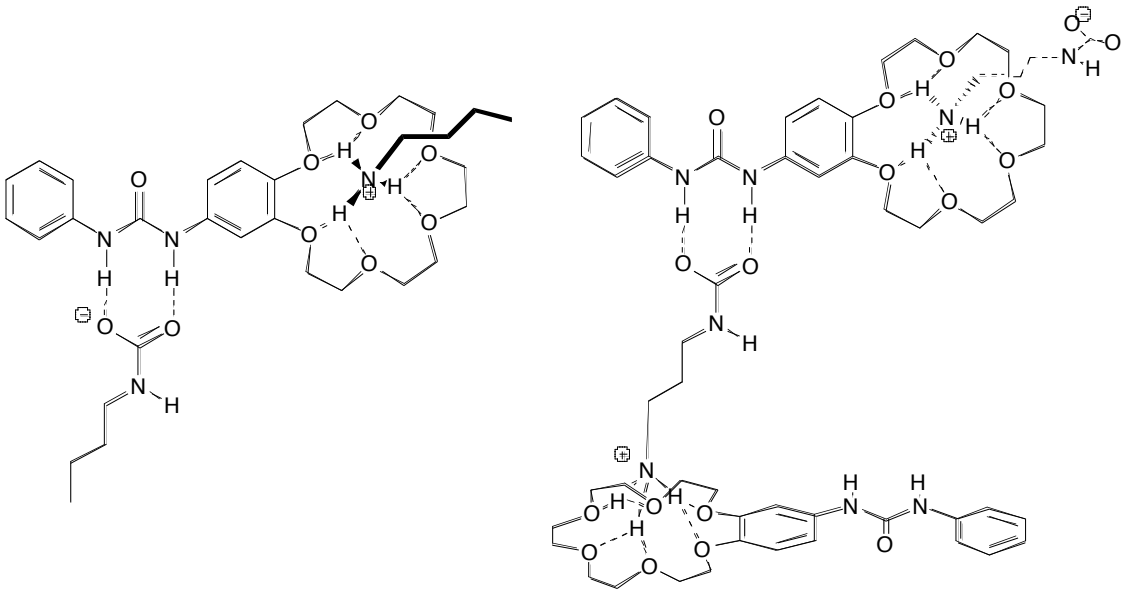

Fig 2.27 Examples of anticipated interactions between AAAC salts and **109**

2.8.3 Chemical shift changes

Solution state studies were performed on **109** with DAP-CO_2 and the AAAC salt formed from n-butlyamine and CO_2, in an identical manner to those carried out on receptors **93** – **101**, (Page 72), (Appendix 2A). These had an average Δδ value of 0.07ppm for both NH protons with the AAAC salt formed from n-butylamine and CO_2, and an average Δδ = 0.10ppm with DAP-CO_2. These values are similar to those observed for the analogous receptor **95**, and do not appear to confirm the hypothesis that a ditopic receptor improves binding. It is possible that this may be due to the electron-donating ether substituents, donating electron density to the urea NH and weakening the hydrogen bonds formed. It is also possible that the two binding sites are separated by too great a distance for **109** to operate as a ditopic receptor.

2.8.4 Solid-state analysis

Introduction

Crystals suitable for X-ray crystallography were obtained by slow evaporation from a methanolic solution of **109**, (Page 90), and DAP-CO_2, (Appendix 1A). When resolved, the structure did not feature DAP-CO_2 or indeed DAP. Instead, it shows receptor **109** with a disordered and unidentified molecule, which is held within a closed cavity, defined by two crown-ether rings from separate receptor molecules, (Figure 2.28). There is significant receptor-receptor hydrogen bonding, including between the crown ether oxygen atoms and the urea NH groups. There are two candidates for the unknown molecule. These are; a) unactivated CO_2 formed by the slow decomposition of DAP-CO_2, and; b) the solvent, methanol. Both are able to fit comfortably in the cavity based on their van der Waals radii, with the evidence split as to which case is more likely.

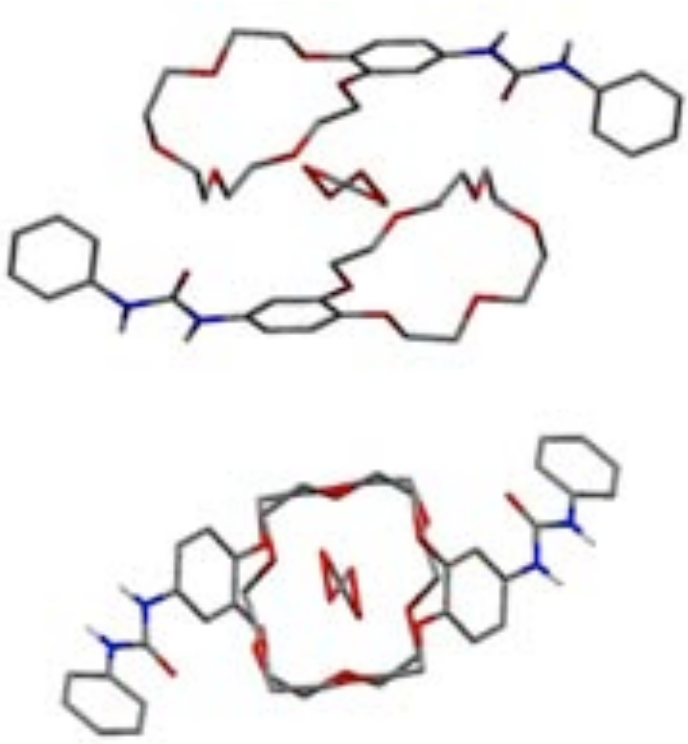

Fig 2.28 Views of the cavity formed by two molecules of **109**.
Central electron density is resolved as CO_2.

Evidence in Favour of Carbon Dioxide

The principle evidence in favour of CO_2 are the bond lengths between the central atom of the unidentified molecule and its satellite atoms, which are calculated to be in the order of 1.26Å. This value correlates well to the C=O bond length in other examples where unbound CO_2 is found in crystal structures, (1.05Å - 1.20Å).[118] The C-O bond length in methanol in crystal structures is longer, between 1.39Å and 1.60Å.[119] There is also circumstantial evidence that the unknown molecule is CO_2, because no hydrogen bonding can be directly observed between it and the receptor molecules. This behaviour would be expected of CO_2, but it is likely that methanol would be involved in at least some hydrogen bonding with the receptor. There is also literature precedent of CO_2 being bound in cavities made from organic dimers, such as seen in the work of Atwood and co-workers.[106-107] Once trapped in the cavity like that seen between the two crown-ethers in this case, it would be hard for CO_2 to diffuse to the atmosphere from a crystalline material such as this.

Evidence in Favour of Methanol

There is also evidence for the presence of methanol in the structure. Firstly, many crystal structures of organic molecules incorporate solvent molecules in the structure. There are few examples with CO_2 present in the structure. In the absence of the evidence presented above, reason would suggest that this crystal is unlikely to be significantly different. Secondly, an electron density image of the unidentified molecule indicates significant electron density on the central atom, (Figure 2.29), (Appendix 1A).

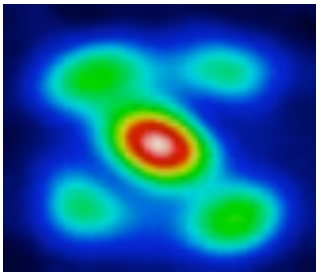

Fig 2.29 Relative electron density image of the unidentified molecule present in the cavity. (Red = High electron density, Green = Moderate electron denisity, Blue = Low electron density).

This is partly due to superposition effects brought about because the unidentified molecule is disordered, but may also indicate that it has the electron-rich oxygen atom at its centre, suggesting methanol inclusion. Another explanation for the intense area of electron density is that the molecule is disordered between four positions, which suggests a bent geometry, also consistent with methanol. The apparent dominance of two of these positions indicates the possibility of weak hydrogen bonding interactions between the unidentified molecule and cavity. Methanol is capable of such interactions, whereas CO_2 is not.

Other Work

Since the partial resolution of this structure, attempts have been made to grow crystals of; a) receptor **109**; b) receptor **109** bubbled with CO_2, and; c) receptor **109** and DAP, (in the absence of CO_2), for the purpose of comparison with the existing data set. Unfortunately, none of these has yielded material suitable for X-ray diffraction. If it was possible to reliably make larger quantities of the material seen in the partially resolved crystal, thermogravimetric analysis, IR spectroscopy, Raman spectroscopy or simple chemical tests would be likely to identify the unknown molecule with certainty. Without this evidence, it is not possible to conclusively prove or disprove the presence of CO_2 or methanol in the crystal structure of **109**.

2.9 CONCLUSION

Chemical shift change experiments have shown that significant hydrogen bonding occurs between neutral receptors and alkylcarbamate anions of AAAC salts, even in the presence of strong electrostatic competition from the alkylammonium counter cation. The removal of the electrostatic competition, either by addition of a secondary receptor for the alkylammonium, 18-crown-6, or changing the substrate to an adduct, THP-CO_2, causes an increase in the hydrogen bond strength. A ternary complex of an alkylammonium-alkylcarbamate salt, complexed to receptor **101** was isolated in the solid state. This led to the design and synthesis of a ditopic receptor, **109**, for AAAC salts. This receptor did not exhibit enhanced hydrogen bond strength with either AAAC salt. A crystal structure of the ditopic receptor appears to contain an unidentified molecule which may be unactivated CO_2, although it is possible that it may be the solvent, methanol.

CHAPTER 3 – SCHIFF-BASE / UREAS AS ANION RECEPTORS AND COLORIMETRIC SENSORS

3.1 COLORIMETRIC ANION SENSORS

There are many literature examples of anion receptors, which undergo colour changes upon anion complexation. Many systems involve deprotonation by basic anions, often involving complete or partial internal electron transfer within a receptor. If chromophores are appended to these, a specific and stark colour change is the likely result, (Figure 3.1).

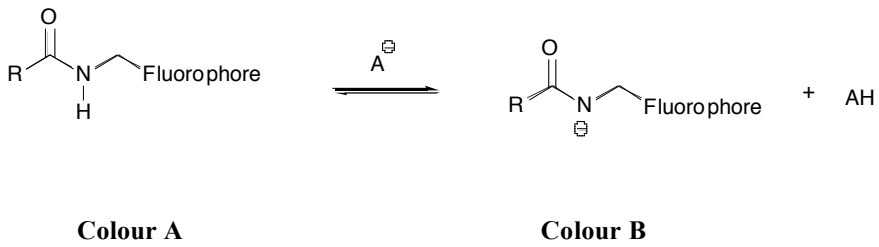

Fig 3.1 Example of complete electron transfer caused by deprotonation of amide NH

Fabbrizzi and co-workers, for example, have developed a two-stage naked-eye anion sensor capable of detecting basic anions by deprotonation. Neutral receptor **103**, consists of two naphthalenimide chromophores linked through a urea, and is yellow in DMSO solution.[120]

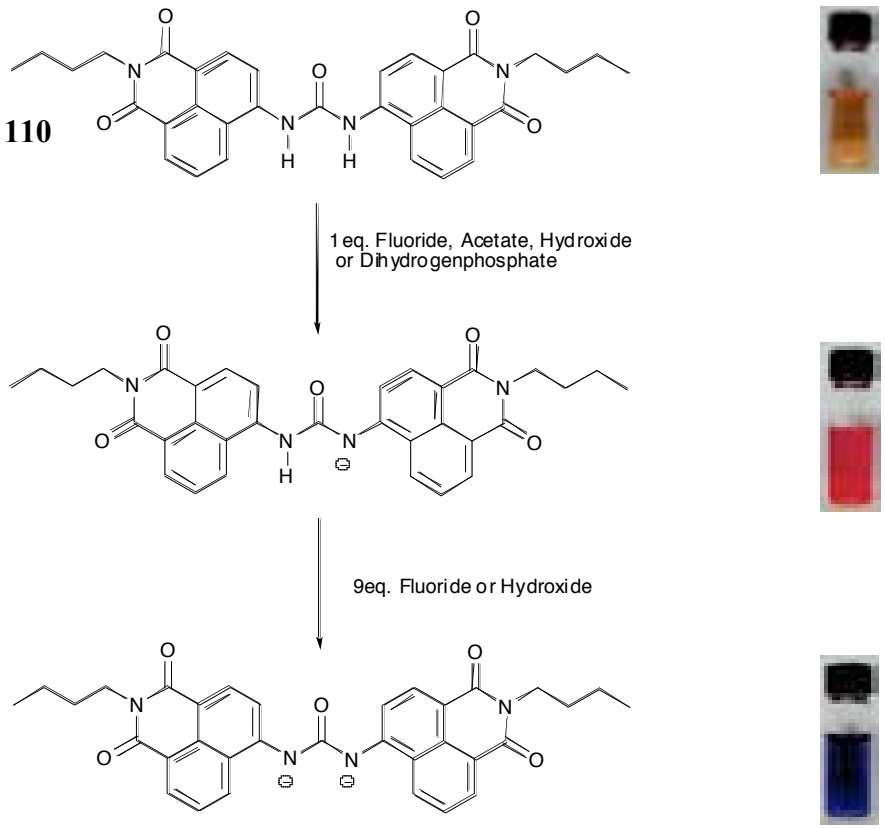

Fig 3.2 Colour changes induced by deprotonation of **110** by various anions. Reproduced in part with permission from *J. Org. Chem.,* **2005**, *70*, 5717. Copyright 2005 American Chemical Society.

The first equivalent of anion causes one urea NH to be deprotonated. This is accompanied by a colour change to bright red, arising from changes in the electronic structure of one of the naphthalenimides, (Figure 3.2). Upon the addition of excess fluoride or hydroxide, the red solution becomes deep blue, caused by the removal of the second urea NH proton, and subsequent changes to the electronic state of the second napthalenimide, (Figure 3.2). This result was not observed when acetate and dihydrogen phosphate were added in excess, and thus this receptor can be used to discriminate between these sets of anions by eye alone.

Gale and co-workers also have developed colorimetric anion sensors, which use a deprotonation mechanism. These include an amido-pyrrole based receptor, **111,** which is insoluble in acetonitrile in the absence of anions.[121]

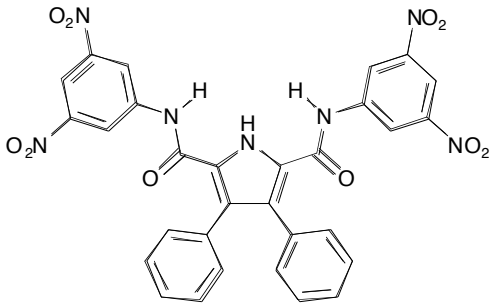

111

The addition of 10eq. of various TBA salts solublises **111**. In the case of fluoride, this solution becomes deep blue, (Figure 3.3). The authors state that the blue colour is due to deprotonation of the central pyrrole molecule and subsequent charge transfer between this and dinitrophenyl appendages.

Fig 3.3 Colour changes seen upon addition of 1 eq. of (left to right), fluoride, chloride, bromide, benzoate, dihydrogenphosphate to an acetonitrile solution of receptor **111**.
Org. Biomol. Chem., **2003**, *1*, 741 – Reproduced with permission of The Royal Society of Chemistry.

More complex systems, such as **112**, have been presented by Gunnlaugsson and co-workers. Receptor **112** is a calixarene appended with four amidourea chains and is colourless in DMSO. It undergoes various colour changes in DMSO solution upon the addition of anions.[122]

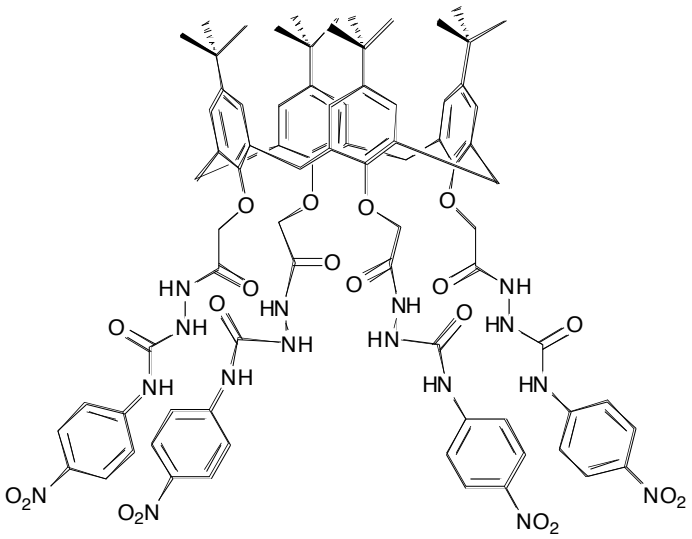

112

The receptor turns deep orange / red in the presence of excess fluoride and pyrophosphate, (Figure 3.4). Strangely, considering its reaction to pyrophosphate, **112** does not change colour in the presence of excess dihydrogenphosphate. The addition of acetate causes the solution to turn yellow, (Figure 3.4). Again, the colour changes are caused by the receptor undergoing deprotonation at the "urea" NH proton adjacent to the *p*-nitrophenyl group, and internal electron transfer to the p-nitrophenyl substituent.

Fig 3.4 Colour changes seen in DMSO solution of receptor **112** (left), upon the addition of (2^{nd} left to right), fluoride, chloride, dihydrogen phosphate, pyrophosphate, acetate, hydrogen sulfate.

The same group have also produced receptors incorporating two amido-thiourea groups appended to a central pyridine ring, to produce receptor **113**.[123]

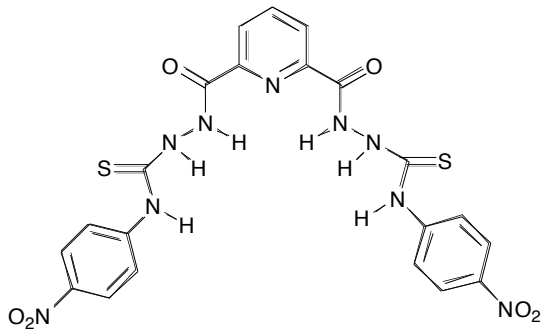

113

This receptor undergoes a stark colour change from colourless to blue upon the addition of the biologically important anions adenosine monophosphate (AMP) and adensosine diphosphate (ADP). Adenosine triphosphate (ATP) does not cause the same response.

The group of Misri and co-workers have also synthesised receptors, which undergo deprotonation-induced colour changes. Receptor **114** consists of a urea appended by naphthyl and a nitro substituted aryl group. It is colourless in DMSO in the absence of any anion.[124]

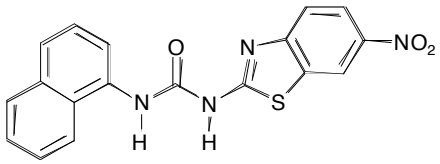

114

With chloride, bromide, iodide and thiocyanate, no change occurs, but with acetate and fluoride the solution changes from colourless to deep orange, caused by deprotonation of the urea NH proton and internal electron transfer to the nitro group.

Others have developed colorimetric anion sensors which operate by switching conformation. Li *et. al*., for example have developed hydrazone based receptors, such as **115**, which binds acetate, (K_a =65,300 M^{-1}) over fluoride, (K_a =27,500 M^{-1}), and dihydrogenphosphate (K_a =12,300 M^{-1}) in DMSO as shown by UV spectroscopy.[125] In the cases of acetate, fluoride and dihydrogen phosphate, the interaction with the receptor is accompanied by a colour change from yellow to dark red, (Figure 3.5).

Fig 3.5 DMSO solutions of receptor **115** (left) and receptor **115** + excess acetate. With kind permission from Springer Science + Business Media: *J. Incl. Phenom. Macrocycl. Chem*. **2009**, *63*, 281. J. Li, Y. Wang, H. Lin and H. Lin.

The authors assert that there is a conformational change upon complexation of the more basic anions, and the selectivity is again due to the relative basicity of the anions, (Figure 3.6).

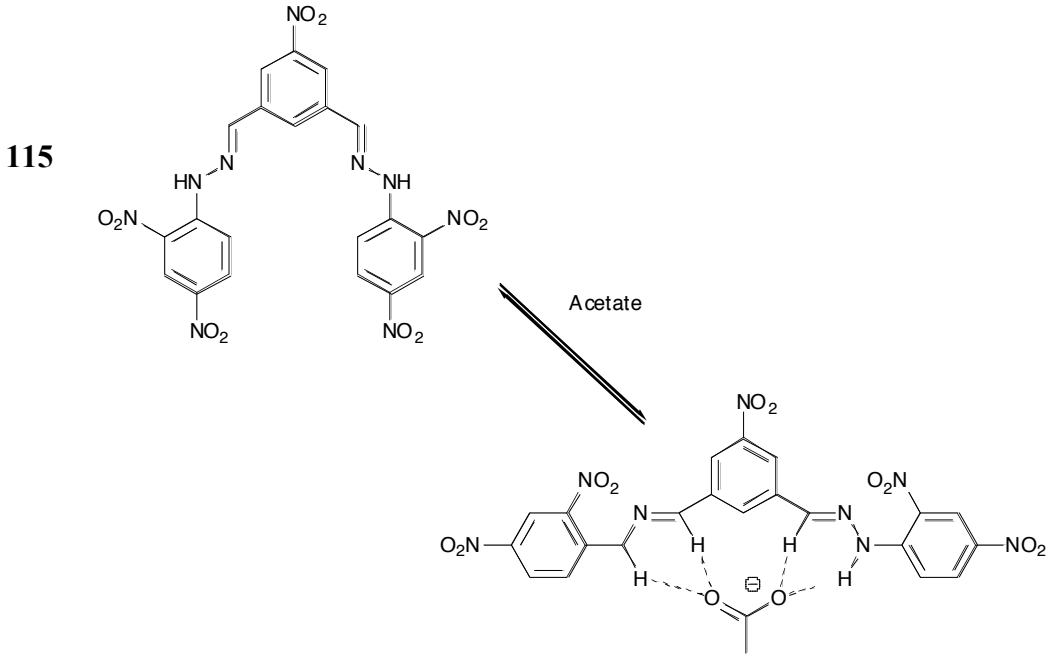

Fig 3.6 Receptor **115** and acetate complex of **115**

Jurczak and co-workers have synthesised a sensor, **116** which has three different colorimetric responses for different anions.[126] Ostensibly a tris-amide with one dinitro substituent, it is colourless in DMSO or acetonitrile.

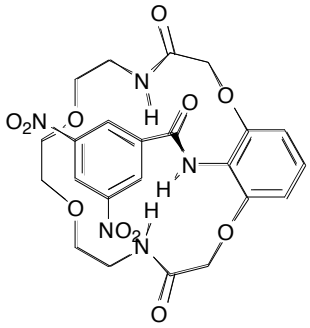

116

Upon addition of excess TBA fluoride in acetonitrile, the solution turns bright blue, (Figure 3.7). With excess TBA acetate, the solution turns orange. With excess dihydrogenphosphate, the solution turns purple. Other anions do not cause colour changes. Binding constants calculated from UV-vis titrations show that the anions are bound according to their basicity in DMSO, ie: fluoride > acetate > dihydrogen phosphate > hydrogensulfate > chloride.

Fig 3.7 Acetonitrile solutions of containing (left to right) **116**, **116** + fluoride, **116** + chloride, **116** + bromide, **116** + acetate, **116** + dihydrogen phosphate, **116** + hydrogen sulfate. *Chem. Commun.,* **2002**, 2450 – Reproduced with permission of The Royal Society of Chemistry.

A colorimetric sensor designed to bind less commonly targeted anions is receptor **117**, developed by Yen and co-workers.[127] This features two ureas, with electron-withdrawing substituents, appended to a central chromophore.

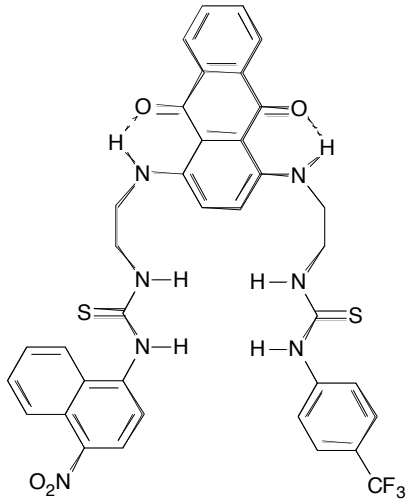

117

The authors found that this receptor is not only capable of differentiating the two isomeric bis-carboxylates, fumarate, (K_a =1,520 M^{-1}), and maleate, (K_a =11,400 M^{-1}) in DMSO (UV-vis), but these same isomers caused two strikingly different colour changes to the solution. The DMSO solution of **117** is bright blue, but with 2 eq. of maleate, it turns a deep red. With 2 eq. of fumarate the solution becomes almost colourless, (Figure 3.8).

Fig 3.8 DMSO solutions of (left to right)receptor **117**, **117** + maleate, **117** + fumarate.
Org. Biomol. Chem., **2007,** *5*, 3592 – Reproduced with permission of The Royal Society of Chemistry.

Displacement Assays

Another method for the detection of anions by colorimetric methods is by displacement assay. In a typical system, the analyte anion is added to a system in which the receptor is already bound to a different anion. If the analyte anion is bound more strongly by the receptor than the other anion, the analyte anion will displace it. For a colorimetric response, the displaced anion will be chosen such that there is a difference between the bound and un-bound colours. Thus, analyte anions may be detected and this method may be used to calculate binding affinities. Sessler and co-workers have used the brightly coloured *p*-nitrophenate anion in a fluoride detection system based on binding to calixpyrrole in DCM.[128] When *p*-nitrophenate is bound to calixpyrrole, it forms a colourless complex. Fluoride is bound far more strongly by this receptor than *p*-nitrophenate, so when a small amount of fluoride is added to the system, this displaces the *p*-nitrophenate, (Figure 3.9). Unbound, the *p*-nitrophenate anion is bright yellow, due to delocalisation of the negative charge onto the nitro group. Even small amounts of free *p*-nitrophenate are visible to the naked-eye, making for a strong naked-eye anion sensor, with potential real-world applications.

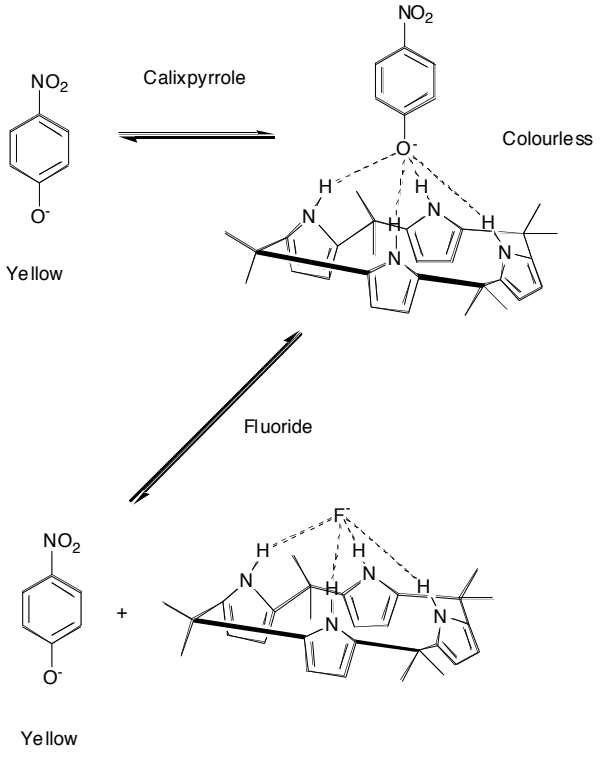

Fig 3.9 Displacement of *p*-nitrophenate by fluoride in the binding site of calixpyrrole in DCM causes a stark change from colourless to yellow

p-Nitrophenate has also been used in a displacement based sensor by Costero and co-workers.[129] Their macrocycles, such as **118** have two amides which bind nitrophenylate until it is displaced from the binding site by fluoride, acetate or dihydrogenphosphate.

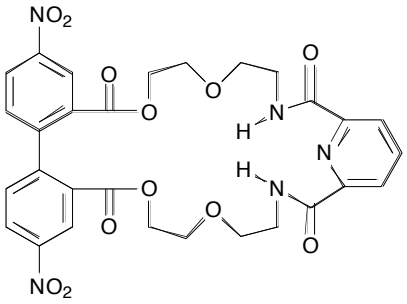

118

In a similar system, Anslyn and co-workers have used 5-carboxyfluoroscein for the detection of citrate in 25%H_2O:MeOH.[130] Their tripodal "pin-wheel" receptor, **119** has three guanidinium groups which bind 5-carboxyfluoroscein in the first instance. Upon addition of the analyte anion citrate, the 5-carboxyfluoroscein is displaced from the binding cleft, and undergoes electronic rearrangement, such that it "switches on" its fluorescence, appearing green to the eye.

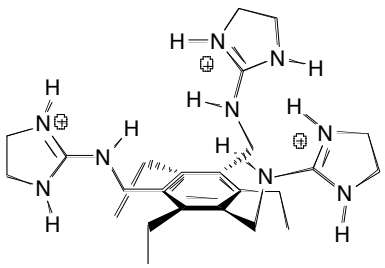

119

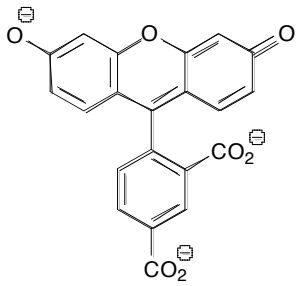

5-Carboxyfluoroscein

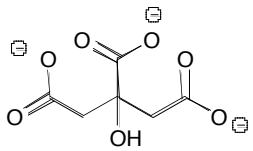

Citrate

A more complicated example has recently been presented by B. D. Smith and co-workers, which is based on a rotaxane, comprising of a thread with a squaraine dye, **120** and macrocycle, **121** which has four amides.[131] When the rotaxane is in aqueous solvent, it adopts a configuration in which the sqauraine moiety is bound to the amides by hydrogen bonds. When chloride is introduced to the system, (as its TBA salt), this competes with the squaraine oxygen atoms, causing displacement of the macrocycle to another point on the thread. This is accompanied by a four-fold increase in fluorescence, from the squaraine dye.

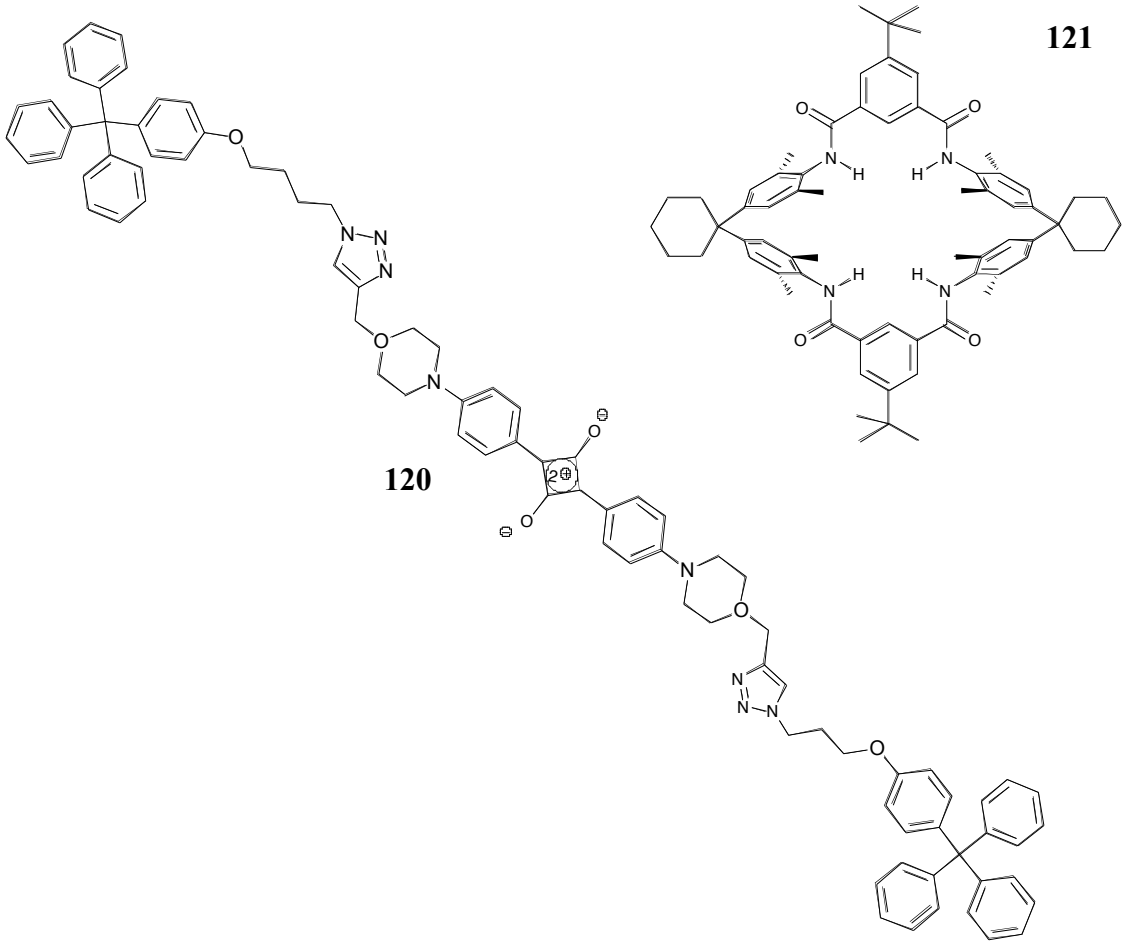

3.2 SCHIFF-BASE / UREA ANION RECEPTORS

3.2.1 Introduction

Schiff-base is another term for the imine group (R-C=N-R') (Figure 3.10). They can be synthesised readily by condensation of the appropriate aldehyde and amine, a process which eliminates water and thus is best conducted under anhydrous conditions.[132] They have found use as spacers and secondary hydrogen bonding groups in various supramolecular structures[133] and in sensors for ions.[134] When two or more Schiff-bases are combined, they can easily bind metals due to the presence of the lone-pair of electrons on the nitrogen atoms.[135] Metallated complexes can also be used as anion receptors.[136] and can form extended systems in the solid state.[137] When combined with pendant hydroxyl groups, a Salen complex of the type **121** is formed, which have found use as catalysts for a vast number of low-temperature organic transformations,[138] including hydrolysis of biologically relevant species[139] and CO_2 /epoxide co-polymerisation.[140]

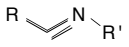

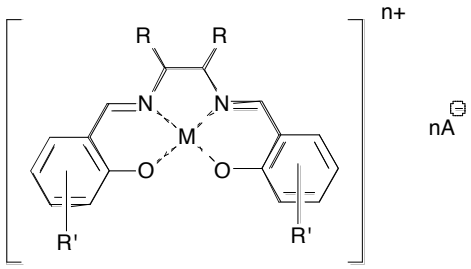

Figure 3.10 Schiff-base (imine) **121**

3.2.2 Synthesis

Four receptors, **122** – **125** were synthesised from commercially available starting materials in three steps, (Scheme 3.1 and Scheme 3.2). Each receptor has either a central benzene or pyridine ring, with two Schiff-bases and two phenyl-urea groups in different positions. It is expected that these should be able to bind anions to a significant extent, as each has two urea NH groups positioned into a cleft.

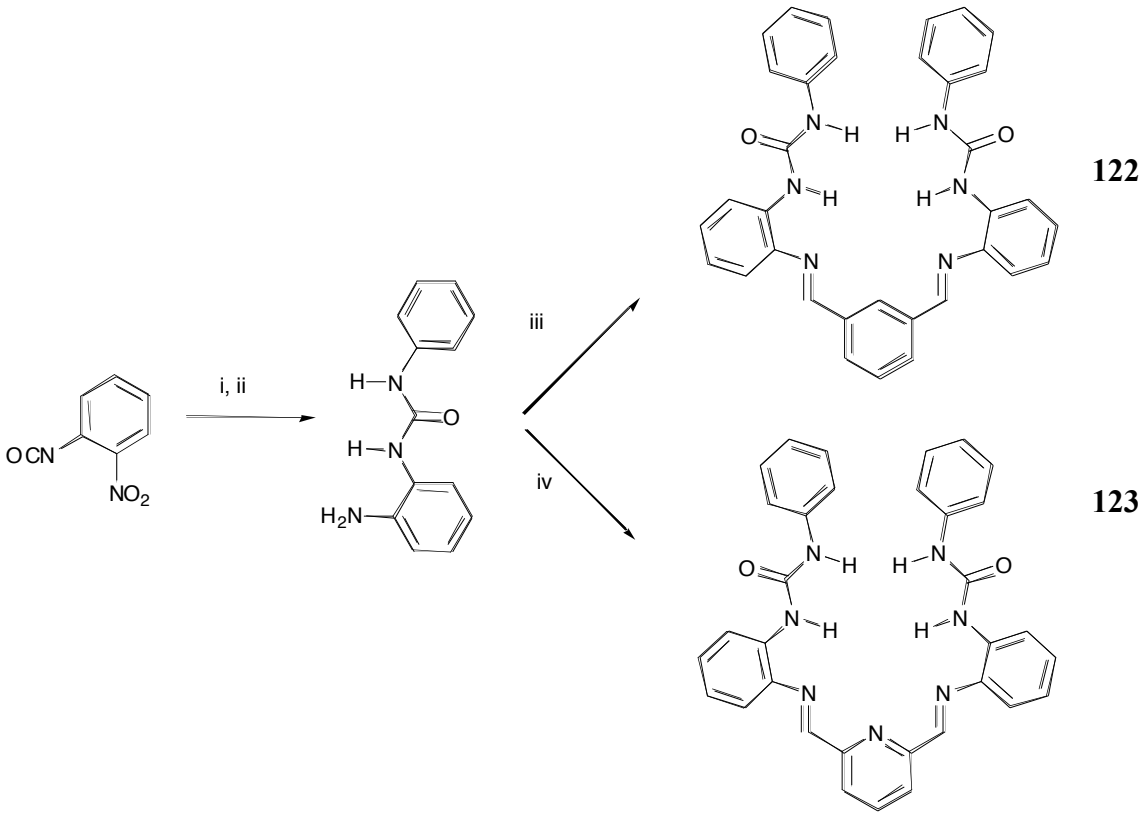

Scheme 3.1 *Reagents and Conditions:* i) Aniline, DCM, RT, 15 min, 98%. ii) NH_2NH_2, Pd/C, EtOH, 24h, 94%. iii) benzene-1,3-dicarbaldehyde, MeOH, reflux under N_2, 48h, 48%, iv) Pyridine-2,6-dicarbaldehyde, MeOH, reflux under N_2, 24h, 44%.

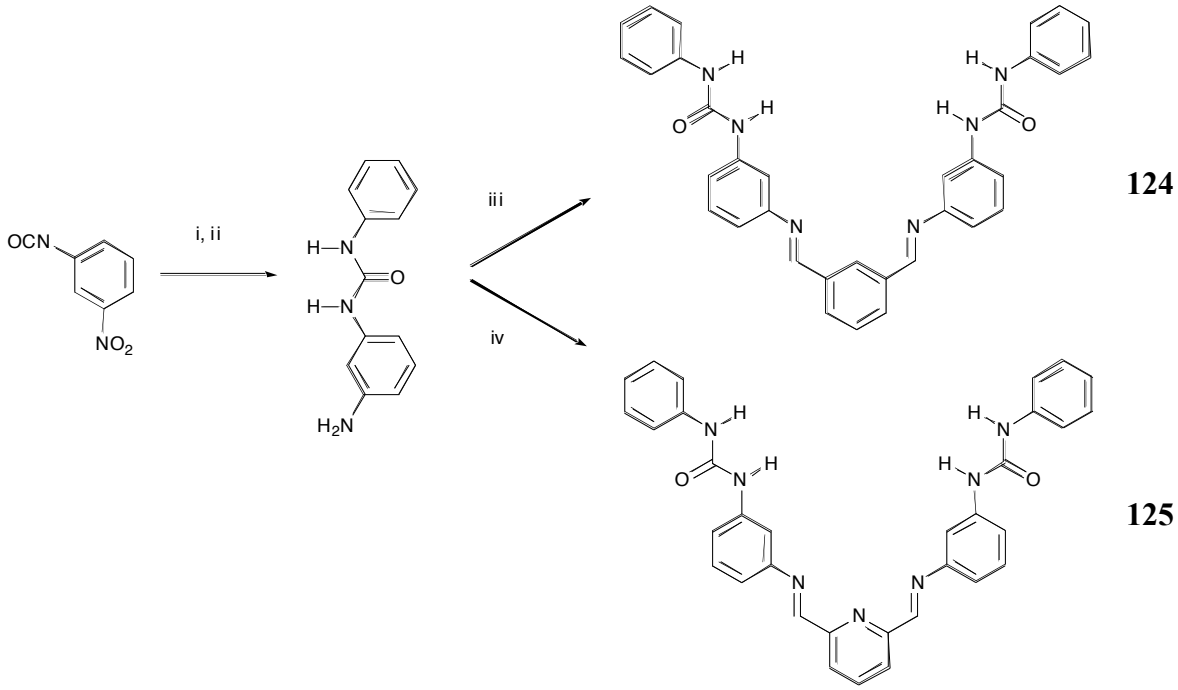

Scheme 3.2 *Reagents and Conditions:* i) Aniline, DCM, RT, 15 min, 93%. ii) H_2, Pd/C, EtOH, 24h, 80%. iii) Benzene-1,3-dicarbaldehyde, MeOH, reflux under N_2, 48h, 60%, iv) Pyridine-2,6-diacarbaldehyde, MeOH, reflux under N_2, xh, 70%.

It is hypothesised that the more open structure of **124** and **125** may make these better receptors for anions, especially carboxylates, because they resemble literature carboxylate receptors such as those by Rebek,[31] Gale,[23] and Werner and Schneider.[32] The series are compared a mono-urea analogue, **95** (Page 72), which has previously been titrated with anions.[36b]

The Schiff-base moieties have been included such that the receptors may be metallated at this position, (Chapter 3.3).

3.2.3 Proton NMR Titration Experiments - Results

Each receptor, **124** – **125**, (Page 108 -109), was studied using ^{1}H NMR titration techniques for binding with benzoate, chloride, hydrogen sulfate and dihydrogen phosphate in 0.5% H_2O:DMSO-d_6 at 298K, (anions added as their TBA salts), (Table 3.1), (Appendix 3). The most downfield urea NH proton was followed in each case. The series is selective for acetate, benzoate and dihydrogen phosphate over chloride and hydrogen sulfate, which is a trend presumably related to the relative basicity of the anions. Each receptor is weaker than a mono-urea comparison compound, **95**.

	AcO^- K_a / M^{-1}	**BzO^-** K_a / M^{-1}	**Cl^-** K_a / M^{-1}	**$H_2PO_4^-$** Ka / M^{-1}	**HSO_4^-** K_a / M^{-1}
122	436 (5)	99 (4)	54 (9)	97 (7)	0
123	69 (3)	37 (7)	0	64 (9)	0
124	45 (20), 2929 (32)	118 (13)	33 (11)	182 (10)	0
125	*a*	262 (10)	0	249 (10)	30 (6)
95	1260	674	31	523	0

Table 3.1 Binding constants (most downfield urea NH proton), (with associated % error) for receptors **122** – **125** with various anions in 0.5%H_2O:DMSO-d_6 at 298K, fitted to a 1:1 (K_a) or 2:1 (K_a , β_2) binding model. (Anions added as TBA salts.) *a* = could not be fitted to a 2:1 or 1:1 binding curve.

Receptors 122 and 123

Receptor **122** binds four of the anions studied in 1:1 complexes. Acetate is bound most strongly, (K_a = 436M^{-1} (± 5%)) with benzoate, (K_a = 99M^{-1} (± 4%), and dihydrogen phosphate, (K_a = 97M^{-1} (± 9%), bound to a similar extent. Chloride, is bound more weakly, (K_a = 54M^{-1} (± 7%), and hydrogen sulfate does not bind to **122**. Receptor **123** also binds acetate most strongly, (K_a = 69M^{-1}(± 3%). Subsequently, a ^{1}H NMR Job plot [122] has shown that this interaction may have a small 2:1 (guest:host) component, with the curve peaking at a molar ratio of host at 0.45. Dihydrogen phosphate, (K_a = 64M^{-1} (± 9%) and benzoate, (K_a = 37M^{-1}(± 7%) are also bound to a moderate extent. Chloride and hydrogen sulfate are not bound by this receptor.

Receptors 124 and 125

Receptors **124** and **125** are both stronger receptors than **122** and **123**. With acetate, receptor **124** forms a 2:1, (guest:host) complex, (K_1 = 45M^{-1} (± 20%), (β_2 = 2,929M^{-1} (± 32%)). The interaction between receptor **125** and acetate could not be fitted to a 1:1 or 2:1 binding model without large errors, and a subsequent Job plot confirmed a mixture of binding stoichiometries, with the molar ratio of host peaking at around 0.40, (Table 3.2), (Appendix 4).[141] With benzoate, receptor **124** forms a 1:1 complex, (K_a = 118M^{-1} (± 13%), whereas **125** adopts a mixture of 1:1 and 2:1 (guest:host) complexes, (Appendix 4). This was confirmed by Job plot in which the molar ratio of host peaks at 0.40, (Table 3.2), (Appendix 4).[141] When ^{1}H NMR titration data for this interaction was fitted to a 1:1 binding model, it gave K_a = 262M^{-1}(± 10%).

Receptor	**Molar Fraction of Host**	
	AcO$^-$	**BzO$^-$**
122	0.50	
123	0.45	
124	0.33	0.50
125	0.40	0.40

Table 3.2 Position of peaks of the Molar Fraction of Host curves for the urea NH protons of receptors **122** – **123** with TBAOAc or TBAOBz (DMSO-d_6), 298K.

With dihydrogen phosphate, receptor **125** is stronger than **124**, (Ka (**125**) = 249M^{-1} (± 10%), K_a (**124**) = 182M^{-1}(± 10%). Receptor **124** binds chloride, (K_a = 33M^{-1}(± 11%), also in a 1:1 complex. Receptor **125** binds hydrogen sulfate weakly, (K_a = 30M^{-1}(± 6%)).

3.2.4 Proton NMR Titration Experiments - Discussion

Despite having twice as many NH hydrogen bond donors as **95**, each receptor in this series is a weaker anion receptor than mono-urea **95**. For receptors **122** and **123**, (Page 105 -106), this result may arise from steric clash between the two pendant urea groups, or urea-stacking, either of which would prevent guest anions from entering the binding cleft. The larger binding constants for oxo-anions are seen for receptors **124**

and **125**. This is presumably because of the open structure of these two receptors, which enable the four urea NH protons to bind the Y-shaped anions simultaneously, (Figure 3.11).

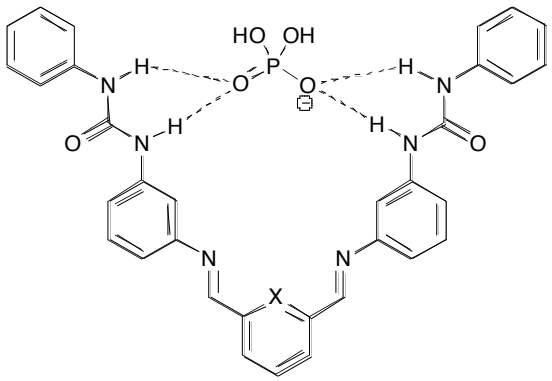

Fig 3.11 Proposed binding mode of dihydrogen phosphate with receptor **124** (X=CH) or **125** (X=N).

Receptor **124** adopts a pure 2:1 (guest:host) binding with acetate, which is a basic anion, strongly attracted to ureas. The pendant urea groups of this receptor are able to rotate freely into divergent positions, in which they are unaffected by other parts of the receptor. In these conformations, there are two efficient oxo-anion binding sites, and 2:1 (guest:host) binding is observed, (Figure 3.12).

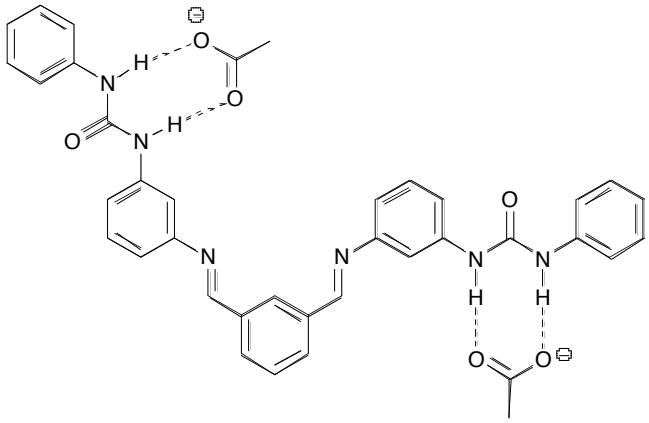

Fig 3.12 Proposed 2:1 binding mode for the interaction between **124** and acetate

When receptor **124** interacts with benzoate, however, a 1:1 complex is observed. It is proposed that this is due to the lower basicity of benzoate compared to acetate. Benzoate does not adopt a 2:1 stoichiometry, because this requires the formation of many relatively weak hydrogen bonds between the receptor and the anion. It is also unfavourable in terms of entropy. The more stable 1:1 complex is formed in this case, because it gives rise to a stronger interaction between host and guest, and there is a lower entropic penalty associated with its formation, (Figure 3.13).

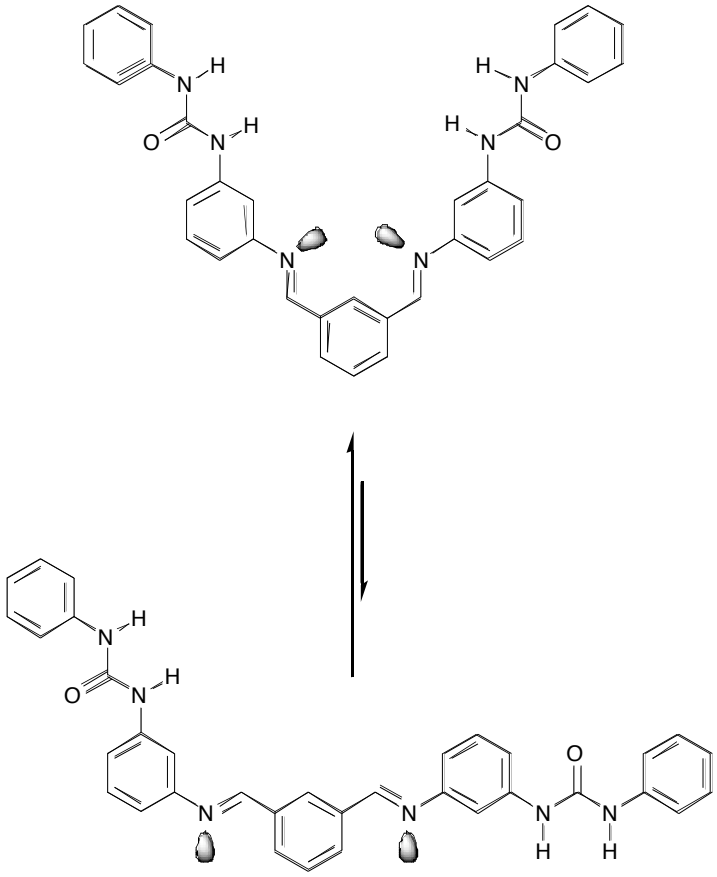

Fig 3.13 Lack of electronic repulsion enables receptor **124** to adopt a predominantly convergent conformation with benzoate.

Receptor **125** binds both acetate and benzoate with a mixture of 1:1 and 2:1 (guest:host) stoichiometries, (Appendix 4). These observations are likely to arise from increased electrostatic repulsion between the three "internal" nitrogen lone-pairs of electrons, which opens up the cleft of **125** into a divergent conformation, (Figure 3.13), in which the urea groups may bind two equivalents of anion. In the case of benzoate, it follows that a higher proportion of 2:1 (guest:host) conformation would be seen, and this is indeed what is observed, (Figure 3.14).

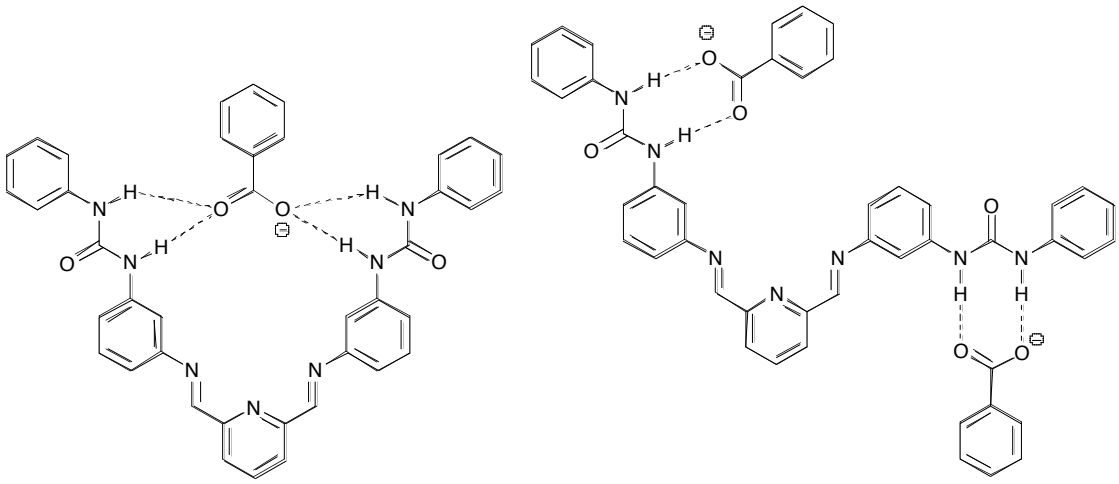

Fig 3.14 Proposed 1:1 and 2:1 binding modes for the interaction between **125** with benzoate

What is less clear, is how this electronic repulsion allows the existence of a 1:1, acetate:**125** complex, whereas a 2:1 (guest:host) complex is exclusively adopted between this anion and receptor **124**. It may be that the presence of a third internal nitrogen lone-pair causes greater conformational mobility around the centre of the receptor, giving an opportunity to form the more entopically favourable 1:1 complex in addition to the 2:1 (guest:host) complex, (Figure 3.15).

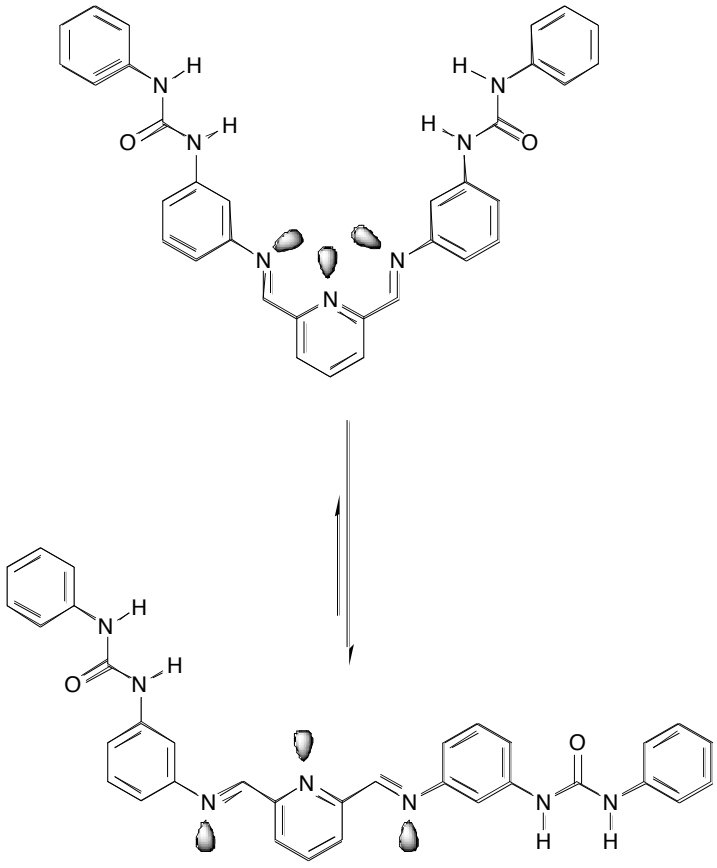

Fig 3.15 Electronic repulsion causes receptor **125** to adopt convergent and divergent conformations in solution.

Receptor **123** adopts a mixture of binding modes with acetate. This is thought to be due to the central pyridine ring encouraging a divergent conformation by electronic repulsion, (Figure 3.16). This forms two binding sites and thus gives rise to a significant proportion of the 2:1 complex. Receptor **122** does not have the same degree of electronic repulsion and so is able to form a convergent cleft. This enables anions to be more strongly bound, and hence enables the weak complexation of chloride.

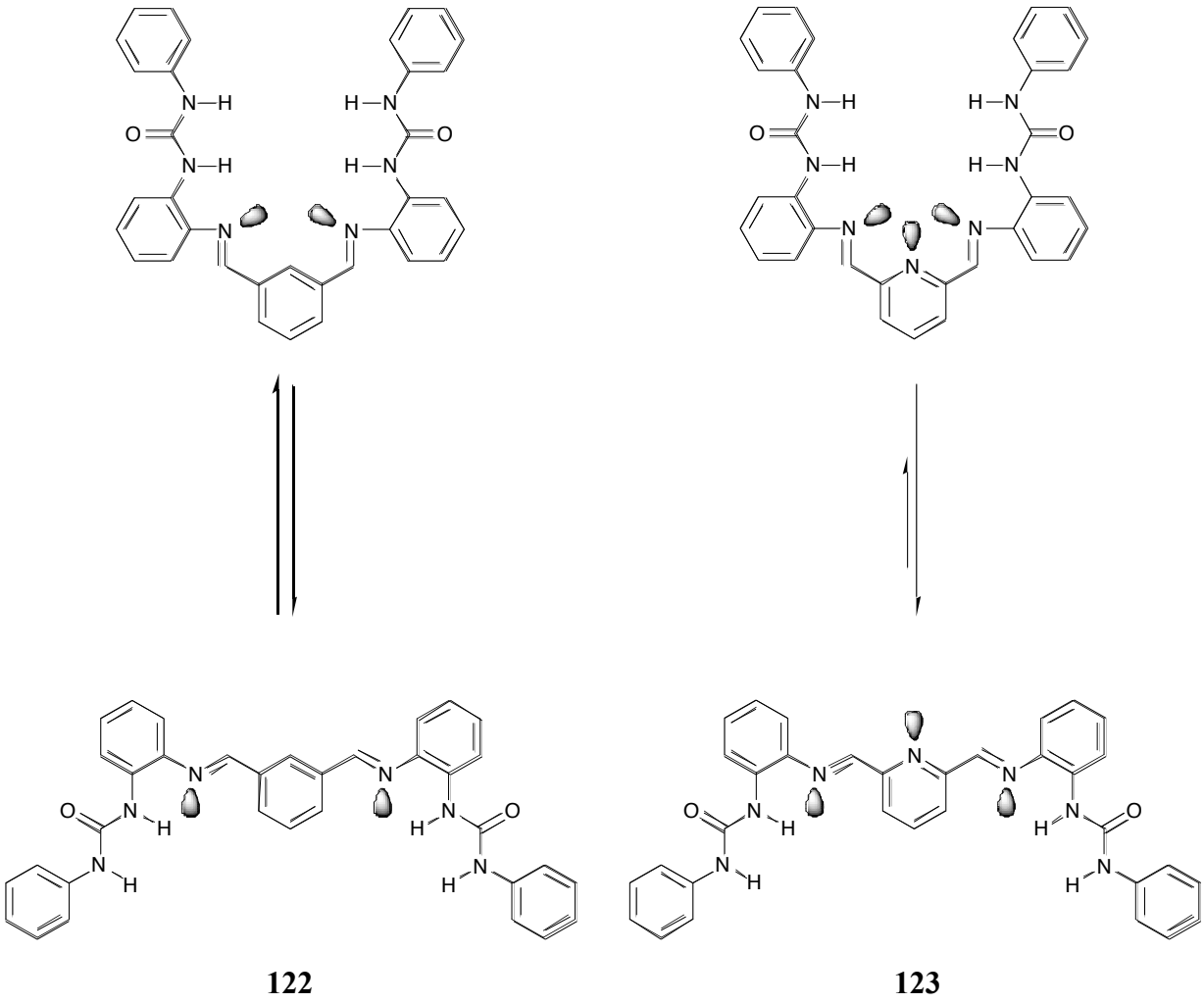

122 **123**

Fig 3.16 Electronic repulsion causes different relative concentrations of 1:1 and 2:1 (guest:host) conformations for receptors **122** and **123** in DMSO solution

3.3 METAL CHLORIDE COMPLEXES OF A SCHIFF-BASE - UREA

3.3.1 Introduction

A cobalt (II) chloride complex, **126**, was synthesised by reaction of receptor **123** with 1eq. of anhydrous cobalt (II) chloride in dry THF. Its formation was associated with a stark colour change from the yellow of the ligand to dark green. Cobalt (II) complexes (d^7) can have a large variety of colours, making them intrinsically interesting targets. For example, the hexa-aquo complex $[Co(H_2O)_6]^{2+}$ is pink, whereas the tetrahedral complex $[CoCl_4]^{2-}$ is bright blue.[142] This is due to the adoption of the low-spin state in the octahedral case and the high-spin state in the tetrahedral case. More subtle changes are observed with different ligands, according to the spectro-chemical series.[143] The wide range of colours produced is widely exploited in biological studies in which UV-vis inactive zinc functions are investigated using cobalt. An analogous zinc complex **127** was also made in parallel.

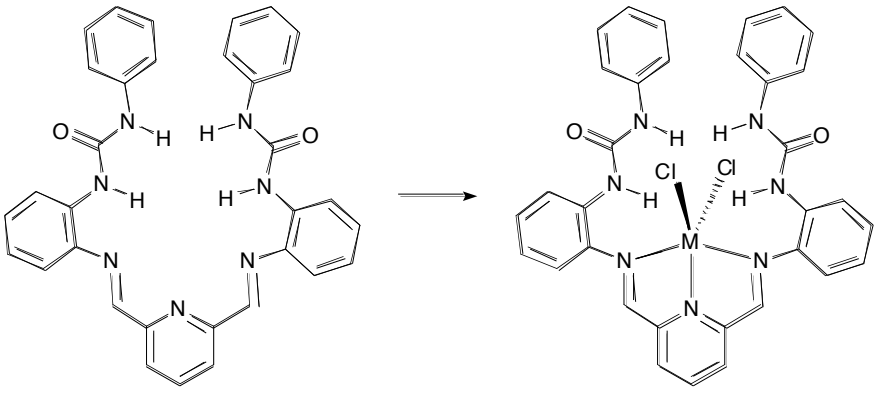

123 → **126** (M = Co^{2+})
127 (M = Zn^{2+})

Scheme 3.3 *Reagents and Conditions:* Under N_2, MCl_2 (anhydrous), THF, 24h, RT, 98% mass rec'd.

3.3.2 Colorimetric Sensor for Anions

It was observed that complex **126** undergoes a stark colour change with various anions in DMSO. A 0.01M solution of complex **126** is yellow in DMSO in the absence

of any anion. Upon addition of 1 eq. various alkyl-ammonium salts, a number of colour changes were observed, (Figure 3.17).

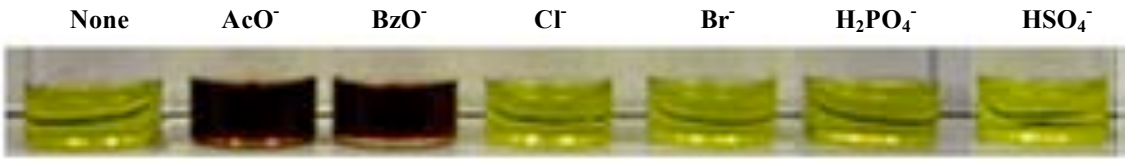

Fig 3.17 Colour changes induced in DMSO solutions of complex **126** by addition of 10eq. of the TBA salts of various anions

With acetate and benzoate the solution becomes deep brown / red. With chloride the solution becomes apple green, and with dihydrogen phosphate the solution becomes slightly blue. These two colours became more intense upon the addition of a further 9 eq. of the appropriate anion, (Figure 3.18). Bromide and hydrogen sulfate did not affect the colour of the solution.

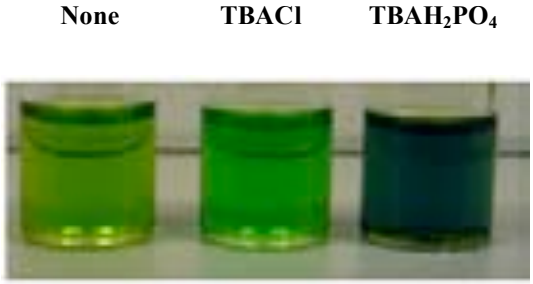

Fig 3.18 Intense colour changes induced in DMSO solutions of **126** upon addition of 10eq. of TBACl or $TBAH_2PO_4$

3.3.3 UV-Visible Spectroscopy - Initial Studies

In order to determine the possible causes of the stark colour changes seen upon the addition of chloride and dihydrogen phosphate, UV-vis experiments were conducted. In the first instance, the following solutions were studied;

a) Complex **126** in DMSO,
b) Complex **126** + 10eq. TBACl in DMSO,
c) Complex **126** + 10eq. $TBAH_2PO_4$ in DMSO.

Complex **126** has υ_{max} = 520nm, but upon addition of chloride, the spectrum changes dramatically, with a new series of peaks emerging from 600 - 700nm, (Figure 3.19). The addition of dihydrogen phosphate causes the emergence of a number of peaks from 580 - 675nm, as well as a reduction in the intensity of the original peak at 520nm. With acetate and benzoate, there is a dramatic increase in the intensity of the peak at 520nm, which unfortunately masks any peaks that may exist in other regions of the spectra.

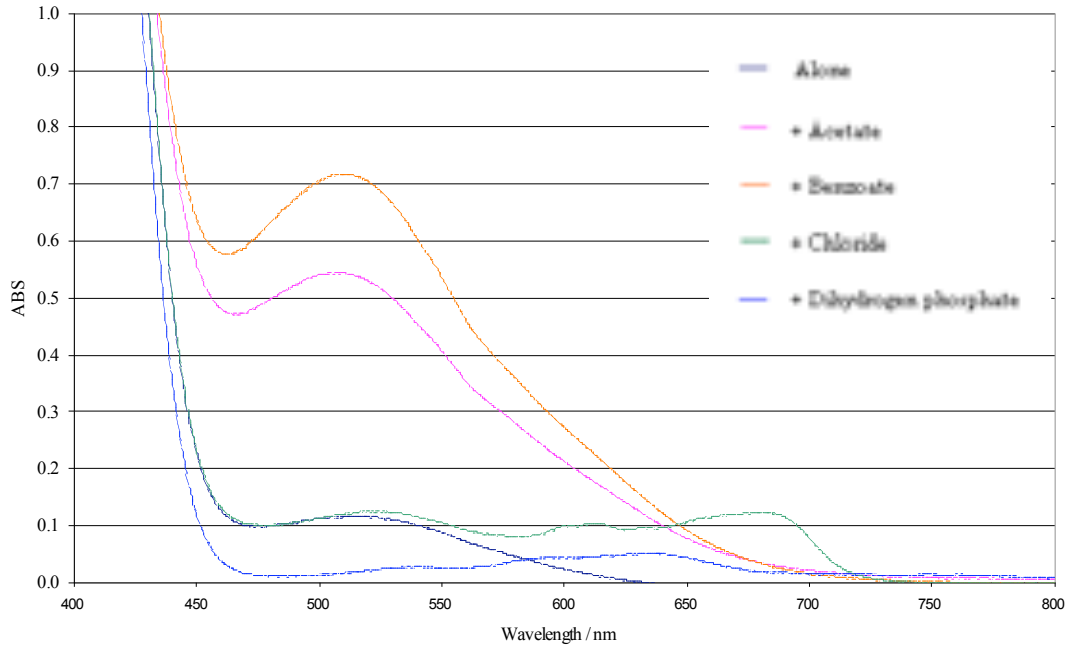

Fig 3.19 UV-visible spectra (DMSO) of complex **126** with 10eq. of various TBA salts

Discussion

The peaks which arise upon addition of chloride are brought about by the presence of the stable $[CoCl_4]^{2-}$ dianion.[143] This peak is not observed in the spectrum of **126** in the absence of TBACl, and so it is thought that the addition of 'free' chloride ions causes **126** to revert to **123** and $CoCl_2$. The $CoCl_2$ then forms $[CoCl_4]^{2-}$ with the "free" chloride. It is not possible to observe if the dianion interacts with the receptor **123**. Upon the addition of dihydrogen phosphate, it is thought that the cobalt is also displaced due to the appearance of the new peaks. This is likely to be due to the formation of other cobalt species such as octahedral mixed cobalt aquo-chloride complexes.

It is thought that a different process is involved upon the addition of carboxylates, because these anions cause a substantial increase in the intensity of the peak at 520nm. It is possible that this is due to deprotonation of **123** as it is formed after displacement of the cobalt. This is thought unlikely, because deprotonation by these anions was not observed during NMR titration, (Chapter 3.2), although it is possible that this could be checked by H/D exchange experiments. It may be possible that the presence of these relatively basic anions deprotonates the complex, **126**, giving rise to the peaks seen.

3.3.4 Further UV-Visible Spectroscopy

To check for the presence of $[CoCl_4]^{2-}$ and analogous tetrahedral cobalt anions, further UV-vis experiments were conducted. Initially, $CoCl_2$ was dissolved in DMSO, (0.002M). A 10eq. excess of the TBA salt of each anion; acetate, benzoate, chloride and dihydrogen phosphate was then added to this stock, and UV-vis experiments were performed on each solution, (Figure 3.20).

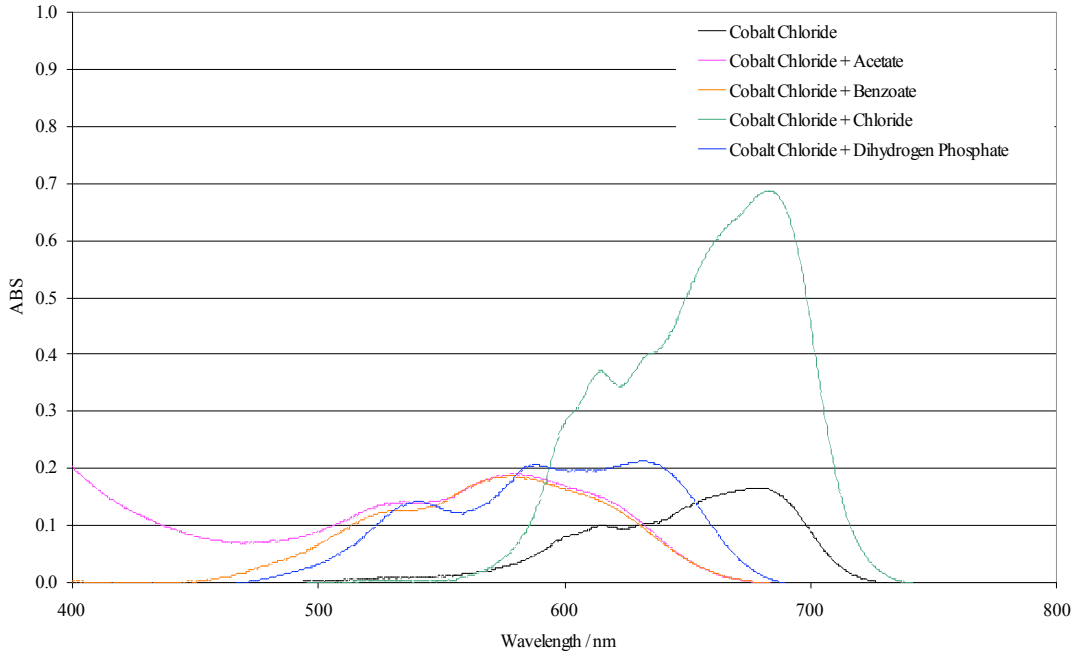

Fig 3.20 UV-visible spectra (DMSO) of $CoCl_2$ with 10eq. of various TBA salts

Results

The solution of $CoCl_2$ produced a spectrum consistent with the formation of $[CoCl_4]^2$ in solution. Upon the addition of chloride, each peak increased in intensity, showing that excess chloride forces the equilibrium of the disproportionation equilibrium to favour a greater proportion of $[CoCl_4]^{2-}$. This confirms that $[CoCl_4]^{2-}$ is the cobalt species formed in the initial experiments (with chloride), and that it is only formed from **126** when excess chloride is supplied. Upon the addition of dihydrogen phosphate, the same set of peaks is observed as seen in Chapter 3.3.3. This is thought to be caused by superposition of the UV-vis spectra of several unidentified mixed cobalt

chloride / aquo species. With acetate and benzoate, a new set of peaks is also seen, which were not seen in the previous experiments, possibly due to being masked by the presence of the peak at 520nm. It is tentatively hypothesised that in both of these cases, the spectrum is the result of a superposition of several cobalt species with differing structures.

3.3.5 Conclusion - (UV-Visible Spectroscopy)

The cobalt complex **126** acts as an effective colorimetric sensor for several common anions, producing a range of colours with different anions. These are thought to arise from the removal of the cobalt centre from the organic ligand, **123**, by competition from the analyte anions, a process which enables the formation of various cobalt complexes. In the case of chloride $[CoCl_4]^{2-}$ is formed. In the case of dihydrogen phosphate it is less clear, although it is possible that a mixture of mixed aqua-chloride cobalt complexes are formed. The apparent colours seen upon the addition of chloride and dihydrogen phosphate are brought about by a superposition of the yellow colour of the ligand and the various blue - green colours of the cobalt complexes. It is not possible to ascertain whether or not any charged cobalt species and **123** interact in solution.

It is thought that **126** is deprotonated by the carboxylates, leading to a more intense ligand peak, due to increased internal electron transfer. It is not possible to tell whether or not cobalt species are formed in this case because the ligand peak masks the rest of the spectrum.

3.4 SOLID STATE ANALYSIS

It was not possible to obtain crystals of **126** that were suitable for X-ray crystallography, but the suitable crystals were obtained of the analogous UV-inactive zinc structure **127**, which was prepared crude from **123** and anhydrous $ZnCl_2$ in THF with no purification. The crystals obtained show the zinc centre bound to the two Schiff-base nitrogen atoms, the pyridyl nitrogen atom and two chloride anions.

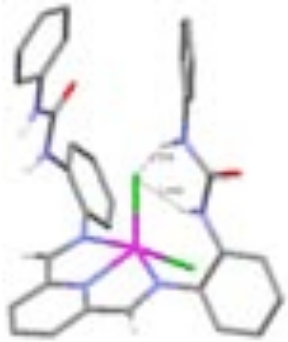

Figure 3.21 View of solid state structure of **127**

One of these is hydrogen bonded to one of the pendant ureas. The other pendant urea is not hydrogen bonded to the other chloride. Instead, this is bound to a pendant urea on a neighbouring molecule. This forms a urea-stack along the c-axis.

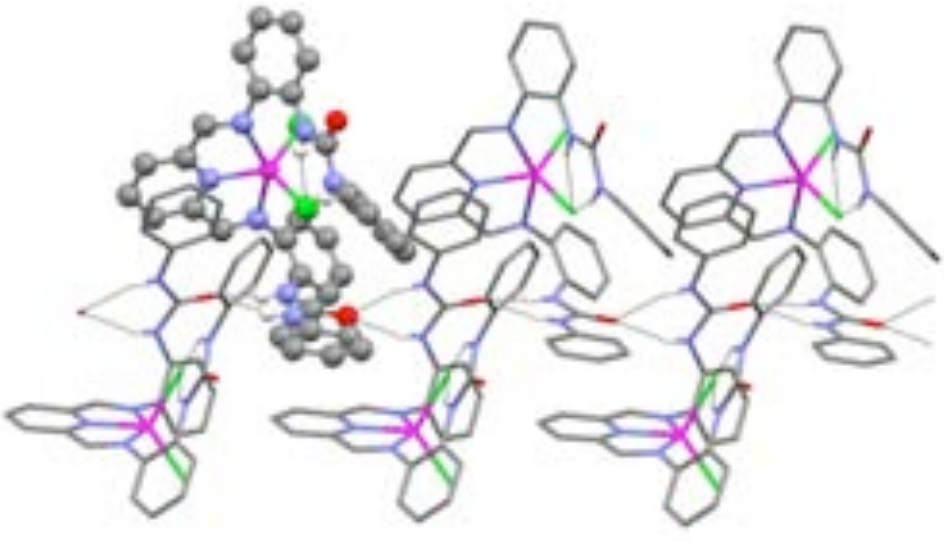

Figure 3.22 Hydrogen bonding chain propagates through **127** by urea stacking down the c-axis

Although it has not been possible to obtain crystals of the UV-vis active cobalt complex **126** it is thought that the zinc structure may be similar. Indeed, the activities of cobalt and zinc are similar to the extent that cobalt can be used as a zinc mimic in order to study biological systems by UV-vis.

3.5 CONCLUSION

The series of ligands **122 - 125** are moderate receptors for anions, which exhibit mixtures of 1:1 and 2:1 (guest:host) stoichiometries in solution. The cobalt chloride complex **126** exhibits interesting colour changes in DMSO solution in the presence of excess (10eq.) TBA chloride and TBA dihydrogen phosphate. The source of these colour changes is due to the formation of $[CoCl_4]^{2-}$ and other cobalt species. These are thought to arise as a result of the displacement of the cobalt centre from the Schiff-base binding site. The system can be described as a pseudo-displacement assay, in which the analyte anions displace the metal centre from one set of ligands to form a new complex, resulting in a colour change. With acetate and benzoate, this is not thought to be the case. Instead, it is thought that these anions may deprotonate **126**.

In order to further characterise the behaviour of this system, one can envisage experiments in which a large excess of a known dihydrogen phosphate or chloride receptor is added to a solution of complex **126** and excess anion. A sufficiently strongly competing receptor would bind the anion, thus allowing the reversibility of the system to be assessed.

CHAPTER 4 – ISOPHTHALAMIDE DERIVATIVES WITH ACTIVATED CH HYDROGEN BOND DONORS

4.1 INTRODUCTION

4.1.1 CH hydrogen bond donors

As seen in the introduction, the vast majority of synthetic neutral anion receptors bind anions using NH hydrogen bond donors. Occasionally, they also incorporate CH hydrogen bond donors, but these are often unintended, as seen in the carbazole crystal structure of Jurcak and co-workers,[47] (Chapter 1.4.4). Generally, CH bonds are not considered particularly acidic, and there was thought to be little scope for successful anion complexation compared with conventional NH hydrogen bond donors. This view has recently been challenged, however, with the development of several excellent CH hydrogen bond receptors.

4.1.2 Receptors containing 1,2,3-triazoles

The principle CH hydrogen bond donor used to date is 1,2,3-triazole, **128**, which has found use in several recent receptors. It has an acidic CH bond (pK_a = 1.2) caused by electron withdrawing effects within the triazole ring, (Figure 4.1).

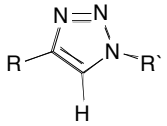

Fig 4.1 1,2,3-triazole, **128**, appended with different R groups. Acidic proton shown.

Several groups have made use of this property in recent anion receptors. For example, Craig and co-workers have made oligotriazole receptors, such as **129** and **130**, which contain two and four 1,2,3-triazole units respectively.[144]

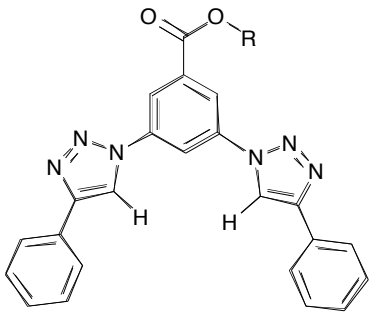

129

Proton NMR experiments in acetone-d_6 show that **129** binds chloride (K_a = 1,260M^{-1}) and benzoate (K_a = 1,150M^{-1}) to a similar extent, (anions added as their TBA salts). Bromide is bound more weakly than these (K_a = 470M^{-1}), and iodide (K_a = 43M^{-1}), hydrogen sulfate (K_a = 160M^{-1}), and nitrate (K_a = 35M^{-1}), are bound to a lesser extent. Receptor **130** is a significantly stronger anion receptor, an unsurprising result considering that it has twice as many hydrogen bond donors as **129**. In this case, the halides are bound most strongly, (K_a (I^-) = 14,000M^{-1}), (K_a (Cl^-) = 12,000M^{-1}),

(K_a (Br^-) = 11,000M^{-1}), followed by benzoate, (K_a = 4,300M^{-1}), hydrogen sulfate (K_a = 2,700M^{-1}), and nitrate (K_a = 910M^{-1}).

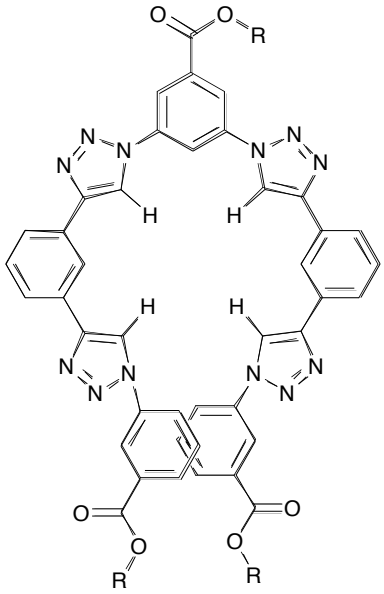

130

The selectivity for halides is due to the ability of **129** to wrap into a roughly spherical central cleft, enabling hydrogen bonding between the halide and all four CH protons. There is also a small contribution from the other internal CH protons. Non-spherical anions cannot be accommodated well in this cleft, and so are bound by a lower number of hydrogen bond donors, and hence are more weakly bound.

Flood and co-workers have also found that a macrocyclic analogue of **130**, receptor **131** is selective for halides.[145] By UV-vis titration in acetonitrile, **131** binds chloride (K_a = 1.1 x 10^7 M^{-1}), over bromide (K_a = 6.7 x 10^6 M^{-1}), fluoride (K_a = 2.8 x 10^5 M^{-1}), and iodide (K_a = 1.7 x 10^4 M^{-1}).

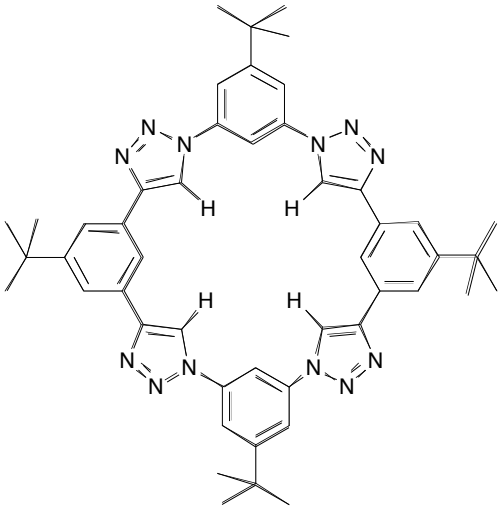

131

The authors suggest using computer modelling, that chloride has the optimum size for complexation to the macrocycle. Bromide is also of a suitable size. In both of these cases, there is also a small hydrogen bonding contribution from the four internal phenyl CH protons. Fluoride was seen to bind only to one triazole CH in computer models, and iodide is too large to fit in the binding cavity. This explains their relatively poor binding affinities compared to chloride, which is of the optimum size for binding to all four triazole CH bonds. This structure has since undergone significant systematic study and adaptation in order to probe its properties.[146]

Gale and co-workers have appended 1,2,3-triazole to the already successful chloride receptor, calixpyrrole, synthesising a strapped calixpyrrole **132,** which has a mixture of NH and CH hydrogen bond donors.[147]

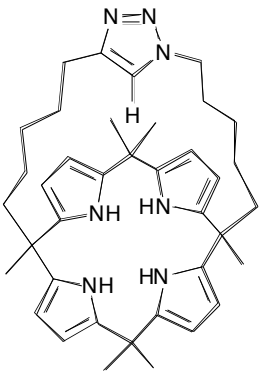

132

Using ^{1}H NMR titration, it was observed that **132** binds chloride strongly. However, the interaction suffered from slow exchange relative to the NMR timescale. Using isothermal titration calorimetry in acetonitrile, the group was able to ascertain that **132** binds chloride one order of magnitude more strongly than calixpyrrole. This technique also identified that the interaction has a very high entropic contribution, arising from a high degree of pre-organisation.

4.1.3 Receptors containing imidazolium salts

Triazoles are by no means the only CH hydrogen bond donors investigated. For example, imidazolium salts have been used by Steed and co-workers in systems such as the appended calixarene **133**.[148]

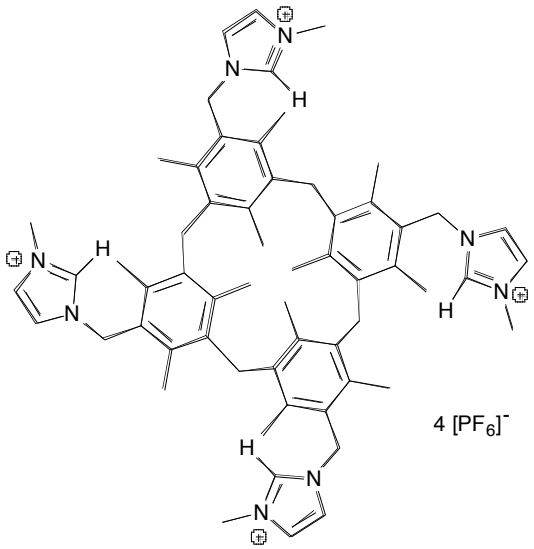

133

As receptor **133** is a charged species, high binding affinity towards anions may be expected. For this receptor ^{1}H NMR Job plots were used to confirm the presence of 2:1 as well as 1:1 binding with nitrate, bromide, chloride, acetate and malonate.[141] This result is due to the flexible nature of calixarenes, which have the ability to rotate into several different conformations, in which the CH protons may be convergent or divergent, and thus can provide multiple binding sites.

Imidazolium salts can also be used in combination with conventional NH hydrogen bond donors. Tomapatanaget and co-workers for example, have synthesised receptor **134**, which combines one imidazolium salt and one amide.[149]

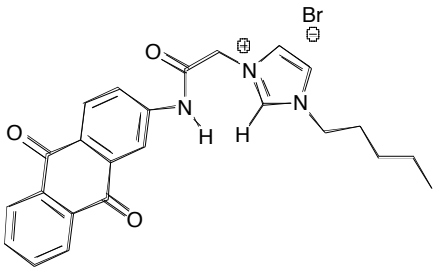

134

Upon addition of fluoride or acetate in DMSO, the UV-vis spectrum undergoes stark changes in the region between 370nm and 600nm. This is due to deprotonation at the amide. Each of the anions studied was seen to bind in a 1:1 complex with **134** according to Job plot analyses carried out by ^{1}H NMR. The binding affinities were found to be linked to the basicity of the anions by UV-vis spectroscopy in DMSO; logK_a (Cl^-) = 3.71, logK_a (Br^-) = 3.63, logK_a ($H_2PO_4^-$), logK_a ($C_6H_5CO_2^-$) = 5.63. Values could not be obtained for fluoride or acetate due to the combined processes of deprotonation and binding.

Others have made biologically relevant imidazolium salt containing receptors, such as Kim and Yoon, who have used multiple imidazolium salts appended with anthracenes to detect ATP by fluorescence.[150] An example of this type of receptor is **135**.

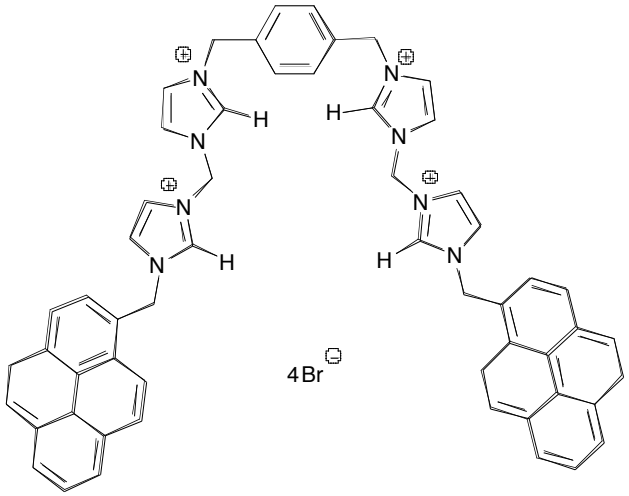

135

Upon addition of ATP to **135**, the authors observed a stark change in fluorescence, which was attributed to the ability of adenosine to undergo π-stacking between the two anthracenes whilst the triphosphate is bound to four imidazolium groups. The effect was not seen upon addition of other the nucleoside-triphosphates, UTP, TTP, GTP and CTP. They caused fluorescence quenching because due to only π-stacking to one anthracene group.

Imidazolium groups have also been used in ditopic receptors and more complex molecular machines by combining imidazolium salts and bipy groups. Fabbrizzi and co-workers have developed **136,** which contains anion and metal binding sites.[151]

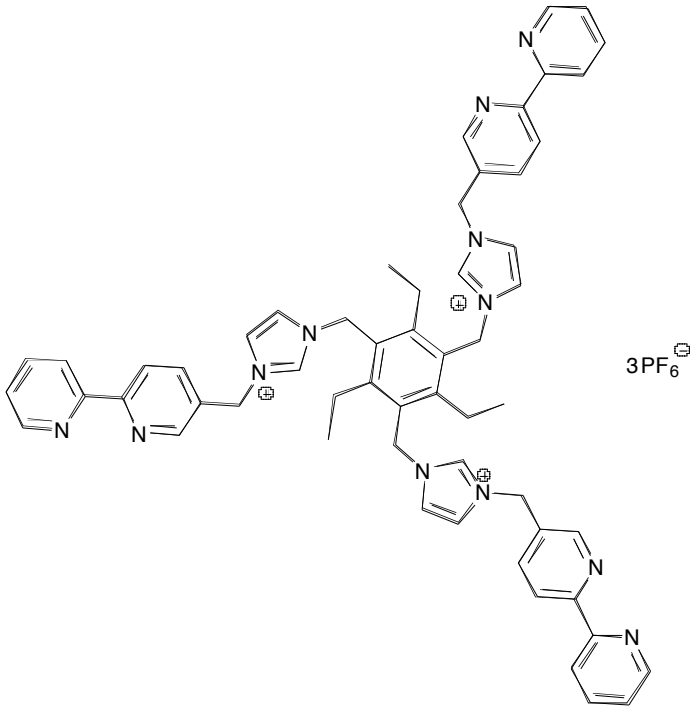

136

When cobalt III is introduced to **136** followed by chloride in acetonitrile, the chloride is bound the three imidazolium salt goups and the cobalt is bound by the three bipy groups (Figure 4.2).

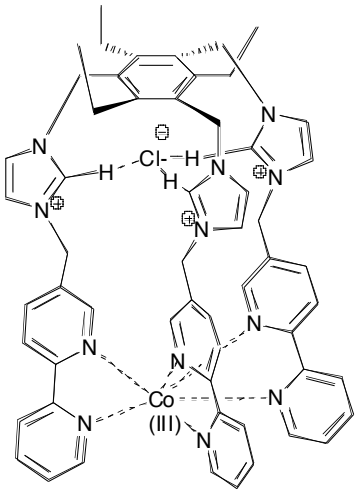

Figure 4.2 Tripodal Co(III) chloride complex formed by **136**

4.2 NITRO-ACTIVATED ISOPHTHALAMIDE DERIVATIVES

4.2.1 Introduction

Since 1997, the "Crabtree" isophthalamide motif, **19** and derivatives of it, such as **23**, have proved to be a popular basis for many larger anion binding motifs, because of the excellent affinity for anions of this type of structure, as described in Chapter 1.

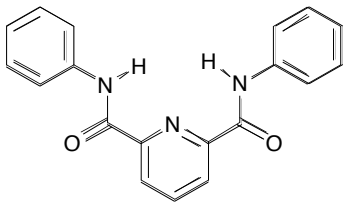

23

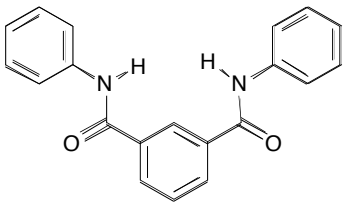

19

A central appended pyridine ring, such as that seen in **23**, is often chosen because of favourable internal electrostatic interactions formed between the pyridine nitrogen and the amide NH protons when the receptor is unbound. This pre-organises the receptor into a *syn-syn* conformation, suitable for hydrogen bonding to anions. In the case of receptor **19** no such interaction is present in the unbound state, leaving it relatively free to rotate about the amide bonds and adopt conformations unfavourable for binding, (Figure 4.3). It is also possible that in the *anti-anti* and *syn-anti* conformations the amide proton clash with the protons on the central ring, further disfavouring these conformations.

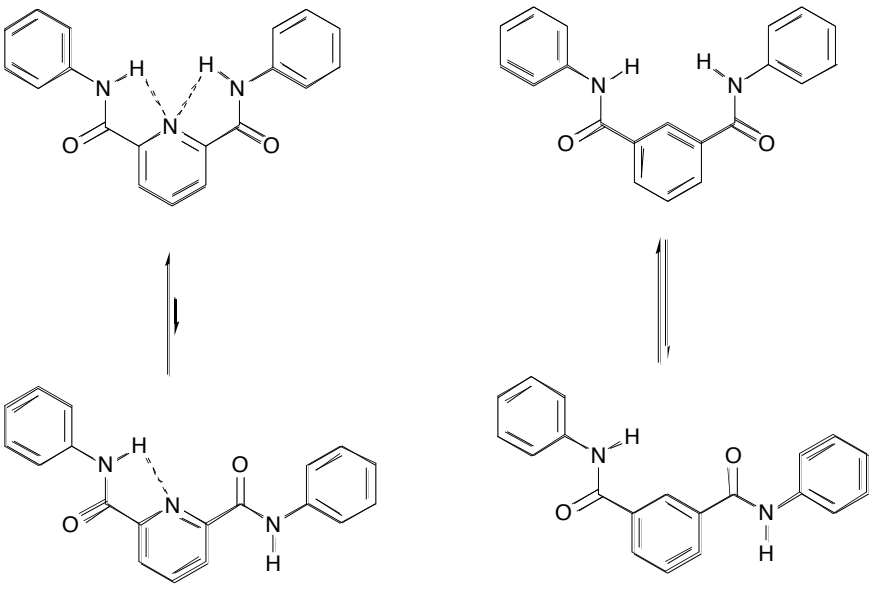

23 **19**

Fig 4.3 Relative proportions of *syn-syn* and *syn-anti* conformations for receptors **23** and **19** are dependant upon intramolecular hydrogen bonds.

4.2.2 CH hydrogen bond donor activation

By addition of electron-withdrawing groups to the pendant phenyl groups it may be possible to activate those CH protons which face into the cleft of the receptor. Nitro groups have been chosen because they are excellent electron withdrawing groups and many nitro derivatives of aniline are readily available. Receptors based on **23**, (**137 – 139**), were synthesised from 2,6-pyridine diacid chloride and the appropriate aniline derivatives in DCM, (Scheme 4.1). These contain two or four nitro groups appended in various positions in order to enhance the binding affinity for anions.

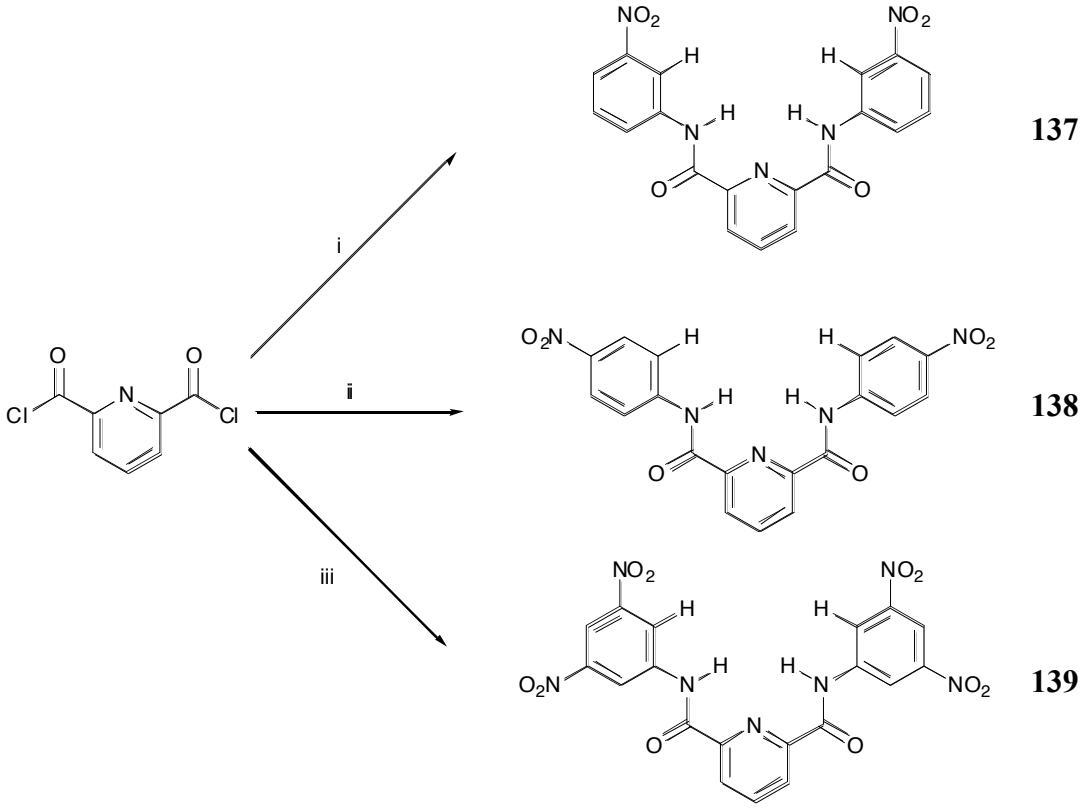

Scheme 4.1 *Reagents and Conditions:* **i)** 2eq. 3-nitroaniline, DCM, 2h, 23%.
ii) 2eq. 4-nitroaniline, DCM, 24h, 63%. **iii)** 2eq. 3,5-dinitroaniline, DCM, 48h, 50%.

In receptor **137**, the CH protons shown are activated by the nitro groups by a mesomeric mechanism. In receptor **138**, it is the amide NH which is activated. In receptor **139**, the CH protons are activated by two nitro substituents, and they have a higher chemical shift, (Chapter 6.3.3). Thus it is expected to be a better anion receptor

than **137** and **138**. For comparison, receptor **23** will also be studied, and is expected to be poor compared to **137** – **139**.

4.2.3 Proton NMR Titration Experiments - Results

The receptors in the series, **137** – **139**, and literature receptor **23** were studied using ^{1}H NMR titration techniques for binding of fluoride, chloride and bromide in DMSO-d_6 at 298K, (Table 4.1), (Appendix 3). The anions were added as their TBA salts.

i	(K_a / M^{-1}) **F** $^-$	(K_a / M^{-1}) **Cl** $^-$	(K_a / M^{-1}) **Br** $^-$
23	s	<10	0
137	s	30 (3)	0
138	s	30 (3)	0
139	s	143 (4)	73 (10)

ii	(K_a / M^{-1}) **F** $^-$	(K_a / M^{-1}) **Cl** $^-$	(K_a / M^{-1}) **Br** $^-$
23	s	<10	0
137	s	33 (3)	0
138	s	25 (38)	0
139	s	138 (3)	103 (9)

Table 4.1 Binding constants (with associated % errors) for receptors **23** and **137**–**139** with halides for; **i**) the NH amide proton, and; ii) the activated CH proton.
(s = strong interaction which does not fit 1:1 or 2:1, (guest : host), binding curve).

4.2.4 Proton NMR Titration Experiments - Discussion

Binding constants were found by fitting the titration data for both the amide NH protons and the CH to a 1:1 binding model. These provide identical binding constants within error, in cases where the anion is bound. As expected, **23** is the poorest halide receptor of the series. It fails to bind chloride (K_a (NH) <10M^{-1}, K_a (CH) < 10M^{-1}, but demonstrates a stronger interaction with fluoride, which could not be fitted to a 1:1 or 2:1(guest:host), binding curve. It does not bind bromide in this solvent system.

Receptors **137** and **128** bind chloride (K_a (**137**-NH) = 30 M^{-1}(± 3%), K_a (**137**-CH) = 33 M^{-1}(± 3%), K_a (**138**-NH) = 30 M^{-1}(± 3%), K_a (**138**-CH) = 25M^{-1}(± 38%)), to similar extents. Both have binding curves with a non-standard shape upon the addition of fluoride, which could not be fitted to a 1:1 or 2:1 (guest:host) binding curve. It is possible that this interaction is partial deprotonation, because the solutions of each receptor change from colourless to deep orange. Neither receptor binds bromide.

Receptor **139** is the strongest chloride receptor in the series, (K_a (NH) = 143M^{-1}(± 4%), K_a (CH) = 138M^{-1}(± 3%). With fluoride, it has a non-standard shape binding curve indicative of a strong interaction, for which a binding constant could not be calculated. It is the only receptor in the series which binds bromide, (K_a (NH) = 73M^{-1}, K_a (CH) = 103M^{-1}(± 9%)), in this competitive solvent system.

It appears therefore, that the number of electron withdrawing substituents on the pendant phenyl groups has a direct effect on the relative magnitudes of the binding affinities, but the nature of the electron withdrawing effects is different for each receptor. In **137**, it is the CH, which is activated by the mesomeric effect and the NH which is activated by the inductive effect. In **138** the opposite is true. Despite activating different hydrogen bond donors, these two receptors have similar binding constants for chloride, which is fairly remarkable. As mesomeric effects are stronger than inductive ones, one can presume that the mesomeric effects dominate in each receptor and are therefore roughly equal. In the case of **137**, it is therefore the CH activation which results in the high affinity for chloride relative to **23**.

The chloride binding constant obtained for receptor **139** is larger than those obtained for receptors **137** and **138**. This enhancement in binding strength relative to **137** shows that the additional nitro groups result in greater activation of the CH protons by the mesomeric effect, and hence the C-H-Cl^- hydrogen bonding interaction is significant. Receptor **139** is the only receptor in the series to bind bromide under these conditions, which is due to the double CH activation, (Figure 4.4).

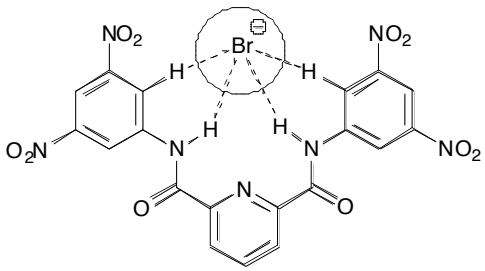

Fig 4.4 Proposed binding modes for the interaction of bromide by receptor **139** in DMSO-d_6.

4.2.5 Consideration of Chemical Shift Changes

Occasionally, binding constants may be calculated for CH protons in instances where it is not possible to use the appropriate NH proton for whatever reason. Often, the CH protons studied are not directly involved in binding, but experience small positive Δδ in strong anion receptors in proportion to those of the binding proton, through resonance effects. They can therefore be used to calculate binding constants. In all of the cases presented here, however, the CH protons experience large positive Δδ of the same order as those experienced by the amide NH for each case where binding is observed, (Table 4.2). Other CH protons in the receptors move negligibly in comparison. Hence, it is inferred that no significant resonance based Δδ effects are observed. In each case with chloride, the non-binding CH protons of receptors **137** - **139** move slightly upfield upon binding, (Figures 4.5 – 4.7). In the case with bromide with **139**, Δδ = 0 for the external CH.

	(Δδ / ppm) NH	**(Δδ / ppm) CH**
137	0.67	0.18
138	0.67	0.19
139	0.92	0.30

Table 4.2 Chemical shift changes (ppm) for NH and CH protons of receptors **126 – 128** upon addition of approx. 6 eq. of TBA chloride in DMSO-d_6 (compared to absence of anion).

Receptor **139**, which has a higher K_a values than **137** and **138** also has larger Δδ values than **137** or **138**. It is not sensible to analyse this further with such a small series of receptors, especially as **137** and **138** provide essentially identical values.

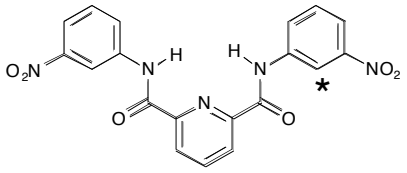

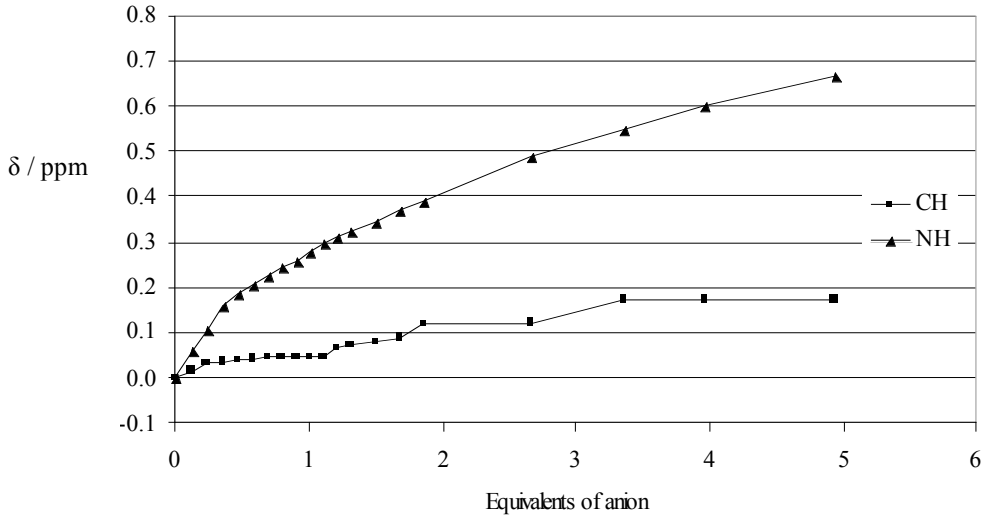

Fig 4.5 Binding profiles for NH and CH proton (*) of receptor **137** upon titration with TBACl in DMSO-d_6 at 298K. ($\Delta\delta$ / ppm (relative to lone receptor) against Eq. of guest).

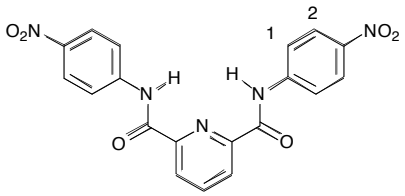

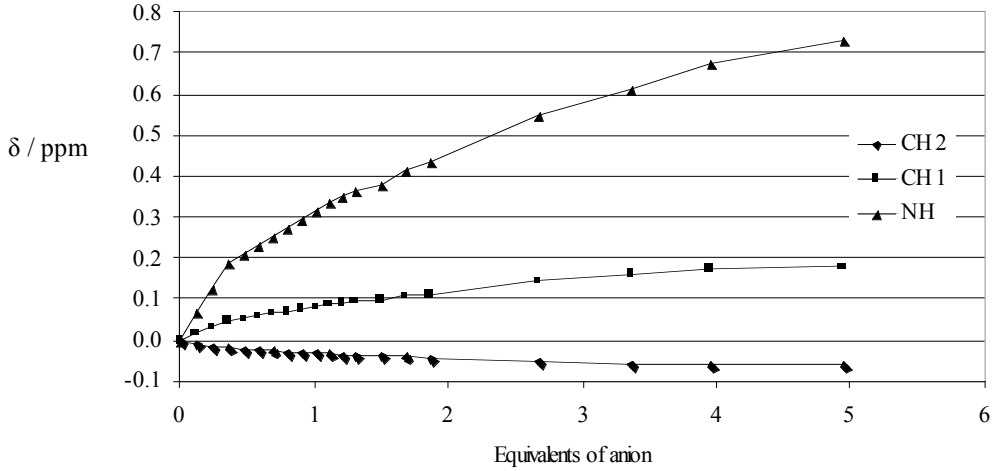

Fig 4.6 Binding profiles for NH and two CH protons of receptor **138** upon titration with TBACl in DMSO-d_6 at 298K. ($\Delta\delta$ / ppm (relative to lone receptor) against Eq. of guest)

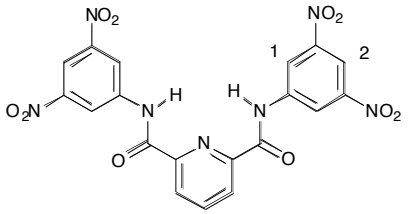

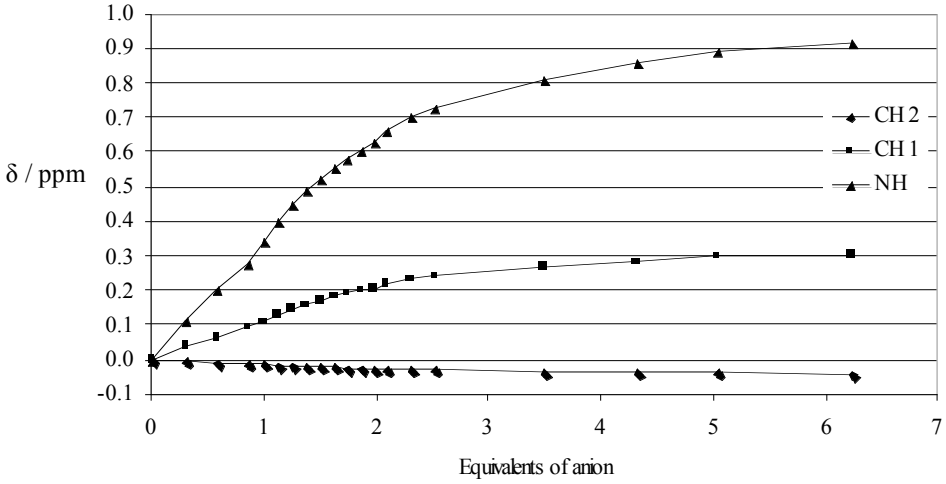

Fig 4.7 Binding profiles for NH and two CH protons of receptor **139** upon titration with TBACl in DMSO-d_6 at 298K. ($\Delta\delta$ / ppm (relative to lone receptor) against Eq. of guest).

4.3 SOLID-STATE ANALYSIS

Crystals suitable for X-ray diffraction were obtained by slow evaporation from DMSO-d_6 mixtures of **138** and **139** with TBACl, (Appendix 1A). Unfortunately, both of the structures, show solvent in their binding clefts and chloride is not present in either structure. Both show the pre-organised bis-amide clefts, with the DMSO-d_6 oxygen atom hydrogen bound to both amides, (Figure 4.7).

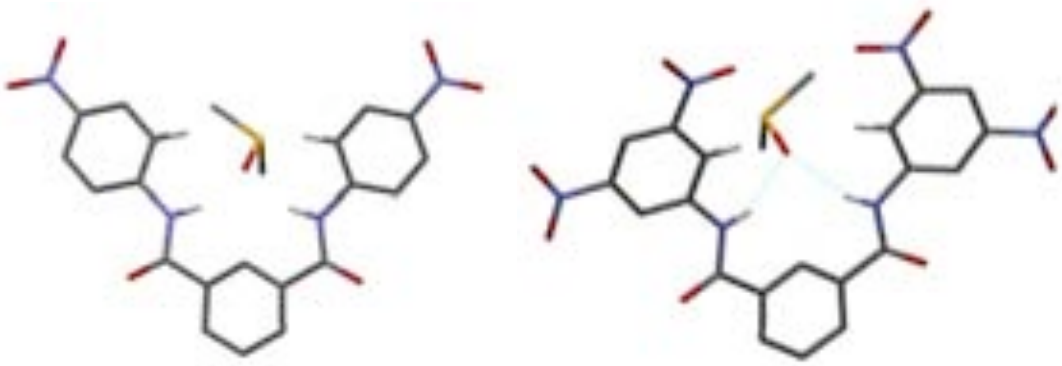

138 **139**

Fig 4.8 Views of the solid-state structures of **138** and **139** bound to solvent DMSO-d_6 molecules

The absence of chloride ions in these structures shows that the halide-receptor interactions are too weak to be retained in the solid state in the presence of a competitive solvent such as DMSO. Unfortunately, due to the poor solubility of this series, other solvents were not suitable for crystallisations.

The crystal structure of **138** is triclinic with space group P-1.The unit cell dimensions are a = 10.02Å, b = 11.11Å, c = 21.88Å, α = 99.15°, β = 94.16° and γ = 112.46°. In contrast, the crystal structure of **139** packs differently. It is monoclinic with space group $P2_1/c$ and unit cell dimensions a = 10.46Å, b = 23.61Å, c = 22.85Å and β = 97.73°.

4.4 CONCLUSION

Binding constants obtained for this series of halide receptors show that it is possible to enhance the chloride binding constant of the Crabtree scaffold, **23**, by activation of appropriately positioned CH protons. In cases where the CH proton is activated by more than one electron-withdrawing substituent, the binding cleft is suitably altered such that bromide binding is observed. This shows that CH activation by pendant nitro substituents can be significant.

Crystalline material obtained from DMSO solutions of receptors **138** and **139** in the presence of excess TBA chloride unfortunately provided only structures that showed the receptors bound to solvent molecules.

CHAPTER 5 – CONCLUSION TO RESEARCH CHAPTERS

5.1 CONCLUSIONS

5.1.1 Chapter 2 - Binding of alkylcarbamates and related species

The work presented in Chapter 2 shows that it is possible for simple hydrogen bond donors (**93–102** and **109)** to bind the alkylcarbamate anions of alkylammonium-alkylcarbamate (AAAC) salts, formed by reaction of CO_2 with primary amines in DMSO solution. The hydrogen bonding interactions occur in the presence of strong ion-pair interactions between the alkylammonium and alkylcarbamate parts of the salt. It was not possible to fully quantify the relative strengths of the interactions seen between the salts and various receptors, because ^{1}H NMR titrations were not reproducible. The irreproducibility is thought to arise from loss of CO_2 from the solution during the titration, which decreases the amount of salt present in solution.

Despite this, experiments involving chemical shift changes ($\Delta\delta$) were designed, which provided evidence of binding and gave a sense of relative strengths and trends. The addition of a suitable crown-ether (18-crown-6) was shown to increase the strength of the hydrogen bonding interaction between the receptors and alkylcarbamates, by binding the alkylammonium cation and thus reducing the extent of charge pairing. This effect was shown to be at play in the solid state, evidenced by a ternary crystal containing the zwitterionic AAAC salt DAP-CO_2, 18-crown-6 and receptor **101**. This represents a novel type of structure.

The adduct formed by the reaction between 1,4,5,6-tetrahydropyrimidine and CO_2 (THP-CO_2) was also investigated using ^{1}H NMR experiments in DMSO. This has very little charge pairing in solution and accordingly gave far higher $\Delta\delta$ values than were seen for the AAAC salts.

In an attempt to overcome some of the entropic penalty associated with the formation of ternary complexes in solution, a ditopic receptor **109** was synthesised, which combined hydrogen bond donors and an 18-crown-6 derivative, in order to bind both the alkylammonium and alkylcarbamate. This did not show an improvement in binding when compared to the two mono-topic receptors (**95** and 18-crown-6), which were studied previously. It is possible that the lack of improvement may due to

electronic changes weakening the anion-binding site, or due to poor relative positioning of the two binding sites.

A crystal obtained from a mixture of ditopic receptor **109** and DAP-CO_2 from methanol provided an intriguing crystal structure, which shows a poorly resolved and thus unidentified molecule positioned between the crown ether rings of two adjacent molecules of **109**. DAP-CO_2 or DAP were not seen in the structure, suggesting that these species have decomposed or are still in solution. The logical candidates for the unidentified molecule are methanol and CO_2, with the evidence split as to which is more likely. Unfortunately, the small quantity of material prevents further non-crystallographic investigation.

5.1.2 Chapter 3 - Schiff-base / urea anion receptors and colorimetric sensor

The work contained in Chapter 3 describes the synthesis, characterisation and anion complexation abilities of a series of Schiff-base urea anion receptors. They are shown to be moderate receptors for acetate, benzoate and dihydrogen phosphate over chloride and hydrogen sulfate in 0.5%H_2O:DMSO-d_6 by ^{1}H NMR titration experiments. A series of Job plots reveals that some of the receptors bind acetate and benzoate using a mixture of 1:1 and 2:1 (guest:host) stoichiometries.

When **123** is metallated using cobalt (II) chloride to produce **126** it acts as a naked-eye colorimetric anion sensor for chloride (apple green) and dihydrogen phosphate (blue). In both cases, UV-vis spectroscopy in DMSO appears to show that upon addition of excess TBA chloride or TBA dihydrogen phosphate, the cobalt centre is displaced from the organic ligand and forms new species, which differ depending on the nature of the anion added. When carboxylates are added, it is thought that they deprotonate the complex, or the organic ligand (**123**) following displacement of the cobalt centre.

In the analogous zinc containing complex **127**, the zinc centre was shown by X-ray crystallography, to be bound by five ligands, namely the pyridine and Schiff-base nitrogen atoms and two chlorides. It is thought that this structure may also be adopted by **126** in the solid state.

5.1.3 Chapter 4 - Isophthalamide derivatives with activated CH protons

Chapter 4 describes the synthesis, characterisation anion binding properties of a series of simple isophthalamide derivatives **137-139**, which were substituted with nitro groups in an effort to activate CH protons for halide binding. ^{1}H NMR titration and Δδ studies appear to confirm the involvement of the CH protons as intended.

The series is selective for chloride over bromide. With fluoride, binding curves were seen that could not be fitted to standard binding models. Crystals were obtained which show **138** and **139** bound to the solvent (DMSO) in preference over the intended guest, chloride.

5.2 FURTHER WORK

5.2.1 Chapter 2 - Binding of alkylcarbamates and related species

- Widen the scope of the Δδ experiments to include other literature receptors.
- Further attempts to reproduce crystals of **109** with unknown guest molecule.
- Investigate synthesis of more adventurous ditopic receptors for DAP-CO_2, possibly including indole and carbazole groups, such as **140** and **141.**

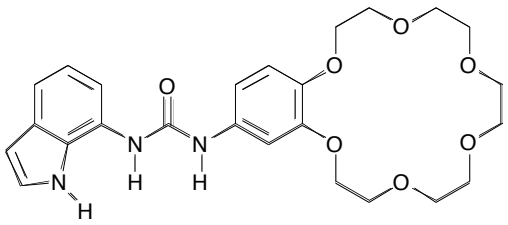

140

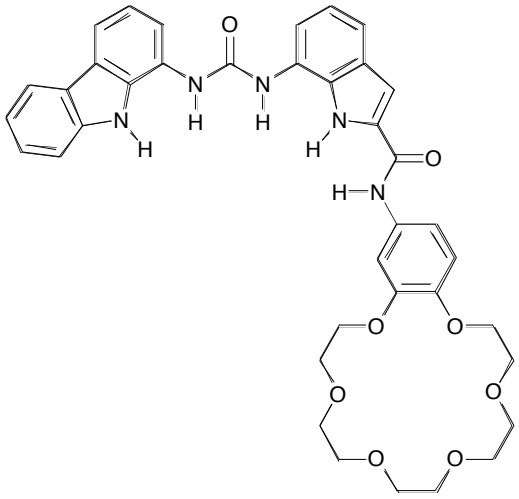

141

- Further attempts to synthesise and study molecules containing primary amines and appropriately positioned hydrogen bond donors, such as **142**, which may undergo internal alkylcarbamate hydrogen bonding upon addition of CO_2.

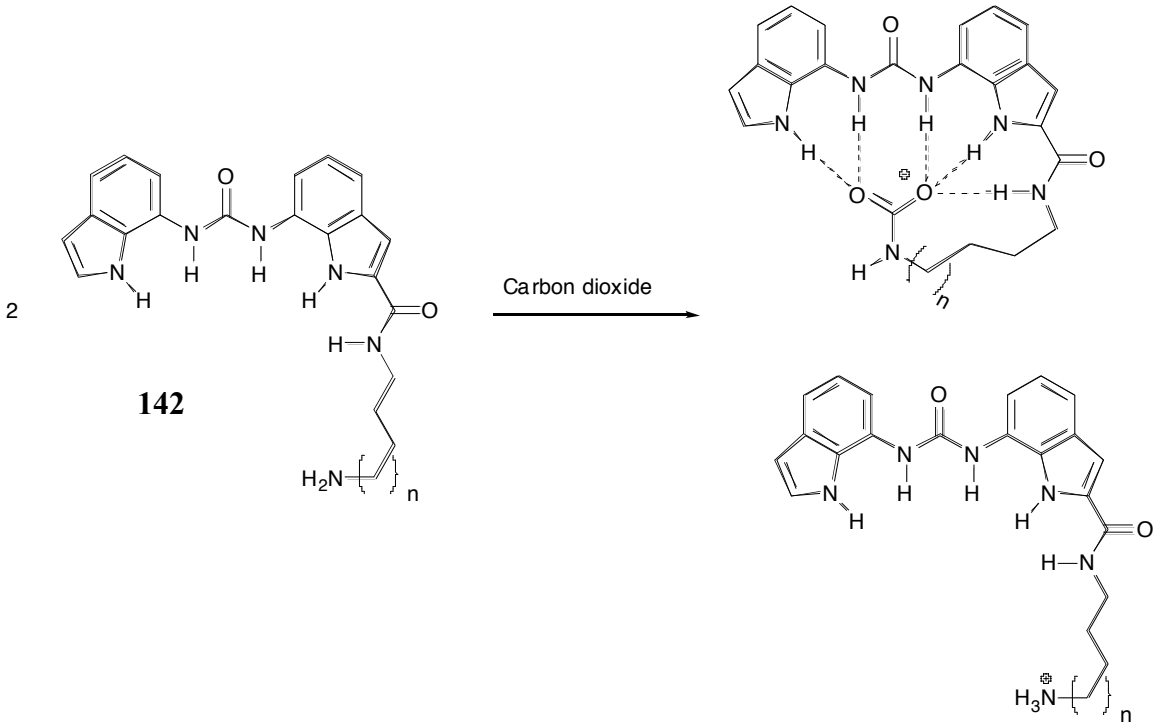

142

- Attempt synthesis of tren based receptors such as **143**.

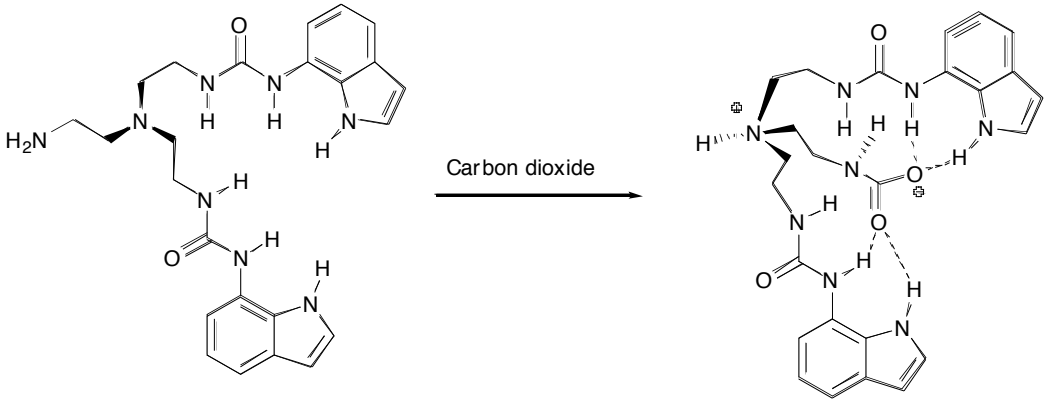

143

5.2.2 Chapter 3 - Schiff-base / urea anion receptors and colorimetric sensor

- Full study of zinc complex **127** and **^{1}H NMR** titrations with anions.
- Investigate possibility of using metal complexes in combination with AAAC salts, as demonstrated by Garcia-España.[91]

5.2.3 Chapter 4 - Isophthalamide derivatives with activated CH protons

- Extend study to other nitro activated receptors with the same scaffold, such as **144**, which was synthesised for inclusion in this chapter, but could not be easily purified due to solubility issues.
- Study of receptors with CH groups activated or deactivated using other groups, such as halides, CF_3, OMe, etc…

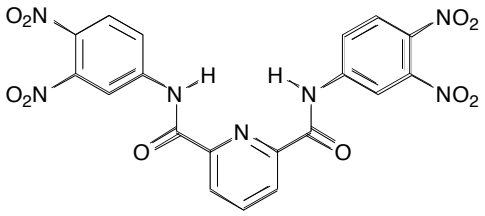

144

CHAPTER 6 – EXPERIMENTAL

6.1 CHEMICALS AND REAGENTS

Unless otherwise stated, reagents were used as supplied from commercial sources without further purification. Solvents used were not dried unless stated in the following procedures (Chapter 5.3).

Compound **95** was obtained from a stock of existing compounds prepared by Dr. S. Brooks at the University of Southampton. Compounds **96** – **101** were originally prepared for publication by Dr. Claudia Caltagirone and Jennifer Hiscock at the University of Southampton,[50-52] and have been re-synthesised by myself according to their procedures where further material has been required.

6.2 INSTRUMENTAL METHODS

NMR data was recorded using Bruker AV300 and AV400 spectrometers. All data is referenced to the residual protio-solvent peak in the case of proton NMR, or the solvent peak set in the case of ^{13}C NMR. Chemical shift values are reported in ppm. Low-resolution mass spectra were recorded on a Waters ZMD single quadrupole spectrometer. High resolution mass spectra were recorded on a Bruker Daltonics DataAnalysis 3.4, FT-ICR-MS, 4.7T magnet. Medac Ltd. performed elemental analyses. Infrared spectra were obtained using a Mattson Satellite (ATR) FTIR ('Golden Gate'), with values reported in wavenumbers (cm^{-1}). Melting points were recorded using open capillary tubes in a Gallenkamp melting point apparatus and are uncorrected. UV-visible spectra were collected using a Shimazdu UV-1601 UV-Visible Spetrophotometer.

6.3 SYNTHETIC PROCEDURES

6.3.1 Syntheses of compounds included in Chapter 2

Novel Compounds

4`-(Phenylureido)benzo-[18]-crown-[6] - (109)

4`-Aminobenzo-18-crown-6, (50mg, 0.15mmol) and phenylisocyanate, (21mg, 0.16mmol), were dissolved in DCM, (10mL), and stirred at ambient temperature for 2h. After this time, the solvent was removed to provide a pale pink powder, which was washed with diethyl ether, (10mL) and hexane (10mL). This provided 4`-(phenylureido)benzo-[18]-crown-[6], **109**, (54mg, 0.12mmol, 82%). **^{1}H NMR (300MHz, d_6-DMSO, δ = ppm):** 8.56 (1H, s, NH), 8.46 (1H, s, NH), 7.43 (2H, d, J = 7.53Hz, CH), 7.26 (2H, t, J = 7.53Hz, CH), 7.19 (1H, s, CH), 6.96 (1H, d, J = 7.53Hz, CH), 6.86 (2H, s, CH), 4.04 (4H, m, CH_2), 3.76 (4H, m, CH_2), 3.60 - 3.53 (12H, m, CH_2). **^{13}C NMR (100MHz, d_6-DMSO, δ = ppm):** 153.2 (q), 148.9 (q), 144.0 (q), 140.4 (q), 134.1 (q), 129.3 (CH), 122.2 (CH), 118.7 (CH), 114.8 (CH), 111.1 (CH), 105.8 (CH), 70.4 (CH_2), 69.5 (CH_2), 69.4 (CH_2), 69.2 (CH_2), 68.7 (CH_2). **IR (ν_{max}/cm^{-1}):** 3325, 3287 (NH), 2905 (CH), 1694 (CO). **LRMS (ES+) m/z:** 469.3 $[M+Na]^+$. **HRMS (ES+) m/z :** $[M+Na]^+$ act: 469.1939, cal: 469.1945. **MPt:** 118-120ºC.

Literature Compounds Synthesised by Independent Synthetic Routes [152, 153]

1-hexyl-3-butylurea, (93)

To a stirring solution of n-butylamine, (106mg, 1.46mmol) in DCM (3mL), was added 1-hexylisocyanate (186mg, 1.46mmol) at RT. The mixture was allowed to stir for 2h before removal of the solvent to provide a white waxy powder, **93,** (286mg, 1.43mmol, 98%). **^{1}H NMR (300MHz, d_6-DMSO, δ = ppm):** 5.69 (2H, s, NH), 2.93 (4H, t, J = 6.39Hz, CH_2), 1.29-1.24 (10H, m, CH_2), 0.85-0.82 (8H, t, J = 7.14, CH_2).

1-phenyl-3-butylurea, (94)

To a stirring solution of n-butylamine, (123mg, 1.68mmol) in DCM (3mL), was added phenylisocyanate (200mg, 1.68mmol) at RT. The mixture was allowed to stir for 2h before removal of the solvent by rotary evaporation. This provided a white powder, **94,** (313mg, 1.63mmol, 97%). **^{1}H NMR (300MHz, d_6-DMSO, δ = ppm):** 8.35 (1H, s, NH), 7.36 (2H, d, J = 7.89Hz, CH), 7.20 (2H, t, J = 7.92Hz, CH), 6.87 (1H, t, J = 7.17Hz, CH), 6.08 (1H, s, NH), 3.08 (2H, dd, J = 12.42Hz, J = 6.39Hz, CH_2), 1.46-1.25 (4H, m, CH_2), 0.89 (2H, t, J = 7.23Hz, CH_3).

6.3.2 Syntheses of compounds included in Chapter 3

Literature Compounds Synthesised by Independent Synthetic Routes [154, 155]

1-(2-Nitrophenyl)-3-phenylurea

To a stirring solution of aniline, (1140mg, 12.20mmol), in DCM, (50mL), was added 2-nitrophenyl isocyanate, (2000mg, 12.20mmol). The mixture was stirred at RT for 15 min, before removal of the DCM by rotary evaporation to provide a white solid, which was dried in vacuo. This provided 1-(2-nitrophenyl)-3-phenylurea, (3080mg, 11.97mmol, 98%). **^{1}H NMR (300MHz, d_6-DMSO, δ = ppm):** 9.80 (1H, s, NH), 9.57 (1H, s, NH), 8.29 (1H, dd, J = 1.13, 7.16Hz, CH), 8.09 (1H, dd, J = 1.50, 8.29Hz, CH), 7.70 (1H, dt, J = 1.51, 7.16Hz, CH), 7.49 (2H, dd, J = 1.13, 8.67 Hz, CH), 7.31 (2H, t, J = 5.65Hz, CH), 7.20 (2H, dt, J = 1.50, 7.53, CH), 7.02 (1H, t, J = 6.40Hz, CH).

1-(2-Aminophenyl)-3-phenylurea

To a stirring solution of 1-(2-nitrophenyl)-3-phenylurea, (1800mg, 7.00mmol), in EtOH (180mL), was added Pd/C (70mg), and hydrazine-hydrate (1.80mL). The mixture was allowed to reflux for 24h under N_2 before hot filtration of the Pd/C and removal of EtOH by rotary evaporation. This provided 1-(2-aminophenyl)-3-phenylurea, (1500mg, 6.60mmol, 94%). **^{1}H NMR (300MHz, d_6-DMSO, δ = ppm):** 8.74 (1H, s, NH), 7.72 (1H, s, NH), 7.44 (2H, d, J = 5.27Hz, CH), 7.34 – 7.26 (3H, m, CH), 6.94 (1H, bs, CH), 6.83 (1H, bs, CH), 6.75, (1H, bs, CH), 6.58 (1H, bs, CH), 4.75 (2H, s, NH_2).

1-(3-Nitrophenyl)-3-phenylurea

To a stirring solution of aniline, (1140mg, 12.20mmol), in DCM, (50mL), was added 3-nitrophenyl isocyanate, (2000mg, 12.20mmol). The mixture was stirred at RT for 15 min, before removal of the DCM by rotary evaporation, to provide a white solid, which was dried in vacuo. This provided 1-(3-nitrophenyl)-3-phenylurea, (2920mg, 11.35mmol, 93%). **^{1}H NMR (300MHz, d_6-DMSO, δ = ppm):** 9.18 (1H, s, NH), 8.80 (1H, s, NH), 8.55 (1H, t, J = 2.26Hz, CH), 7.82 (1H, dd, J = 1.88, 8.29Hz, CH), 7.70 (1H, dd, J = 1.89, 7.16Hz, CH), 7.59 (1H, t, J = 7.91Hz, CH), 7.47 (2H, d, J = 7.54Hz, CH), 7.30 (2H, t, J = 5.65Hz, CH), 7.00 (1H, t, J = 7.54Hz, CH).

1-(3-Aminophenyl)-3-phenylurea

To a stirring solution of 1-(3-nitrophenyl)-3-phenylurea, (900mg, 3.50mmol), in EtOH, (100mL), was added Pd/C, (35mg), and hydrazine-hydrate, (0.90mL). The mixture was allowed to reflux for 24h under N_2 before hot filtration of the Pd/C and removal of EtOH by rotary evaporation. This provided 1-(3-aminophenyl)-3-phenylurea, (681mg, 2.81mmol, 80%). **^{1}H NMR (300MHz, d_6-DMSO, δ = ppm):** 8.52 (1H, s, NH), 8.33 (1H, s, NH), 7.34 (2H, d, J = 7.54Hz, CH), 7.26 (2H, t, J = 7.53Hz, CH), 6.97 – 6.86 (2H, m, CH), 6.77 (1H, t, J = 3.76Hz, CH), 6.55 (1H, dd, J = 1.13, 7.92 Hz), 6.19 (1H, dd, J = 1.51, 7.91Hz, CH), 4.99 (2H, s, NH_2).

Novel Compounds

***Bis*-[N-2-(phenylureido)phenyl]-1,3-phenylenedimethanimine – (122)**

1-(2-Amino-phenyl)-3-phenylurea, (500mg, 2.20mmol), and benzene-1,3-dicarbaldehyde, (148mg, 1.10mmol) were dissolved in methanol, (250mL), and the mixture was allowed to reflux under nitrogen for 48h. After this time, the methanol was removed by rotary evaporation, providing a yellow powder, which was carefully washed with methanol (3 x 10mL). The powder was dried in vacuo to provide *bis*-[N-2-(phenylureido)phenyl]-1,3-phenylenedimethanimine, **122**, (295mg, 0.53mmol, 48%). **^{1}H NMR (300MHz, d_6-DMSO, δ = ppm):** 9.56 (2H, s, NH), 8.90 (2H, s, NH), 8.64 (1H, s, CH), 8.48 (2H, s, CH), 8.39 (2H, d, J = 7.32 Hz, CH), 8.29 (2H, d, J = 8.05 Hz,

CH), 7.79 (1H, t, J = 7.68 Hz, CH), 7.49 (4H, d, J = 7.68 Hz, CH), 7.39 (2H, d, J = 7.68 Hz, CH), 7.32-7.23 (6H, m, CH), 7.05 (2H, t, J = 7.32 Hz, CH), 6.98 (2H, t, J = 7.32 Hz, CH). **^{13}C NMR (75MHz, *d*$_6$-DMSO, δ = ppm):** 159.2 (CH), 152.2 (q), 139.6 (q), 138.1 (q), 136.6 (q), 134.6 (q), 131.5 (CH), 130.9 (CH), 129.3 (CH), 128.8 (CH), 127.3 (CH), 121.9 (CH), 118.7 (CH), 118.4 (CH), 117.4 (CH). **IR (ν_{max} / cm^{-1}):** 3307 (NH), 3041 (CH), 2341 (C=N). **LRMS (ES+) m/z:** 553.4 $[M+H]^+$, **MPt:** 198-200ºC. **Microanalysis:** ($C_{34}H_{28}N_6O_2$ + 0.125 CH_2Cl_2) Theory: C 72.77%, H 5.06%, N 14.92%. Found: C 72.93%, H 5.02%, N 14.76%.

***Bis*-[N-2-(phenylureido)phenyl]-pyridine-2,6-diyldimethanimine – (123)**

1-(2-Amino-phenyl)-3-phenylurea, (788mg, 3.25mmol), and pyridine-2,6-dicarbaldehyde, (0.220g, 1.63mmol), were dissolved in methanol, (150mL), and the mixture was allowed to reflux under nitrogen for 24h. After this time, the methanol was removed by rotary evaporation, providing a yellow powder, which was carefully washed with methanol (3 x 10mL). The powder was dried in vacuo to provide *bis*-[N-2-(phenylureido)phenyl]-pyridine-2,6-diyldimethanimine, **123**, (0.806g, 1.46mmol, 44%). **^{1}H NMR (300MHz, *d*$_6$-DMSO, δ = ppm):** 9.57 (2H, s, NH), 8.87 (2H, s, NH), 8.64 (2H, d, J = 8.05, CH), 8.58 (2H, s, CH), 8.32 (3H, m, CH), 7.53-7.49 (6H, m, CH), 7.34 – 7.28 (6H, m, CH), 7.05 (2H, t, J = 7.32Hz, CH), 7.00 (2H, t J = 7.32Hz, CH). **^{13}C NMR (75MHz, *d*$_6$-DMSO, δ = ppm):** 158.6 (CH), 154.2 (q), 152.2 (q), 139.6 (q), 137.8 (CH), 136.7 (q), 135.1 (q), 128.8 (CH), 128.3 (CH), 123.7 (CH), 122.0 (CH), 118.8 (CH), 118.4 (CH), 117.3 (CH). **IR (ν_{max} / cm^{-1}):** 3335 (NH), 3296 (NH), 3057 (CH), 2354 (C=N). **LRMS (ES+) m/z:** 554.3 $[M+H]^+$, 576.3 $[M+Na]^+$. **MPt:** 235 - 237ºC. **Microanalysis:** ($C_{33}H_{27}N_7O_2$ + 0.167 CH_2Cl_2) Theory: C 70.16%, H 4.85%, N 17.27%. Found: C 70.30%, H 4.86%, N 17.15%.

***Bis*-[N-3-(phenylureido)phenyl]-1,3-phenylenedimethanimine – (124)**

1-(3-Amino-phenyl)-3-phenylurea, (500mg, 2.20mmol) and benzene-1,3-dicarbaldehyde, (148mg, 1.10mmol) were dissolved in methanol, (250mL) and the mixture was allowed to reflux under nitrogen for 48h. After this time, the methanol was removed by rotary evaporation, providing a yellow powder which was carefully washed with methanol, (3 x 10mL). The powder was dried in vacuo to provide *bis*-[N-3-

(phenylureido)phenyl]-1,3-phenylenedimethanimine, **117**, (365mg, 0.66mmol, 60%). **^{1}H NMR (300MHz, d_6-DMSO, δ = ppm):** 8.76 (2H, s, NH), 8.71 (4H, d, J = 9.40 Hz, CH), 8.54, (1H, s, CH), 8.11 (2H, dd, J = 1.51 Hz, 7.91 Hz, CH), 7.69 (1H, t, J = 7.54 Hz, CH), 7.49 (2H, d, J = 1.51 Hz, CH), 7.45 (4H, dd, J = 8.66 Hz, 1.51 Hz, CH), 7.34-7.26 (8H, m, CH), 6.96 (4H, q, J = 7.91 Hz, CH). **^{13}C NMR (75MHz, d_6-DMSO, δ = ppm):** 160.0 (CH), 152.5 (q), 151.7 (q), 140.6 (q), 139.6 (q), 136.6 (q), 131.5 (CH), 129.5 (CH), 128.8 (CH), 128.3 (CH), 121.9 (CH), 116.0 (CH), 114.2 (CH), 111.1 (CH). **IR (ν_{max} / cm^{-1}):** 3302 (NH), 3055 (CH), 2359 (C=N), 2341 (C=N). **LRMS (ES+) m/z:** 553.4 $[M+H]^+$. **MPt:** 222-224ºC. **Microanalysis: (**$C_{34}H_{28}N_6O_2$ + 0.25 CH_2Cl_2) Theory: C 71.68%, H 5.01%, N 14.64%. Found: C 71.38%, H 5.09%, N 14.35%.

***Bis*-[N-2-(phenylureido)phenyl]-pyridine-2,6-diyldimethanimine – (125)**

1-(3-amino-phenyl)-3-phenylurea, (500mg, 2.20mmol) and pyridine-2,6-dicarbaldehyde, (0.148g, 1.1mmol) were dissolved in methanol, (250mL), and the mixture was allowed to reflux under N_2 for 48h. After this time, the methanol was removed by rotary evaporation, providing a yellow powder, which was carefully washed with MeOH (3 x 10mL). The powder was dried in vacuo to provide *bis*-[N-3-(phenylureido)phenyl]-pyridine-2,6-diyldimethanimine, **118**, (427mg, 0.77mmol, 70%). **^{1}H NMR (300MHz, d_6-DMSO, δ = ppm):** 8.79 (2H, s, NH), 8.72 (2H, s, NH), 8.68 (2H, s, CH), 8.29 (2H, d, J = 12.66Hz), CH), 8.14 (1H, t, J = 7.13Hz, CH), 7.60 (2H, d, J = 1.51Hz, CH), 7.47 (4H, d, J = 5.82Hz, CH), 7.39 – 7.26 (8H, m, CH), 7.02 – 6.95 (4H, m, CH). **^{13}C NMR (75MHz, d_6-DMSO, δ = ppm):** 160.0 (CH), 154.1 (q), 152.5 (q), 150.9 (q), 140.7 (q), 139.6 (q), 138.1 (CH), 129.6 (CH), 128.8 (CH), 123.0 (CH), 121.9 (CH), 118.3 (CH), 116.7 (CH), 114.3 (CH), 111.1 (CH). **IR (ν_{max} / cm^{-1}):** 3372 (NH), 3057 (CH). **LRMS (ES+) m/z:** 554.3 $[M+H]^+$, 576.3 $[M+Na]^+$. **MPt:** 245 - 247ºC. **Microanalysis:** ($C_{33}H_{27}N_7O_2$ + 0.083 CH_2Cl_2) Theory: C 70.87%, H 4.88%, N 17.49%. Found: C 70.98%, H 4.77%, N 17.50%.

Cobalt(II)chloride complex of *Bis*-[N-2-(phenylureido)phenyl]-pyridine-2,6-diyldimethanimine – (126)

Cobalt(II)chloride, (43mg, 0.32mmol), and *bis*-[N-2-(phenylureido)phenyl]-pyridine-2,6-diyldimethanimine, (200mg, 0.36mmol), were dissolved in THF (dried by distillation over sodium), (25mL), and stirred at RT under N_2 for 24h. After this time, the THF was removed by rotary evaporation to provide a dark green microcrystalline solid, **126**, (230mg, 0.21mmol, 98%).**^{1}H NMR (300MHz, d_6–DMSO, δ = ppm):** 9.62 (2H, broad s, NH), 8.79 (2H, broad s, CH), 8.58 (4H, broad s, NH and CH), 8.22 (3H, broad s, CH), 7.44 (6H, broad s, CH), 7.22 (6H, broad s, CH), 6.91 (4H, broad s, CH). **IR (ν_{max} / cm^{-1}):** 3283 (NH), 3055, 2960 (CH). **LRMS (ES-) m/z:** 576.3 [M-Co-2Cl+Na]$^+$, 1129.7 [2M-Co-2Cl+Na]$^+$. **HRMS (ES+) m/z :** [M-Cl]$^+$ act: 647.1234, cal: 647.1241. **MPt:** disc. > 200ºC, dec. >220ºC. **Microanalysis:** ($C_{33}H_{27}Cl_2CoN_7O_2$) Theory: C 57.99%, H 4.11%, N 14.34%, Cl 10.37%. Found: C 56.43%, H 4.12%, N 13.68%, 10.11%. **UV-vis (λ_{max} /nm):** 520.

Zinc(II)chloride complex of *Bis*-[N-2-(phenylureido)phenyl]-pyridine-2,6-diyldimethanimine – (127)

Zinc(II)chloride, (43mg, 0.32mmol), and *bis*-[N-2-(phenylureido)phenyl]-pyridine-2,6-diyldimethanimine, (200mg, 0.36mmol), were dissolved in THF (dried by distillation over sodium), (25mL), and stirred at RT under N_2 for 24h. After this time, the THF was removed by rotary evaporation to provide a bright yellow powder, **127**. The material was prepared crudely and was not characterised by methods other than X-ray crystallography, (See Page 123 or Appendix 1, Part A).

6.3.3 Syntheses of compounds included in Chapter 4

Novel Compounds

N^2,N^6-bis(3-nitrophenyl)pyridine-2,6-dicarboxamide – (137)

To a stirring solution of pyridine-2,6-dicarboyl dichloride, (170mg, 1.25mmol), DMAP, (catalytic amount) and dry triethylamine, (1.50mL) in DCM, (dried by distillation over calcium hydride), (25mL), was added dropwise, a solution of 3-nitroaniline, (500mg, 2.50mmol) in DCM (25mL) under argon. The reaction was left for 2h and an orange precipitate was observed. DCM was removed by rotary evaporation and the residue washed with MeOH to provide a pale yellow precipitate. This was collected by filtration and washed with MeOH (3 x 30mL), DCM (1 x 30mL) and Et_2O, (3 x 30mL). The product was dried in vacuo to provide N^2,N^6-(3-dinitrophenyl)pyridine-2,6-dicarboxamide, **137**, (117mg, 0.29mmol, 23%). **^{1}H NMR (300MHz, d_6-DMSO, δ = ppm):** 11.36 (2H, s, NH), 8.99 (2H, s, CH), 8.47 (2H, d, J = 7.15 Hz, CH), 8.35 (3H, t, CH), 8.07 (2H, d, J = 7.54 Hz, CH), 7.78 (2H, t, J = 7.91Hz, CH). **^{13}C NMR (75MHz, d_6-DMSO, δ = ppm):** (1eq. TBAF added for solubility): 163.2 (q), 148.8 (q), 147.6 (q), 141.0 (q), 139.5 (CH), 129.2 (CH), 127.1 (CH), 124.8 (CH), 117.8 (CH), 114.9 (CH). **IR (Golden Gate, ν_{max} / cm^{-1}):** 3308 (NH), 3078 (CH). **LRMS (ES-) m/z:** 406.2 $[M-H]^-$, 442.2 $[M+Cl]^-$, 849.3 $[2M+Cl]^-$. **HRMS (ES+) m/z:** $[M+H]^+$ act: 408.0929, cal: 408.0939. **MPt:** > 240 ºC.

N^2,N^6-bis(4-nitrophenyl)pyridine-2,6-dicarboxamide – (138)

To a stirring solution of pyridine-2,6-dicarboyl dichloride, (170mg, 1.25mmol), DMAP, (catalytic amount) and dry triethylamine, (1.50mL) in dry DCM, (25mL), was added dropwise, a solution of 4-nitroaniline, (500mg, 2.50mmol) in DCM, (dried by distillation over calcium hydride), (25mL) under Ar. The reaction was left for 24h and a bright yellow precipitate was observed. DCM was removed by rotary evaporation and the residue washed with MeOH to provide a bright yellow precipitate. This was collected by filtration and washed with MeOH (3 x 30mL), DCM (1 x 30mL) and Et_2O, (3 x 30mL). The product was dried in vacuo to provide N^2,N^6-(4-nitrophenyl)pyridine-2,6-dicarboxamide, **138**, (321g, 0.79mmol, 63%). **^{1}H NMR (300MHz, d_6-DMSO, δ =**

ppm): 11.45 (2H, s, NH), 8.47 (2H, d, J = 6.95Hz, CH), 8.38 – 8.33 (5H, m, CH), 8.28 – 8.24 (2H, m, CH). **^{13}C NMR (75MHz, d_6-DMSO, δ = ppm):** 162.2 (q), 148.2 (q), 144.2 (q), 142.9 (q), 140.4 (CH), 126.2 (CH), 124.9 (CH), 120.4 (CH). **IR (Golden Gate, ν_{max} / cm^{-1}):** 3357, 3334 (NH), 3087 (CH). **LRMS (ES-) m/z:** 406.2 $[M-H]^-$, 442.2 $[M+Cl]^-$, 849.3 $[2M+Cl]^-$. **HRMS (ES-) m/z:** act: 406.0787, cal. 406.0793. **MPt:** > 240 ºC.

N^2,N^6-bis(3,5-dinitrophenyl)pyridine-2,6-dicarboxamide – (139)

To a stirring solution of pyridine-2,6-dicarboyl dichloride, (0.400g, 1.96mmol), DMAP, (catalytic amount) and diisopropylethylamine, (1.20mL) in DCM, (dried by distillation over calcium hydride), (25mL), was added dropwise, a solution of 3,5-dinitroaniline, (0.718g, 3.92mmol) in DCM (25mL) under argon. The reaction was left for 48h and a bright yellow precipitate was observed. DCM was removed by rotary evaporation and the residue washed with MeOH to provide a bright yellow precipitate. This was collected by filtration and washed with MeOH (3 x 30mL), DCM (1 x 30mL) and Et_2O, (3 x 30mL). The product was dried in vacuo to provide N^2,N^6-bis(3,5-dinitrophenyl)pyridine-2,6-dicarboxamide, **139**, (0.485g, 0.97mmol, 50%). **^{1}H NMR (300MHz, d_6 -DMSO, δ = ppm):** 11.90 (2H, s, NH), 9.40 (4H, s, CH), 8.65 (2H, s, CH), 8.51 (2H, d, J = 7.53Hz), 8.41 (1H, t, J = 7.53Hz). **^{13}C NMR:** Could not be obtained due to poor solubility of compound, even in the presence of anions. Overnight experiment attempted in presence of TBAF, but resultant spectra indicates destruction of compound. **IR (Golden Gate, ν_{max} / cm^{-1}):** 3330, (NH), 3088 (CH). **LRMS (ES-) m/z:** 496.2 $[M-H]^-$, 532.1 $[M+Cl]^-$, 993.5 $[2M-H]^-$. **HRMS (ES+) m/z:** $[M-H]^-$, act: 496.0499, cal: 496.0495. **MPt:** disc. > 200 ºC.

References

1 Lehn, J. M. *Angew. Chem. Int. Ed.,* **1988,** *27*, 89.

2 Connors, K. A. *Binding Constants,* 1st Ed. John Wiley and Sons: New York, **1987**, 24.

3 Knowles, M.R; Gatzy, J.Tl Boucher, R. C. *N. Eng. J. Med*., **1981**, *305*, 1489. Quinton PM, *Nature*, **1983,** *30*1,421.

4 Levene, P. *J Biol. Chem.* **1919,** *40*, 415.

5 Bartram, J; Carmichael, W.W; Chorus, I; Jones, G; Skulberg, O. M. "*Toxic Cyanobacteria in Water: A guide to their public health consequences, monitoring and management*." **1999**, The World Health Organisation. E & FN Spon, London and New York.

6 Tu, A. T; Gaffield, W. *ACS Symposium Series.* **2000**, *745*, 304.

7 Simmons, H. E; Park, C. H. *J. Am. Chem. Soc.,* **1968**, *90*, 2428. Simmons, H. E; Park, C. H. *J. Am. Chem. Soc.,* **1968**, *90*, 2429. Simmons, H. E; Park, C. H. *J. Am. Chem. Soc.,* **1968**, *90*, 2431.

8 Lehn, J. M; Sonveaux, E; Willard, A. K. *J. Am. Chem. Soc.,* **1978**, *100*, 4914. Kintzinger, J. P; Lehn, J. M; Kauffmann, E; Dye, J. L; Popov, A. I. *J. Am. Chem. Soc.,* **1983**, *105*, 7549.

9 Kimura, E; Sakonaka, A; Yatsunami, T. *J. Am .Chem. Soc.,* **1981**, *103*, 3041.

10 Davis, A. P; Sheppard, D. N; Smith, B. D. *Chem. Soc. Rev.,* **2007**, *36*, 348. Santacroce, P. V; Davis, J. T; Light, M. E; Gale, P. A; Iglesias-Sánchez, J.C; Prados, P; Quesada, R. *J. Am. Chem. Soc.,* **2007**, *129*, 1886. Fisher, M. G; Gale, P. A; Hiscock, J. R; Hursthouse, M. B; Light, M.E; Schmidtchen, F. P; Tong, C. C. *Chem. Commun.,* **2009**, 3017. Davis, J. T; Gale, P. A; Okunola, O; Prados, P; Iglesias-Sánchez, J. C; Torroba, T; Quesada, R. *Nat. Chem.,* **2009**, *1*, 138. Berezin, S. K; Davis, J. T. *J. Am. Chem. Soc.,* **2009***, 131*, 2458.

11 Martell, A. E; Motekaitis, R. J. *J. Am. Chem. Soc.,* **1988**, *110*, 8059.Lu, Q; Reibenspies, J. H; Carroll, R. I; Martell, A. E; Clearfiled, A. *Inorg. Chim. Acta.,* **1998**, *270*, 207.

12 Hosseini, M. W; Lehn, J-. M; Mertes, M. P *Helv. Chim. Acta,* **1983**, *66*, 2454. Hosseini, M. W; Lehn, J-. M. *J.. Chem. Soc. Chem. Commun.,* **1985**, 1155.

13 Boyer, P. D; Walker, J. E; Skou, J. C. *Nobel Prize for Chemistry*, **1997**.

14 Schmidtchen, F. P. *Angew. Chem. Int. Ed.,* **1977**, *16*, 720. Schmidtchen, F. P. *Chem. Ber.,* **1980***, 113*, 864. Schmidtchen, F. P. *Chem. Ber.,* **1981***, 114*, 597.Schmidtchen, F. P; Muller, G. *J. Chem. Soc. Chem. Commun..,* **1984**, 1115.

15 Schmidtchen, F. P; Schier, A; Schafer, A; Hesse, M. *Angew. Chem. Int. Ed.,* **1994***, 33*, 327. Schmidtchen, F. P; Schier, A; Schafer, A; Hesse, M. *Angew. Chem. Int. Ed.,* **1995***, 34*, 65.

16 Dietrich, B; Fyles, T.M; Lehn, J-M; Pease, L.G; Fyles, D.L. *J. Chem. Soc. Chem. Commun.,* **1978**, 934.

17 Echavarren, A; Galán, A; Lehn, J-M; de Mendoza, J. *J. Am. Chem. Soc.,* **1989**, *111*, 4994.

18 Beer, P. D; Gale, P. A. *Angew. Chem. Int. Ed. Engl*, **2001**, *40*, 486; Angew. Chem. **2001**, *113*, 502-532.Gale, P. A. *Coord. Chem. Rev*., **2001**, *213*, 79. Gale, P. A. *Coord. Chem. Rev*. **2003**, *240*, 191. Gale, P. A. *Acc. Chem. Res*. **2006**, *39*, 465. Gale, P. A; García-Garrido, S.E; Garric, J. *Chem. Soc. Rev*. **2008**, *37*, 151. Caltagirone, C; Gale, P. A. *Chem. Soc. Rev*., **2009**, *38*, 301. Fitzmaurice, R. J; Kyne, G. M; Douheret, D; Kilburn, J. D *J. Chem. Soc., Perkin Trans. 1,* **2002**, 841.

19 Pascal, R. A; Spergel, J; Engbersen. *Tetrahedron Lett.,* **1986***, 27*, 4099.

20 Valiyaveettil, S; S; Engbersen, J. F. J; Verboom, W; Reinhouldt, D. N. *Angew. Chem. Int. Ed.,* **1993**, *32*, 900.

21 Kavillieratos, K; de Gala, S. R; Austin, D. J; Crabtree, R. H. *J. Am. Chem. Soc.,* **1997,** *119*, 2325.

22 Hughes, M. P; Smith, B. D. *J. Org. Chem.,* **1997**, *62*, 4492.

23 Brooks, S. J; Edwards, P. R; Gale, P. A; Light, M. E; *New. J. Chem.,* **2006**, *30*, 65.

24 Kondo, S.-I; Hiraoka, Y; Kurumantani, N; Yano, Y. *Chem. Commun.,* **2005**, 1720.

25 Korendovych, I. V; Cho, M; Makhlynets, O. V; Butler, P. L; Staples, R. J; Rybak-Akimova, E. V. *J. Org. Chem.,* **2008**, *73*, 4771.

26 Hossain, M. A; Kang, S. O; Llinares, J. M; Powell, D; Bowman-James, K. *Inorg, Chem.,* **2003**, *42*, 5043. Kang, S. O; Llinares, J. M; Powell, VanderVelde, D; Bowman-James, K. *J. Am. Chem. Soc.,* **2003**, *125*, 10152. Kang, S, O; VanderVelde, D; Powell, D; VanderVelde, D; Bowman-James, K. *J. Am. Chem. Soc.,* **2004**, *126*, 12272.

27 Meshcheryakov, D; Arnaud-Neu, F; Böhmer, V; Bolte, M; Hubscher-Bruder, V; Jobin, E; Thorndorf, I; Werner, S. *Org. Biomol. Chem.,* **2008**, *6,* 1004. Meshcheryakov, D; Arnaud-Neu, F; Böhmer, V; Bolte, M; Cavaleri, J; Hubscher-Bruder,V; Thorndorf, I; Werner, S. *Org. Biomol. Chem.,* **2008**, *6¸* 3244. Meshcheryakov, D; Böhmer, V; Bolte, M; Hubscher-Bruder,V; Arnaud-Neu, F. *Chem. Eur. J.,* **2009**, *15¸* 4811. Meshcheryakov, D; Bolte, M; Böhmer, V; *Org. Biomol. Chem.,* **2009**, *7*, 4386.

28 Bisson, A. P; Lynch, M; Hirose, Monahan, K. C; Anslyn, E. V. *Angew. Chem. Int. Ed.,* **1997**, *36*, 2340.

27 Kubik, S; Kirchner, R; Nolting, D; Seidel, J. *J. Am. Chem. Soc.,* **2002**, *124*, 12752. Otto, S; Kubik, S. *J. Am. Chem. Soc.,* **2003**, *125*, 7804.

30 Smith, P. J; Reddington, M. V; Wilcox, C. S. *Tetrahedron. Lett.,* **1992**, *35*, 6085.

31 Hamann, B. C; Branda, N. R; Rebek Jr, J. *Tetrahedron Lett.,* **1993**, *34*, 6837.

32 Werner, F; Schneider, H. –J. *Helv. Chim. Acta.,* **2000**, *83*, 465.

33 Lakshminarayanan, P. S; Ravikumar, I; Suresh, E; Ghosh. *Chem. Commun.,* **2007**, 5214.

34 Custelcean, R; Remy, P; Bonnesen, P. V; Jiang, D; Moyer, B. A. *Angew. Chem. Int. Ed.,* **2008**, *47,* 1866.

35 Hisaki, I; Sasaki, S-I; Hirose, K; Tobe, Y. *Eur. J. Org. Chem.,* **2007,** 607.

36 **a)** Brooks, S. J; Garcia-Garrido, S. E; Light, M. E; Cole, P. A; Gale, P. A. *Chem. Eur. J.* **2007**, *13*, 3320. **b)** Caltagirone, C; Gale, P. A; Hiscock, J. R; Brooks, S. J; Hursthouse, M. B; Light, M. E. *Chem. Commun.,* **2008**, 3007. **c)** Brooks, S. J; Gale, P. A; Light, M.E. Chem. Commun., **2006**, 4344.

37 Brooks, S. J; Gale, P. A; Light, M. E. *Supramol. Chem.,* **2006**, *19*, 9.

38 Gale, P. A; Sessler, J. L; Král, V; Lynch, V. *J. Am. Chem. Soc.,* **1996**, *118*, 5140.

39 Baeyer, A. *Dtsch. Chem. Ges.,* **1886**, *19*, 2184.

40 Katayev, E. A; Ustynyuk, Y. A; Lynch, V. M; Sessler, J. L. *Chem. Commun.,* **2006**, 4682.

41 Katayev, E. A; Myshkovskaya, E. N; Boev, N. V; Khrustalev, V. N. *Supramol.Chem.,* **2008,** *20*, 619.

42 Chang, K-J; Moon, D; Lah, M. S; Jeong, K. –S. *Angew. Chem. Int. Ed.,* **2005**, *44*, 7926.

43 Kim, N. K; Chang, K-J; Moon, D; Jeong, K. –S. *Chem. Commun.,* **2007**, 3401.

44 Lee, J. –Y; Lee, M. –H; Jeong, K. –S. *Supramol. Chem.,* **2007**, *19*, 257.

45 Ju, J; Park, M; Suk, J; Lah, M. S; Jeong, K. –S. *Chem. Commun.,* **2008**, 3546.

46 Curiel, D; Cowley, A; Beer, P. D. *Chem. Commun.,* **2005**, 236.

47 Chmielewski, M. J; Charon, M; Jurczak, J. *Org. Lett.,* **2004**, *6*, 3501.

48 Pfeffer, F. M; Lim, K. F; Sedgwick, K. J. *Org. Biomol. Chem.,* **2007**, *5*, 1795.

49 Bates, G. B; Gale, P. A; Light, M. E. *Chem Commun.,* **2007**, 2121.

50 Zieliński, T; Dydio, P; Jurczak, J. *Tetrahedron,* **2008**, *64*, 568.

51 Caltagirone, C; Mulas, A; Isaia, F; Lippolis, V; Gale, P. A, Light, M. E. *Chem. Commun.,* **2009**, 6279.

52 **a)** Caltagirone, C; Gale, P. A; Hiscock, J. R; Brooks, S. J; Hursthouse, M. B; Light, M. E. *Chem. Commun.,* **2008**, 3007. **b)** Caltagirone, C; Hiscock, J. R; Hursthouse, M. B; Light, M. E; Gale, P. A. *Chem. Eur. J.* **2008**, *14*, 10236.

53 Caltagirone, C; Hiscock, J. R; Light, M. E; Hursthouse, M. B; Gale, P. A. *Org. Biomol. Chem.,* **2009**, *7*, 1781.

54 Gale, P. A; Hiscock, J. R; Moore, S. J; Caltagirone, C; Hursthouse, M. B; Light, M. E. *Chem. Asian. J.,* **2010**, *5*, 555.

55 Aresta, M; Dibendetto, A. *Dalton. Trans.,* **2007**, 2975.

56 Tans, P. NOAA/ESRL (www.esrl.noaa.gov/gmd/ccgg/trends) (06/11/2009).

57 Solomon, S; Qin, D; Manning, M; Chen, Z; Marqius, M; Averyt, K. B; Tignor, M; Miller, H. L (eds.) "*IPCC, 2007: Summary for Policymakers. In: Climate Change 2007: The Physical Science Basis. Contribution of Working Group 1 to the Fourth Assessment Report of the Intergovernmental Panel of Climate Change."* Cambridge University Press, Cambridge, United Kingdom and New York, NY, USA, **2007**.

58 REN21. "*Renewables: Global Status Report: Update"*, **2009**, 24.

59 Metz, B., Davidson, O; de Coninck, H; Loos, M, Meyer, L (Eds.)*"IPCC special report on Carbon Dioxide Capture and Storage*: *Prepared by working group III of the Intergovernmental Panel on Climate Change*." Cambridge University Press, Cambridge, United Kingdom and New York, NY, USA, **2005**.

60 Caplow, M. *J. Am. Chem. Soc.,* **1968**, *90,* 6795.

61 George, M; Weiss, R. M. *Langmuir*, **2003**, *19*, 8168.

62 Danckwerts, P. V. *Chem. Eng. Sci.,* **1979**, *34*, 443.Glasscock, D. A; Critchfield, J. E; Rochelle, G. T. *Chem. Eng. Sci.,* **1991**, *46*, 2829.Choi, W-J; Cho, K-C; Lee, S-S; Shim, J-G, Hwang, H-R; Park, S-W; Oh, W-J. *Green Chem.,* **2007**, *9*, 594.

63 Hampe, E. R; Rudkevich, D. M. *Chem. Commun.,* **2002**, 1450.

64 da Silva, A. P; Gunaratne, H. Q. N; Gunnlaugsson, T; Huxley, A. J. M; McCoy, C. P; Rademacher, J. T; Rice, T.E. *Chem. Rev.,* **1997**, *97*, 1515.

65 Xu, H; Rudkevich, D. M. *Chem. Eur. J.* **2004**, *10*, 5432.

66 Zhang, H; Rudkevich, D. M. *Chem. Commun.,* **2007**, 4893.

67 Stastny, V; Anderson, A; Rudkevich, D. M. *J. Org. Chem.,* **2006**, *71*, 8696.

68 Stastny, V; Rudkevich, D. M. *J. Am. Chem. Soc.,* **2007**, *129*, 1018.

69 Heldebrandt, D. J; Jessop, P. G; Thomas, C. A; Eckert, C. A; Liotta, C. L. *J. Org. Chem.,* **2005**, *70*, 5335.

70 Seçkin, T; Bülent, A; Çetinkaya, E; Özdemir, I. *J. Polym. Sci., Part A: Polym. Chem.,* **1997**, *35*, 2411.

71 Endo, T; Nagai, D; Monma, T; Yamaguchi, H; Ochiai, B. *Macromol.* **2004**, *37*, 2007.

72 Jessop, P. G; Heldebrant, D. J; Li, X; Eckert, C. A; Liotta, L. C. *Nature,* **2005**, *436*, 1102. Phan, L; Jessop, P.G. *Green Chem.,* **2009**, *11*, 307.

73 Yamada, T; Lukac, P. J; George, M; Weiss, R. G. *Chem. Mater.,* **2007**, *19*, 967.

74 Yoshida, M' Komatsuzaki, Y; Ihara, M. *Org. Lett.,* **2008**, *10*, 2085.

75 Zhao, H; Zhang, W. Z; Liu, C. H; Qu, J. P; Lu, X. B; *J. Org. Chem.,* **2008**, *73*, 8039. Kayaki, Y; Yamamoto, M; Ikariya, T. *Angew. Chem. Int. Ed.,* **2009**, *48*, 4194.

76 An, J; Fiorella, R. P; Geib, S. J; Rosi, N. L. *J. Am. Chem. Soc.,* **2009**, *131*, 8401.

77 Johnston, A. G; Leigh, D. A; Murphy, A; Smart, J. P; Deegan, M. D. *J. Am. Chem. Soc.,* **1996**, *118*, 10662.

78 Hunter, C. A. *J. Am. Chem. Soc. Chem. Commun.,* **1991**, 749.

79 Johnston, A. G; Leigh, D. A; Pritchard, R. J; Deegan, M. D; *Angew. Chem. Int. Ed Eng.,* **1995**, *34*, 1209.

80 Quinn, R; Appleby, J. B; Pez, G. P. *J. Am. Chem. Soc.,* **1995**, *117*, 329.

81 Brooks, S. J; Gale, P. A; Light, M. E. *Chem. Commun.,* **2006**, 4344.

82 Tossel, J. A. *Inorg. Chem.,* **2009**, *48*, 7105.

83 Gunnlaugsson, T; Kruger, P. E; Jensen, P; Pfeffer, F. M; Hussey, G. M. *Tetrahedron. Lett.,* **2003**, *44*, 8909.

84 Calderazzo, F; Ianelli, S; Pampaloni, G; Pelizzi, G; Sperrle, M. *J. Chem. Soc. Dalton. Trans.,* **1991**, 693.

85 Belforte, A; Belli Dell`Amico, D; Calderazzo, F; Devillers, M; Englert, U. *Inorg. Chem.,* **1993**, *32*, 2283.

86 Nilsson Lill, S. O; Köhn, U; Anders, E.,*Eur. J. Org. Chem.,* **2004**, 2686.

87 Schumann, H; Meese-Marktscheffel, J; Diederich, A; Görlitz, H. *J. Organomet. Chem.,* **1992**, *430*, 299. Evans, W.J; Miller, K.A; Ziller, J. W. *Inorg. Chem.,* **2006,** *45*, 424.Baisch, U; Belli Dell'Amico, D; Calderazzo, F; Labella, L; Marchetti, F; Mergio, A. *Eur. J. Inorg. Chem.,* **2004**, 1219.

88 Farugia, L. J; Lopinski, S; Lovatt, P. A; Peacock, R. D. *Inorg. Chem.,* **2001**, *40*, 558. Evans, W. J; Seibel, A; Ziller, J. W. *Inorg. Chem.,* **1998**, *37*, 770.Evans, W. J; Perotti, J.M; Brady, J. C; Ziller, J. W. *J. Am. Chem. Soc.,* **2003**, *215*, 5204.

89 Lindskog, S. *Pharmacol. Theraput.,* **1997**, *74*, 1.

90 Bazzicalupi, C; Bencini, A; Bencini, A; Bianchi, A; Corana, F; Fusi, V; Giorgi, C; Paoli, P; Valtancoli, B; Zanchini, C. *Inorg. Chem.,* **1996**, *35*, 5540.

91 Garcia-España, E; Gaviña, P; Latorre, J; Soriano, C; Verdejo, B. *J. Am. Chem. Soc.,* **2004**, *126*, 5082. Verdejo, B; Blasco, S; González, J; Garcia-España, E; Gaviña, P; Tatay, S; Doménech, A; Doménech-Carbó M. T; Jiménez H. R, Soriano, C. *Eur. J. Inorg. Chem.,* **2008**, 84.

92 Pierce, J; Andrews, T. J; Lorimer, G. H. *J. Biol. Chem.,* **1986**, *261*, 10248.

93 Walther, D; Fugger, C; Schreer, H; Kilian, R; Görls, H. *Chem. Eur. J.,* **2001**, *7*, 5216.

94 **Cyclic:** Darensbourg, D.J; Mackiewicz, R. M; Phelps, A.L; Billodeaux, D.R. *Acc. Chem. Res.,* **2004**, *37*, 836. Fukuoka, S; Kawumura, M; Komiya, K; Tojo, M; Hachiya, H; Hasegawa, K, Aminaka, M; Okamoto, H; Fukawa, I; Konno, S. *Green Chem.,* **2003**, *5*, 497. Beckmann, E.J. *Science,* **1999**, 946. **Polymers:** Inoue, S; Koinuma, H; Tsuruta, T. *Makromol. Chem.,* **1969**, *130*, 210. Inoue, S; Koinuma, H; Tsuruta, T. *J. Polym. Sci.,* **1969**, *7*, 287. Super, M. S; Beckmann, E.J. *Trends Polym. Sci.,* **1997**, 236.Darensbourg, D.J; Holtcamp, M.W; *Coord. Chem. Rev.,* **1996**, 155. Srivastava, R; Srinavas, D; Ratnasamy, P. *Catal. Lett.,* **2003**, *89*, 81. Srivastava, R; Srinavas, D; Ratnasamy, P. *Catal. Lett.,* **2003**, *91*, 133.Darensbourg, D. J. *Chem. Rev.,* **2007**, *107*, 2388. Jacobsen, E. N. *Acc. Chem. Res.,* **2000**, *33*, 421.Byrne, C. M; Allen, S. D; Lobkovsky, E. B; Coates, G. W. *J. Am. Chem. Soc.,* **2004**, *126*, 11404.

95 Shi, F; Zhang, Q; Ma, Y; He, Y; Deng, Y. *J. Am. Chem. Soc.,* **2005**, *125*, 4183.

96 Salvatore, R. N; Shin, S. I; Nagle, A. S; Jung, K. W. *J. Org. Chem.,* **2001**, *66*, 1035. Kim, S.-I; Chu, F; Dueno, E, E; Jung, K.W. *J. Org. Chem.,* **1999**, *64*, 4578. Chu, F; Dueno, E. E; Jung, K. W. *Tetrahedron Lett.,* **1999**, *40*, 1847.

97 Gu, Y; Zhang, Q; Duan, Z; Zhang, J; Deng, Y. *J. Org. Chem.,* **2005**, *70*, 7376. Tekavec, T. N; Arif, A, M; Louie, J. *Tetrahedron.,* **2004**, *60*, 7431.

98 Zhan, Z; Kobsiriphat, W; Wilson, J. R; Pillai, M; Kim, I; Barnett, S. A. *Energ. Fuel.,* **2009**, *23*, 3089.

99 Laitar, D. S; Müller, P; Sadighi, J. P. *J. Am. Chem. Soc.,* **2005**, *127*, 17196.

100 Cavenati, S; Grande, C. A; Rodrigues, A. E. *J. Chem. Eng. Data.,* 2004, *49*, 1095. Ko, D; Siriwaedene, R; Biegler, L. T. *Ind. Eng. Chem. Res.,* **2003**, *42*, 339.

101 Choudhury, V.R; Mayadevi, S. *Langmuir.,* **1996**, *12,* 980. Zhao, X-X; Xu, X-L; Sun, L-B; Zhang L-L; Liu, X-Q. *Energ. Fuel.,* **2009**, *23,* 1534. Li, S; Falconer, J. L; Noble, R.D. *J. Membr. Sci.,* **2004**, *241*, 121.

102 **a)** Chui, S. S-Y; Lo, S. M-F; Charmant, J. P. H; Orpen, A. G; Williams, I. D. *Science,* **1999**, *19*, 1148. **b)** Millward, A. R; Yaghi, O. M. *J. Am. Chem. Soc.,* **2005**, *127*, 17998. **c)** Wang, Q; Shen, D; Buelow, M; Lau, M; Deng, S; Fitch, F. R; Lemcoff, N. O; Semanscin, J. *Micro. Meso. Mater.,* **2002**, *55*, 217. **d)** Liang, Z; Marshall, M; Chaffee, A. L. *Energ. Fuel.,* **2009**, *23*, 2785.**e)** Wang, B; Côté, A. P; Furukawa, H; O'Keeffe, M; Yaghi, O. M. *Nature,* **2008**, *453*, 207. Millward, A. R; Yaghi, O. M. *J. Am. Chem. Soc.,***2005**, *127*, 17998. Banerjee, R; Phan, A; Wang, B; Knobler, C; Furukawa, H; O'Keeffe, M; Yaghi, O. *Science,* **2008**, *319*, 939. Chae, H. K; Siberio-Pérez, D. Y; Kim, J; Go, Y; Eddaoudi, M; Matzger, A. J; O'Keeffe, M; Yaghi, O. M. *Nature,* **2004**, *427*, 523.

103 Chen, C; Yang, S-T; Ahn, W-S; Ryoo, R. *Chem. Commun.,* **2009**, 3627.

104 Jadhev, P. D; Chatti, R. V; Biniwale, R. B; Labhsetwar, N. K; Devotta, S; Rayalu, S. S. *Energ. Fuel.* **2007**, *21*, 3555.

105 Couck, S; Denayer, J. F. M; Baron, G. V; Rémy, T; Gascon, J; Kapteijn, F. *J. Am. Chem. Soc.,* **2009**, *131*, 6326.

106 Atwood, J. L; Barbour, L. J; Jerga, A. *Angew. Chem. Int. Ed.,* **2004**, *43*, 2948.

107 Dalgarno, S. J; Tian, J; Warren, J. E; Clark, T. E; Makha, M; Raston, C. L; Atwood, J. L. *Chem. Commun.***, 2007**, 4848 – 4850.4

108 Hynes, M. *J.Chem. Soc. Dalton. Trans.,* **1993**, 311.

109 Makuc, D; Lenarčič, M; Bates, G. W; Gale, P. A; Plavec, J. *Org. Biomol. Chem.,* **2009**, *7*, 3505.

110 Bordwell, F. E; Drucker, G. E; Fried, H. E. *J. Org. Chem.,* **1981**, *46*, 632.

111 Späth, A; König, B. *Tetrahedron,* **2010**, *66*, 1859.

112 Lu, G; Lui, F; Song, W; He, W; Prados, P; de Mendoza, J. *Mater. Sci. Eng.,* **1999***, 10*, 29.

113 Lankshear, M. D; Dudley, I. M; Chan, K-M, Cowley, A. R; Santos, S. M; Felix, V; Beer, P.D. Chem. Eur. J.

114 Tumcharern, G; Tuntulani, T; Coles, S. J; Hursthouse, M. B; Kilburn, J. D. *Org. Lett.,* **2003**, *5*, 4971.

115 Custelcean, R; Delmau, L. H; Moyer, B. A; Sessler, J. L; Cho, W-S; Gross, D; Bates, G. W; Brooks, S. J; Light, M.E; Gale, P. A. Angew. Chem. Int. Ed., 2005, 44, 2537.

116 Qureshi, N; Yufit, D.S; Howard, J. A. K; Steed, J. W. *Dalton Trans.,* **2009**, 5708.

117 Tasker, P. A; Tong, C. C; Westra, A. N. *Coord. Chem. Rev.,* **2007**, *251*, 1868.

118 Tian, Y-Q; Zhao, Y-M; Xu, H-J; Chi, C-Y. *Inorg. Chem.,* **2007**, *46*, 1612. Takamizawa, S; Nakata, E; Yokoyama, H;Mochizuki, K; Mori, W. *Angew. Chem. Int. Ed.,* **2003**, *42*, 4331. Takamizawa, S; Saito, T. *Inorg. Chem. Commun.,* **2004***, 7*, 1. Maji, T. K; Motafa, G; Kitagawa, S. *J. Am. Chem. Soc.,* **2005***, 127*, 17152.

119 Berl, V; Huc, I; Khoury, R. G; Lehn, J-M. *Chem. Eur. J.,* **2001**, *7*, 2798. Harata, J. *Bull. Chem. Soc. Jpn.,* **1978**, *51*, 1644. Gunnes, S; Romming, C; Undheim, K. *Tetrahedron.,* **2006**, *62*, 6090. Deskus, J. A; Epperson, J. R; Sloan, C. P; Cipollina, J. A; Dextraze, P; Jingfang, Q-C; Gao, Q; Ma, B; Beno, B.R; Mattson, G. K; Molski, T. F; Krause, R. G; Taber, M. T; Lodge, N. J; Mattson, R. J. *Bioorg, Med. Chem. Lett.,* **2007**, *17*, 3099.

120 Esteban-Goméz, D; Fabbrizzi, L; Licchelli, M. *J. Org. Chem.,* **2005**, *70*, 5717.

121 Camiolo, S; Gale, P. A; Hursthouse, M. B; Light, M.E. *Org. Biomol. Chem.,* **2003**, *1*, 741.

122 Quinlan, E; Matthews, S. E; Gunnlaugsson, T. *J. Org. Chem.,* **2007**, *72*, 7497.

123 Duke, R. M; O'Brien, J. E; McCabe, T, Gunnlaugsson, T. *Org. Biomol. Chem.,* **2008**, *6*, 4089.

124 Misri, A; Shahid, M; Dwivedi, P. *Talanta.,* **2009**, *80*, 532.

125 Li, J; Wang, Y; Lin, H; Lin H. *J. Incl. Phenom. Macrocycl. Chem.,* **2009**, *63*, 281.

126 Piątek, P; Jurczak, J; *Chem. Commun.,* **2002**, 2450.

127 Tseng, Y-P; Tu, G-M; Lin, C-H; Chang, C-T; Lin, C-Y, Yen, Y-P. *Org. Biomol. Chem.,* **2007,** *5*, 3592.

128 Gale, P. A; Twyman, L. P; Handlin, C. I; Sessler, J. L. *Chem. Commun.,* **1999**, 1851.

129 Costero, A. M; Banuls, M; J; Aurell, M .J; Ramirez de Arellano, M. C. *J. Incl. Phenom. Macrocycl. Chem.,* **2006**, *54*, 61.

130 Wisjur, S. L; Lavigne, J. L; Metzger, A; Tobey, S. L; Lynch, V; Anslyn, E. V. *Chem. Eur. J.,* **2004**, *10*, 3792.

131 Gassensmith, J. J; Mattys, S; Lee, J-J; Wojcik, A; Kamat, P. V; Smith, B. D. *Chem. Eur, J.,* **2010**, *16*, 2916.

132 Borisnova, N. E; Reshetova, M. D; Ustynyuk, Y. A. *Chem. Rev.,* **2007**, *107*, 46.

133 Sivakumar, R; Reena, V; Ananthi, N; Babu, M; Anandan, S; Velmethi, S. *Spectrochim. Acta A*. **2010**, *75*, 1146. Kumar, M; Babu, J. N; Bhalla, V. *J. Incl. Phenom. Macrocycl. Chem.,* **2010***, 66*, 139. Sessler, J. L; Katayev, E; Dan Pantos, G; Ustynyuk, Y. A. *Chem. Comm.,* **2004**, 1276. Sessler, J. L; Katayev, E; Dan Pantos, G; Scherbakov, P; Reshetova, M. D; Khrustalev, V. N; Lynch, V. M; Ustynyuk, Y. A. *J. Am. Chem. Soc.,* **2005**, *127*, 11442. Roznyatovsky, V. V; Borisova, N. E; Reshetova, M. D; Buyanovskaya, A. G; Ustynyuk, Y. A. *Russ. Chem. B*+. **2005***, 54*, 2219. Mateus, P; Delgado, R; Brandão, P; Carvalho, S; Félix, V. *Org. Biomol. Chem.,* **2009**, *7*, 4661.

134 Fernandes, L; Boucher, M; Fernandéz-Lodeiro, J; Oliveira, E; Nuñez, C; Santos, H. M; Capelo, J. L; Faza, O. N; Bértolo, E; Lodeiro, C. *Inorg .Chem. Commun.,* **2009**, *12*, 905. Li, L; Dang, Y-Q; Li, H-W; Wang, B; Wu, Y. *Tetrahedron Lett.,* **2010***, 51*, 618. Aksuner, N; Henden, E; Yilmez, I; Cukurovali, A. *Dyes Pigments,* **2009***, 83*, 211. Singh, N; Kuar, N; Choitir, C. N; Callan, J. F. *Tetrahedron Lett.,* **2009***, 50*, 4201.

135 Geest, D. J; Noble, A; Moubaraki, B; Murray, K. S; Larsen, D. S; Brooker, S. *Dalton Trans.,* **2007***,* 467.

136 Katayev, E. A; Ustynyuk, Y. A; Lynch, V. M; Sessler, J. L. *Chem. Commun.,* **2006,** 4682. Natale, D; Mareque-Rivas, J. C. *Chem. Commun.,* **2008**, 425.

137 Marinescu, G; Marin, G; Madalan, A. M; Vezenu, A; Tiseanu, C; Andruh, M. *Cryst. Growth Des.,* **2010**, *10*, 2096. Agapiou, K; Mejía, M. L; Yang, X; Holliday, B. J. *Dalton. Trans.,* **2009**, 4154. Basu-Baul, T.S; Masharing, C; Ruisi, G; Jirasko, R; Holcapek, M; de Vas, D; Wolsternholme, D; Linden, A. *J. Organomet. Chem.,* **2007**, *692*, 4849.

138 Gupta, K. C; Sutar, A. A. *Coord. Chem. Rev.,* **2008**, *252*, 1420.

139 Hu, W; Li, J; Zhang, J; Wang, J; Zou, L; Du, J; Wang, X. *J. Disper. Sci. Technol.,* **2010***, 4*, 529.

140 Yoo, J; Na, S-J; Park, H.C; Cyriac, A; Lee, B-Y. *Dalton Trans.,* **2010***, 39*, 2622.

141 Job, P. *Ann. Chim.* **1928**, *9*, 113.

142 Cotton, F.A; Wilkinson, G. *"Advanced Inorganic Chemistry - (3rd Ed.)",* **1972**. John Wiley and Sons, USA.

143 Shriver, D. F; Atkins, P. W. '*Inorganic Chemistry'* 3rd Ed., **2001**, Oxford University Press.

144 Jurwarker, H; Lenhardt, J. M; Castillo, J. C; Zhao, E; Krishnamurthy, S; Jamiolkowski, R. M; Kim, K-H; Craig, S. L. *J. Org. Chem.,* **2009**, *74*, 8924.

145 Li, Y; Flood, A. H. *J. Am. Chem. Soc.,* **2009**, *130*, 12111.

146 Zahran, E; Hua, Y; Li, Y; Flood, A. H; Bachas, L. G. *Anal. Chem.* **2010**, *82*, 368.

147 Fisher, M. G; Gale, P. A; Hiscock, J. R; Hursthouse, M. B; Light, M. E; Schmidtchen, F. P; Tong, C. C. *Chem. Commun.,* **2009**, 3017.

148 Willans, C. R; Anderson, K. M; Potts, L. C. Steed, J. W. *Org. Biomol. Chem.,* **2009**, *7*, 2756.

149 Wannalerse, B; Tuntulani, T; Tomapatanaget, B. *Tetrahedron.,* **2008**, *64*, 10619.

150 Xu, Z; Singh, N. J; Lim, J; Pan, J; Kim, H. N; Park, S; Kim, K.S, Yoon, J. *J. Am. Chem. Soc.,* **2009**, *131*, 15528.

151 Amendola, V; Boiocchi, M; Colasson, B; Fabbrizzi, L; Monzani, E; Douton-Rodriquez, M-J; Spadini, C. *Inorg. Chem.,* **2008***, 47*, 4808

152 McElroy, N.R; Jurs, P.C. *J. Med. Chem.,* **2003**, *46*, 1066.

153 Mizuno, T; Kino, T; Ito, T; Miyata, T. *Synth. Commun.,* **2000**, *30*, 1675.

154 Perry, C. J; Holding, K; Tyrrell, E. *Synthetic. Commun.,* **2008**, *38*, 3354.

155 Song, D-Q; Du, N-N; Wang, Y-M; He, W-Y; Jiang, E-Z; Cheng, S-X; Wang, Y-X; Li, Y-H; Wang, Y-P; Li, X; Jiang, J-D. *Bioorg. Med. Chem.,* **2009**, *17*, 3873.

156 Clegg, W. *J. Chem. Soc. Dalton. Trans.,* **2000**, 3223.

APPENDIX 1 – X-RAY CRYSTAL STRUCTURE DATA

Part A

The following crystal structures were solved by the EPSRC National Crystallography Service, (Dr. M. E. Light):

In Chapter 2	Receptor **109** with unknown guest (resolved as CO_2)
	Receptor **109** with unknown guest (resolved as MeOH)
In Chapter 3	Complex **127**
In Chapter 4	Receptor **138,** Receptor **139**

The refinement of the structures and fractional coordinates are reported for the sake of completeness and so that the structures can be reproduced from this text if necessary.

Part B

The structure of the ternary complex of receptor **101** (included in chapter 2) was collected using the synchrotron source at Diamond, (Prof. W. Clegg)[156] before resolution at the EPSRC National Crystallography Service, (Dr. Mark Light). The refinement of the structure and fractional coordinates are reported for the sake of completeness and so that the structures can be reproduced from this text if necessary.

PART A

STRUCTURES FROM CHAPTER 2

Receptor 109 with unknown guest (resolved as CO_2)

Table 1. Crystal data and structure refinement details.

Empirical formula	$C_{47}H_{60}N_4O_{16}$ $2(C_{23}H_{30}N_2O_7), CO_2$
Formula weight	936.99
Temperature	273(2) K
Wavelength	0.71073 Å
Crystal system	Monoclinic
Space group	$P2_1/c$
Unit cell dimensions	a = 7.96450(10) Å b = 12.1599(2) Å β = 93.3390(10)° c = 23.8549(4) Å
Volume	2306.37(6) Å^3
Z	2
Density (calculated)	1.349 Mg / m^3
Absorption coefficient	0.102 mm^{-1}
F(000)	996
Crystal	Prism; Pink
Crystal size	0.20 × 0.20 × 0.12 mm^3
θ range for data collection	3.00 – 27.54°
Index ranges	$-10 \le h \le 10$, $-15 \le k \le 15$, $-30 \le l \le 31$
Reflections collected	31529
Independent reflections	5299 [R_{int} = 0.0505]
Completeness to θ = 27.50°	99.8 %
Absorption correction	Semi–empirical from equivalents
Max. and min. transmission	0.9879 and 0.9799
Refinement method	Full-matrix least-squares on F^2
Data / restraints / parameters	5299 / 0 / 313
Goodness-of-fit on F^2	1.068
Final R indices [$F^2 > 2\sigma(F^2)$]	*R1* = 0.0636, *wR2* = 0.1394
R indices (all data)	*R1* = 0.0795, *wR2* = 0.1494
Largest diff. peak and hole	0.342 and –0.323 e Å^{-3}

Diffractometer: *Nonius KappaCCD* area detector (ϕ scans and ω scans to fill *asymmetric unit*). **Cell determination:** DirAx (Duisenberg, A.J.M.(1992). J. Appl. Cryst. 25, 92-96.) **Data collection:** Collect (Collect: Data collection software, R. Hooft, Nonius B.V., 1998). **Data reduction and cell refinement**: *Denzo* (Z. Otwinowski & W. Minor, *Methods in Enzymology* (1997) Vol. **276**: *Macromolecular Crystallography*, part A, pp. 307–326; C. W. Carter, Jr. & R. M. Sweet, Eds., Academic Press). **Absorption correction**: Sheldrick, G. M. SADABS - Bruker Nonius area detector scaling and absorption correction - V2.10 S**tructure solution**: *SHELXS97* (G. M. Sheldrick, Acta Cryst. (1990) A**46** 467–473). S**tructure refinement**: *SHELXL97* (G. M. Sheldrick (1997), University of Göttingen, Germany). **Graphics:** Cameron - A Molecular Graphics Package. (D. M. Watkin, L. Pearce and C. K. Prout, Chemical Crystallography Laboratory, University of Oxford, 1993).

Special details: All hydrogen atoms were placed in idealised positions and refined using a riding model.

Table 2. Atomic coordinates [× 10^4], equivalent isotropic displacement parameters [Å^2 × 10^3] and site occupancy factors. U_{eq} is defined as one third of the trace of the orthogonalized U^{ij} tensor.

Atom	*x*	*y*	*z*	U_{eq}	*S.o.f.*
O102	5190(15)	9414(10)	5449(4)	165(4)	0.50
C101	5000	10000	5000	88(2)	1
O103	3789(15)	10263(12)	5251(7)	216(6)	0.50
O1	1334(2)	8689(1)	2930(1)	30(1)	1
O2	2057(2)	7645(1)	4906(1)	27(1)	1
O3	961(2)	9211(1)	5656(1)	30(1)	1
O4	3236(2)	9202(1)	6621(1)	31(1)	1
O5	6083(2)	8257(1)	7238(1)	33(1)	1
O6	6837(2)	6695(1)	6335(1)	32(1)	1
O7	4910(2)	6727(1)	5224(1)	28(1)	1
N1	2337(2)	8080(2)	2104(1)	27(1)	1
N2	3436(2)	7407(2)	2939(1)	27(1)	1
C1	1714(3)	8639(2)	1151(1)	24(1)	1
C2	1064(3)	9387(2)	758(1)	28(1)	1
C3	363(3)	10374(2)	924(1)	29(1)	1
C4	358(3)	10611(2)	1492(1)	29(1)	1
C5	991(3)	9874(2)	1892(1)	27(1)	1
C6	1654(2)	8867(2)	1724(1)	23(1)	1
C7	2294(3)	8109(2)	2682(1)	24(1)	1
C8	3815(3)	7297(2)	3521(1)	23(1)	1
C9	2692(3)	7610(2)	3925(1)	23(1)	1
C10	3102(3)	7416(2)	4487(1)	23(1)	1
C11	4642(3)	6922(2)	4662(1)	25(1)	1
C12	5761(3)	6655(2)	4261(1)	28(1)	1
C13	5345(3)	6835(2)	3694(1)	27(1)	1
C14	629(3)	8328(2)	4770(1)	27(1)	1
C15	–184(3)	8567(2)	5312(1)	29(1)	1
C16	442(3)	9336(2)	6213(1)	31(1)	1
C17	1811(3)	9909(2)	6552(1)	34(1)	1
C18	4741(3)	9784(2)	6779(1)	34(1)	1
C19	6192(3)	9015(2)	6781(1)	34(1)	1
C20	7352(3)	7424(2)	7259(1)	37(1)	1
C21	6843(3)	6433(2)	6914(1)	34(1)	1
C22	6269(3)	5785(2)	6001(1)	29(1)	1
C23	6346(3)	6066(2)	5391(1)	28(1)	1

Table 6. Hydrogen bonds [Å and °].

D–H···*A*	*d*(*D*–H)	*d*(H···*A*)	*d*(*D*···*A*)	∠(*D*H*A*)
N1–H901···O4^{ii}	0.88	2.26	3.104(2)	160.0
N2–H902···O5^{ii}	0.88	2.09	2.881(2)	148.8

Symmetry transformations used to generate equivalent atoms:
(i) –x+1,–y+2,–z+1 (ii) x,–y+3/2,z–1/2

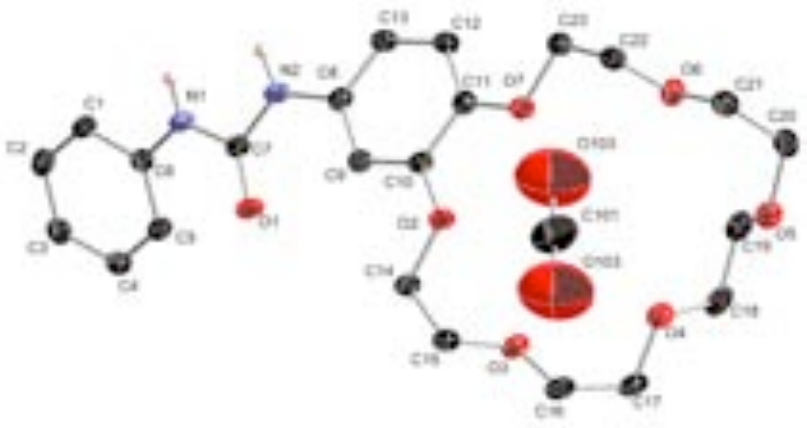

Thermal ellipsoids drawn at the 35% probability level

RECEPTOR 109 with unknown guest (resolved as MeOH)

Table 1. Crystal data and structure refinement details.

Empirical formula	$C_{47}H_{64}N_4O_{15}$ $2C_{23}H_{30}N_2O_7, CH_3OH$
Formula weight	925.02
Temperature	120(2) K
Wavelength	0.71073 Å
Crystal system	Monoclinic
Space group	$P2_1/c$
Unit cell dimensions	a = 7.96450(10) Å b = 12.1599(2) Å β = 93.3390(10)° c = 23.8549(4) Å
Volume	2306.37(6) Å^3
Z	2
Density (calculated)	1.332 Mg / m^3
Absorption coefficient	0.099 mm^{-1}
F(000)	988
Crystal	Prism; Pink
Crystal size	0.20 × 0.20 × 0.12 mm^3

θ range for data collection	3.00 – 25.03°
Index ranges	$-9 \le h \le 9$, $-14 \le k \le 14$, $-28 \le l \le 28$
Reflections collected	26868
Independent reflections	4086 [R_{int} = 0.0481]
Completeness to θ = 25.03°	99.9 %
Absorption correction	Semi–empirical from equivalents
Max. and min. transmission	0.9882 and 0.9804
Refinement method	Full-matrix least-squares on F^2
Data / restraints / parameters	4086 / 21 / 301
Goodness-of-fit on F^2	1.049
Final R indices [$F^2 > 2\sigma(F^2)$]	$R1$ = 0.0567, $wR2$ = 0.1316
R indices (all data)	$R1$ = 0.0665, $wR2$ = 0.1387
Largest diff. peak and hole	0.535 and –0.266 e Å^{-3}

Diffractometer: *Nonius KappaCCD* area detector (ϕ scans and ω scans to fill *asymmetric unit*). **Cell determination:** DirAx (Duisenberg, A.J.M.(1992). J. Appl. Cryst. 25, 92-96.) **Data collection:** Collect (Collect: Data collection software, R. Hooft, Nonius B.V., 1998). **Data reduction and cell refinement**: *Denzo* (Z. Otwinowski & W. Minor, *Methods in Enzymology* (1997) Vol. **276**: *Macromolecular Crystallography*, part A, pp. 307–326; C. W. Carter, Jr. & R. M. Sweet, Eds., Academic Press). **Absorption correction**: Sheldrick, G. M. SADABS - Bruker Nonius area detector scaling and absorption correction - V2.10 S**tructure solution**: *SHELXS97* (G. M. Sheldrick, Acta Cryst. (1990) A**46** 467–473). S**tructure refinement**: *SHELXL97* (G. M. Sheldrick (1997), University of Göttingen, Germany). **Graphics:** Cameron - A Molecular Graphics Package. (D. M. Watkin, L. Pearce and C. K. Prout, Chemical Crystallography Laboratory, University of Oxford, 1993).

Special details: The identity of the solvent proved very difficult to ascertain. As the experiment involved CO2 it was initially considered as a possibility, however, it was finally decided that methanol was the most likely culprit. It is modelled as disordered over 4 positions with the oxygens involved in hydrogen bonding to the bowl. Hydrogen atoms were included in the UNIT instruction but not the model.

Table 2. Atomic coordinates [× 10^4], equivalent isotropic displacement parameters [Å^2 × 10^3] and site occupancy factors. U_{eq} is defined as one third of the trace of the orthogonalized U^{ij} tensor.

Atom	*x*	*y*	*z*	U_{eq}	*S.o.f.*
O102	5161(12)	9412(8)	5454(4)	91(1)	0.25
O103	3781(11)	10266(8)	5289(4)	91(1)	0.25
C101	5000	10000	5000	91(1)	1
O1	1334(2)	8688(1)	2930(1)	30(1)	1
O2	2057(2)	7645(1)	4906(1)	27(1)	1
O3	961(2)	9211(1)	5656(1)	30(1)	1
O4	3235(2)	9202(1)	6621(1)	32(1)	1
O5	6083(2)	8257(1)	7238(1)	34(1)	1
O6	6837(2)	6695(1)	6335(1)	33(1)	1
O7	4910(2)	6727(1)	5225(1)	29(1)	1
N1	2334(2)	8080(1)	2105(1)	27(1)	1
N2	3436(2)	7407(1)	2939(1)	27(1)	1
C1	1713(2)	8641(2)	1152(1)	25(1)	1
C2	1062(2)	9387(2)	758(1)	28(1)	1
C3	364(2)	10375(2)	924(1)	29(1)	1
C4	356(2)	10611(2)	1492(1)	30(1)	1
C5	990(2)	9874(2)	1891(1)	28(1)	1
C6	1654(2)	8866(2)	1723(1)	23(1)	1
C7	2294(2)	8107(2)	2681(1)	24(1)	1

C8	3813(2)	7297(2)	3522(1)	24(1)	1
C9	2693(2)	7612(2)	3925(1)	23(1)	1
C10	3104(2)	7416(2)	4488(1)	23(1)	1
C11	4642(2)	6922(2)	4661(1)	25(1)	1
C12	5758(2)	6655(2)	4261(1)	28(1)	1
C13	5345(2)	6834(2)	3695(1)	28(1)	1
C14	628(2)	8329(2)	4770(1)	28(1)	1
C15	−184(2)	8568(2)	5313(1)	30(1)	1
C16	444(3)	9336(2)	6214(1)	32(1)	1
C17	1809(3)	9909(2)	6552(1)	34(1)	1
C18	4741(3)	9783(2)	6780(1)	35(1)	1
C19	6191(3)	9013(2)	6781(1)	35(1)	1
C20	7352(3)	7422(2)	7259(1)	37(1)	1
C21	6843(3)	6433(2)	6914(1)	35(1)	1
C22	6269(3)	5784(2)	6000(1)	30(1)	1
C23	6341(2)	6064(2)	5391(1)	29(1)	1

Table 3. Hydrogen bonds [Å and °].

D–H···*A*	*d*(*D*–H)	*d*(H···*A*)	*d*(*D*···*A*)	∠(*D*H*A*)
N1–H901···O4^{ii}	0.88	2.26	3.104(2)	160.0
N2–H902···O5^{ii}	0.88	2.09	2.881(2)	148.8

Symmetry transformations used to generate equivalent atoms:
(i) −x+1,−y+2,−z+1 (ii) x,−y+3/2,z−1/2

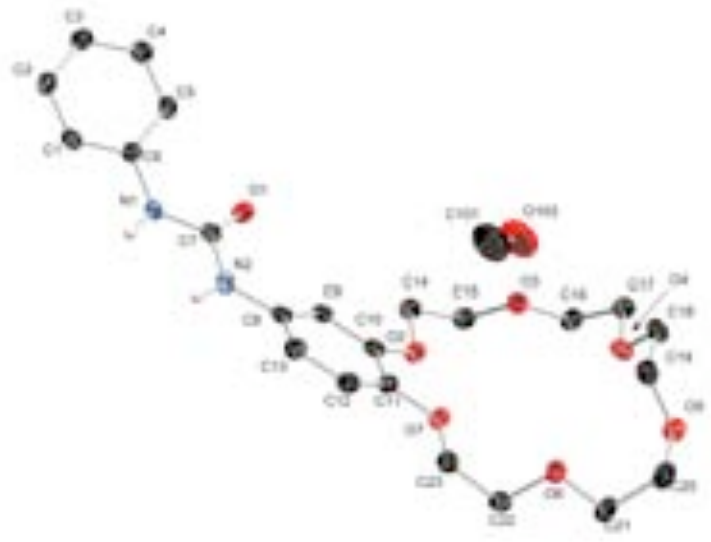

Thermal ellipsoids drawn at the 35% probability level

STRUCTURES FROM CHAPTER 3

Complex 127

Table 1. Crystal data and structure refinement details.

Empirical formula	$C_{33}H_{27}Cl_2N_7O_2Zn$
Formula weight	689.89
Temperature	120(2) K
Wavelength	0.71073 Å
Crystal system	Monoclinic
Space group	*Cc*
Unit cell dimensions	a = 22.3441(6) Å b = 14.6549(4) Å β = 94.119(2)° c = 9.2561(2) Å
Volume	3023.09(13) Å^3
Z	4
Density (calculated)	1.516 Mg / m^3
Absorption coefficient	1.034 mm^{-1}
F(000)	1416
Crystal	Blade; Yellow
Crystal size	0.2 × 0.09 × 0.05 mm^3
θ range for data collection	3.07 – 27.48°
Index ranges	$-28 \le h \le 26$, $-19 \le k \le 17$, $-12 \le l \le 10$
Reflections collected	15749
Independent reflections	6056 [R_{int} = 0.0368]
Completeness to θ = 27.48°	99.3 %
Absorption correction	Semi–empirical from equivalents
Max. and min. transmission	0.9501 and 0.8299
Refinement method	Full-matrix least-squares on F^2
Data / restraints / parameters	6056 / 8 / 337
Goodness-of-fit on F^2	1.051
Final R indices [$F^2 > 2\sigma(F^2)$]	*R1* = 0.0518, *wR2* = 0.1139
R indices (all data)	*R1* = 0.0629, *wR2* = 0.1218
Absolute structure parameter	0.109(15)
Largest diff. peak and hole	0.843 and –0.534 e Å^{-3}

Diffractometer: *Nonius KappaCCD* area detector (ϕ scans and ω scans to fill *asymmetric unit*). **Cell determination:** DirAx (Duisenberg, A.J.M.(1992). J. Appl. Cryst. 25, 92-96.) **Data collection:** Collect (Collect: Data collection software, R. Hooft, Nonius B.V., 1998). **Data reduction and cell refinement**: *Denzo* (Z. Otwinowski & W. Minor, *Methods in Enzymology* (1997) Vol. **276**: *Macromolecular Crystallography*, part A, pp. 307–326; C. W. Carter, Jr. & R. M. Sweet, Eds., Academic Press). **Absorption correction**: Sheldrick, G. M. SADABS - Bruker Nonius area detector scaling and absorption correction - V2.10 S**tructure solution**: *SHELXS97* (G. M. Sheldrick, Acta Cryst. (1990) A**46** 467–473). S**tructure refinement**: *SHELXL97* (G. M. Sheldrick (1997), University of Göttingen, Germany). **Graphics:** Cameron - A Molecular Graphics Package. (D. M. Watkin, L. Pearce and C. K. Prout, Chemical Crystallography Laboratory, University of Oxford, 1993).

Special details: The 2 phenyl rings are modelled as disordered over 2 rotationally related positions. The structure was refined as a racemic twin.

Table 2. Atomic coordinates [$\times 10^4$], equivalent isotropic displacement parameters [$Å^2 \times 10^3$] and site occupancy factors. U_{eq} is defined as one third of the trace of the orthogonalized U^{ij} tensor.

Atom	*x*	*y*	*z*	U_{eq}	*S.o.f.*
C1A	9759(6)	6226(6)	8432(13)	63(1)	0.382(12)
C2A	10169(5)	5576(9)	8972(18)	63(1)	0.382(12)
C3A	10013(5)	4970(8)	10037(14)	63(1)	0.382(12)
C4A	9446(7)	5014(9)	10562(12)	63(1)	0.382(12)
C5A	9036(5)	5664(10)	10022(18)	63(1)	0.382(12)
C6A	9192(6)	6270(7)	8957(15)	63(1)	0.382(12)
C1B	9778(4)	6279(5)	8928(12)	63(1)	0.618(12)
C2B	10127(3)	5587(5)	9582(13)	63(1)	0.618(12)
C3B	9853(3)	4839(5)	10182(10)	63(1)	0.618(12)
C4B	9231(3)	4783(5)	10128(11)	63(1)	0.618(12)
C5B	8883(3)	5474(6)	9473(12)	63(1)	0.618(12)
C6B	9156(4)	6222(5)	8874(10)	63(1)	0.618(12)
C7	8911(2)	7809(4)	8043(5)	34(1)	1
C8	8426(2)	9215(4)	7046(5)	31(1)	1
C9	8857(2)	9842(4)	7526(5)	37(1)	1
C10	8850(2)	10724(4)	6999(6)	42(1)	1
C11	8405(3)	11008(4)	6014(6)	43(1)	1
C12	7962(2)	10395(3)	5518(5)	35(1)	1
C13	7972(2)	9500(3)	6017(5)	29(1)	1
C14	7371(2)	8869(3)	4147(5)	29(1)	1
C15	6863(2)	8309(3)	3565(5)	30(1)	1
C16	6731(2)	8196(4)	2101(5)	37(1)	1
C17	6244(3)	7659(4)	1637(6)	44(1)	1
C18	5891(2)	7291(4)	2654(5)	35(1)	1
C19	6048(2)	7455(3)	4112(5)	31(1)	1
C20	5685(2)	7113(4)	5273(5)	33(1)	1
C21	5506(2)	7000(4)	7723(5)	32(1)	1
C22	5148(2)	7608(4)	8412(6)	41(1)	1
C23	4826(2)	7329(5)	9558(6)	46(1)	1
C24	4864(2)	6429(4)	10014(5)	43(1)	1
C25	5222(2)	5821(4)	9352(5)	39(1)	1
C26	5553(2)	6096(4)	8196(5)	34(1)	1
C27	6345(2)	4934(3)	8245(5)	35(1)	1
C28A	7252(4)	4042(9)	7763(15)	47(1)	0.61(2)
C29A	7545(5)	3753(9)	6569(13)	47(1)	0.61(2)
C30A	8060(4)	3222(8)	6765(11)	47(1)	0.61(2)
C31A	8282(4)	2981(8)	8154(12)	47(1)	0.61(2)
C32A	7989(4)	3270(8)	9347(11)	47(1)	0.61(2)
C33A	7474(4)	3800(8)	9151(14)	47(1)	0.61(2)
C28B	7292(5)	4140(13)	7810(20)	47(1)	0.39(2)
C29B	7671(7)	3900(11)	6745(17)	47(1)	0.39(2)
C30B	8200(7)	3431(11)	7116(17)	47(1)	0.39(2)
C31B	8352(5)	3202(11)	8553(18)	47(1)	0.39(2)
C32B	7973(7)	3442(10)	9619(15)	47(1)	0.39(2)

C33B	7444(7)	3911(12)	9250(20)	47(1)	0.39(2)
N1	8771(2)	6923(3)	8342(5)	40(1)	1
N2	8427(2)	8302(3)	7487(5)	36(1)	1
N3	7512(2)	8879(3)	5514(4)	27(1)	1
N4	6519(2)	7959(3)	4559(4)	27(1)	1
N5	5853(2)	7305(3)	6570(4)	30(1)	1
N6	5930(2)	5484(3)	7525(4)	36(1)	1
N7	6741(2)	4577(3)	7386(5)	40(1)	1
O1	9416(2)	8126(3)	8270(4)	39(1)	1
O2	6344(2)	4778(3)	9559(4)	43(1)	1
Cl1	6505(1)	9278(1)	8101(2)	49(1)	1
Cl2	7261(1)	6968(1)	7863(2)	47(1)	1
Zn1	6725(1)	8110(1)	6744(1)	30(1)	1

Table 3. Hydrogen bonds [Å and °].

D–H···*A*	*d*(*D*–H)	*d*(H···*A*)	*d*(*D*···*A*)	∠(*D*H*A*)
N1–H91···Cl2	0.88	2.56	3.372(4)	154.3
N2–H92···Cl2	0.88	2.45	3.294(4)	161.2
N6–H93···O2^{i}	0.88	2.20	2.984(5)	147.6
N7–H94···O2^{i}	0.88	2.01	2.863(6)	162.9

Symmetry transformations used to generate equivalent atoms:
(i) x,–y+1,z–1/2

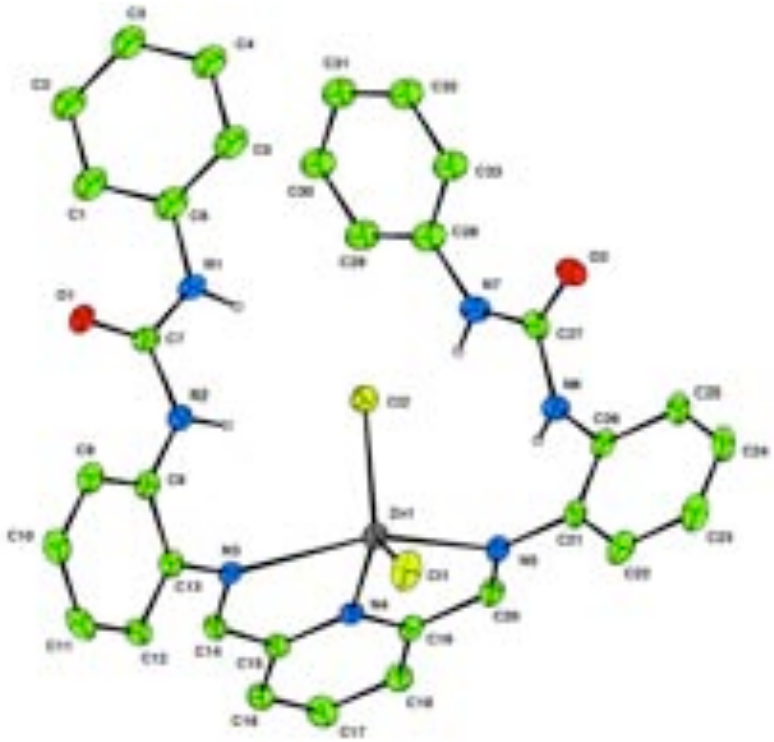

STRUCTURES FROM CHAPTER 4

Receptor 138

Table 1. Crystal data and structure refinement details.

Empirical formula	$C_{21}H_{19}N_5O_7S$	
Formula weight	485.47	
Temperature	120(2) K	
Wavelength	0.71073 Å	
Crystal system	Triclinic	
Space group	*P*–1	
Unit cell dimensions	a = 10.0218(3) Å	α = 99.149(2)°
	b = 11.1125(3) Å	β = 94.159(2)°
	c = 21.8751(6) Å	γ = 112.463(2)°
Volume	2198.84(11) Å^3	
Z	4	
Density (calculated)	1.466 Mg / m^3	
Absorption coefficient	0.202 mm^{-1}	
F(000)	1008	
Crystal	Fragment; Colourless	
Crystal size	0.20 × 0.15 × 0.10 mm^3	
θ range for data collection	2.96 – 27.48°	
Index ranges	$-13 \le h \le 12$, $-14 \le k \le 14$, $-28 \le l \le 28$	
Reflections collected	32447	
Independent reflections	9954 [R_{int} = 0.0590]	
Completeness to θ = 27.48°	98.7 %	
Absorption correction	Semi–empirical from equivalents	
Max. and min. transmission	0.9801 and 0.9607	
Refinement method	Full-matrix least-squares on F^2	
Data / restraints / parameters	9954 / 0 / 617	
Goodness-of-fit on F^2	1.073	
Final *R* indices [$F^2 > 2\sigma(F^2)$]	*R1* = 0.0796, *wR2* = 0.1621	
R indices (all data)	*R1* = 0.1196, *wR2* = 0.1852	
Largest diff. peak and hole	0.344 and –0.441 e Å^{-3}	

Diffractometer: *Nonius KappaCCD* area detector (ϕ scans and ω scans to fill *asymmetric unit*). **Cell determination:** DirAx (Duisenberg, A.J.M.(1992). J. Appl. Cryst. 25, 92-96.) **Data collection:** Collect (Collect: Data collection software, R. Hooft, Nonius B.V., 1998). **Data reduction and cell refinement**: *Denzo* (Z. Otwinowski & W. Minor, *Methods in Enzymology* (1997) Vol. **276**: *Macromolecular Crystallography*, part A, pp. 307–326; C. W. Carter, Jr. & R. M. Sweet, Eds., Academic Press). **Absorption correction**: Sheldrick, G. M. SADABS - Bruker Nonius area detector scaling and absorption correction - V2.10 **Structure solution**: *SHELXS97* (G. M. Sheldrick, Acta Cryst. (1990) A**46** 467–473). **Structure refinement**: *SHELXL97* (G. M. Sheldrick (1997), University of Göttingen, Germany). **Graphics:** Cameron - A Molecular Graphics Package. (D. M. Watkin, L. Pearce and C. K. Prout, Chemical Crystallography Laboratory, University of Oxford, 1993).

Special details: All hydrogen atoms were placed in idealised positions and refined using a riding model.

Table 2. Atomic coordinates [× 10^4], equivalent isotropic displacement parameters [Å^2 × 10^3] and site occupancy factors. U_{eq} is defined as one third of the trace of the orthogonalized U^{ij} tensor.

Atom	*x*	*y*	*z*	U_{eq}	*S.o.f.*
O1	226(3)	303(3)	–2143(1)	44(1)	1
O2	–194(4)	–920(3)	–1450(1)	60(1)	1
O3	4015(3)	6366(2)	–238(1)	39(1)	1
O4	5734(3)	7610(3)	3021(1)	39(1)	1
O5	2128(3)	1223(3)	4134(1)	50(1)	1
O6	3685(3)	2857(3)	4834(1)	43(1)	1
N1	314(3)	164(3)	–1599(1)	34(1)	1
N2	3120(3)	4705(3)	311(1)	27(1)	1
N3	4461(3)	6487(3)	1394(1)	27(1)	1
N4	4137(3)	5558(3)	2477(1)	29(1)	1
N5	3038(3)	2376(3)	4296(1)	35(1)	1
C1	1070(4)	1340(3)	–1103(2)	26(1)	1
C2	1703(4)	2553(3)	–1269(2)	29(1)	1
C3	2406(4)	3691(3)	–806(2)	29(1)	1
C4	2454(3)	3591(3)	–179(1)	24(1)	1
C5	1830(4)	2347(3)	–17(2)	28(1)	1
C6	1132(4)	1209(3)	–483(2)	29(1)	1
C7	3867(4)	5985(3)	260(2)	28(1)	1
C8	4556(4)	6953(3)	862(2)	27(1)	1
C9	5285(4)	8293(3)	849(2)	29(1)	1
C10	5947(4)	9184(4)	1409(2)	33(1)	1
C11	5859(4)	8706(4)	1956(2)	33(1)	1
C12	5103(4)	7356(4)	1931(2)	29(1)	1
C13	5032(4)	6858(4)	2533(2)	31(1)	1
C14	3899(4)	4811(3)	2952(2)	27(1)	1
C15	2893(4)	3486(3)	2785(2)	29(1)	1
C16	2618(4)	2686(3)	3220(2)	29(1)	1
C17	3344(4)	3212(3)	3827(2)	28(1)	1
C18	4346(4)	4517(4)	4005(2)	30(1)	1
C19	4622(4)	5333(3)	3570(2)	28(1)	1
O7	2540(3)	–431(3)	297(1)	49(1)	1
O8	1919(3)	–1587(3)	1015(1)	41(1)	1
O9	7485(3)	5396(3)	2125(1)	45(1)	1
O10	9255(3)	6678(2)	5388(1)	33(1)	1
O11	6006(3)	287(3)	6504(1)	50(1)	1
O12	7457(3)	1965(3)	7209(1)	49(1)	1
N6	2616(3)	–542(3)	849(1)	34(1)	1
N7	6523(3)	3769(3)	2679(1)	26(1)	1
N8	8062(3)	5521(3)	3756(1)	24(1)	1
N9	7977(3)	4561(3)	4825(1)	26(1)	1
N10	6845(4)	1460(3)	6668(1)	38(1)	1
C20	3600(4)	603(3)	1324(2)	28(1)	1
C21	4434(4)	1741(4)	1133(2)	32(1)	1

C22	5420(4)	2815(4)	1575(2)	31(1)	1
C23	5551(4)	2724(3)	2206(2)	26(1)	1
C24	4661(4)	1559(3)	2382(2)	25(1)	1
C25	3677(4)	484(3)	1947(2)	25(1)	1
C26	7365(4)	5022(3)	2623(2)	28(1)	1
C27	8160(4)	5980(3)	3224(2)	26(1)	1
C28	8941(4)	7301(3)	3202(2)	31(1)	1
C29	9623(4)	8203(3)	3756(2)	34(1)	1
C30	9509(4)	7750(3)	4313(2)	30(1)	1
C31	8745(4)	6402(3)	4285(2)	25(1)	1
C32	8687(4)	5899(3)	4889(2)	25(1)	1
C33	7734(4)	3836(3)	5307(2)	26(1)	1
C34	6715(4)	2527(4)	5149(2)	32(1)	1
C35	6427(4)	1745(4)	5595(2)	37(1)	1
C36	7140(4)	2290(4)	6199(2)	30(1)	1
C37	8134(4)	3590(4)	6367(2)	29(1)	1
C38	8450(4)	4366(3)	5918(2)	27(1)	1
S1	401(1)	3975(1)	1532(1)	32(1)	1
O13	1818(3)	3886(2)	1407(1)	29(1)	1
C39	–858(5)	3160(5)	829(2)	58(1)	1
C40	623(5)	5627(4)	1507(2)	51(1)	1
S2	7233(1)	1291(1)	3376(1)	37(1)	1
O14	6957(3)	2444(2)	3702(1)	33(1)	1
C41	7687(5)	513(4)	3967(2)	56(1)	1
C42	8994(5)	1987(5)	3144(2)	61(1)	1

Receptor 139

Table 1. Crystal data and structure refinement details.

Empirical formula	$C_{23}H_{23}N_7O_{12}S_2$ $C_{19}H_{11}N_7O_{10}$, $2(C_2H_6OS)$
Formula weight	653.60
Temperature	120(2) K
Wavelength	0.71073 Å
Crystal system	Monoclinic
Space group	$P2_1/c$
Unit cell dimensions	a = 10.4595(3) Å b = 23.6137(7) Å β = 97.7270(10)° c = 22.8537(6) Å
Volume	5593.3(3) Å^3
Z	8
Density (calculated)	1.552 Mg / m^3
Absorption coefficient	0.267 mm^{-1}
F(000)	2704
Crystal	Block; Colourless
Crystal size	0.2 × 0.07 × 0.03 mm^3
θ range for data collection	2.97 – 25.03°
Index ranges	$-12 \le h \le 12$, $-28 \le k \le 28$, $-27 \le l \le 27$
Reflections collected	43828
Independent reflections	9851 [R_{int} = 0.0655]
Completeness to θ = 25.03°	99.6 %
Absorption correction	Semi–empirical from equivalents
Max. and min. transmission	0.9920 and 0.9384
Refinement method	Full-matrix least-squares on F^2
Data / restraints / parameters	9851 / 0 / 817
Goodness-of-fit on F^2	1.137
Final R indices [$F^2 > 2\sigma(F^2)$]	$R1$ = 0.0756, $wR2$ = 0.1358
R indices (all data)	$R1$ = 0.1053, $wR2$ = 0.1499
Largest diff. peak and hole	0.516 and –0.367 e Å^{-3}

Diffractometer: *Nonius KappaCCD* area detector (ϕ scans and ω scans to fill *asymmetric unit*). **Cell determination:** DirAx (Duisenberg, A.J.M.(1992). J. Appl. Cryst. 25, 92-96.) **Data collection:** Collect (Collect: Data collection software, R. Hooft, Nonius B.V., 1998). **Data reduction and cell refinement**: *Denzo* (Z. Otwinowski & W. Minor, *Methods in Enzymology* (1997) Vol. **276**: *Macromolecular Crystallography*, part A, pp. 307–326; C. W. Carter, Jr. & R. M. Sweet, Eds., Academic Press). **Absorption correction**: Sheldrick, G. M. SADABS - Bruker Nonius area detector scaling and absorption correction - V2.10 S**tructure solution**: *SHELXS97* (G. M. Sheldrick, Acta Cryst. (1990) A**46** 467–473). S**tructure refinement**: *SHELXL97* (G. M. Sheldrick (1997), University of Göttingen, Germany). **Graphics:** Cameron - A Molecular Graphics Package. (D. M. Watkin, L. Pearce and C. K. Prout, Chemical Crystallography Laboratory, University of Oxford, 1993).

Special details: All hydrogen atoms were placed in idealised positions and refined using a riding model, except those of the NH which were freely refined.

Table 2. Atomic coordinates [× 10^4], equivalent isotropic displacement parameters [Å^2 × 10^3] and site occupancy factors. U_{eq} is defined as one third of the trace of the orthogonalized U^{ij} tensor.

Atom	*x*	*y*	*z*	U_{eq}	*S.o.f.*
O1	–4004(3)	7546(2)	10520(2)	44(1)	1
O2	–5223(3)	7490(2)	9676(2)	38(1)	1
O3	–3903(3)	6368(1)	8104(1)	34(1)	1
O4	–2037(3)	5961(2)	8241(1)	34(1)	1
O5	–821(3)	6414(1)	11272(1)	26(1)	1
O6	4228(3)	4605(1)	10787(1)	24(1)	1
O7	5979(3)	3522(2)	9544(1)	37(1)	1
O8	5444(4)	3357(2)	8613(2)	43(1)	1
O9	1912(3)	4394(2)	7511(1)	37(1)	1
O10	972(3)	5051(2)	7951(1)	44(1)	1
N1	–4256(4)	7365(2)	10012(2)	28(1)	1
N2	–2892(4)	6244(2)	8410(2)	26(1)	1
N3	–401(3)	6157(2)	10346(2)	20(1)	1
N4	1667(3)	5575(2)	10824(2)	20(1)	1
N5	2859(4)	5016(2)	10040(2)	21(1)	1
N6	5312(4)	3608(2)	9067(2)	26(1)	1
N7	1768(4)	4674(2)	7948(2)	31(1)	1
C1	–1654(4)	6227(2)	9400(2)	19(1)	1
C2	–2688(4)	6444(2)	9030(2)	21(1)	1
C3	–3559(4)	6819(2)	9209(2)	23(1)	1
C4	–3327(4)	6973(2)	9799(2)	22(1)	1
C5	–2306(4)	6779(2)	10196(2)	20(1)	1
C6	–1462(4)	6392(2)	9991(2)	18(1)	1
C7	–144(4)	6188(2)	10947(2)	22(1)	1
C8	1081(4)	5879(2)	11201(2)	21(1)	1
C9	1523(4)	5919(2)	11803(2)	26(1)	1
C10	2621(4)	5620(2)	12024(2)	26(1)	1
C11	3234(4)	5293(2)	11642(2)	25(1)	1
C12	2722(4)	5288(2)	11043(2)	20(1)	1
C13	3350(4)	4936(2)	10614(2)	20(1)	1
C14	3141(4)	4716(2)	9543(2)	21(1)	1
C15	4114(4)	4314(2)	9562(2)	21(1)	1
C16	4285(4)	4041(2)	9040(2)	22(1)	1
C17	3557(4)	4148(2)	8502(2)	24(1)	1
C18	2608(4)	4551(2)	8507(2)	23(1)	1
C19	2375(4)	4830(2)	9007(2)	21(1)	1
O11	7289(3)	3933(1)	6503(1)	34(1)	1
O12	9079(3)	3491(2)	6459(2)	43(1)	1
O13	9458(3)	2327(2)	4758(2)	45(1)	1
O14	8262(3)	2511(2)	3931(2)	48(1)	1
O15	5010(3)	3705(1)	3503(1)	24(1)	1
O16	511(3)	5536(1)	4521(1)	25(1)	1
O17	–526(3)	6539(2)	6031(2)	42(1)	1

O18	371(4)	6604(2)	6941(2)	45(1)	1
O19	3958(3)	5408(2)	7661(1)	37(1)	1
O20	4776(3)	4865(2)	7050(1)	41(1)	1
N8	8007(4)	3643(2)	6243(2)	32(1)	1
N9	8554(4)	2570(2)	4467(2)	33(1)	1
N10	4921(3)	3884(2)	4481(2)	20(1)	1
N11	2860(3)	4548(2)	4205(2)	20(1)	1
N12	2105(3)	5070(2)	5121(2)	21(1)	1
N13	288(4)	6402(2)	6446(2)	32(1)	1
N14	3993(4)	5209(2)	7168(2)	29(1)	1
C20	6455(4)	3741(2)	5340(2)	21(1)	1
C21	7538(4)	3478(2)	5626(2)	22(1)	1
C22	8243(4)	3088(2)	5358(2)	26(1)	1
C23	7811(4)	2974(2)	4772(2)	24(1)	1
C24	6734(4)	3224(2)	4457(2)	23(1)	1
C25	6043(4)	3613(2)	4749(2)	19(1)	1
C26	4480(4)	3920(2)	3896(2)	20(1)	1
C27	3278(4)	4268(2)	3755(2)	19(1)	1
C28	2667(4)	4302(2)	3177(2)	22(1)	1
C29	1583(4)	4631(2)	3058(2)	25(1)	1
C30	1134(4)	4922(2)	3518(2)	23(1)	1
C31	1808(4)	4868(2)	4081(2)	20(1)	1
C32	1389(4)	5190(2)	4595(2)	20(1)	1
C33	2057(4)	5329(2)	5670(2)	21(1)	1
C34	1158(4)	5741(2)	5770(2)	23(1)	1
C35	1226(4)	5965(2)	6334(2)	23(1)	1
C36	2124(4)	5802(2)	6805(2)	24(1)	1
C37	2996(4)	5397(2)	6681(2)	21(1)	1
C38	3001(4)	5163(2)	6133(2)	21(1)	1
S1	1929(1)	6488(1)	9265(1)	26(1)	1
O21	1319(3)	5952(1)	9466(1)	25(1)	1
C39	813(4)	6771(2)	8689(2)	40(1)	1
C40	3116(5)	6269(2)	8824(2)	42(1)	1
S2	1595(1)	2263(1)	7395(1)	26(1)	1
O22	2211(3)	2483(2)	6882(1)	38(1)	1
C41	506(5)	2794(2)	7570(2)	33(1)	1
C42	2738(5)	2336(2)	8044(2)	41(1)	1
S3	3124(1)	3530(1)	5777(1)	23(1)	1
O23	3563(3)	4058(1)	5492(1)	28(1)	1
C43	2334(5)	3765(2)	6379(2)	40(1)	1
C44	1731(5)	3285(2)	5317(3)	50(2)	1
S4	3256(1)	7177(1)	2722(1)	28(1)	1
O24	3024(4)	7425(2)	3301(2)	43(1)	1
C45	4786(4)	6836(2)	2859(2)	36(1)	1
C46	3715(5)	7748(2)	2287(2)	39(1)	1

PART B

STRUCTURE FROM CHAPTER 2

Receptor 101 / 18-crown-6 / DAP-CO_2 ternary complex

Table 1. Crystal data and structure refinement details.

Empirical formula	$C_{87}H_{135}N_{16}O_{22.50}S_{0.50}$ $2(C_{27}H_{32}N_6O_3)$, $2(C_{12}H_{24}O_6)$, $2(C_4H_{10}N_2O_2)$, $0.5(C_2H_6OS)$	
Formula weight	1781.14	
Temperature	293(2) K	
Wavelength	0.68890 Å	
Crystal system	Triclinic	
Space group	P-1	
Unit cell dimensions	a = 12.626(7) Å	α = 84.204(10)°
	b = 14.165(9) Å	β = 77.246(8)°
	c = 27.564(17) Å	γ = 72.121(9)°
Volume	4573(5) $Å^3$	
Z	2	
Density (calculated)	1.294 Mg / m^3	
Absorption coefficient	0.105 mm^{-1}	
F(000)	1914	
Crystal	Colourless block	
Crystal size	0.05 × 0.03 × 0.02 mm^3	
θ range for data collection	2.90 – 24.21°	
Index ranges	$-13 \le h \le 14$, $-14 \le k \le 16$, $-30 \le l \le 32$	
Reflections collected	34055	
Independent reflections	14794 [R_{int} = 0.0680]	
Completeness to θ = 24.21°	91.7 %	
Max. and min. transmission	0.9979 and 0.9948	
Refinement method	Full-matrix least-squares on F^2	
Data / restraints / parameters	14794 / 0 / 1151	
Goodness-of-fit on F^2	1.052	
Final R indices [$F^2 > 2\sigma(F^2)$]	*R1* = 0.0649, *wR2* = 0.1813	
R indices (all data)	*R1* = 0.0854, *wR2* = 0.1936	
Largest diff. peak and hole	0.283 and –0.484 e $Å^{-3}$	

Diffractometer: *Nonius KappaCCD* area detector (ϕ scans and ω scans to fill *asymmetric unit*). **Cell determination:** DirAx (Duisenberg, A.J.M.(1992). J. Appl. Cryst. 25, 92-96.) **Data collection:** Collect (Collect: Data collection software, R. Hooft, Nonius B.V., 1998). **Data reduction and cell refinement**: *Denzo* (Z. Otwinowski & W. Minor, *Methods in Enzymology* (1997) Vol. **276**: *Macromolecular Crystallography*, part A, pp. 307–326; C. W. Carter, Jr. & R. M. Sweet, Eds., Academic Press). **Absorption correction**: Sheldrick, G. M. SADABS - Bruker Nonius area detector scaling and absorption correction - V2.10 S**tructure solution**: *SHELXS97* (G. M. Sheldrick, Acta Cryst. (1990) A**46** 467–473). S**tructure refinement**: *SHELXL97* (G. M. Sheldrick (1997), University of Göttingen, Germany). **Graphics:** Cameron - A Molecular Graphics Package. (D. M. Watkin, L. Pearce and C. K. Prout, Chemical Crystallography Laboratory, University of Oxford, 1993).

Special details: All hydrogen atoms were placed in idealised positions and refined using a riding model.

Table 2. Atomic coordinates [× 10^4], equivalent isotropic displacement parameters [Å^2 × 10^3] and site occupancy factors. U_{eq} is defined as one third of the trace of the orthogonalized U^{ij} tensor.

Atom	*x*	*y*	*z*	U_{eq}	*S.o.f.*
O1	1760(2)	2700(2)	3245(1)	41(1)	1
O2	6919(2)	4379(2)	2280(1)	38(1)	1
O3	5950(2)	1405(2)	−52(1)	40(1)	1
N1	1216(2)	2676(2)	4084(1)	33(1)	1
N2	3377(2)	3623(2)	3276(1)	26(1)	1
N3	5104(2)	4325(2)	2574(1)	28(1)	1
N4	5872(2)	4127(2)	1752(1)	31(1)	1
N5	5894(2)	2940(2)	934(1)	29(1)	1
N6	4630(2)	1765(2)	651(1)	32(1)	1
C1	1467(3)	−563(3)	4454(1)	45(1)	1
C2	1435(3)	415(2)	4160(1)	40(1)	1
C3	441(3)	1263(2)	4393(1)	33(1)	1
C4	305(3)	2239(2)	4099(1)	35(1)	1
C5	1878(2)	2872(2)	3658(1)	28(1)	1
C6	2760(2)	3316(2)	3705(1)	27(1)	1
C7	3165(3)	3450(2)	4105(1)	29(1)	1
C8	4086(3)	3852(2)	3920(1)	27(1)	1
C9	4841(3)	4128(2)	4140(1)	34(1)	1
C10	5671(3)	4474(2)	3838(1)	36(1)	1
C11	5785(3)	4549(2)	3315(1)	33(1)	1
C12	5058(2)	4287(2)	3089(1)	27(1)	1
C13	4198(2)	3947(2)	3398(1)	26(1)	1
C14	6045(3)	4280(2)	2211(1)	28(1)	1
C15	6695(3)	4025(2)	1311(1)	30(1)	1
C16	7555(3)	4476(2)	1211(1)	32(1)	1
C17	8346(3)	4343(2)	760(1)	39(1)	1
C18	8301(3)	3779(3)	396(1)	40(1)	1
C19	7435(3)	3320(2)	480(1)	34(1)	1
C20	6646(2)	3455(2)	936(1)	30(1)	1
C21	7112(3)	2708(2)	203(1)	37(1)	1
C22	6179(3)	2485(2)	483(1)	31(1)	1
C23	5574(3)	1853(2)	343(1)	32(1)	1
C24	3988(3)	1161(2)	531(1)	38(1)	1
C25	3234(3)	1677(2)	163(1)	37(1)	1
C26	2365(3)	2645(2)	347(1)	42(1)	1
C27	1615(3)	3144(3)	−19(1)	53(1)	1
O4	8760(2)	6683(2)	4956(1)	37(1)	1
O5	8325(2)	11633(2)	2912(1)	36(1)	1
O6	13503(2)	7488(2)	1869(1)	40(1)	1
N7	10165(2)	6706(2)	4298(1)	30(1)	1
N8	9002(2)	8769(2)	4115(1)	27(1)	1
N9	9251(2)	10463(2)	3431(1)	30(1)	1
N10	10080(2)	10574(2)	2613(1)	29(1)	1
N11	11861(2)	9304(2)	1883(1)	26(1)	1

N12	14129(2)	7652(2)	1040(1)	34(1)	1
C28	13152(4)	6366(3)	4956(2)	61(1)	1
C29	12440(3)	6328(3)	4584(1)	44(1)	1
C30	11601(3)	5753(2)	4782(1)	34(1)	1
C31	10868(3)	5720(2)	4417(1)	32(1)	1
C32	9181(3)	7130(2)	4591(1)	29(1)	1
C33	8581(3)	8180(2)	4488(1)	29(1)	1
C34	7570(3)	8739(2)	4754(1)	33(1)	1
C35	7352(3)	9718(2)	4546(1)	30(1)	1
C36	6490(3)	10609(2)	4657(1)	36(1)	1
C37	6571(3)	11439(2)	4367(1)	37(1)	1
C38	7477(3)	11417(2)	3963(1)	34(1)	1
C39	8336(3)	10554(2)	3840(1)	28(1)	1
C40	8272(2)	9709(2)	4144(1)	27(1)	1
C41	9151(3)	10952(2)	2973(1)	28(1)	1
C42	10179(2)	10808(2)	2097(1)	27(1)	1
C43	9487(3)	11599(2)	1882(1)	30(1)	1
C44	9665(3)	11764(2)	1362(1)	36(1)	1
C45	10529(3)	11146(2)	1049(1)	37(1)	1
C46	11255(3)	10324(2)	1254(1)	30(1)	1
C47	11071(3)	10162(2)	1777(1)	28(1)	1
C48	12197(3)	9518(2)	1056(1)	32(1)	1
C49	12538(3)	8910(2)	1445(1)	29(1)	1
C50	13427(2)	7959(2)	1469(1)	30(1)	1
C51	15025(3)	6714(2)	994(1)	35(1)	1
C52	14814(3)	5992(2)	686(1)	37(1)	1
C53	13835(3)	5595(2)	925(1)	41(1)	1
C54	13651(3)	4878(3)	602(1)	46(1)	1
O7	3519(2)	3727(2)	2221(1)	32(1)	1
O8	3932(2)	2871(2)	1530(1)	34(1)	1
N14	4973(2)	−357(2)	2488(1)	32(1)	1
C55	3443(2)	3051(2)	1974(1)	27(1)	1
N13	2771(2)	2484(2)	2211(1)	28(1)	1
C57	2637(2)	1661(2)	1989(1)	30(1)	1
C58	3659(3)	742(2)	1968(1)	29(1)	1
C59	3808(3)	313(2)	2483(1)	34(1)	1
O9	11643(2)	8884(1)	2900(1)	32(1)	1
O10	11036(2)	7943(2)	3537(1)	33(1)	1
N16	9736(2)	6091(2)	2485(1)	31(1)	1
C60	11570(2)	8055(2)	3102(1)	28(1)	1
N15	12132(2)	7235(2)	2831(1)	30(1)	1
C62	12200(2)	6236(2)	3017(1)	30(1)	1
C63	11127(3)	5961(2)	3020(1)	32(1)	1
C64	10937(3)	5965(2)	2500(1)	37(1)	1
O11	26(2)	5260(2)	1521(1)	39(1)	1
O12	−173(2)	4140(2)	2463(1)	40(1)	1
O13	−1594(2)	5147(2)	3304(1)	38(1)	1
O14	−1772(2)	7183(2)	3347(1)	35(1)	1
O15	−1356(2)	8241(2)	2433(1)	35(1)	1
O16	37(2)	7220(2)	1575(1)	41(1)	1

C65	630(3)	4241(2)	1594(1)	45(1)	1
C66	−63(3)	3757(2)	1988(1)	42(1)	1
C67	−812(3)	3671(2)	2846(1)	43(1)	1
C68	−962(3)	4130(2)	3326(1)	44(1)	1
C69	−1744(3)	5628(3)	3754(1)	40(1)	1
C70	−2430(3)	6677(3)	3705(1)	41(1)	1
C71	−2369(3)	8192(2)	3266(1)	36(1)	1
C72	−1604(3)	8667(2)	2905(1)	36(1)	1
C73	−547(3)	8609(2)	2087(1)	38(1)	1
C74	−433(3)	8274(2)	1582(1)	40(1)	1
C75	72(3)	6817(3)	1120(1)	48(1)	1
C76	669(3)	5740(3)	1147(1)	48(1)	1
O17	6752(2)	9054(2)	1554(1)	37(1)	1
O18	5818(2)	7662(2)	2129(1)	43(1)	1
O19	5067(2)	7802(2)	3189(1)	42(1)	1
O20	4636(2)	9667(2)	3553(1)	41(1)	1
O21	5809(2)	10932(2)	2977(1)	38(1)	1
O22	6321(2)	10895(2)	1915(1)	37(1)	1
C77	6608(3)	8242(3)	1341(1)	48(1)	1
C78	6734(3)	7406(2)	1720(1)	47(1)	1
C79	5737(3)	6850(2)	2466(2)	51(1)	1
C80	4783(3)	7193(3)	2891(1)	48(1)	1
C81	4179(3)	8166(3)	3603(1)	50(1)	1
C82	4534(3)	8835(3)	3873(1)	48(1)	1
C83	5026(3)	10340(3)	3770(1)	44(1)	1
C84	5013(3)	11221(3)	3430(1)	43(1)	1
C85	5893(3)	11776(2)	2659(1)	39(1)	1
C86	6729(3)	11450(2)	2194(1)	39(1)	1
C87	7091(3)	10598(2)	1459(1)	42(1)	1
C88	6723(3)	9894(2)	1220(1)	41(1)	1
C89	8914(4)	427(5)	141(2)	111(2)	1
S1	9952(2)	−435(2)	306(1)	54(1)	0.50
O23	9687(6)	−1331(4)	209(2)	79(2)	0.50

Table 3. Hydrogen bonds [Å and °].

D–H···*A*	*d*(*D*–H)	*d*(H···*A*)	*d*(*D*···*A*)	∠(*D*H*A*)
N13–H13···O1	0.86	2.01	2.860(3)	168.7
N15–H15···O6	0.86	2.03	2.885(3)	170.1
N2–H2···O7	0.86	2.04	2.866(4)	159.8
N3–H3···O7	0.86	2.01	2.782(3)	148.2
N4–H4···O7	0.86	2.43	3.163(3)	143.5
N5–H5···O8	0.86	1.84	2.677(3)	163.2
N6–H6···O8	0.86	1.98	2.840(3)	174.7
N7–H7A···O10	0.86	2.01	2.846(3)	164.7

N8–H8···O10	0.86	1.84	2.688(3)	167.5
N9–H9A···O9	0.86	2.62	3.291(3)	135.6
N10–H10A···O9	0.86	1.95	2.767(3)	158.7
N11–H11A···O9	0.86	1.95	2.775(3)	160.6
N1–H1···O4^{ii}	0.86	2.05	2.893(4)	167.1
N12–H12···O3^{iii}	0.86	2.08	2.916(4)	165.4
N14–H14A···O18^{iv}	0.89	2.03	2.872(4)	157.6
N14–H14B···O20^{iv}	0.89	2.04	2.875(4)	154.9
N14–H14B···O19^{iv}	0.89	2.52	3.073(4)	120.9
N14–H14C···O22^{iv}	0.89	2.07	2.940(3)	166.1
N14–H14C···O17^{iv}	0.89	2.56	3.016(3)	112.7
N16–H16A···O12^{v}	0.89	2.06	2.738(4)	132.1
N16–H16A···O13^{v}	0.89	2.19	2.966(3)	144.8
N16–H16B···O11^{v}	0.89	2.14	2.919(4)	145.2
N16–H16B···O16^{v}	0.89	2.23	2.852(3)	126.5
N16–H16C···O15^{v}	0.89	2.20	2.935(4)	140.1
N16–H16C···O14^{v}	0.89	2.20	2.932(3)	139.6

Symmetry transformations used to generate equivalent atoms:
(i) –x+2,–y,–z (ii) –x+1,–y+1,–z+1 (iii) –x+2,–y+1,–z
(iv) x,y–1,z (v) x+1,y,z

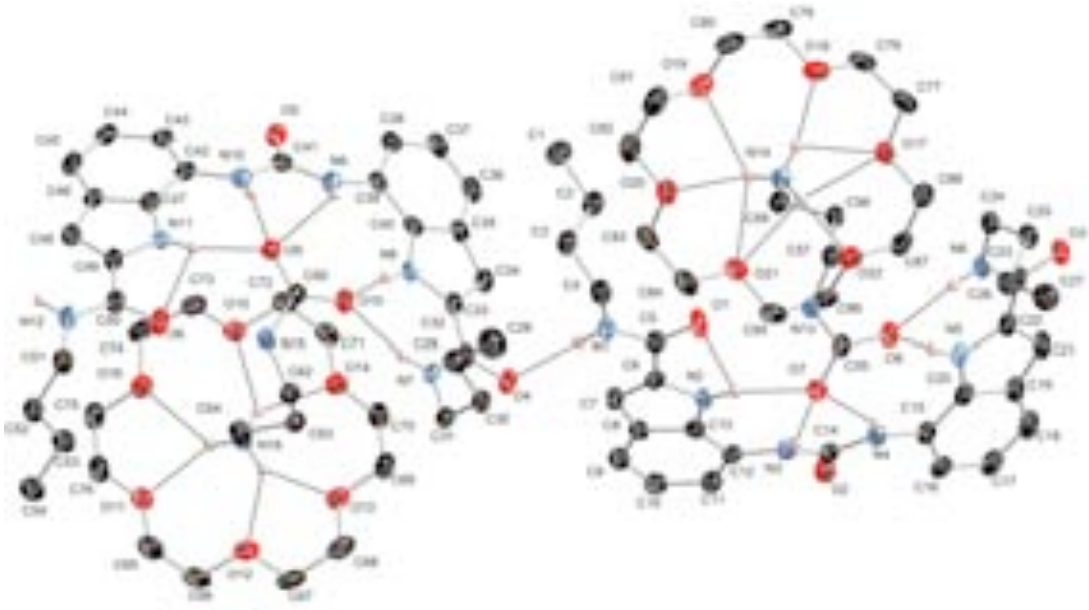

Thermal ellipsoids drawn at the 35% probability level

APPENDIX 2 – SPECTRA SUPPORTING CO_2 EXPERIMENTS

Example ^{1}H NMR (300MHz) spectra determined on a Bruker AV300 spectrometer. Chemical shifts are reported in parts per million (ppm) calibrated to the residual protio-solvent peak. All spectra were obtained at 298K.

PART A – Chemical shift changes with AAAC salts and THP-CO_2 adduct

DMSO-d_6 solutions, (0.01M), of each receptor, **93** - **101** and **109** were made and the ^{1}H NMR spectrum acquired. Subsequently either,

a) 1,3-diaminopropane, (1eq, 0.01M, 0.73 mg/mL, 0.8 μL/mL),
b) n-butylamine, (2eq, 0.02M, 1.46 mg/mL, 2.0 μL/mL),
c) 1,3-diaminopropane, (1eq, 0.01M, 0.73 mg/mL, 0.8 μL/mL) and 18-crown-6, (1eq, 0.01M, 2.64mg/mL),
d) n-butylamine, (2eq, 0.02M, 1.46mg/mL, 2.0μL/mL) and 18-crown-6, (1eq, 0.01M, 2.64mg/mL), or,
e) 1,4,5,6-tetrahydropyrimidine, (1eq, 0.01M, 0.84mg/mL).

…were added to the solution of receptor. Receptor **109** was not studied with cases **c)**, **d)**, or **e)**.

Carbon dioxide was bubbled through each solution for 3 minutes. After this time, a second ^{1}H NMR spectrum was acquired. The chemical shift change for each urea NH proton was calculated accordingly. This process was repeated three times for each receptor in each case a-e.

Chemical Shift Changes with AAAC salts and THP-CO_2 adduct

RECEPTOR 93

93 a) lone receptor, b) receptor + 2eq. n-butylamine, bubbled with CO_2 for 3 minutes.

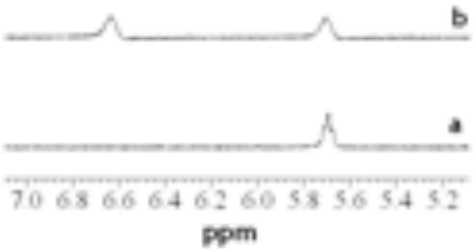

93 a) lone receptor, b) receptor + 1eq. 1,3-diaminopropane, bubbled with CO_2 for 3 minutes.

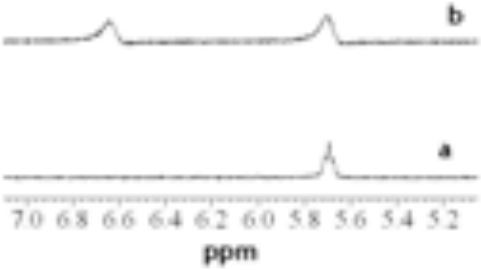

93 a) lone receptor, b) receptor + 2eq. n-butylamine and 1eq. 18-crown-6, bubbled with CO_2 for 3 minutes.

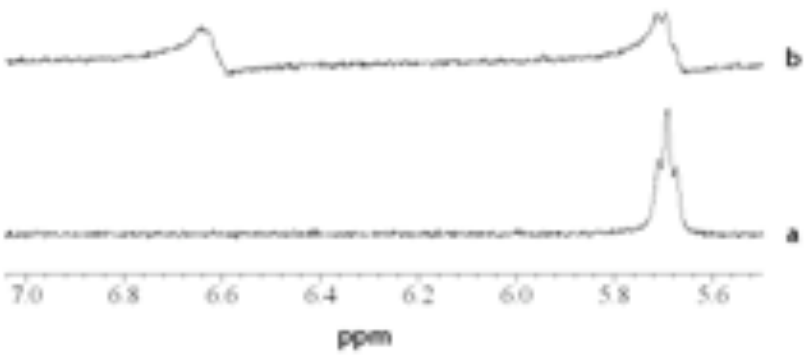

93 a) lone receptor, b) receptor + 1eq. 1,3-diaminopropane and 1eq. 18-crown-6, bubbled with CO_2 for 3 minutes.

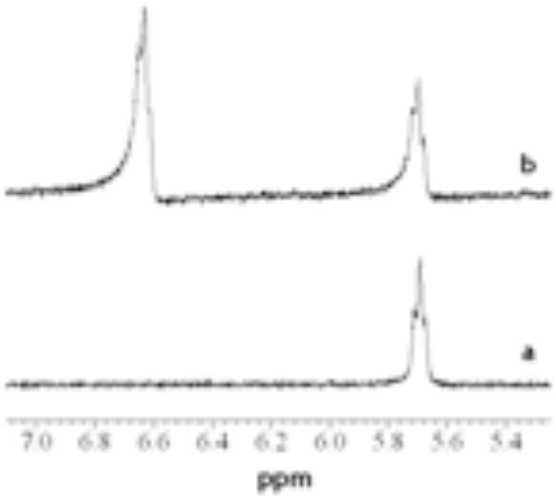

93 a) lone receptor, b) receptor + 1eq. 1,4,5,-tetrahydropyrimidine, bubbled with CO_2 for 3 minutes.

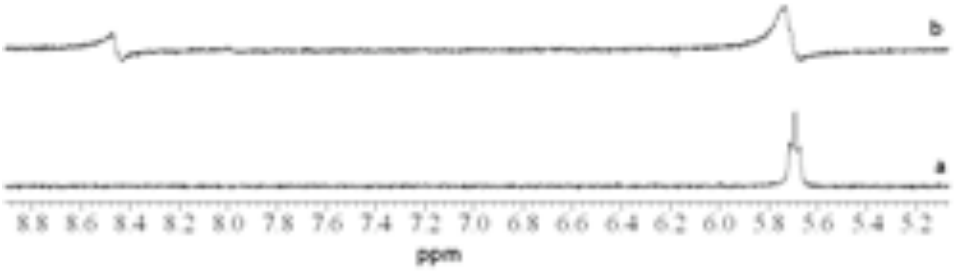

RECEPTOR 94

94 a) lone receptor, b) receptor + 2eq. n-butylamine, bubbled with CO_2 for 3 minutes.

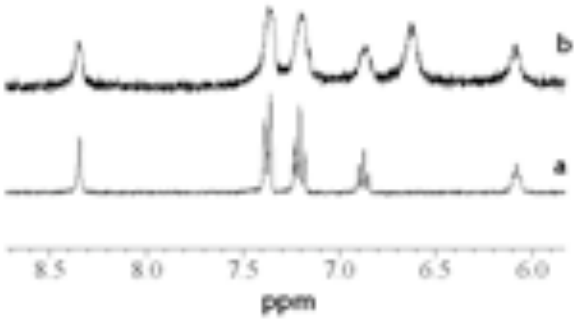

94 a) lone receptor, b) receptor + 1eq. 1,3-diaminopropane, bubbled with CO_2 for 3 minutes.

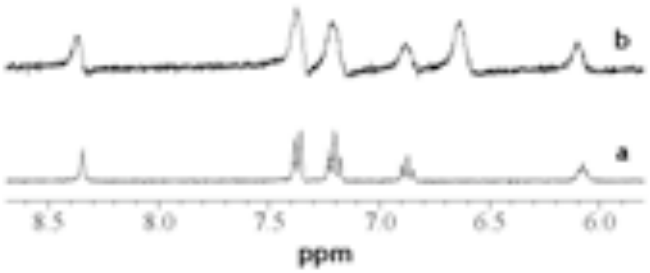

94 a) lone receptor, b) receptor + 2eq. n-butylamine and 1eq. 18-crown-6, bubbled with CO_2 for 3 minutes.

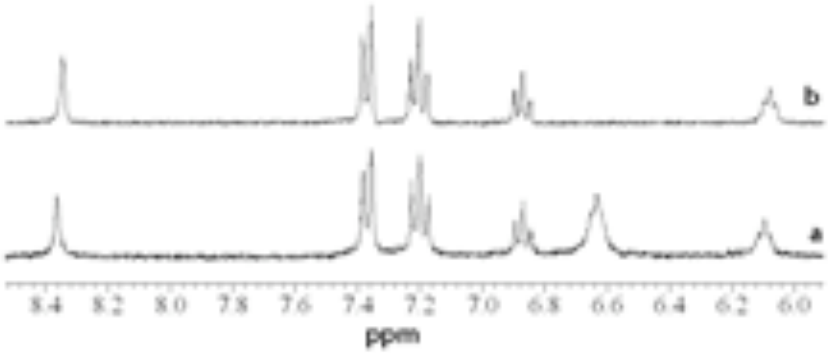

94 a) lone receptor, b) receptor + 1eq. 1,3-diaminopropane and 1eq. 18-crown-6, bubbled with CO_2 for 3 minutes.

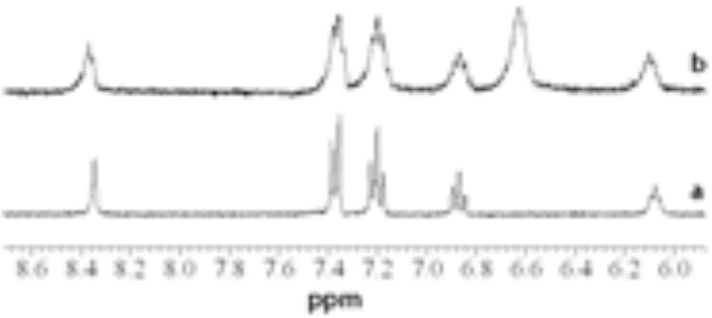

94 a) lone receptor, b) receptor + 1eq. 1,4,5,6-tetrahydropyrimidine, bubbled with CO_2 for 3 minutes.

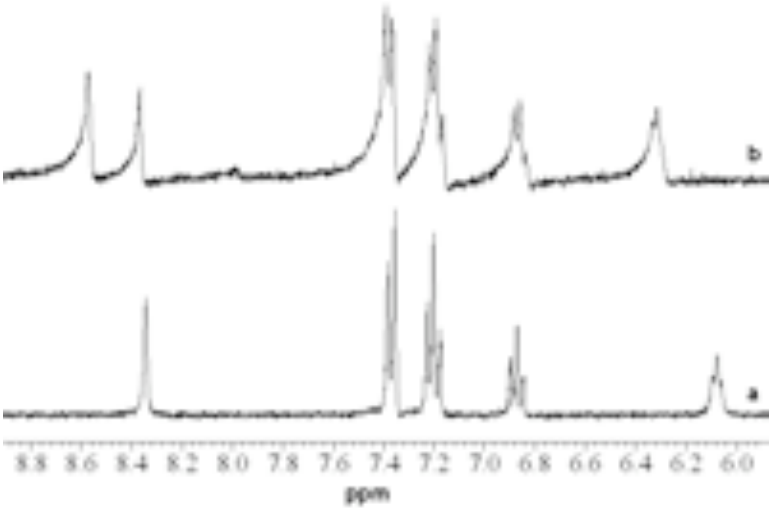

RECEPTOR 95

95 a) lone receptor, b) receptor + 2eq. n-butylamine, bubbled with CO_2 for 3 minutes.

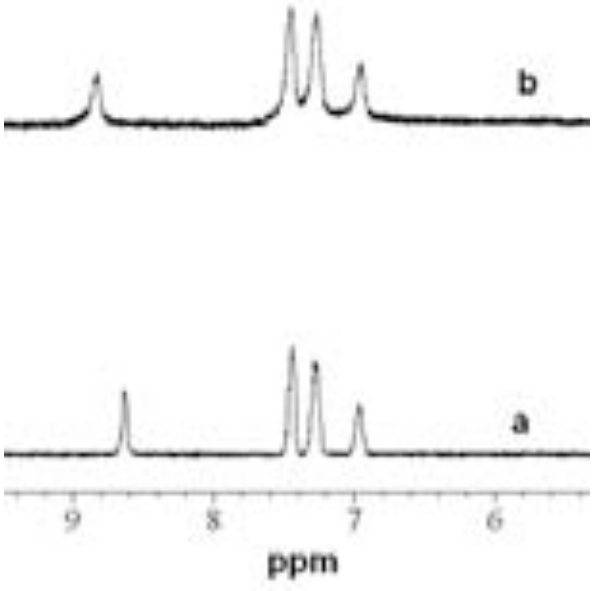

95 a) lone receptor, b) receptor + 1eq. 1,3-daiminopropane, bubbled with CO_2 for 3 minutes.

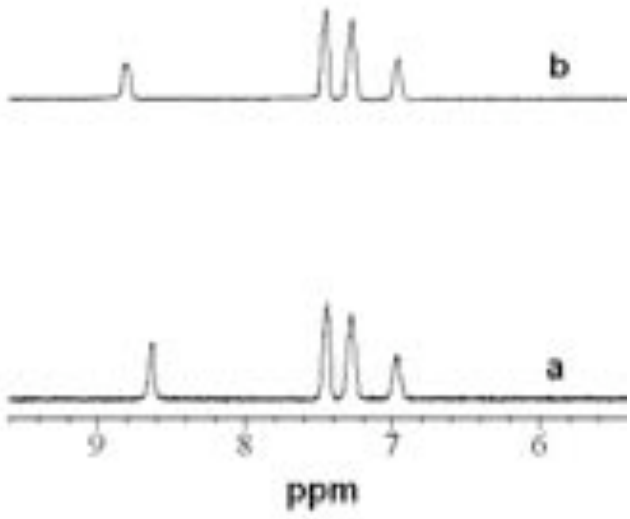

95 a) lone receptor, b) receptor + 2eq. n-butylamine and 1eq. 18-crown-6, bubbled with CO_2 for 3 minutes.

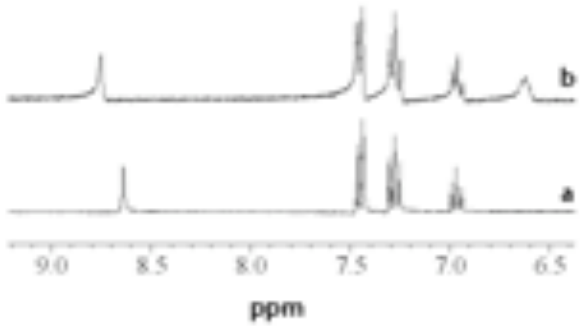

95 a) lone receptor, b) receptor + 1eq. 1,3-diaminopropane and 1eq. 18-crown-6, bubbled with CO_2 for 3 minutes.

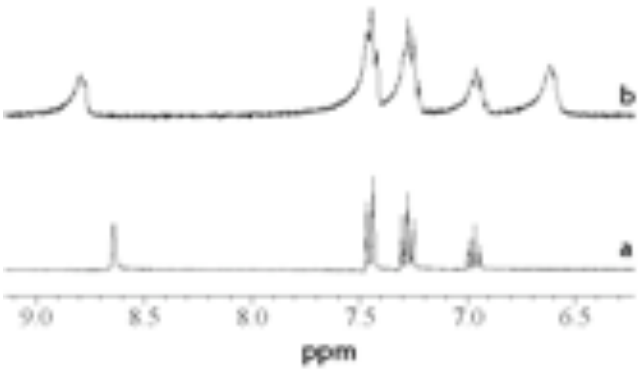

95 a) lone receptor, b) receptor + 1eq. 1,4,5,6-tetrahydropyrimidine, bubbled with CO_2 for 3 minutes.

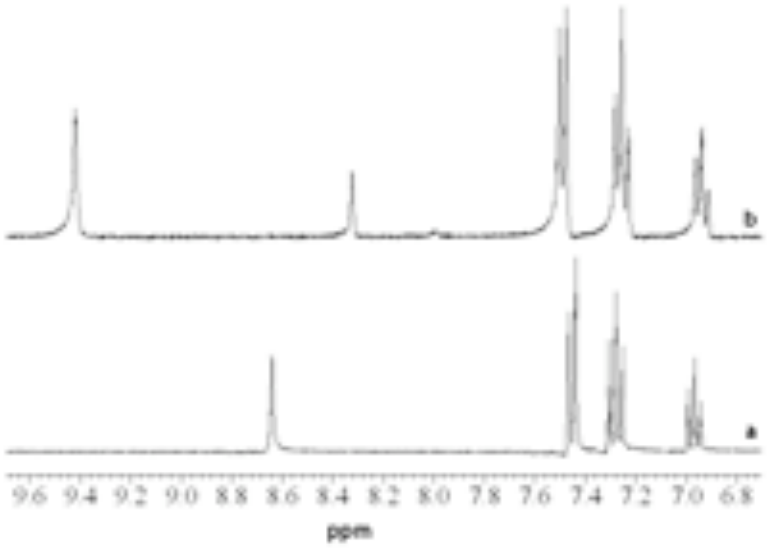

RECEPTOR 96

96 a) lone receptor, b) receptor + 2eq. n-butylamine, bubbled with CO_2 for 3 minutes.

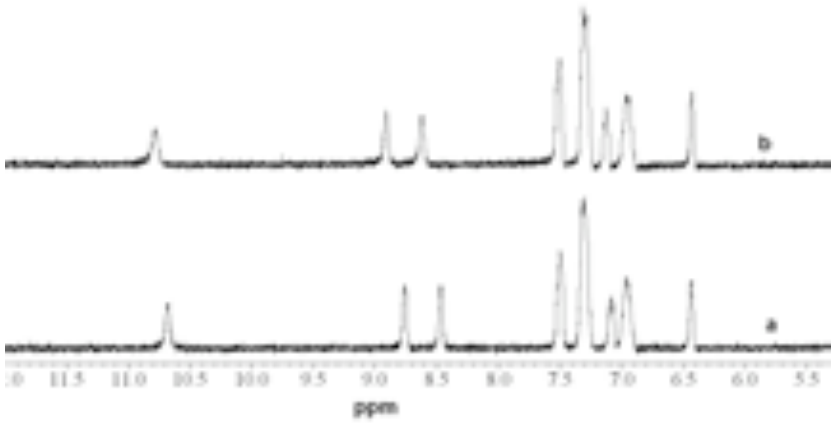

96 a) lone receptor, b) receptor + 1eq. 1,3-diaminopropane, bubbled with CO_2 for 3 minutes.

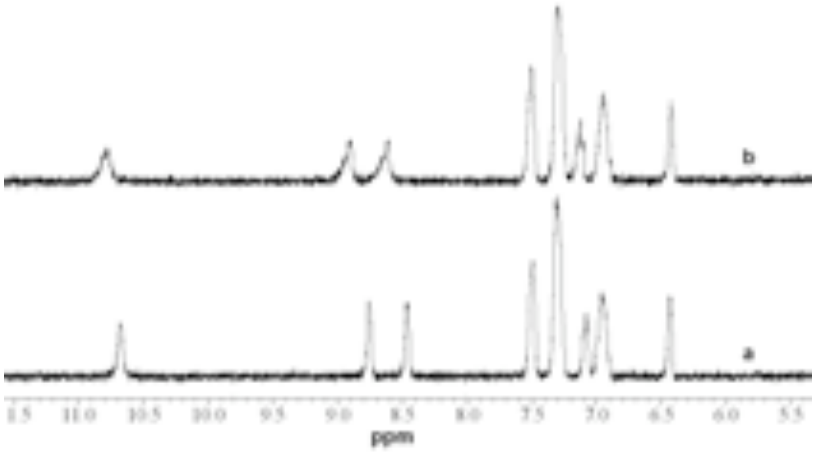

96 a) lone receptor, b) receptor + 2eq. n-butylamine and 1eq. 18-crown-6, bubbled with CO_2 for 3 minutes.

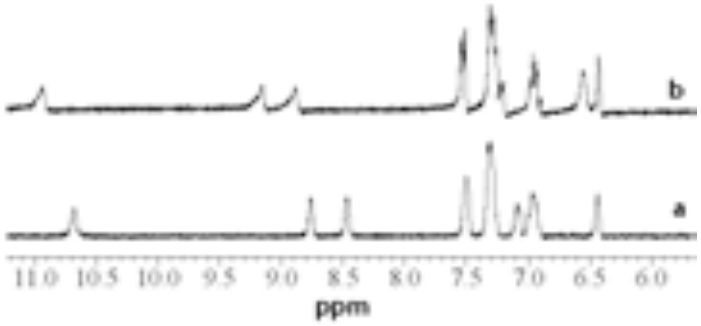

96 a) lone receptor, b) receptor + 1eq. 1,3-diaminopropane and 1eq. 18-crown-6, bubbled with CO_2 for 3 minutes.

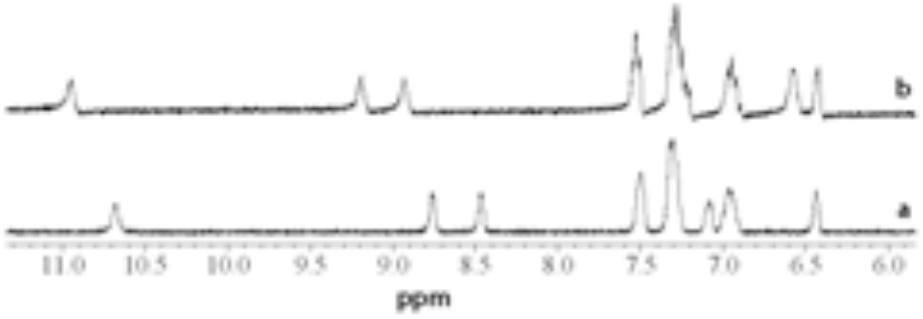

96 a) lone receptor, b) receptor + 1eq. 1,4,5,6-tetrahydropyrimidine, bubbled with CO_2 for 3 minutes.

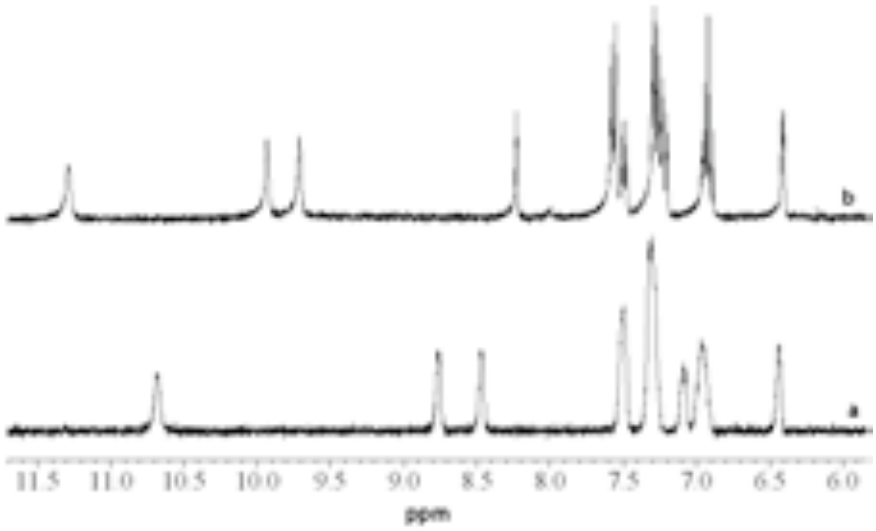

RECEPTOR 97

97 a) lone receptor, b) receptor + 2eq. n-butylamine, bubbled with CO_2 for 3 minutes.

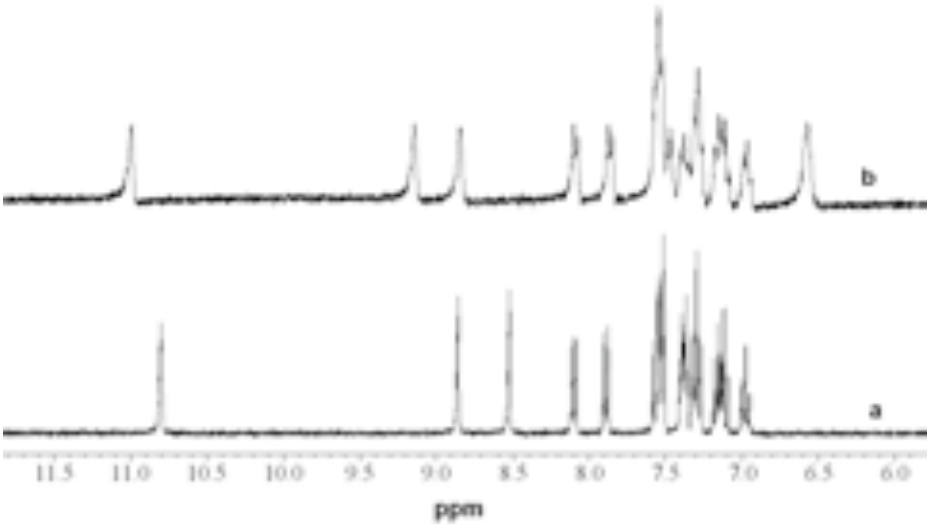

97 a) lone receptor, b) receptor + 1eq. 1,3-diaminopropane, bubbled with CO_2 for 3 minutes.

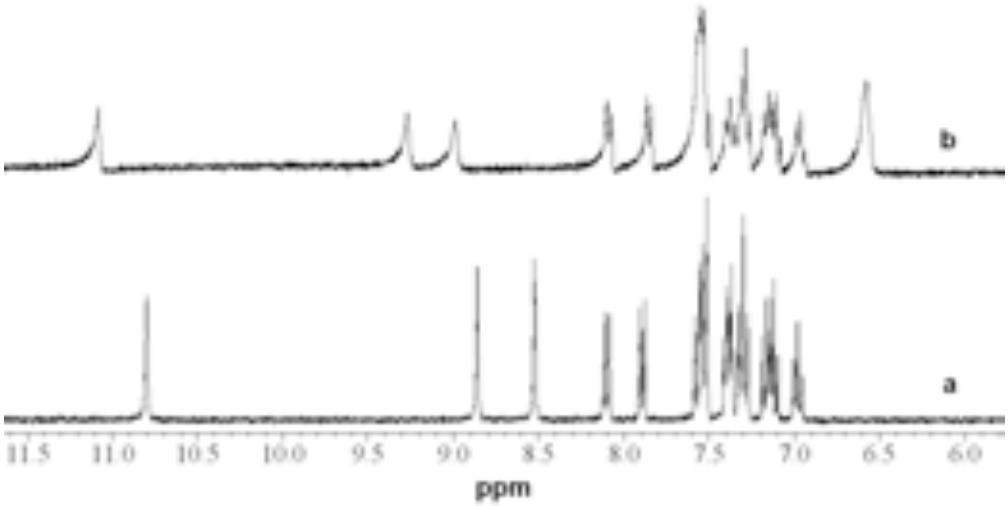

97 a) lone receptor, b) receptor + 2eq. n-butylamine and 1eq. 18-crown-6, bubbled with CO_2 for 3 minutes.

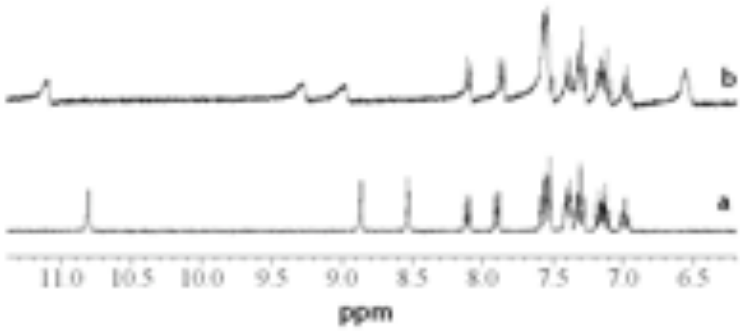

97 a) lone receptor, b) receptor + 1eq. 1,3-diaminopropane and 1eq. 18-crown-6, bubbled with CO_2 for 3 minutes.

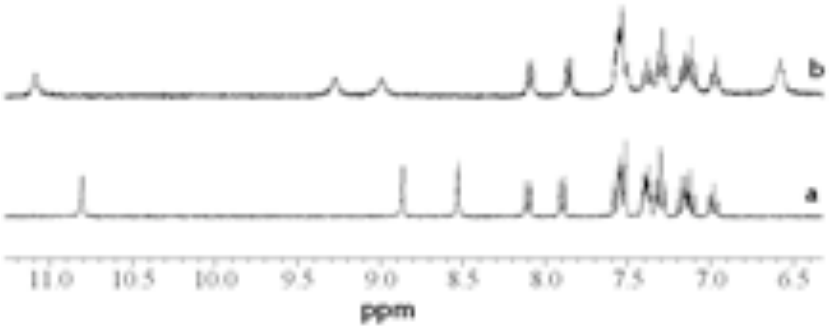

97 a) lone receptor, b) receptor + 2eq. 1,4,5,6-tetrahydropyrimidine, bubbled with CO_2 for 3 minutes.

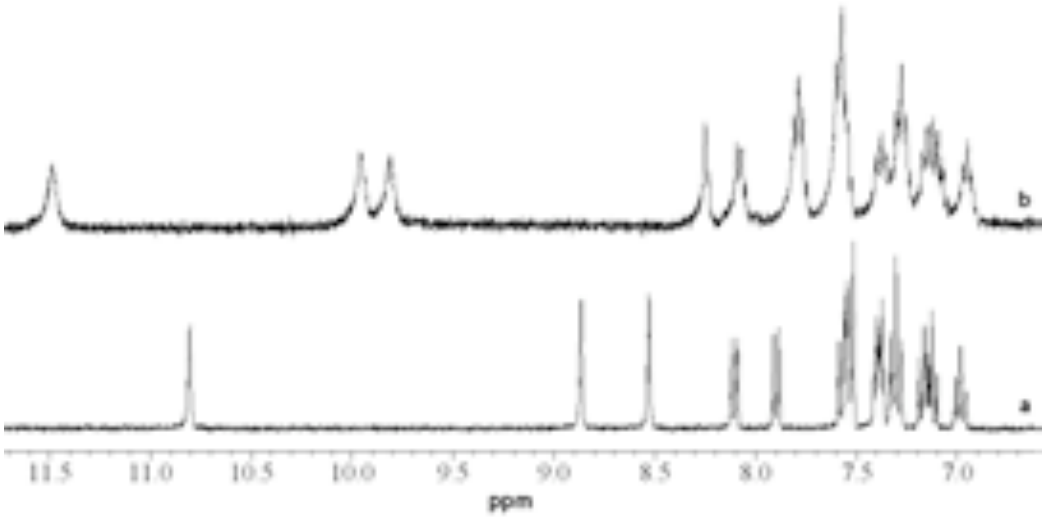

RECEPTOR 98

98 a) lone receptor, b) receptor + 2eq. n-butylamine, bubbled with CO_2 for 3 minutes.

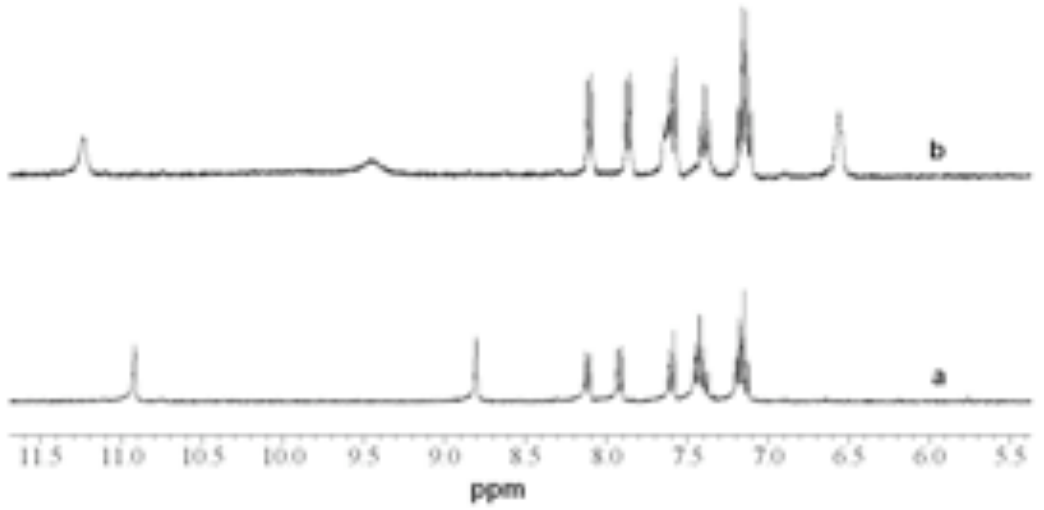

98 a) lone receptor, b) receptor + 1eq. 1,3-diaminopropane, bubbled with CO_2 for 3 minutes.

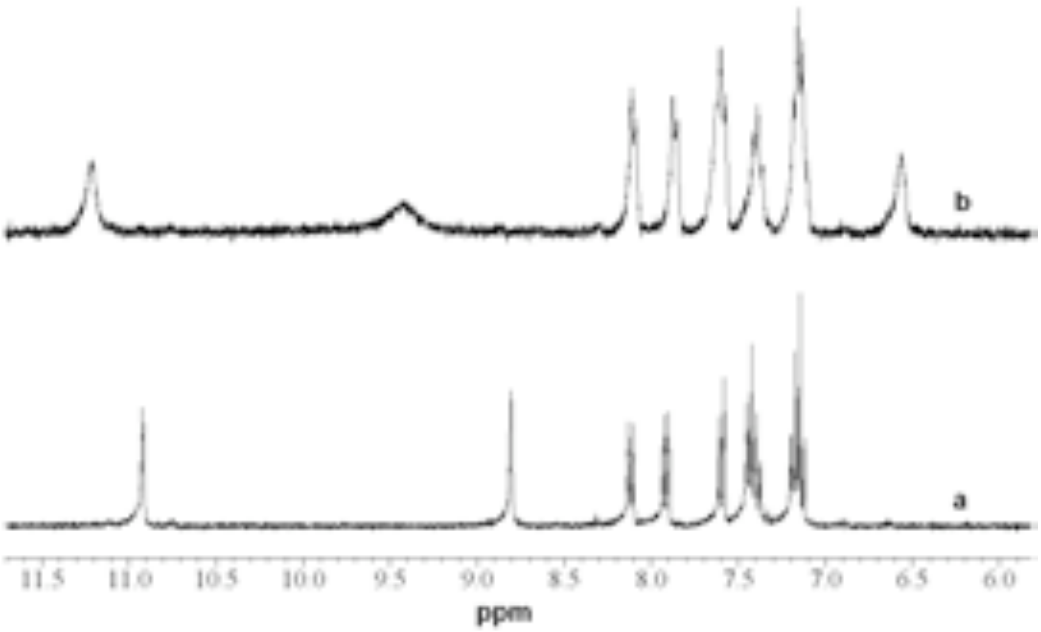

98 a) lone receptor, b) receptor + 2eq. n-butylamine and 1eq. 18-crown-6, bubbled with CO_2 for 3 minutes.

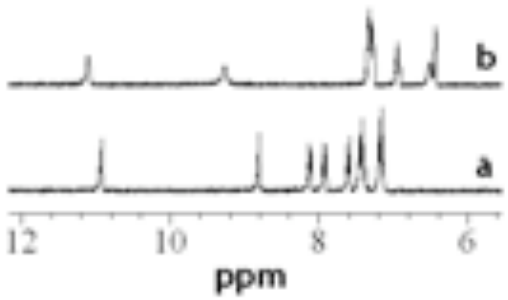

98 a) lone receptor, b) receptor + 1eq. 1,3-diaminopropane and 1eq. 18-crown-6, bubbled with CO_2 for 3 minutes.

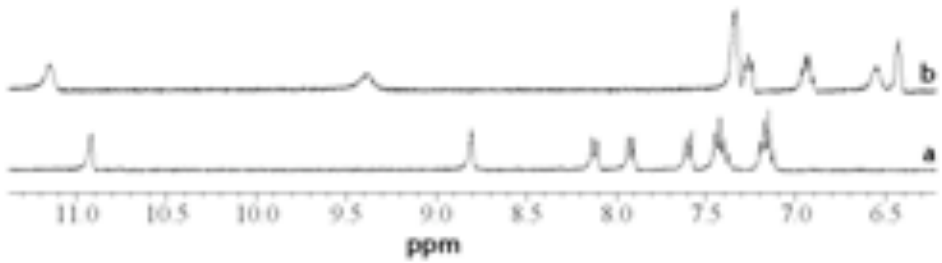

98 a) lone receptor, b) receptor + 1eq. 1,4,5,6-tetrahydropyrimidine, bubbled with CO_2 for 3 minutes.

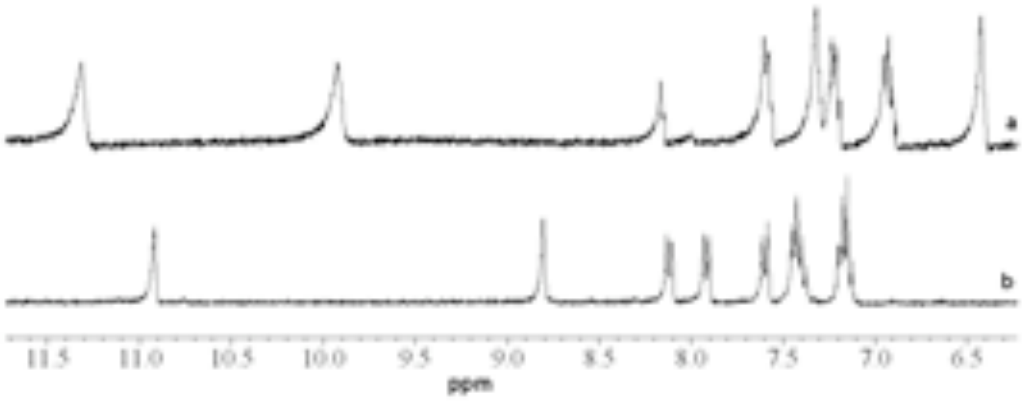

RECEPTOR 99

99 a) lone receptor, b) receptor + 2eq. n-butylamine, bubbled with CO_2 for 3 minutes.

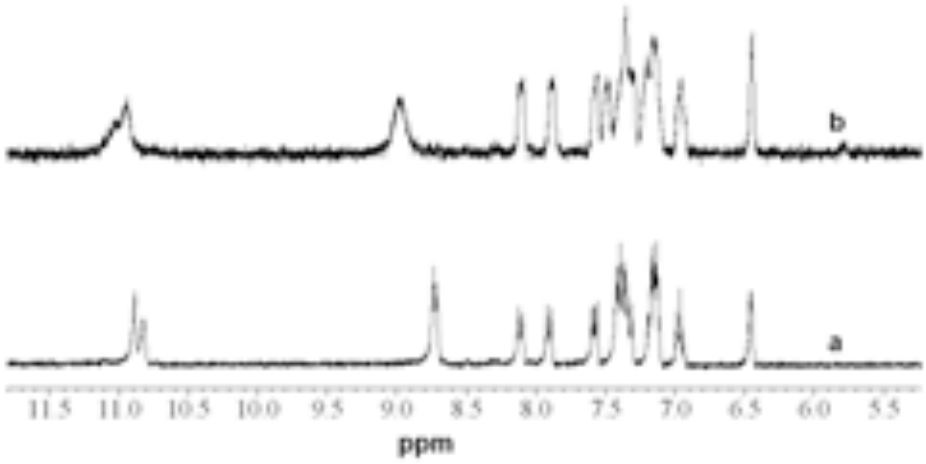

99 a) lone receptor, b) receptor + 1eq. 1,3-diaminopropane, bubbled with CO_2 for 3 minutes.

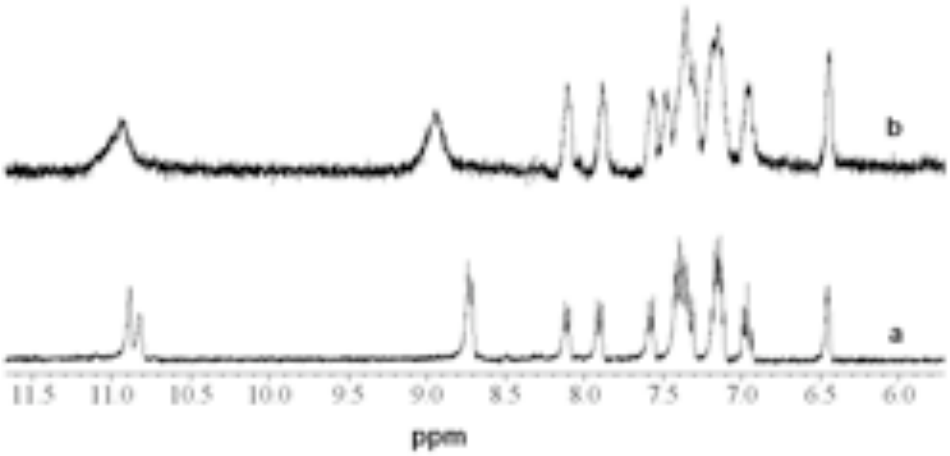

99 a) lone receptor, b) receptor + 2eq. n-butylamine and 1eq. 18-crown-6, bubbled with CO_2 for 3 minutes.

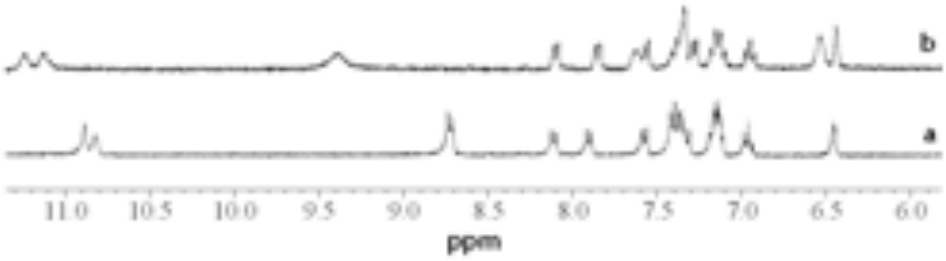

99 a) lone receptor, b) receptor + 1eq. 1,3-diaminopropane and 1eq. 18-crown-6, bubbled with CO_2 for 3 minutes.

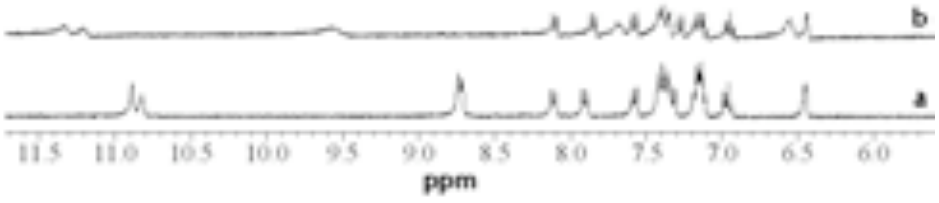

99 a) lone receptor, b) receptor + 1eq. 1,4,5,6-tetrahydropyrimidine, bubbled with CO_2 for 3 minutes.

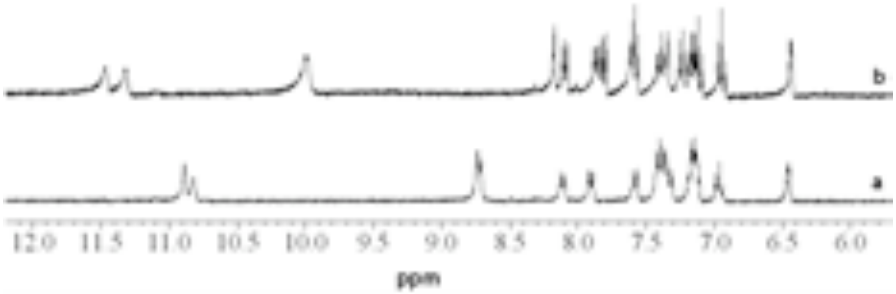

RECEPTOR 100

100 a) lone receptor, b) receptor + 2eq. n-butylamine, bubbled with CO_2 for 3 minutes.

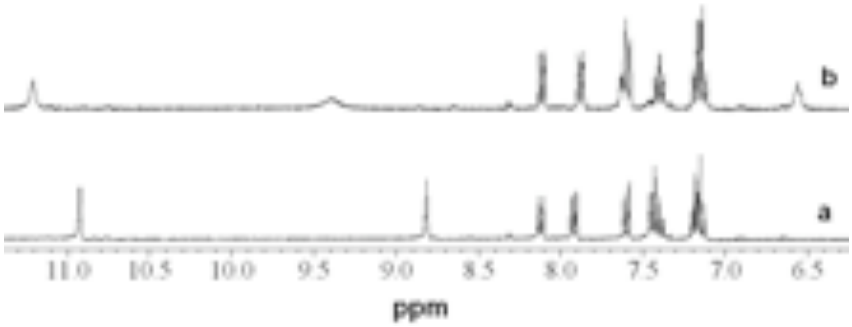

100 a) lone receptor, b) receptor + 1eq. 1,3-diaminopropane, bubbled with CO_2 for 3 minutes.

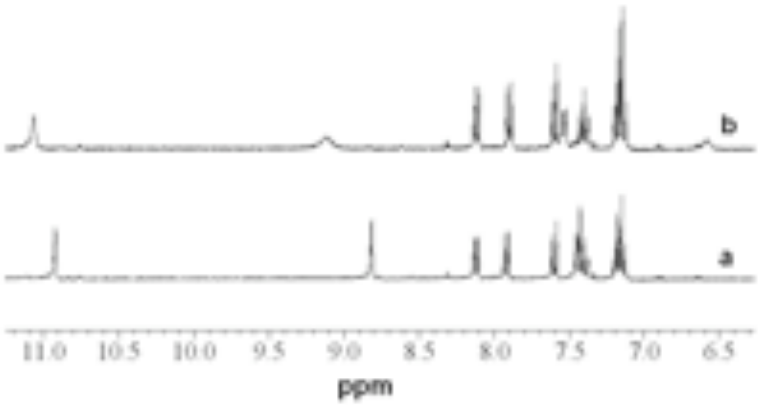

100 a) lone receptor, b) receptor + 2eq. n-butylamine and 18-crown-6, bubbled with CO_2 for 3 minutes.

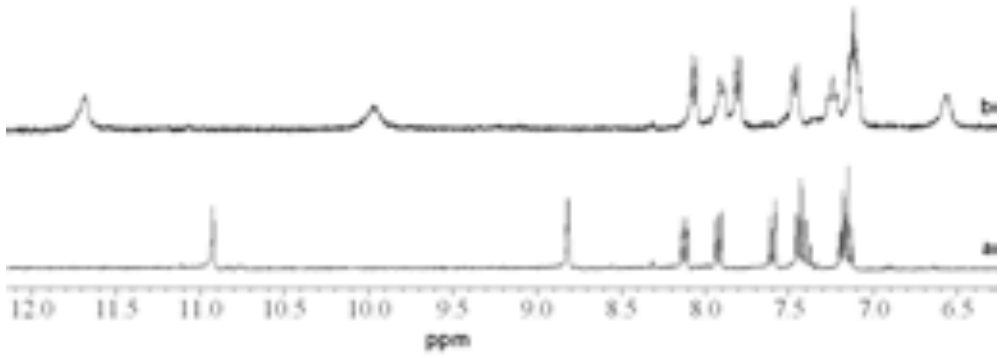

100 a) lone receptor, b) receptor + 1eq. 1,3-diaminopropane and 18-crown-6, bubbled with CO_2 for 3 minutes.

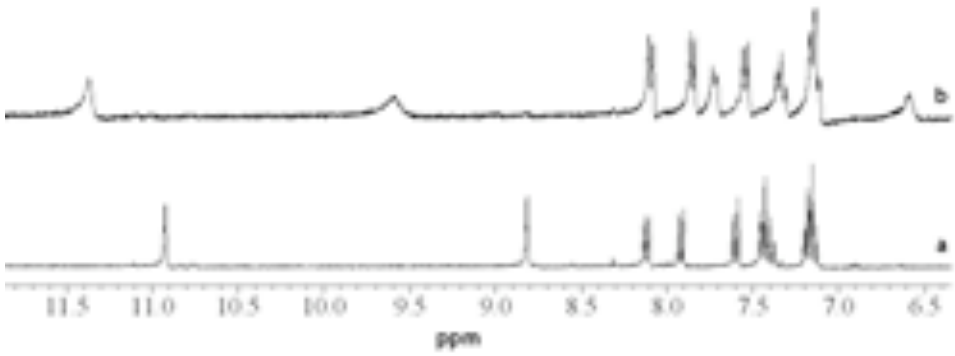

100 a) lone receptor, b) receptor + 1eq. 1,4,5,6-tetrahydropyrimidine, bubbled with CO_2 for 3 minutes.

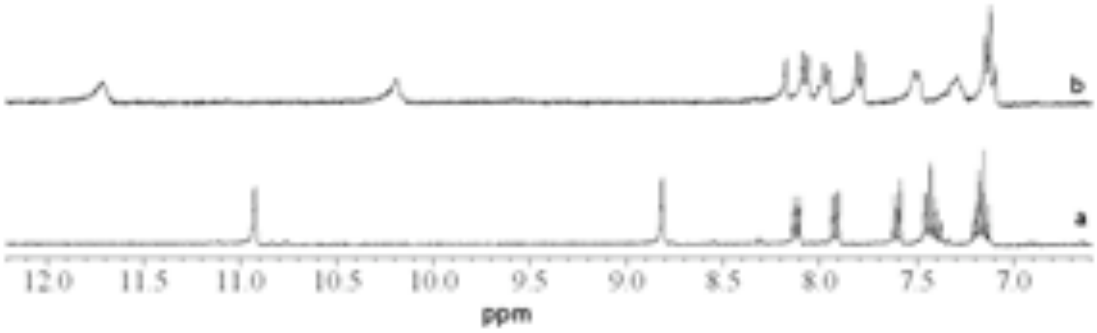

RECEPTOR 101

101 a) lone receptor, b) receptor + 2eq. n-butylamine, bubbled with CO_2 for 3 minutes.

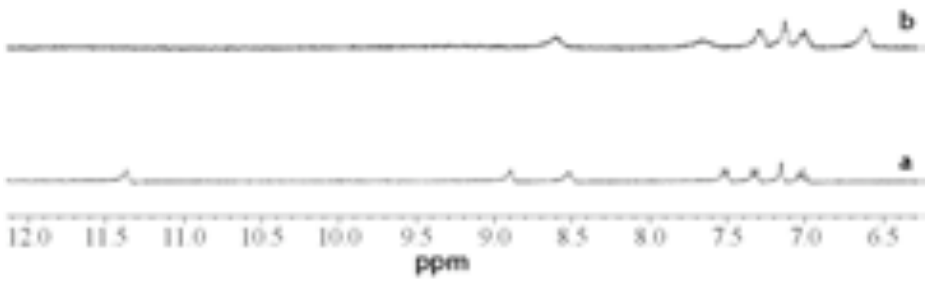

101 a) lone receptor, b) receptor + 1eq. 1,3-diaminopropane, bubbled with CO_2 for 3 minutes.

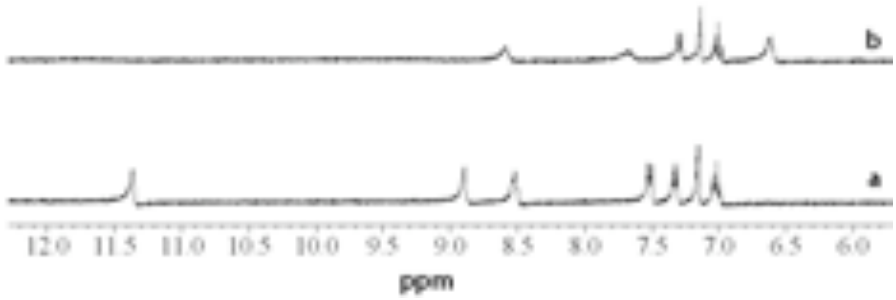

101 a) lone receptor, b) receptor + 2eq. n-butylamine and 18-crown-6, bubbled with CO_2 for 3 minutes.

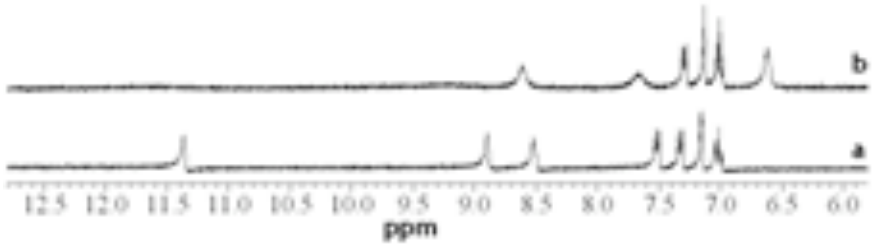

101 a) lone receptor, b) receptor + 1eq. 1,3-diaminopropane and 18-crown-6, bubbled with CO_2 for 3 minutes.

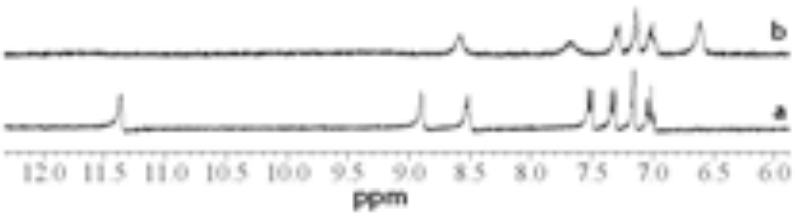

101 a) lone receptor, b) receptor + 1eq. 1,4,5,6-tetrahydropyrimidine, bubbled with CO_2 for 3 minutes.

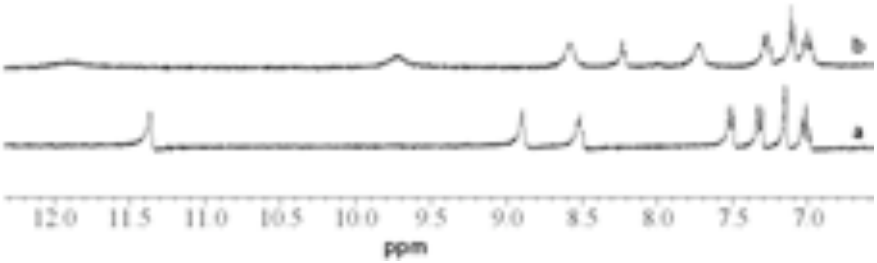

RECEPTOR 109

109 a) lone receptor, b) receptor + 2eq. n-butylamine, bubbled with CO_2 for 3 minutes.

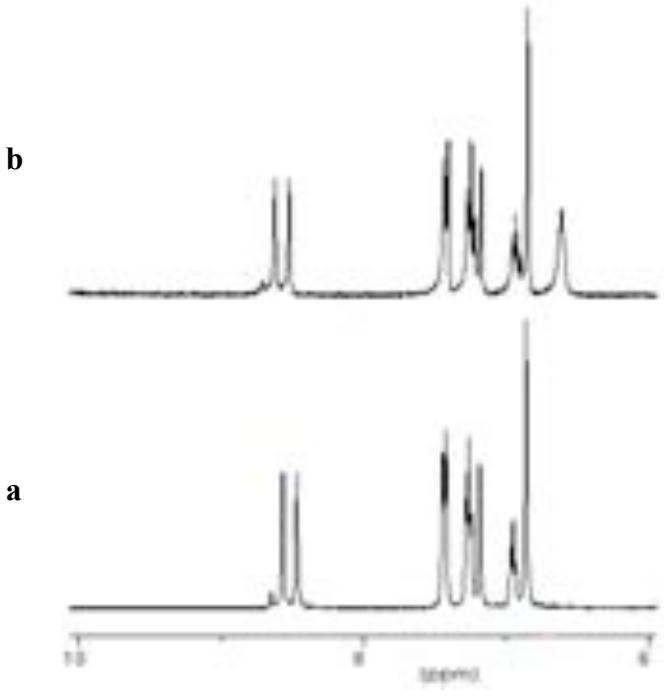

109 a) lone receptor, b) receptor + 1eq. 1,3-diaminopropane, bubbled with CO_2 for 3 minutes.

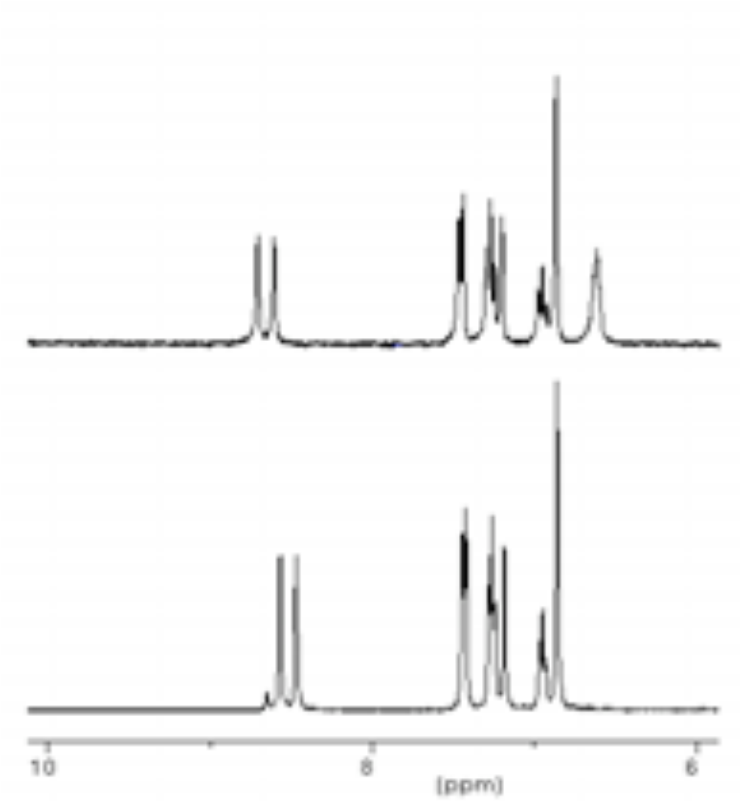

PART B – Chemical shift changes with CO_2 only

DMSO-d_6 solutions, (0.01M), of each receptor, **93 - 101** were made and the ^{1}H NMR spectrum acquired. Carbon dioxide was bubbled through each solution for 3 minutes. After this time, a second ^{1}H NMR spectrum was acquired. No chemical shift changes were observed. All spectra were obtained at 298K.

93 a) lone receptor, b) bubbled with CO_2 for 3 minutes.

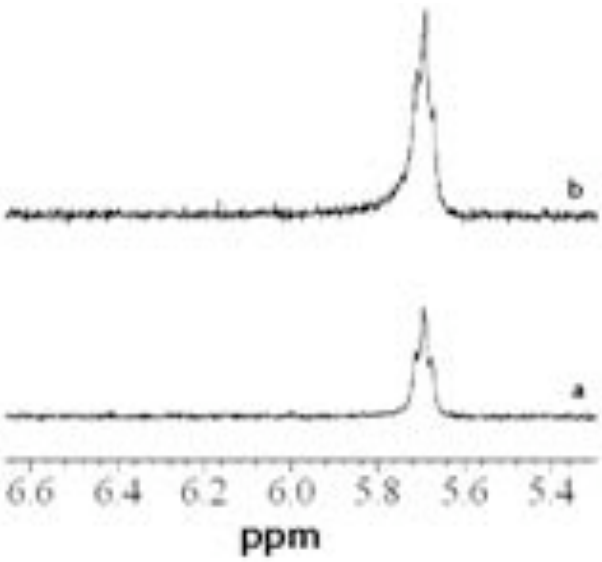

94 a) lone receptor, b) bubbled with CO_2 for 3 minutes.

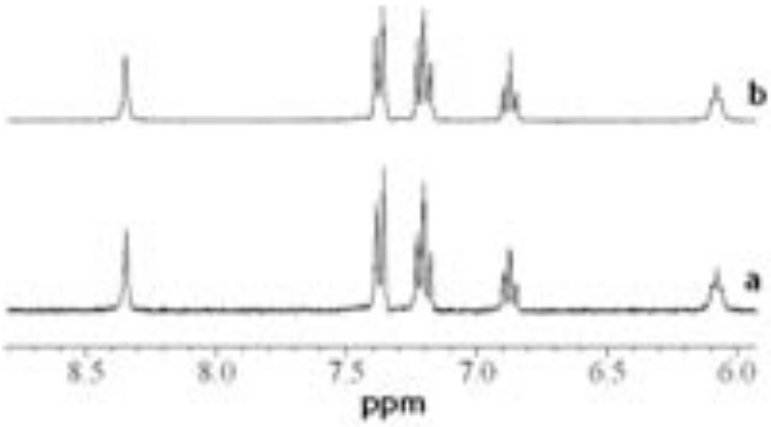

95 a) lone receptor, b) bubbled with CO_2 for 3 minutes.

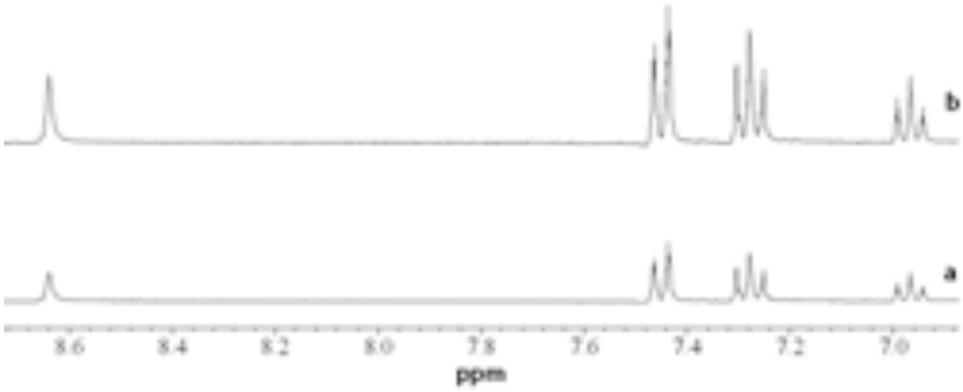

96 a) lone receptor, b) bubbled with CO_2 for 3 minutes.

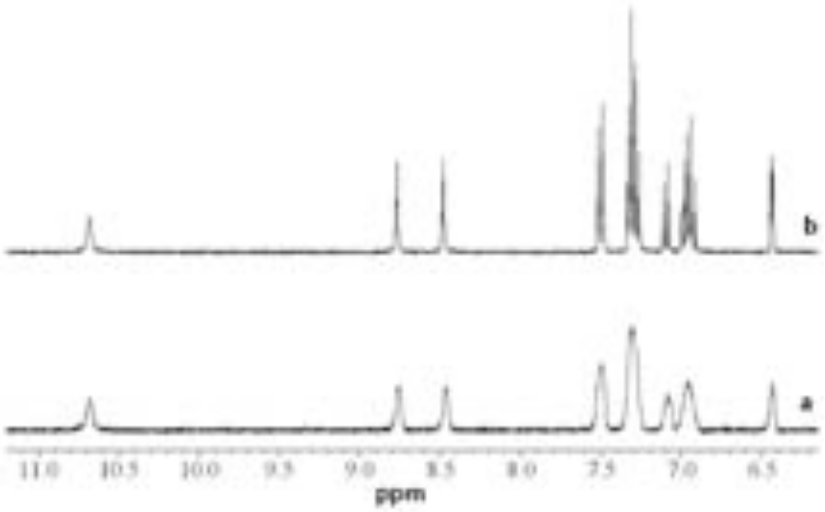

97 a) lone receptor, b) bubbled with CO_2 for 3 minutes.

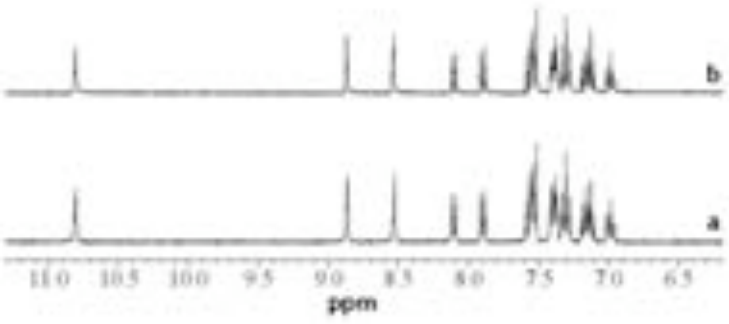

98 a) lone receptor, b) bubbled with CO_2 for 3 minutes.

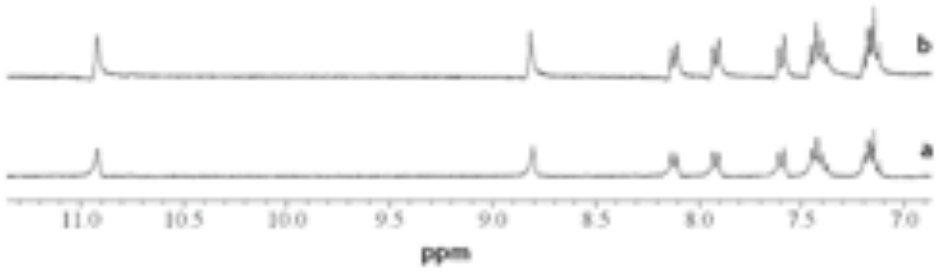

99 a) lone receptor, b) bubbled with CO_2 for 3 minutes.

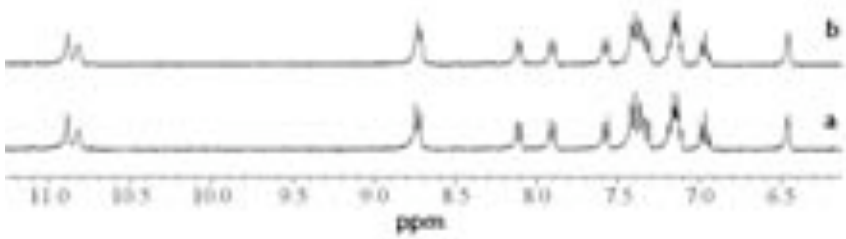

100 a) lone receptor, b) bubbled with CO_2 for 3 minutes.

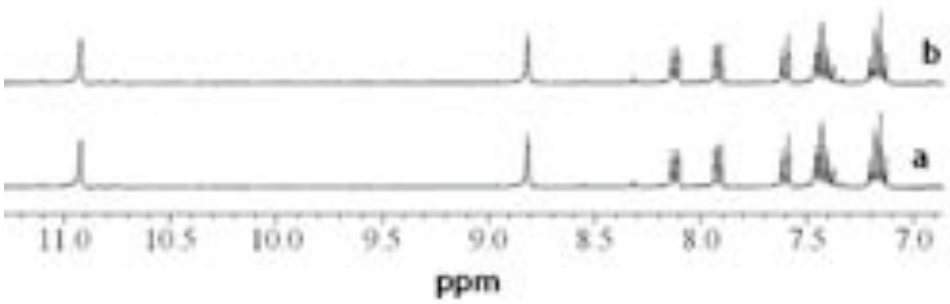

101 a) lone receptor, b) bubbled with CO_2 for 3 minutes.

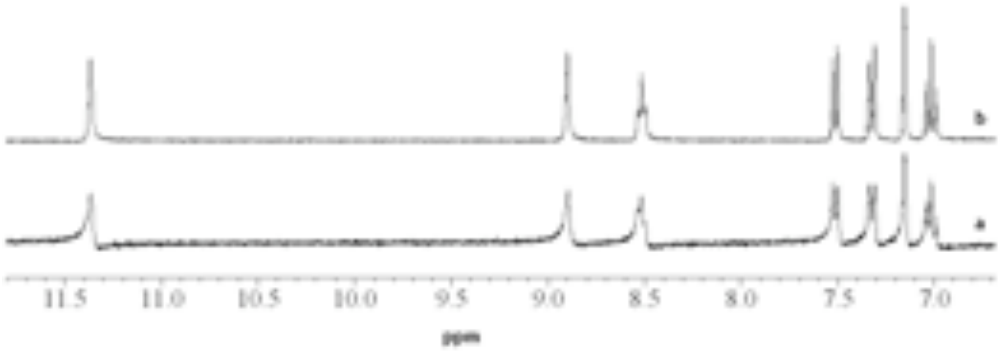

PART C – Chemical shift changes after different lengths of exposure to CO_2

To ensure DMSO solutions were saturated by CO_2, experiments were conducted in which 1mM DMSO-d_6 solutions of **95** and **100** were combined with 2eq. n-butylamine. Each solution was then bubbled with CO_2, with aliquots of each solution removed every minute for up to 10 minutes. Each solution underwent ^{1}H NMR spectroscopy, and the chemical shift change was recorded. All spectra were obtained at 298K.

Receptor 95 vs. AAAC salt formed from n-butlyamine and CO_2

Time / min	CSC (1eq.)
1	0.079
2	0.074
3	0.076
4	0.074
5	0.077
Mean	**0.076**
Error	**3%**

Table A2C.1 Chemical shift changes (ppm) for urea NH proton of receptor **95** induced by presence of AAAC salt formed by reaction of n-butylamine and CO_2 after different lengths of time (min).

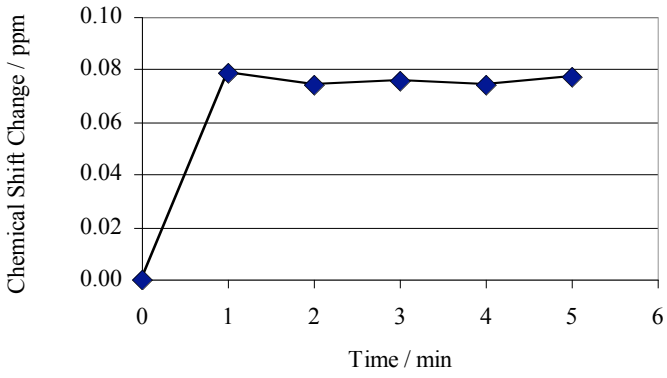

Fig A2C.1 Chemical shift changes (ppm) for urea NH proton of receptor **95** induced by presence of AAAC salt formed by reaction of n-butylamine and CO_2 after different lengths of time (min).

Receptor 100 vs. AAAC salt formed from n-butlyamine and CO_2

Time / min	CSC (1eq.)
1	0.732
2	0.679
3	0.714
4	0.732
5	0.712
6	0.722
7	0.716
8	0.726
9	0.710
10	0.749
Mean	**0.719**
Error	**3%**

Table A2C.2 Chemical shift changes (ppm) for urea NH proton of receptor **100** induced by presence of AAAC salt formed by reaction of n-butylamine and CO_2 after different lengths of time (min).

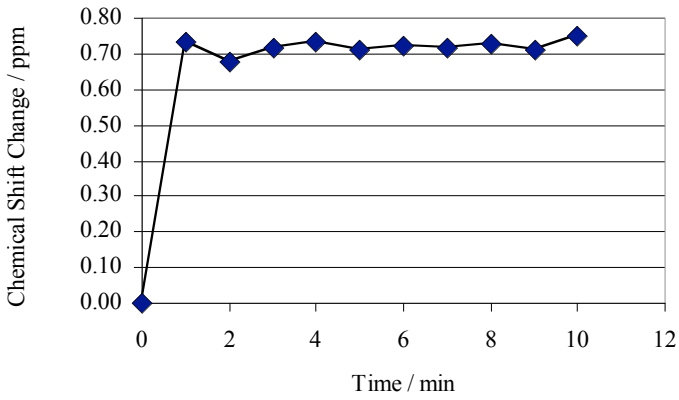

Fig A2C.2 Chemical shift changes (ppm) for urea NH proton of receptor **100** induced by presence of AAAC salt formed by reaction of n-butylamine and CO_2 after different lengths of time (min).

In each case, there is no difference in chemical shift change after 1 minute and the percentage error (from standard deviation) of the chemical shift changes recorded after this time is 3% in both cases.

APPENDIX 3 – ^{1}H NMR TITRATION CURVES

CURVES FROM CHAPTER 2

Receptor 93

TBAOBz

$K_a < 20M^{-1}$

0.5%H_2O:DMSO-d_6. 298K

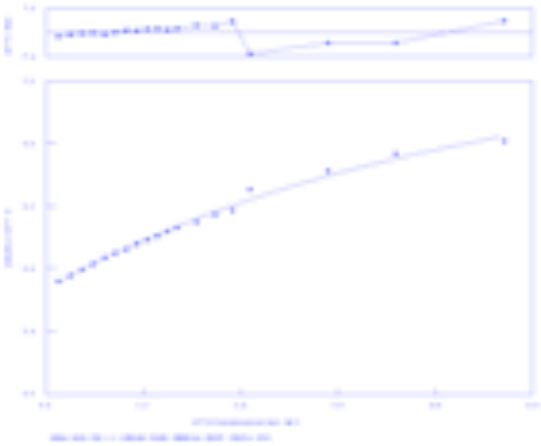

Receptor 94

TBAOBz

$K_a = 140M^{-1}$ (± 9%)

0.5%H_2O:DMSO-d_6 298K

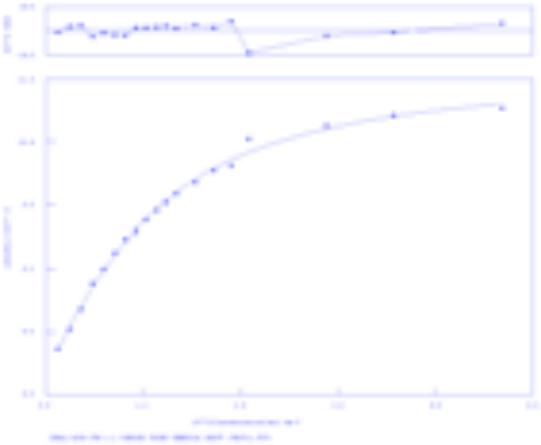

Receptor 97

TBAOBz

$K_a > 10{,}000M^{-1}$

0.5%H_2O:DMSO-d_6 298K

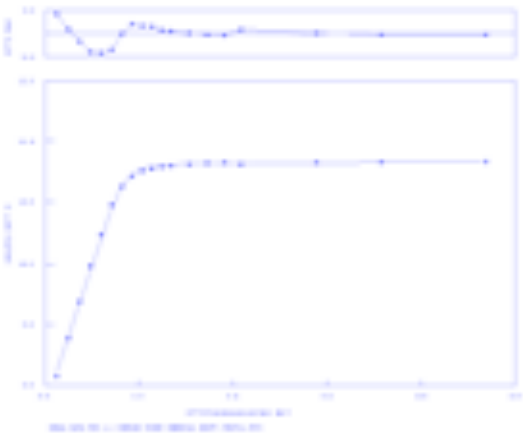

Receptor 101

DAP-CO_2 (Attempt 1)

K_a = 4,000M^{-1} (± 16%)

0.5%H_2O:DMSO-d_6 298K

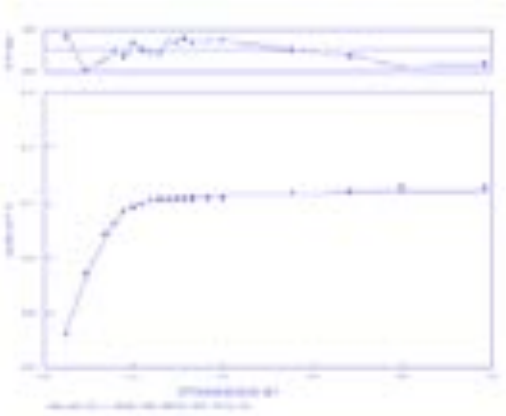

Receptor 101

DAP-CO_2 (Attempt 2)c

K_a = 724M^{-1} (± 10%)

0.5%H_2O:DMSO-d_6 298K

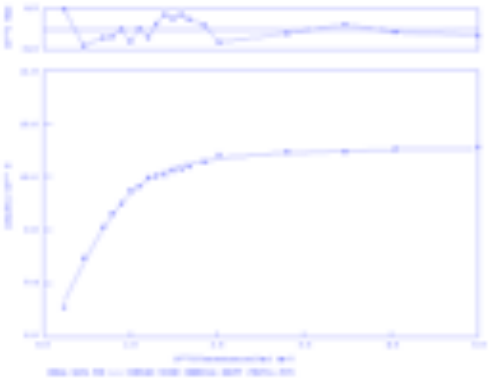

Receptor 101

DAP-CO_2 (Attempt 3)

K_a = 1,194M^{-1} (± 11%)

0.5%H_2O:DMSO-d_6 298K

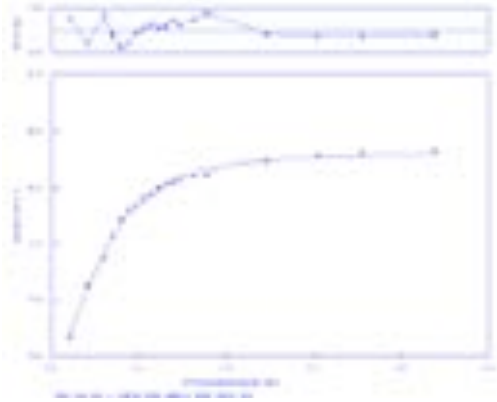

Receptor 102

DAP-CO_2

K_a = 711M^{-1} (± 11%)

0.5%H_2O:DMSO-d_6 298K

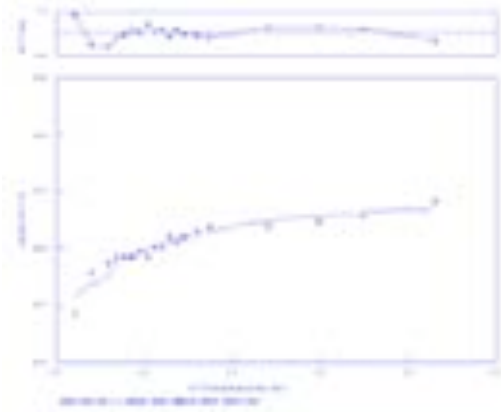

CURVES FROM CHAPTER 3

Receptor 122

TBAOAc

K_a = 436 M^{-1} (± 5%)

0.5%H_2O:DMSO-d_6 298K

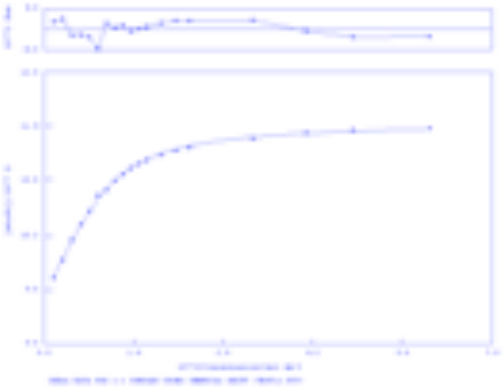

Receptor 122

TBAOBz

K_a = 99 M^{-1} (± 4%)

0.5%H_2O:DMSO-d_6 298K

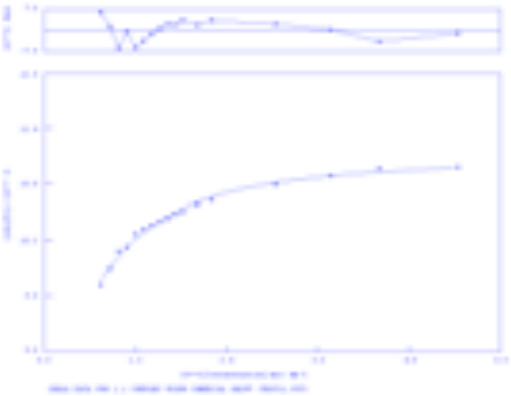

Receptor 122

TBACl

K_a = 54 M^{-1} (± 9%)

0.5%H_2O:DMSO-d_6 298K

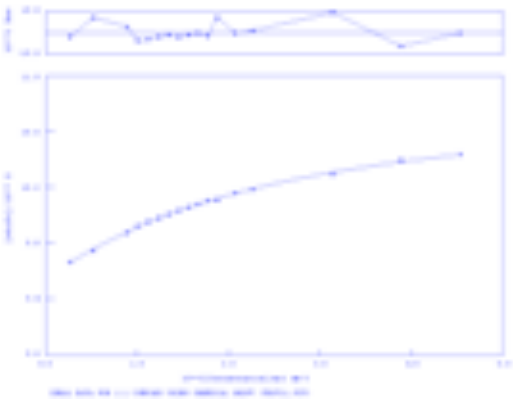

Receptor 122

$TBAH_2PO_4$

K_a = 97 M^{-1} (± 7%)

0.5%H_2O:DMSO-d_6 298K

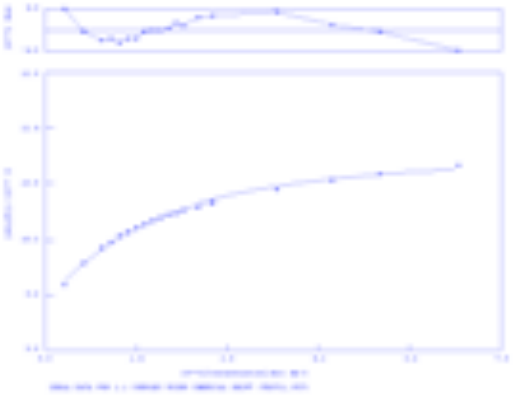

Receptor 123

TBAOAc

K_a = 69 M^{-1} (± 3%)

0.5%H_2O:DMSO-d_6 298K

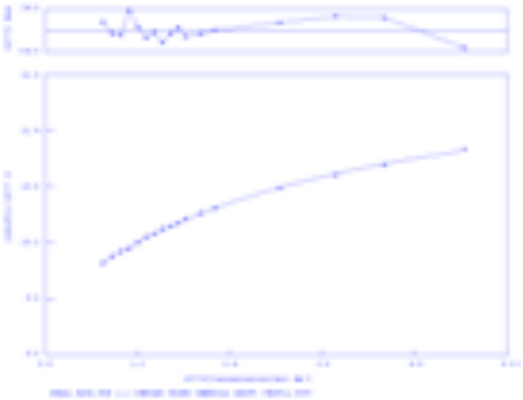

Receptor 123

TBAOBz

K_a = 37 M^{-1} (± 7%)

0.5%H_2O:DMSO-d_6 298K

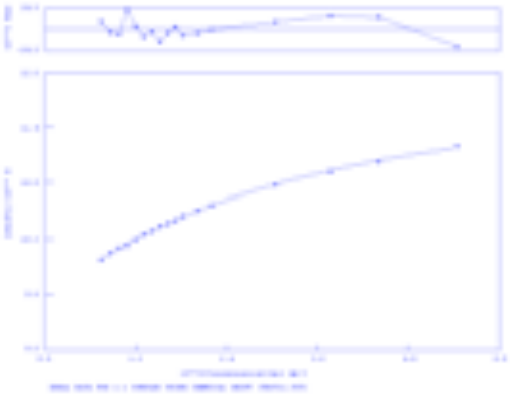

Receptor 123

TBAH_2PO_4

K_a = 64 M^{-1} (± 9%)

0.5%H_2O:DMSO-d_6 298K

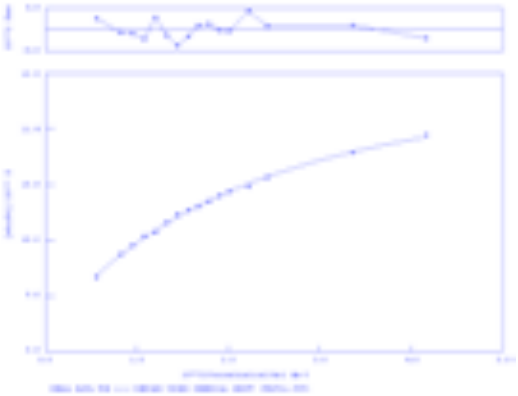

Receptor 124

TBAOAc

K_1 = 45 M^{-1} (± 20%)
β_2 = 2,929 M^{-1} (± 30%)

0.5%H_2O:DMSO-d_6 298K

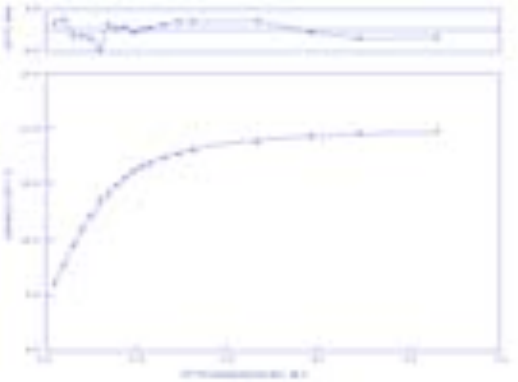

Receptor 124

TBAOBz

K_a = 118 M^{-1} (± 13%)

0.5%H_2O:DMSO-d_6 298K

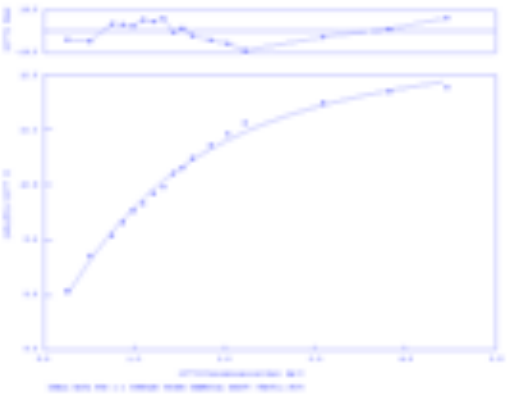

Receptor 124

TBACl

K_a = 33 M^{-1} (± 11%)

0.5%H_2O:DMSO-d_6 298K

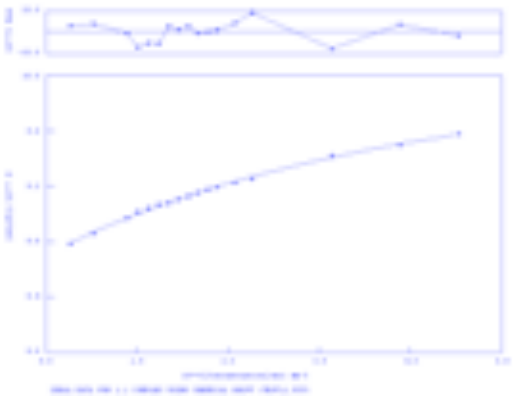

Receptor 124

TBAH_2PO_4

K_a = 182 M^{-1} (± 10%)

0.5%H_2O:DMSO-d_6 298K

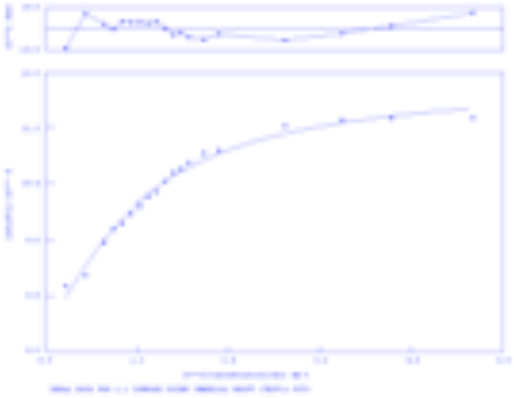

Receptor 125

TBAOAc

Strong1:1 and 2:1 interactions –
Curve did not fit either model

0.5%H_2O:DMSO-d_6 298K

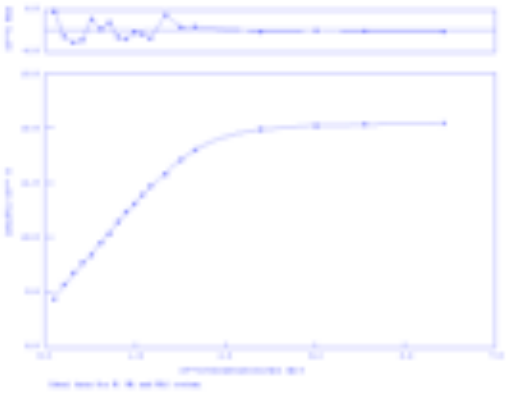

Receptor 125

TBAOBz

K_a = 262 M^{-1} (± 10%)

0.5%H_2O:DMSO-d_6 298K

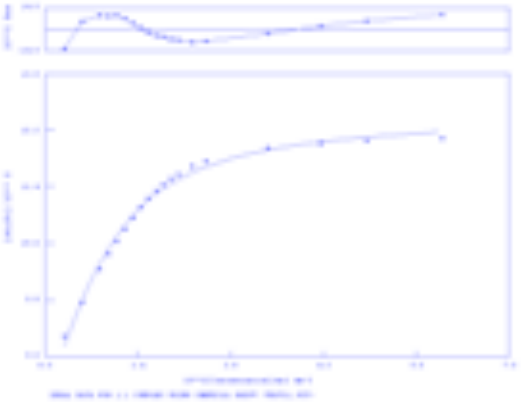

Receptor 125

$TBAH_2PO_4$

K_a = 249 M^{-1} (± 10%)

0.5%H_2O:DMSO-d_6 298K

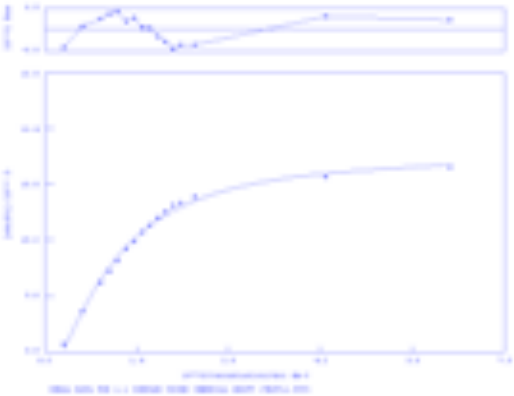

Receptor 125

$TBAHSO_4$

K_a = 30 M^{-1} (± 6%)

0.5%H_2O:DMSO-d_6 298K

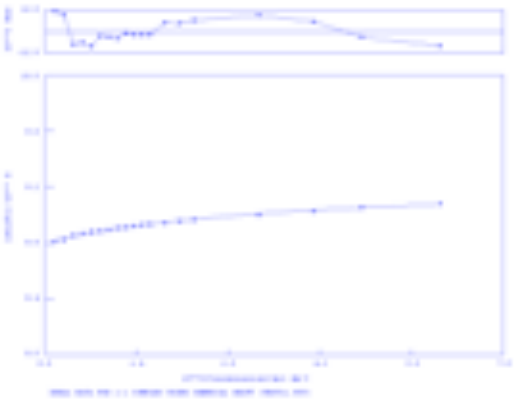

CURVES FROM CHAPTER 4

Receptor 23 (NH Proton)

TBACl

$K_a < 10\ M^{-1}$

DMSO-d_6 298K

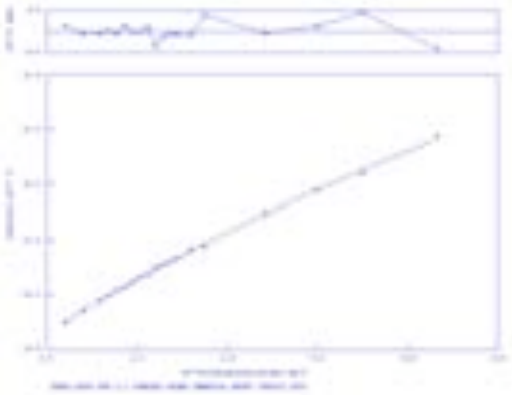

Receptor 23 (CH Proton)

TBACl

$K_a < 10\ M^{-1}$

DMSO-d_6 298K

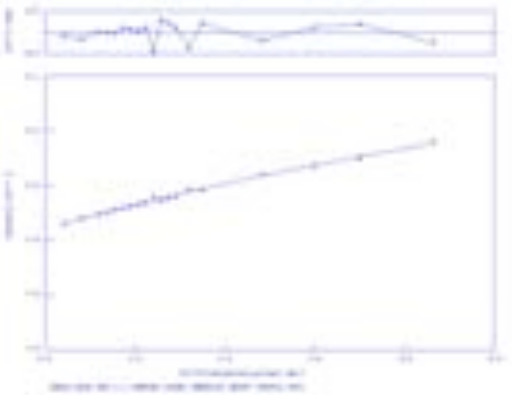

Receptor 137 (NH Proton)

TBACl

$K_a = 30 M^{-1}$ (± 3%)

DMSO-d_6 298K

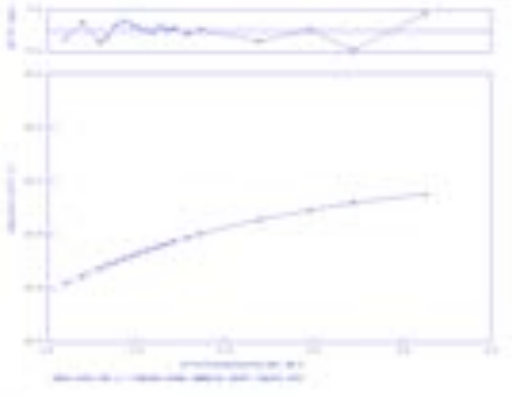

Receptor 137 (CH Proton)

TBACl

K_a = 33M^{-1} (± 3%)

DMSO-d_6 298K

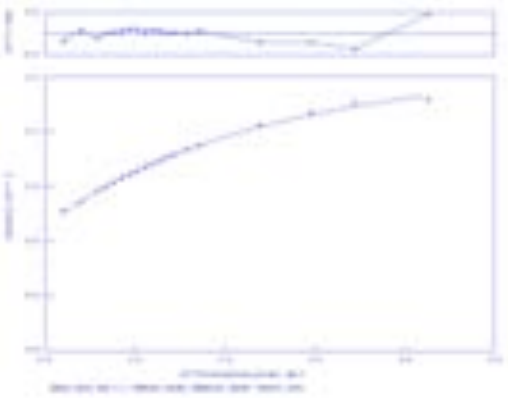

Receptor 138 (NH Proton)

TBACl

K_a = 30M^{-1} (± 3%)

DMSO-d_6 298K

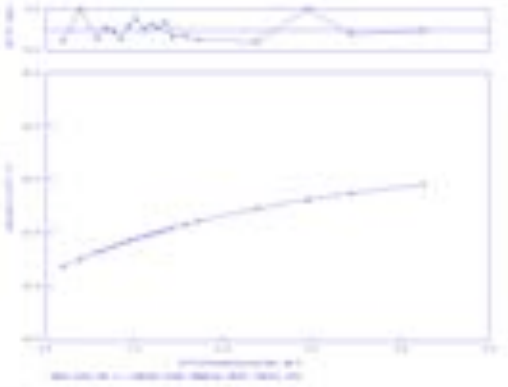

Receptor 138 (CH Proton)

TBACl

K_a = 25M^{-1} (± 38%)

DMSO-*d* 298K

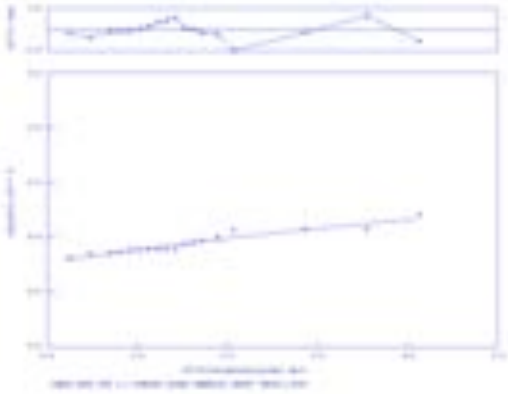

Receptor 139 (NH Proton)

TBACl

K_a = 143 M^{-1} (± 4%)

DMSO-d_6 298K

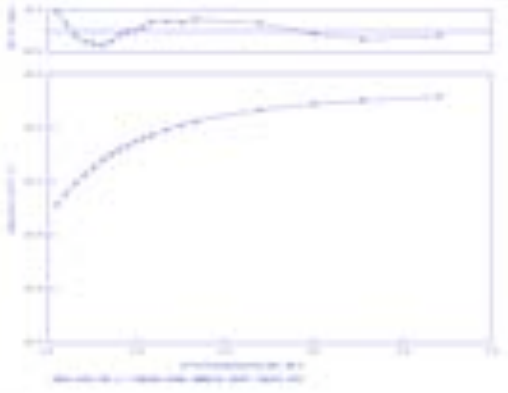

Receptor 139 (CH Proton)

TBACl

K_a = 138 M^{-1} (± 3%)

DMSO-d_6 298K

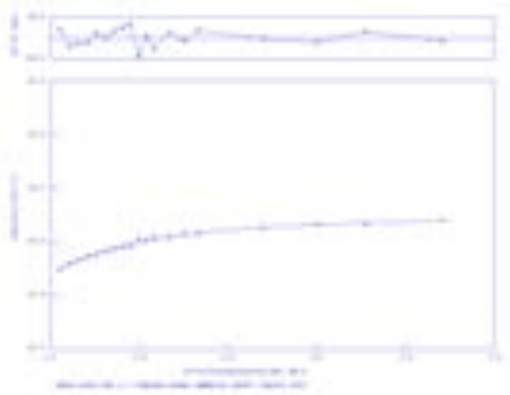

Receptor 139 (NH Proton)

TBABr

K_a = 73 M^{-1} (± 10%)

DMSO-d_6 298K

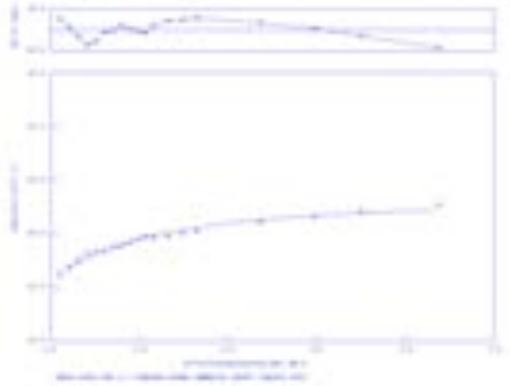

Receptor 139 (CH Proton)

TBABr

K_a = 103 M^{-1} (± 9%)

DMSO-d_6 298K

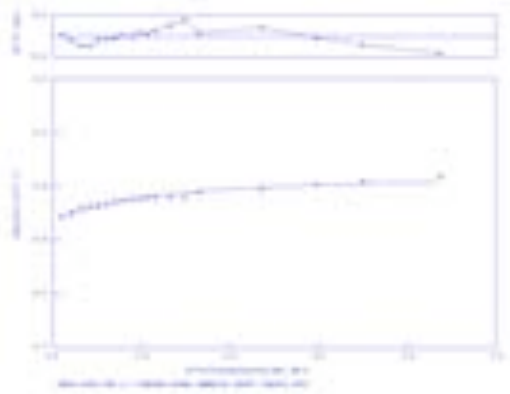

APPENDIX 4 – Job Plots Included in Chapter 3

Receptor 122 vs TBAOAc

DMSO-d_6 298K

Molar Fraction Host peaks at 0.5, indicative of 1:1 binding

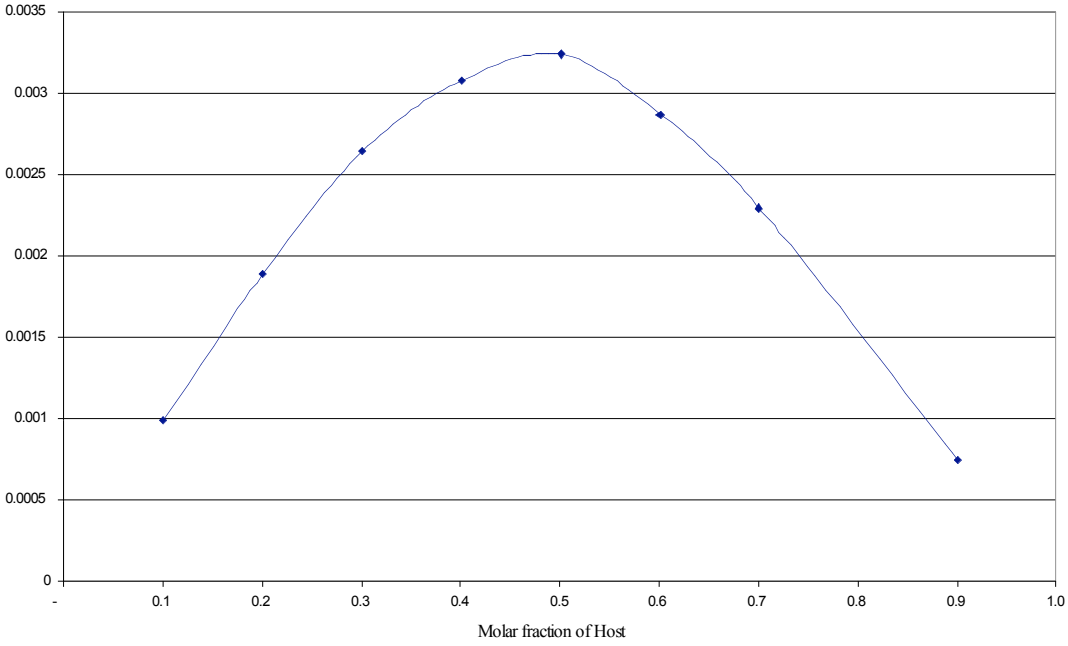

Receptor 123 vs TBAOAc

DMSO-d_6 298K

Molar Fraction Host peaks at 0.45, indicative of 1:1 binding with minor 2:1 (guest:host) component

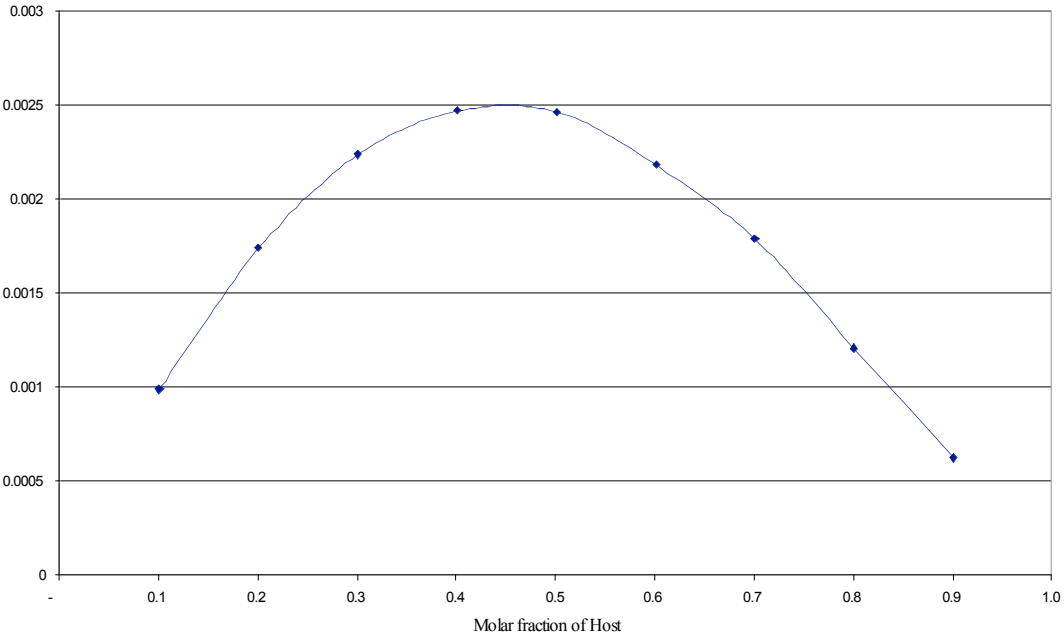

Receptor 124 vs TBAOAc

DMSO-d_6 298K

Molar Fraction Host peaks at 0.33, indicative of 2:1 (guest:host) binding

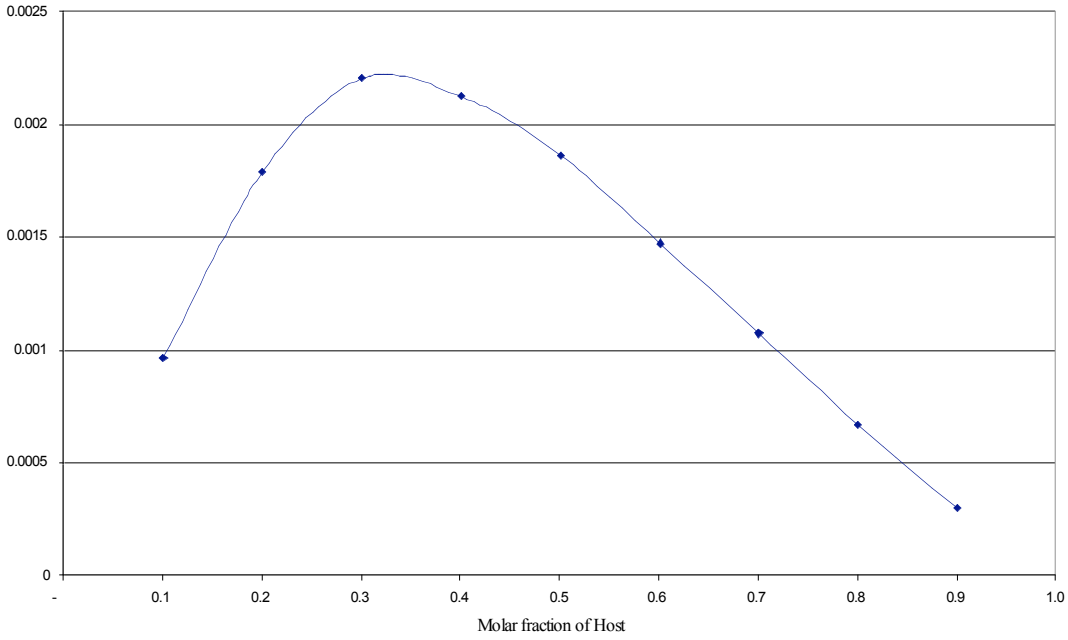

Receptor 125 vs TBAOAc

DMSO-d_6 298K

Molar Fraction of Host peaks at 0.40, indicative of a mixture of 1:1 and 2:1 (guest:host) binding modes.

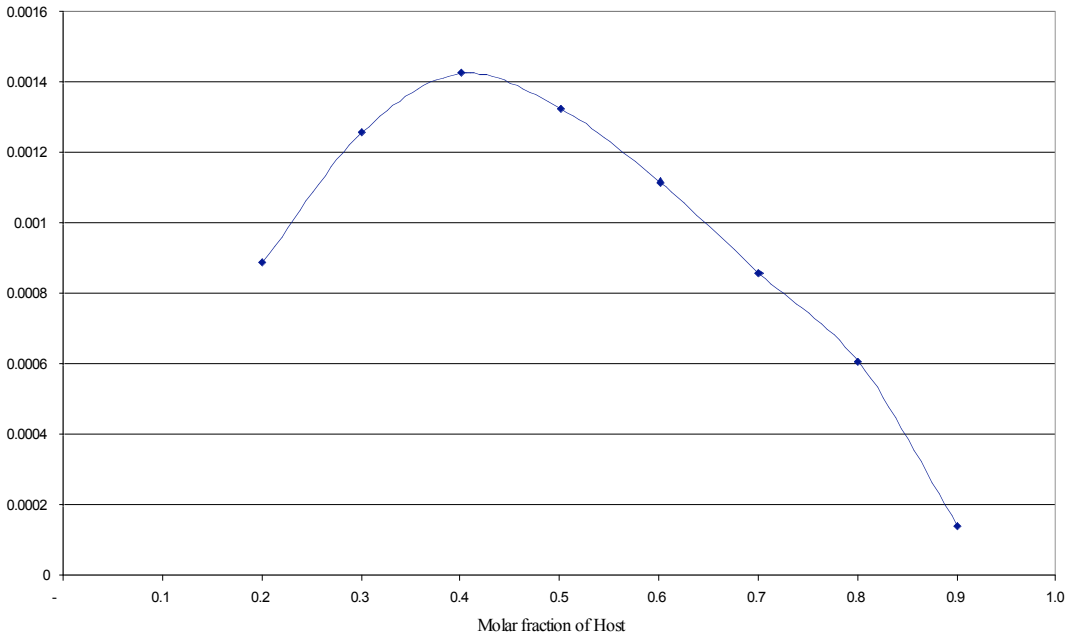

Receptor 124 vs TBAOBz

DMSO-d_6 298K

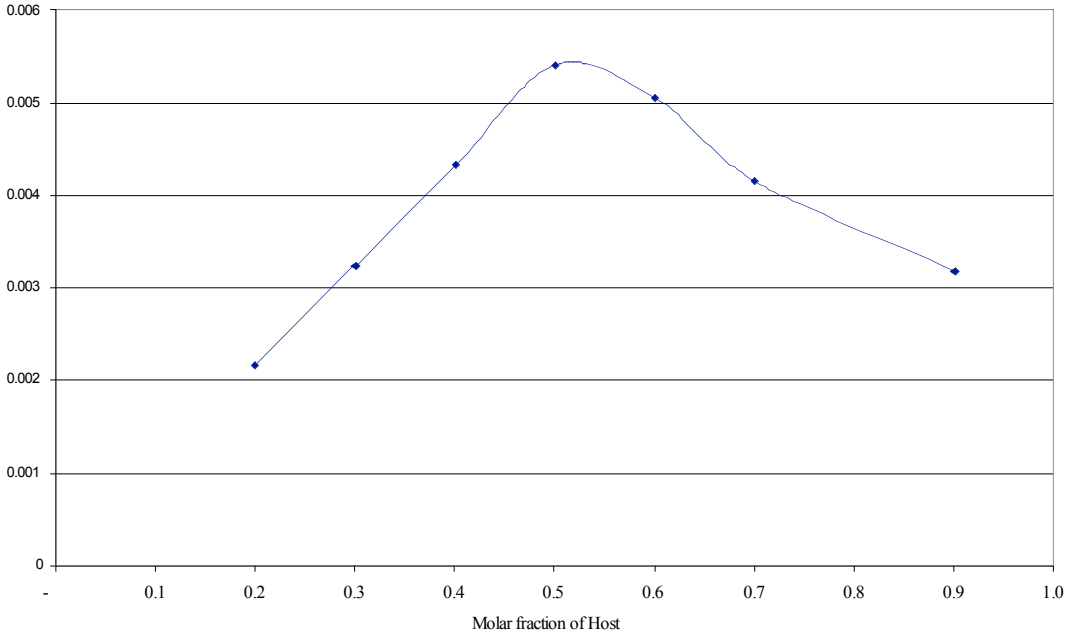

Receptor 125 vs TBAOBz

DMSO-d_6 298K

Molar Fraction Host peaks at 0.41, indicative of a mixture of 1:1 and 2:1 (guest:host) binding modes